GENERAL ACID AND GENERAL BASE CATALYSIS OF THE ENOLIZATION OF ACETONE. AN EXTENSIVE STUDY.

By

KEVIN PAUL SHELLY

B.Sc., University College Galway, 1981
M.Sc., University of British Columbia, 1984

A THESIS SUBMITTED IN PARTIAL FULFILMENT OF

THE REQUIREMENTS FOR THE DEGREE OF

DOCTOR OF PHILOSOPHY

in

THE FACULTY OF GRADUATE STUDIES

DEPARTMENT OF CHEMISTRY

We accept this thesis as conforming

to the required standard

THE UNIVERSITY OF BRITISH COLUMBIA
May 1988

In presenting this thesis in partial fulfilment of the requirements for an advanced degree at the University of British Columbia, I agree that the Library shall make it freely available for reference and study. I further agree that permission for extensive copying of this thesis for scholarly purposes may be granted by the head of my department or by his or her representatives. It is understood that copying or publication of this thesis for financial gain shall not be allowed without my written permission.

Department of CHEMISTRY

The University of British Columbia
Vancouver, Canada

Date June 1, 1988

ABSTRACT

The enolization of acetone is subject to both general acid and general base catalysis, eqs. [1.10] and [1.78]. The Bronsted equation relates the catalyzing power of the acid or base to the equilibrium acid or base strength of the species involved, eqs. [1.14] and [1.13].

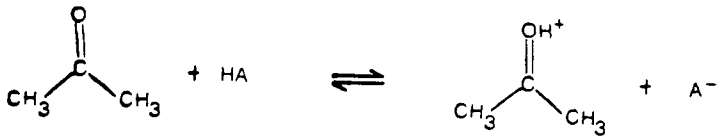

[1.10a]

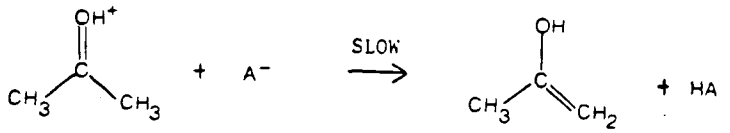

[1.10b]

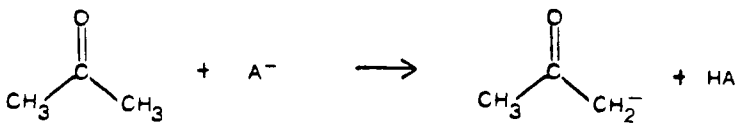

[1.78]

$$\log k_{HA} = \alpha \log k_{HA} + \text{Constant} \qquad [1.14]$$

$$\log k_{A^-} = -\beta \log k_{HA} + \text{Constant} \qquad [1.13]$$

This work involved measuring enolization rate constants for over 130 acid and base catalysts. These include monoprotic and diprotic carboxylic acids, phosphonic acids, carboxylate monoanions and dianions and phosphonate dianions. A number of the conjugate bases of the diprotic acids, i.e. bifunctional monoanions, were also examined. A

number of effects were probed by an examination of the resulting Bronsted plots.

In the case of general acid catalysis, a number of sterically crowded catalysts displayed enhanced catalytic activity. That is to say, they are more effective in the enolization process than their equilibrium acid strengths would suggest. This result was evident in both carboxylic acid and phosphonic acid catalysis, but not in general base catalysis. The role of steric factors in these processes is unclear.

A group of bifunctional monoanions are shown to act as general acids in the enolization process. A comparison of 5- and 2-substituted isophthalate monoanions reveals a steric accelerating effect for the 2-substituted species, a result consistent with earlier observations.

Species with polarizable substituents are better catalysts, in both acid and base catalysis, and this result is explained.

A set of carboxylate dianions, whose conjugate monoanions possess no hydrogen-bonding, form a reasonable Bronsted line. A pair of dianions deviate below this line, and the degree of deviation is shown to be related to the degree of hydrogen-bonding present in the conjugate monoanions.

The group of phosphonate dianions gives a curved Bronsted plot suggesting a changing transition state as the base strength of the catalyst is varied. In terms of the Hammond postulate, a more favourable proton transfer (involving a stronger base) is leading to an earlier, more reactant-like transition state i.e. the proton transfer is occurring earlier along the reaction coordinate. The curvature is analyzed

in terms of Marcus Theory and gives experimental support to the concepts of transition state energetics that are encompassed in the Hammond and Marcus models. A correlation of primary isotope effects with the curved Bronsted line is presented and this further maps out the varying degrees of proton transfer in the transition state. A number of other examples of experimental evidence for the Hammond postulate are presented.

Carboxylic monoprotic acids, free from both polarizability and steric factors, appear to form a curved Bronsted line. While the curvature is in the direction predicted by Marcus Theory, primary isotope effects suggest that a changing transiiton state is not a cause of the curvature.

As well as the topics mentioned here, a number of other facets of the reaction are discussed, including electrostatic factors. It is shown, for example, that including catalysts of varying charge in a single Bronsted correlation must be done with caution.

TABLE OF CONTENTS

LIST OF TABLES

LIST OF FIGURES

LIST OF ABBREVIATIONS

α	The Bronsted exponent when the cataylsts are proton donors
β	The Bronsted exponent when the catalysts are proton acceptors
p	Number of equivalent acidic protons
q	Number of equivalent sites for proton attachment
k_{HA}	Rate constant for a monoprotic acid
k_{H_2A}	Rate constant for a diprotic acid
k_{A^-}	Rate constant for a monoanionic base
$k_{A^{2-}}$	Rate constant for a dianionic base
k_{HA^-}	Rate constant for a bifunctional monoanion of a diprotic acid
$k_{A^-\cdot HA}$	Rate constant for the simultaneous involvement of acid and base with the substrate (Third order term)
k_{H^+}	Rate constant for hydronium ion
$k_{^-OH}$	Rate constant for hydroxide ion
k_{H_2O}	Rate constant for water
k_H/k_D	Primary kinetic isotope effect, i.e. ratio of rate constants for a particular catalyst with the ^1H substrate (k_H) and the ^2H substrate (k_D)
K_{HA}	Equilibrium acid constant for a monoprotic acid
K_{A^-}	Equilibrium base constant for a monoanionic base
K_W	Autocatalysis constant for water

n	Buffer ratio of neutral acid to monoanion
m	Buffer ratio of monoanion to dianion
ℓ	Buffer ratio of dianion to trianion
G_r^o	Free energy of reactants
G_p^o	Free energy of products
$G^{\neq}$	Free energy of transition state
ΔG^o	Free energy of reaction
$\Delta G^{\neq}$	Free energy of activation
$\Delta G_o^{\neq}$	Intrinsic barrier
W_r	Work term for encounter of reactants
W_p	Work term for separation of products
$(\Delta G^o)_{obs}$	Observed free energy of reaction
$(\Delta G^{\neq})_{obs}$	Observed free energy of activation
ρ	Hammett reaction constant
σ	Hammett substituent constant
σ^n	Modified substituent constant
σ_I^o	Inductive substituent constant for an ortho group
ρ_I	Coefficient for the ortho inductive parameter
E_s^o	Steric substituent constant for an ortho group
δ	Coefficient for the ortho steric parameter

ACKNOWLEDGEMENTS

While only my name appears on the front of this thesis, I would like to give credit to a few people, for without their help, there would be no thesis.

I would like to thank Dr. Ross Stewart for the opportunity to work with him, and for many helpful suggestions throughout the course of the research and the writing of the thesis. I also want to acknowledge the members of the research group, past and present, whose results I have used in my work. In this regard, the synthetic work of Dr. Kasinathan Nagarajan and Dr. Sampath Venimadhavan deserve special mention. These colleagues, along with a few summer students, namely Lisa Wong, Alex Lee, Lackbir Rai and Oliver Lee, were also responsible for many pK determinations.

The assistance of the elemental analyses, nmr, mass spectroscopy, secretarial and workshop staff in the department, is appreciated.

Thanks are also due to my guidance committee, especially Dr. Pincock for helpful comments in the preparation of this thesis. A big thank you to Rani Theeparajah for her efficient typing of same. Dr. Sampath Venimadhavan deserves special mention for his help and advice in the writing of the manuscript.

Regards to all the friends that I met at the Chemistry Department and at International House. You all helped to make UBC and Vancouver such a great place to be.

Finally, thanks to my family, just for 'being there'.

FOR RITA

INTRODUCTION

1.1 PHYSICAL ORGANIC CHEMISTRY

The subject of physical organic chemistry is the study of organic chemistry by "quantitative and mathematical methods." This definition and the naming of the subject date back to Hammett's landmark book in 1940 (H40). The organic chemist who claims that physical organic chemistry is a branch of physical chemistry is reflecting the opinion of the physical chemist who suggests the topic is a branch of organic chemistry. Such opinions prompt the questions: Is chemistry a branch of physics? Is biochemistry a branch of chemistry? While physical organic chemistry is on the borders of our defined areas of specialized chemistry fields, in essence, chemistry, like science, knows no boundaries. Each area merges with many around it, eventually comprising the whole. By its very nature, physical organic chemistry is a meeting of concepts and methods of several areas of chemistry. In conducting my research and preparing this thesis, I had to consult various texts and journals. These included Faraday Transactions I, The Journal of Organic Chemistry, The Journal of Physical Chemistry and Advances in Chemical Physics. The scope of these journals is a comment on the scope of physical organic chemistry, a scope that is only limited by the minds of those researching the topic.

A main aim of physical organic chemists is to attain a thorough understanding of reaction mechanism energetics and transition state

structures. In approaching such problems we need experimental results as a basis for further refinement and development of our concepts. Much progress has been made in this regard and much more has still to be achieved. This thesis contributes one very small part to that progress.

1.2 ENOLIZATION

In 1904, Lapworth suggested that enol formation was the rate-limiting step in the halogenation of ketones, eq. [1.1] (L04).

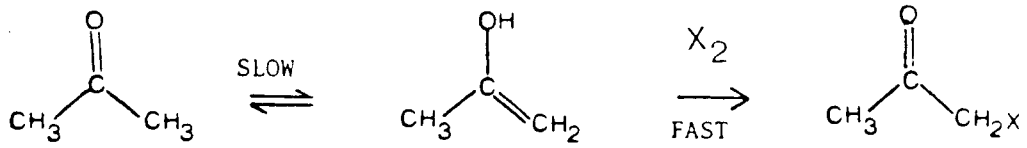

[1.1]

Since then many scientists have turned their attention to the process of enolization of keto compounds. There are two main reasons for this. First, is the relevance of enolization to many reaction pathways. Secondly, enolization is an example of a proton transfer reaction, "a fundamental reaction in Chemistry", as Koch recently described it (K84). The subject of the enolization of simple carbonyl compounds was reviewed in 1982 by Toullec (T82).

Reactions of these compounds are of two general types; addition of a nucleophile to a carbonyl compound, eq. [1.2], and removal of a proton from the α-carbon, eq. [1.3]. Co-ordinating a Lewis acid, e.g. a proton, to the carbonyl oxygen will help these two processes. Lowry and

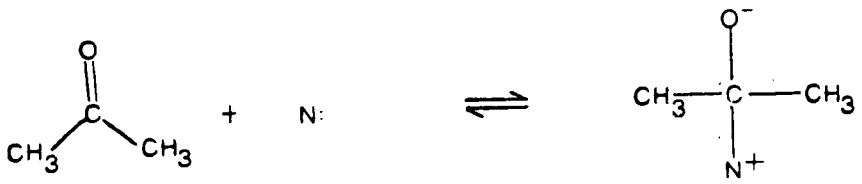

[1.2]

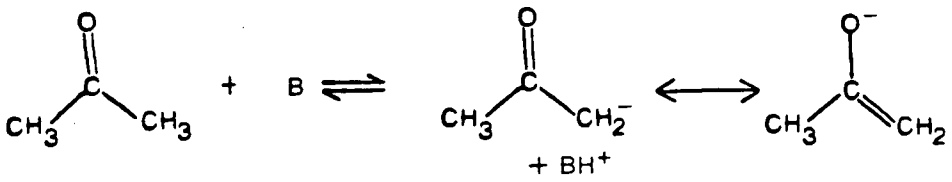

[1.3]

Richardson describe catalysis by acids and bases as a "central theme of carbonyl reactions" (LR87a). In particular the process of enolization is of great importance in organic and bio-organic chemistry, being involved in condensation, oxidation, halogenation, racemization and isotope exchange reactions.

The keto-enol equilibrium in most carbonyl compounds is well over to the keto side, and so the tautomer cannot be studied directly. Rather, kinetic studies are frequently used to follow the conversion of ketone to enol or enolate anion. The enols of simple ketones have recently been detected in aqueous solution allowing the kinetics of the enol-keto conversion to be measured (CH87). The enols of a carboxylic acid and an ester have also been reported (NH87).

Enolization is catalyzed by acids and bases. A relationship exists between the equilibrium strength (pK) of the acid or base and its effectiveness in catalyzing the enolization (rate constant). The relationship, named after its co-discoverer, is described in the following section.

1.3 BRONSTED RELATIONSHIP

In 1913, Dawson and Powis published a study of the enolization of acetone catalyzed by a number of acids ranging in strength from acetic to hydrochloric acid (DP13). This was ten years before Bronsted defined acids as species that give up protons and bases as species that accept protons (B23). In 1913, the Arrhenius definition of acids was popular; it defines acids as substances which give rise to hydrogen ions in aqueous solution. An interesting account of the early history of acid and base definitions has been compiled by Bell, going from the late eighteenth century to Bronsted's defintion (B73a). Dawson and Powis stated in their paper that "evidence has been obtained in support of the view that the catalyzing power of an acid is not entirely due to the hydrogen ion, but that the undissociated acid also contributes to the observed effect." They measured the rate constant for the enolization catalyzed by hydrogen ion and the undissociated acids. Of course, catalysis by undissociated hydrochloric acid was subsequently disproven (B73b). The authors drew attention to the fact that the "catalyzing power of the undissociated acid diminishes rapidly as the ionization tendency decreases, a relation which has already been pointed out by Snethlage." However they could not find any quantitative relationship between these two factors. Within the decade, Bronsted and Pederson were studying the decomposition of nitramide in aqueous solution, eq. [1.4], (BP 24).

$$NH_2NO_2 \longrightarrow H_2O + N_2O \qquad [1.4]$$

Like many scientists, before and after, their initial aim in studying this reaction proved fruitless while a far more interesting result became evident: a simple relationship was seen to exist between the rate constants for the base catalyzed decomposition of nitramide, k_B, and the basicity constants of the catalysts, K_B, eq. [1.5]. A detailed discussion of this reaction and its mechanism is available (B73c).

$$k_B = (6.2 \times 10^{-5})(K_B)^{0.83} \qquad [1.5]$$

This relationship has become known as the Bronsted relationship. One wonders how close Dawson was to uncovering the correlation, and if perhaps we might now be discussing the Dawson relationship. Before discussing the relationship further it is worth outlining some concepts of catalysis.

A catalyst is a substance that increase the rate of reaction without itself being consumed. In the acid hydrolysis of most acetals the mechanism given in eq. [1.6] operates (S85a).

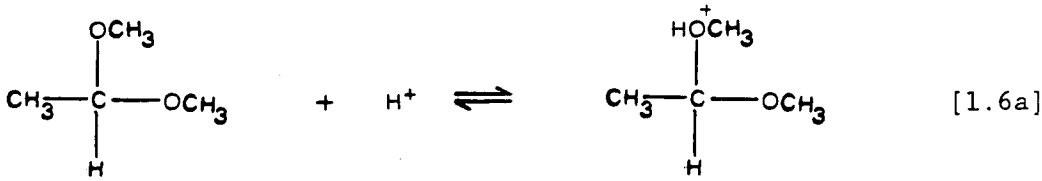

[1.6a]

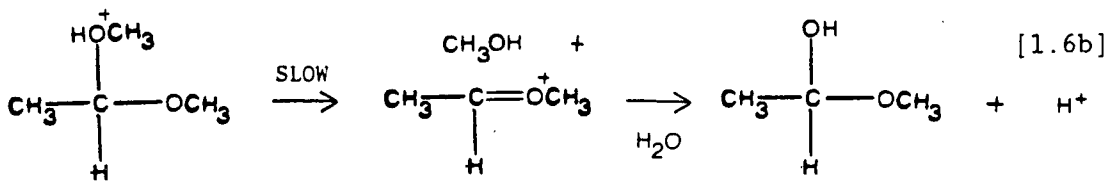

[1.6b]

The rate of this reaction depends only on the equilibrium activity of the proton, i.e. in dilute aqueous solution, on the pH. Reactions of this type can be represented by eq. [1.7].

$$Z + H^+ \rightleftharpoons ZH^+ \qquad [1.7a]$$

$$ZH^+ \xrightarrow{\text{rate controlling step}} \text{products} \qquad [1.7b]$$

There is no proton transfer in the rate controlling step of this reaction. Such catalysis is called specific acid catalysis. In specific base catalysis the rate depends only on the equilibrium activity of hydroxide ion. On the other hand when the rate controlling step of a reaction involves proton transfer, general acid and/or general base catalysis will be evident. The base catalyzed decomposition of nitramide is an example of general base catalysis. The rate depends on the nature and concentration of all the bases present in the system, hydroxide and acetate in an acetate buffer, for example. The two routes by which general acid catalyzed reactions proceed are shown in eqs. [1.8] and [1.9].

A-2 mechanism

$$Z + HA \rightleftharpoons ZH^+ + A^- \qquad [1.8a]$$

$$ZH^+ + A^- \xrightarrow{\text{slow}} \text{products} \qquad [1.8b]$$

A-S_E-2 mechanism

$$Z + HA \xrightarrow{\text{slow}} \text{products} \qquad [1.9]$$

The acid catalyzed enolization of ketones is an example of an A-2 mechanism, eq. [1.10]. It can be shown that the A-2 and A-S_E-2 mechanisms are kinetically equivalent (S85b).

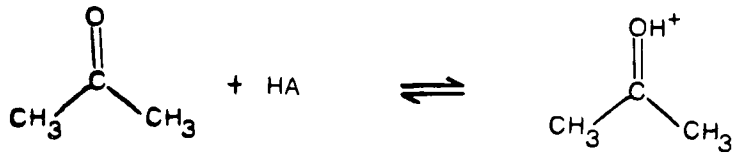

[1.10a]

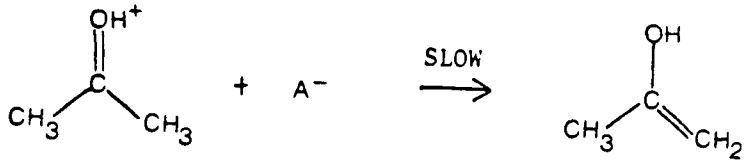

[1.10b]

Reactions subject to general acid and/or general base catalysis can be treated by eqs. [1.11a] and [1.12a] where HA is the general acid and k_{HA} the rate constant for that acid; and A^- is the general base and k_{A^-} the rate constant for that base. Since $K_{A^-}.K_{HA} = K_w$, eq. [1.11a] can be rewritten as eq. [1.11b].

Base Catalysis

$$k_{A^-} = (\text{const})(K_{A^-})^{\beta} \qquad [1.11a]$$

$$k_{A^-} = (\text{const})(K_{HA})^{-\beta} \qquad [1.11b]$$

Acid Catalysis

$$k_{HA} = (\text{const})(K_{HA})^{\alpha} \qquad [1.12a]$$

These equations are expressed as linear relationships in eqs. [1.13] and [1.14]. Since $-\log K_{HA} = pK$, eqs. [1.15a] and [1.16a] result.

$$\log k_{A^-} = -\beta \log K_{HA} + C \qquad [1.13]$$

$$\log k_{HA} = \alpha \log K_{HA} + C \qquad [1.14]$$

$$\log k_{A^-} = \beta \, pK + C \qquad [1.15a]$$

$$\log k_{HA} = -\alpha \, pK + C \qquad [1.16a]$$

In a situation where both general acid and general base catalyses operate, two Bronsted lines would result as shown in Fig. 1.

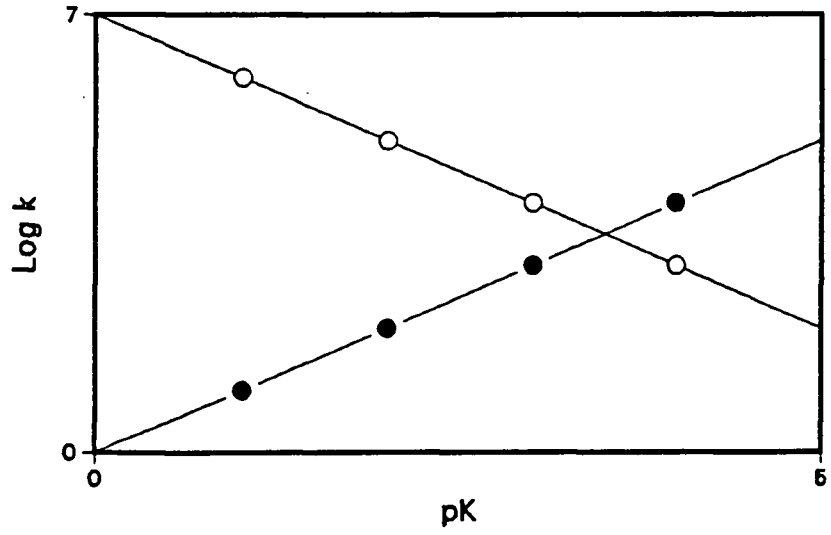

Fig. 1: Bronsted plots resulting from both general acid catalysis (open circles) and general base catalysis (closed circles)

The Bronsted equation which began as an empirical observation, has over many years proven its relevance to the study of proton transfer reactions. As stated by Bell in 1978, "In conjunction with isotope effects, a study of Bronsted relations constitutes the most powerful method for elucidating the detailed structure of proton transfer reactions, one of the most important classes of reactions in chemistry and biology" (B78).

1.4 STATISTICAL FACTORS

In a comparison of polyprotic acids or bases with monoacids or bases, rate and equilibrium constants must be corrected statistically (B73d, BL65). Thus Bronsted and Pedersen proposed the form of the Bronsted equation, eqs. [1.11c] and [1.12b], where p and q are statistical factors (BP24).

Base Catalysis

$$k_{A^-}/q = (\text{const})(qK_{HA}/p)^{-\beta} \qquad [1.11c]$$

Acid Catalysis

$$k_{HA}/p = (\text{const})(qK_{HA}/p)^{\alpha} \qquad [1.12b]$$

The number of equivalent acidic protons is represented by p, while q is the number of equivalent sites for proton attachment. These eqs. can be expressed as eqs. [1.15b] and [1.16b].

Base Catalysis

$$\log {}^{k}/_{q} = \beta(pK + \log {}^{p}/_{q}) + C \qquad [1.15b]$$

Acid Catalysis

$$\log {}^{k}/_{p} = -\alpha(pK + \log {}^{p}/_{q}) + C \qquad [1.16b]$$

Thus, in comparing oxalic acid, $(COOH)_2$, with acetic acid, CH_3COOH, p = 2 and 1 respectively. While the former acid has two

protons available, the latter has only one. The value of q in both cases is 2, as a carboxylate has two sites for proton attachment. For phenol, C_6H_5OH, p = 1 and q = 1. With respect to the base catalysts oxalate dianion, acetate and phenoxide, p = 1, q = 4 for $(COO^-)_2$, p = 1, q = 2 for CH_3COO^-, and p = 1 and q = 1 for $C_6H_5O^-$.

The values of p and q chosen for a homogeneous set of acids or bases is immaterial, as it only moves the Bronsted line vertically or horizontally while keeping the slope the same. These statistical corrections become important, however, when comparing the catalytic effects of acids or bases that have differing values of p and q. A deviation from a Bronsted line which is solely dependent on the choice of values for p and q would have to be treated with caution. Generally deviations are sufficiently large that they cannot be attributed to an incorrect choice of values for p and q.

The hydronium ion, H_3O^+ is such an example. It frequently deviates markedly from acid catalyzed Bronsted correlations. Values of p = 3 and q = 1 are commonly used for H_3O^+, the value of q being derived from the number of equivalent sites for proton attachment in the conjugate base of the hydronium ion, H_2O. Gold and Waterman have suggested that q = 2 as the oxygen atom has two lone pairs in H_2O (GW68). Regardless of whether a value of q = 2 or 1 is used, the hydronium ion exhibits a marked negative deviation from most Bronsted lines, (i.e. decreased catalytic activity).

1.5 MEANING OF THE BRONSTED EXPONENT

The Bronsted exponent, α or β, is a measure of the sensitivity of the reaction to change in structure of the catalyzing acid or base. These exponents lie between the value of 0 and 1 for most reactions. The use of α or β depends on whether the catalysts are proton donors (α) or acceptors (β).

What is the theoretical meaning of the exponent? The relationship can be considered a quantification of the Hammond postulate, which states that in an exothermic reaction the transition state should resemble the reactants, whereas in an endothermic reaction the transition state should resemble the products (LR87b).

Consider eq. [1.17]. When HA is a much weaker acid than BH^+, the reaction profile shown in Fig. 2 results. The transition state resembles products. Small structural changes that change the free energy of the products G_p^o, cause similar changes in the free energy of activation $G^{\neq}$. Conversely changes in the free energy of reactants G_r^o have very little effect on $G^{\neq}$. In such an example $\alpha = 1$ and the reverse reaction (base catalysis by A^-) will be diffusion controlled, resulting in a β value of 0.

$$B + HA \longrightarrow BH^+ + A^- \qquad [1.17]$$

Consider the opposite extreme, when HA is a much stronger acid than BH^+, as shown in Fig. 3. The transition state resembles reactants and so $G^{\neq}$ will be dependent on G_r^o, not G_p^o. The acid catalyzed forward

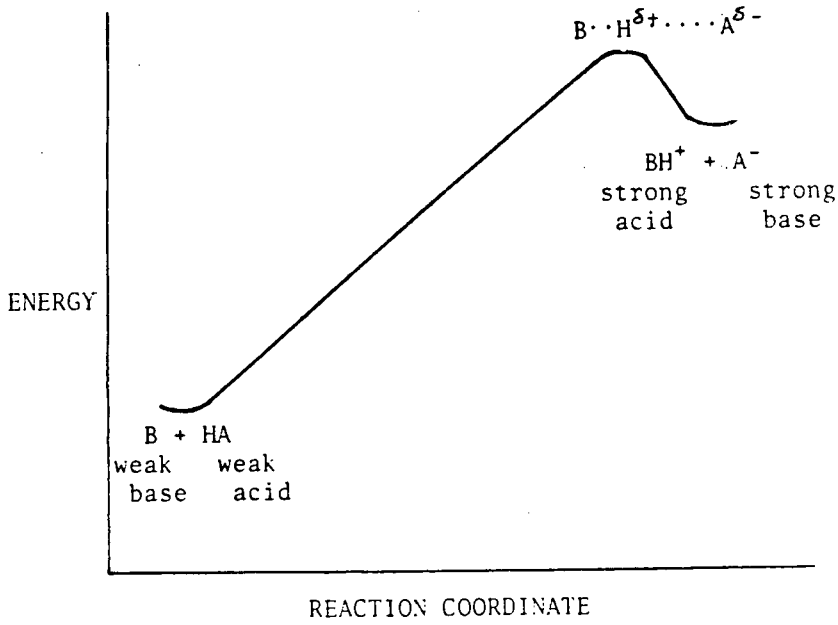

Fig. 2: Energy profile for eq. [1.17], HA being a much weaker acid than BH^+

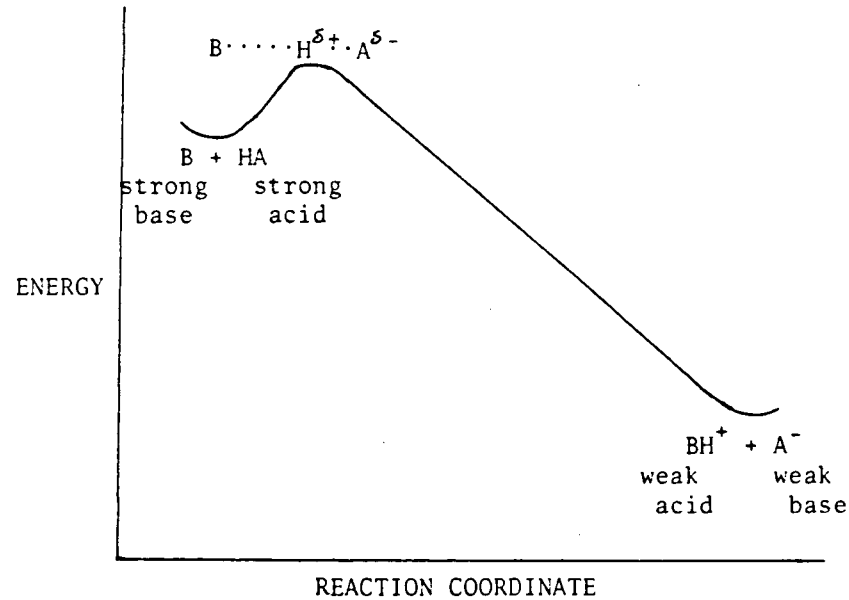

Fig. 3: Energy profile for eq. [1.17], HA being a much stronger acid than BH^+

reaction will be diffusion controlled ($\alpha = 0$) and the reverse reaction will have $\beta = 1$.

In the region where BH^+ and HA are similar in acid strength, α and β values between 0 and 1 will be observed. Leffler and Grunwald have quantified the Hammond postulate using eq. [1.18] where δ denotes the effect of substituent changes on the quantity it precedes (LG63). Since $\beta = 1-\alpha$, $\Delta G^{\neq} = G^{\neq} - G_r^o$, and $\Delta G^o = G_p^o - G_r^o$ eqs. [1.19], [1.20] and [1.21] result.

$$\delta G^{\neq} = \alpha\, \delta G_p^o + \beta\, \delta G_r^o \qquad [1.18]$$

$$\delta G^{\neq} = \alpha\, \delta G_p^o + \delta G_r^o - \alpha\, \delta G_r^o \qquad [1.19]$$

$$\delta G^{\neq} - \delta G_r^o = \alpha\, (\delta G_p^o - \delta G_r^o) \qquad [1.20]$$

$$\alpha = \delta\, \Delta G^{\neq} / \delta\, \Delta G^o \qquad [1.21]$$

Thus α can be defined as a "ratio of substituent effects, namely, the substituent effect on the free energy of activation divided by the substituent effect upon the standard free energy change of the reaction" (K75). We can also interpret α as a measure of the position of the transition state. A small value of α implies a transition state resembling reactants with little transfer of the proton. A large value of α implies a transition state resembling products, with a substantial degree of proton transfer in the transition state. Many good discussions of the Bronsted exponent and its meaning are available (B73e,B78,K73,K75 and S85c).

1.6 CURVATURE IN BRONSTED PLOTS I

The Bronsted relationship was the first linear free energy relationship to be discovered, predating the Hammett equation by ten years. It relates the free energy of activation $\Delta G^{\neq}$, a kinetic parameter, to the free energy of reaction ΔG^{o}, a thermodynamic parameter. Recall that α can be considered as $\delta\Delta G^{\neq}/\delta\Delta G^{o}$, which in the limit is $d\Delta G^{\neq}/d\Delta G^{o}$. This correlation between rate and equilibria is a purely empirical observation and bears no relationship to the laws of equilibrium thermodynamics.

An inherent assumption in our discussion of the Bronsted exponent and the Hammond postulate is the following; the position of the transition state along the reaction co-ordinate (i.e. the extent of proton transfer) will not change as the strength of the acid HA or the base B changes. This will be true over a small range of acid or base strength, but over an extensive range of pK, changes in the Bronsted coefficient may result.

Bronsted predicted in his original paper that log k would be a curved rather than a linear function of log K (BP24). This curvature can be understood further and in fact used (with care) to determine free energies of activation with the aid of Marcus theory (CM68).

1.7 MARCUS THEORY

1.7.1 Derivation and Application

Marcus developed an equation relating the rate of electron transfer processes to certain parameters, and it has since been applied with success to both proton transfer and atom transfer reactions. Only a brief relevant discussion of the theory will be given here, as a number of review articles and recent papers address the issue (B78, K73, F75, LS81, JB82, K83, KL84, SA84, HP84, SK85, ES87 and LR87C).

The approach to Marcus theory used here owes a great deal to refs. K73 and LR87c, with some modification introduced by this author. Marcus theory allocates two contributions to an activation barrier; (1) a thermodynamic part resulting from the overall free energy change of the reaction; (2) an intrinsic kinetic part which is the reaction barrier that would exist if the reactants and products had the same free energy.

Consider, for example, the proton transfer reaction, eq. [1.17], where AH could be acetone and B any base.

$$B + HA \longrightarrow BH^+ + A^- \qquad [1.17]$$

Marcus theory envisages the reaction coordinate as two intersecting parabolas, one representing the potential energy surface for stretching the A—H bond in the reactants and the other representing the stretching of the B—H bond in the products. The locations of these parabolas are determined by the overall free energy change and the

intrinsic barrier.

The intrinsic barrier is obtained by considering symmetrical reactions, such as those shown in eqs. [1.22] and [1.23], represented by the two parabolas in Fig. 4.

$$AH + A^- \longrightarrow A^- + HA \qquad [1.22]$$

$$B + HB^+ \longrightarrow BH^+ + B \qquad [1.23]$$

The parabolas are drawn so as to intersect at the activation energies of eq. [1.22], $\Delta G^{\neq}_{eq.\ [1.22]}$ (Fig.4(a)) and eq. [1.23], $\Delta G^{\neq}_{eq.\ [1.23]}$ (Fig. 4(b)).

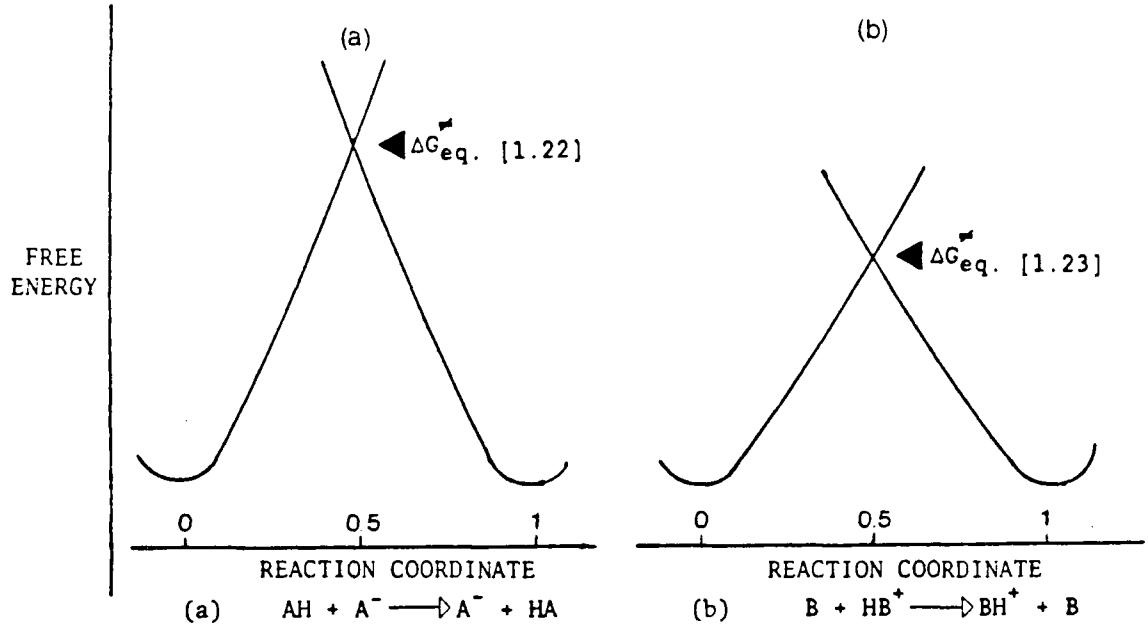

Fig. 4: Parabolas representing eqs. [1.22], Fig. 4(a) and [1.23], Fig. 4(b).

A new pair of parabolas is drawn so as to intersect at the average of the activation energies of the two processes represented by eqs. [1.22] and [1.23]. This average is the intrinsic barrier, $\Delta G_o^{\neq}$, of the proton transfer process represented by eq. [1.17] (Fig. 5).

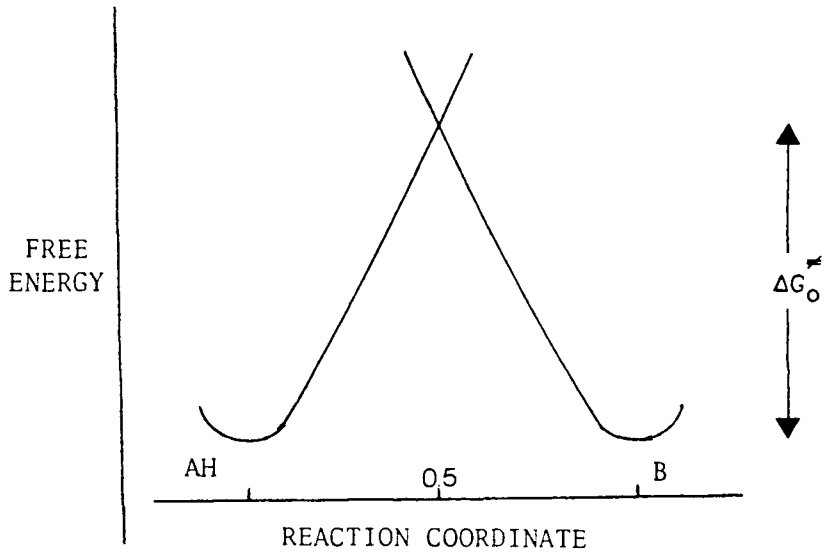

Fig. 5: Intersecting parabolas at $\Delta G = 1/2\ (\Delta G_{eq.[1.22]}^{\neq} + \Delta G_{eq.[1.23]}^{\neq})$, representing the intrinsic barrier of the proton transfer process represented by eq. [1.17], $\Delta G_o^{\neq}$

The parabolas representing the actual reaction are shown in Fig. 6(a) and (b). They are generated by displacing the parabolas of Fig. 5 vertically relative to one another by the observed free energy change, ΔG^o. The reaction might be exergonic, $\Delta G^o < 0$, Fig. 6(a) or endergonic $\Delta G^o > 0$, Fig. 6(b). The new point of intersection of the two parabolas is the activation free energy barrier, $\Delta G^{\neq}$, for the reaction. It can be

expressed in terms of $\Delta G_o^{\neq}$, the intrinsic barrier and ΔG^o, the observed free energy change by deriving the mathematical expression for the point of intersection of the two parabolas in Fig. 6(a) or (b).

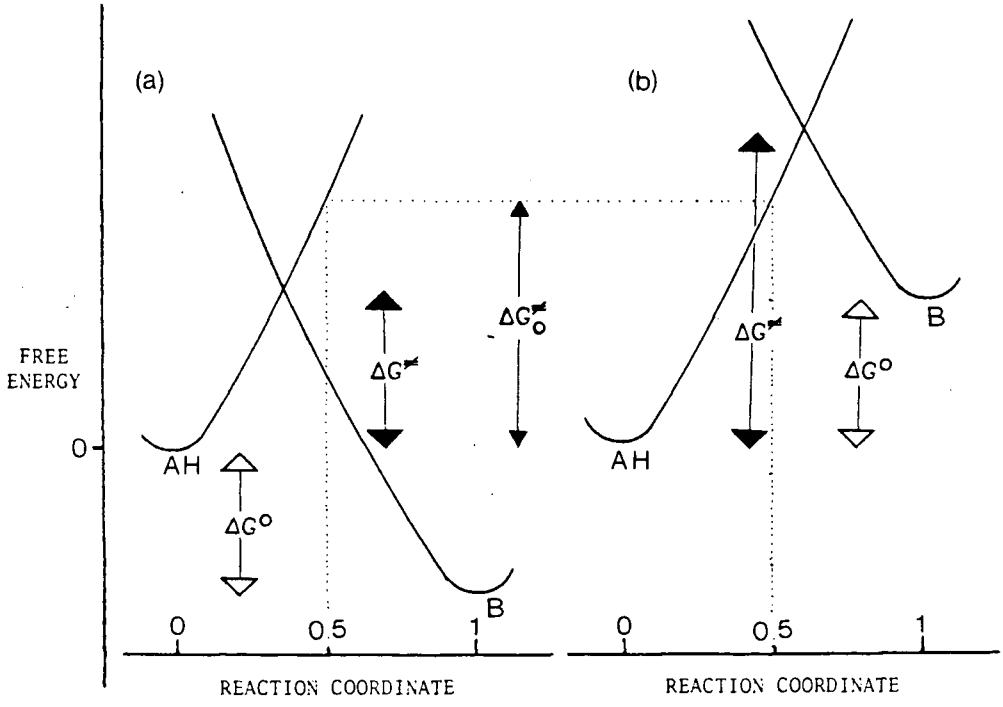

Fig. 6: Displaced parabolas from Fig. 5 so as to give an overall free energy change $\Delta G^o < 0$ (a) or $\Delta G^o > 0$ (b).

The general expression for the parabolas in Fig. 5 are $X^2 = C_1\Delta G$ for parabola AH and $(X-1)^2 = C_2\Delta G$ for parabola B, where X is the reaction coordinate and C_1 and C_2 are parabola constants. For both parabolas at a X value of 0.5, $\Delta G = \Delta G_o^{\neq}$, the intrinsic barrier. Thus the constants C_1 and C_2 can be determined, $C_1 = 1/4\Delta G_o$ and $C_2 = 1/4\Delta G_o^{\neq}$ We can now write the equations for the parabolas as follows.

Parabola AH
Fig. 5

$$X^2 = (1/4\Delta G_o^{\neq})\ \Delta G \qquad [1.24]$$

Parabola B
Fig. 5

$$(X - 1)^2 = (1/4\Delta G_o^{\neq})\ \Delta G \qquad [1.25]$$

In Fig. 6(a) or (b) parabola B has been moved vertically by a factor ΔG^o, and hence this parabola is now expressed by eq. [1.26]. Parabola AH is Fig. 6(a) or (b) is the same as in Fig. 5, represented by eq. [1.24].

Parabola B
Fig. 6

$$(X - 1)^2 = 1/4\Delta G_o^{\neq}\ (\Delta G - \Delta G^o) \qquad [1.26]$$

The point of intersection of parabolas AH and B in Fig. 6(a) or (b) is at $\Delta G = \Delta G^{\neq}$ and can be determined by substituting the value for X at the point of intersection from eq. [1.24], $(\Delta G^{\neq}/4\Delta G_o^{\neq})^{1/2}$, into eq. [1.26] to give eq. [1.27].

$$[(\Delta G^{\neq}/4\Delta G_o^{\neq})^{1/2} - 1]^2 = 1/4\Delta G_o^{\neq}\ (\Delta G^{\neq} - \Delta G^o) \qquad [1.27]$$

Eq. [1.27] is rearranged to give an expression for $\Delta G^{\neq}$, as shown.

$$\Delta G^{\neq}/4\Delta G_o^{\neq} + 1 - 2\ (\Delta G^{\neq}/4\Delta G_o^{\neq})^{1/2} = \Delta G^{\neq}/4\Delta G_o^{\neq} - \Delta G^o/4\Delta G_o^{\neq} \qquad [1.28]$$

$$(\Delta G^{\neq}/\Delta G_o^{\neq})^{1/2} = (1 + \Delta G^o/4\Delta G_o^{\neq}) \qquad [1.29]$$

$$\Delta G^{\neq} = (1 + \Delta G^o/4\Delta G_o^{\neq})^2\ \Delta G_o^{\neq} \qquad [1.30]$$

The position of the transition state along the reaction coordinate X can be determined by substituting for ΔG, which is equivalent to $\Delta G^{\neq}$, from eq. [1.30] into eq. [1.24]. The result is given in eq. [1.31] and is equivalent to α (or β), the Bronsted exponent determined by taking the derivative of eq. [1.30] with respect to ΔG^{o}.

$$X = 1/2\ (1 + \Delta G^{o}/4\Delta G_{o}^{\neq}) = d\Delta G^{\neq}/d\Delta G^{o} = \alpha \qquad [1.31]$$

In Fig. 6(a), where $\Delta G^{o} < 0$, an α value of less than 0.5 would be observed. For Fig. 6(b), where $\Delta G^{o} > 0$, an α value greater than 0.5 would result.

The degree of curvature present in a Bronsted plot will be represented by eq. [1.32]. When the intrinsic barrier is small a large degree of curvature will result. Conversely, with large values of intrinsic barriers, Bronsted plots will show little or no curvature.

$$d\alpha/d\Delta G^{o} = 1/8\Delta G_{o}^{\neq} \qquad [1.32]$$

Our discussion thus far has not considered the work expended in bringing the reactants from an infinite distance apart to the position where the proton transfer can occur and then separating the products to infinite distance. We should treat the encounter of reactants, involving a work term W_r, and the separation of products, involving a work term W_p, as distinct steps separate from the actual proton transfer itself and involving a free energy change. A three step process representing the mechanism of proton transfer is shown below.

$$AH + B \underset{}{\overset{W_r}{\rightleftharpoons}} A - H \cdots B \qquad \text{ENCOUNTER} \qquad [1.33]$$

$$A - H \cdots B \overset{\Delta G^o}{\rightleftharpoons} A \cdots H - B \qquad \text{PROTON TRANSFER} \qquad [1.34]$$

$$A \cdots H - B \overset{W_p}{\rightleftharpoons} A^- + HB^+ \qquad \text{SEPARATION} \qquad [1.35]$$

The observed free energy of reaction $(\Delta G^o)_{obs}$ will then be represented by eq. [1.36]. The observed free energy of activation $(\Delta G^{\neq})_{obs}$ will be represented by eq. [1.37]. An energy profile diagram for an endothermic reaction is shown in Fig. 7.

$$(\Delta G^o)_{obs} = \Delta G^o + W_r - W_p \qquad [1.36]$$

$$(\Delta G^{\neq})_{obs} = \Delta G^{\neq} + W_r \qquad [1.37]$$

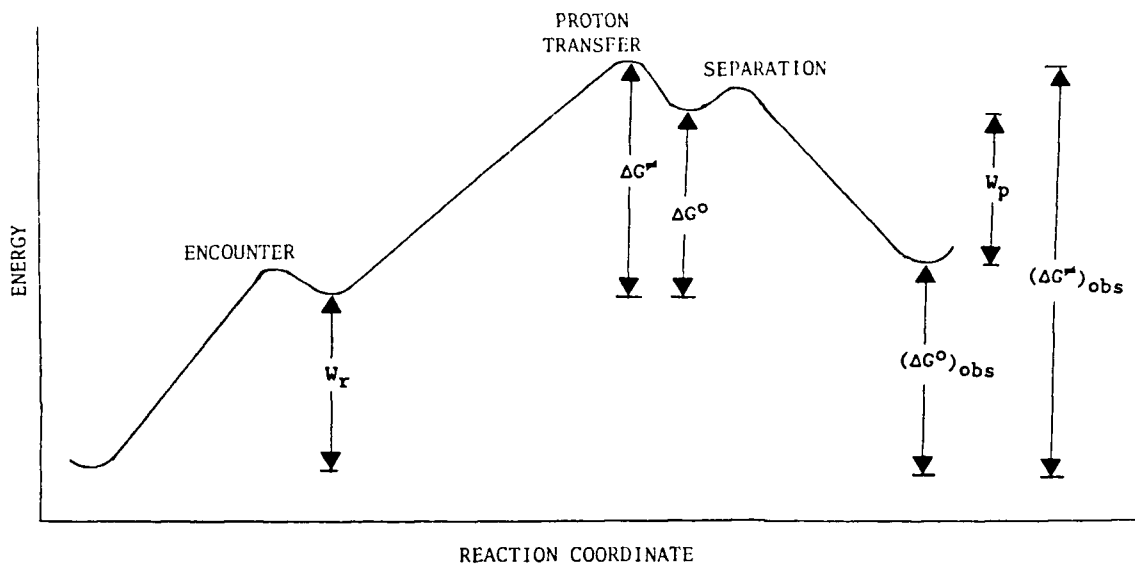

Fig. 7: Energy profile diagram describing eqs. [1.33]-[1.37] for an endothermic proton transfer ($\Delta G^o > 0$)

Substituting $\Delta G^{\neq}$ from eq. [1.30] into eq. [1.37] gives eq. [1.38]. We can now substitute ΔG^{o} from eq. [1.36] into eq. [1.38] giving eq. [1.39].

$$(\Delta G^{\neq})_{obs} = (1 + \Delta G^{o}/4\Delta G_{o}^{\neq})^{2} \Delta G_{o}^{\neq} + W_{r} \qquad [1.38]$$

$$(\Delta G^{\neq})_{obs} = [1 + ((\Delta G^{o})_{obs} - W_{r} + W_{p})/4\Delta G_{o}^{\neq}]^{2} \Delta G_{o}^{\neq} + W_{r} \qquad [1.39]$$

The work terms W_r and W_p and the intrinsic barrier $\Delta G_o^{\neq}$ are assumed to be constants along a reaction series. These assumptions together with limitations to this approach, will be discussed later.

The parabolas shown in Fig. 6(a) are a quantification of the Hammond postulate showing an early transition state for a reaction with $\Delta G^{o} < 0$ and the Bronsted coefficient (i.e. the reaction coordinate) less than 0.5. A quantification of the Hammond postulate showing a later transition state with $\Delta G^{o} > 0$ and the Bronsted coefficient (i.e. the reaction coordinate) greater than 0.5 is shown in Fig. 6(b).

The expression relating the observed free energy of activation, $(\Delta G^{\neq})_{obs}$ to the observed free energy of reaction, $(\Delta G^{o})_{obs}$, eq. [1.39] can be stated as a quadratic expression eq. [1.40], where the coefficients a, b and c are defined by eqs. [1.41], [1.42] and [1.43] respectively.

$$(\Delta G^{\neq})_{obs} = a + b\,(\Delta G^{o})_{obs} + c\,(\Delta G^{o})^{2}_{obs} \qquad [1.40]$$

$$a = \Delta G^{\neq} + (W_p + W_r)/2 + 1/16\Delta G^{\neq}_{o}\,(W_p - W_r)^2 \qquad [1.41]$$

$$b = 1/2 + 1/8\Delta G^{\neq}_{o}\,(W_p - W_r) \qquad [1.42]$$

$$c = 1/16\Delta G^{\neq}_{o} \qquad [1.43]$$

Expressions for $\Delta G^{\neq}$, W_r and W_p can be determined using eqs. [1.41]-[1.43] giving eqs. [1.44]-[1.46].

$$\Delta G^{\neq}_{o} = 1/16c \qquad [1.44]$$

$$W_r = a - b^2/4c \qquad [1.45]$$

$$W_p = W_r + 1/4c\,(2b - 1) \qquad [1.46]$$

The observed free energy of activation, $(\Delta G^{\neq})_{obs}$ is related to the observed rate constant k_{cat} for the catalyst (be it HA or B) by eq. [1.47] where h, $\underline{k}$ and T are Planck's constant, Boltzmann's constant and Kelvin temperature respectively. The observed free energy of the reaction, $(\Delta G^{o})_{obs}$, is related to the equilibrium constants of HA and BH^{+} by eq. [1.48].

$$(\Delta G^{\neq})_{obs} = - RT\,\ln(k_{cat}h/\underline{k}T) \qquad [1.47]$$

$$(\Delta G^{o})_{obs} = - RT \ln [A^{-}][BH^{+}]/[AH][B] = - RT \ln K_{HA}/K_{BH^{+}} \qquad [1.48]$$

The quadratic expression, eq. [1.40] can be expanded in terms of log k_{cat}, log k_{HA} and log $k_{BH^{+}}$ to give a complex equation. Generally in a Bronsted plot, one species will be kept constant (the substrate) while the other is varied (the catalyst). In eq. [1.17], HA could be the acid catalyst with B being the substrate. Since B remains unchanged, log $K_{BH^{+}}$ will be a constant and the expansion of eq. [1.40] reduces to eq. [1.49]. The parameters $\Delta G_{o}^{\neq}$, W_r and W_p are defined in eqs. [1.50]-[1.52].

$$\log k_{HA} = A + B (\log K_{HA}) + C (\log K_{HA})^2 \qquad [1.49]$$

$$\Delta G_{o}^{\neq} = - 2.3 RT/16C \qquad [1.50]$$

$$W_r = 2.3 RT (\log \underline{k}T/h - A + B^2/4C) \qquad [1.51]$$

$$W_p = W_r + 2.3 RT (1/4C - B/2C - \log K_{BH^{+}}) \qquad [1.52]$$

The work term W_r and the intrinsic barrier can be determined from the coefficients of the Bronsted plot that shows curvature, without knowing the pK of the protonated substrate, BH^{+}. This latter quantity is needed in order to determine the work term W_p.

The other possibility involves HA in eq. [1.17] being the substrate and B being a series of base catalysts. Now log K_{HA} will be a constant and eq. [1.53] results, with the parameters $\Delta G_{o}^{\neq}$, W_r and W_p being defined by eqs. [1.54]-[1.56].

$$\log k_B = D + E (\log K_{BH^+}) + F (\log K_{BH^+})^2 \qquad [1.53]$$

$$\Delta G_o^{\neq} = - 2.3RT/16F \qquad [1.54]$$

$$W_r = 2.3RT (\log \underline{k}T/h - D + E^2/4F) \qquad [1.55]$$

$$W_p = W_r + 2.3RT (1/4F + E/2F + \log K_{HA}) \qquad [1.56]$$

Both acid and base catalysis give the same result in relating the quadratic coefficients to the energy parameters, except for changes of sign in the definition of W_p.

Kreevoy and Oh have compiled a number of reactions and determined their intrinsic barriers, $\Delta G_o^{\neq}$ and work terms W_r (KO73). Albery and co-workers have applied the same treatment to several other reactions (AC72). All these data have been collected and discussed by Kresge (K73). The resulting intrinsic barriers, $\Delta G_o^{\neq}$, are small (averaging 4 kcal mol^{-1}) while the work terms W_r are generally much larger (averaging 12 kcal mol^{-1}) in proton transfer reactions.

1.7.2 Limitations to Marcus Theory

One of the assumptions in the treatment just described is that $\Delta G_o^{\neq}$, W_r and W_p are constant along a reaction series. This assumption is valid where, for example, HA is acetone and the bases are a series of oxygen anions. The bulk of $\Delta G_o^{\neq}$ can be attributed to $\Delta G^{\neq}$ for the

symmetrical reactions involving HA represented by eq. [1.22]. The free energy of activation for the symmetrical reaction represented by eq. [1.23] will be small for an oxygen anion, B.

$$AH + A^- \longrightarrow A^- + HA \qquad [1.22]$$

$$B + HB^+ \longrightarrow BH^+ + B \qquad [1.23]$$

A discussion of situations where the intrinsic barrier is not a constant is available (K73).

Other assumptions in 'simple' Marcus theory involve the use of the parabolas in Fig. 6; the distance moved by the hydrogen atom, d_H, is assumed to be constant as either AH or B is varied; and the force constants of the A——H bond, k_1, and that of the H—B bond, k_2, are assumed equal. Kresge and Koeppl determined an expression for the free energy of activation involving these parameters, (an equation which reduces to eq. [1.30] if $k_1 = k_2$ and d_H is constant) (KK73). The authors determine that in considering variations in k_1, k_2 and d_H, a sigmoid dependence of α upon ΔG results. In the range of $\alpha = 0.2 - 0.8$, the dependence is almost linear, as predicted by Marcus theory. But the slopes of these lines are greater than those predicted by Marcus theory, by about a factor of two. Other approaches to the proton transfer process give the same result, i.e. intrinsic barriers resulting from simple Marcus theory may be underestimated by as much as a factor of two (K73, LS81). For example a treatment by Lewis and co-workers invoked a hyperbolic modification of the Bronsted relationship and determined that Marcus theory "provides a lower limit for and indeed must underestimate

the (intrinsic) barrier" (LS81). The equation relating $\Delta G^{\neq}$ and ΔG^{o} used by these authors is shown below, eq. [1.57], and differs from Marcus theory, eq. [1.30] in the magnitude of the coefficient of the squared term. This approach therefore leads to $\Delta G_o^{\neq}$ values twice that of Marcus theory.

$$\Delta G^{\neq} = \Delta G_o^{\neq} + \Delta G^o/2 + (\Delta G^o)^2/8\Delta G_o^{\neq} \qquad [1.57]$$

$$\Delta G^{\neq} = \Delta G_o^{\neq} + \Delta G^o/2 + (\Delta G^o)^2/16\Delta G_o^{\neq} \qquad [1.30]$$

While simple Marcus theory may underestimate $\Delta G_o^{\neq}$, the relative values of $\Delta G_o^{\neq}$ and work terms obtained from the readily applicable equations are valid. Despite the limitations of Marcus theory, it gives results which have support from other theoretical approaches to proton transfer. As Kresge emphasizes in his review, a number of theoretical studies, as well as Marcus theory, predict that the degree of curvature in a Bronsted plot will depend on the magnitude of $\Delta G_o^{\neq}$ (K73).

There exists an experimental limitation to a treatment involving Marcus theory. A curved Bronsted plot, free from artifacts resulting from the use of catalysts of different types, is needed. The presence of curvature in some of the literature examples treated with Marcus theory is questionable in this regard (see p. 45 for example).

The most serious criticism of Marcus theory is whether it is valid to separate the 'setting-up' of the reagents involving reagent positioning and solvent reorganization from the actual proton transfer itself, an aspect which will be discussed later.

1.8 PRIMARY ISOTOPE EFFECTS

The use of the Bronsted relationship is often coupled with studies of primary isotope effects as probes of proton transfer reaction pathways and energetics, and reviews of the subject are available (M75, L76, and K76).

The Westheimer principle suggests how isotope effects can be related to the extent of proton transfer in the transition state for those reactions in which a bond to protium (deuterium, tritium) is broken. The principle states that a maximum isotope effect should be found for a transition state in which the hydrogen is half transferred between the donor and acceptor atoms (W61). If there is no breaking of a bond to the isotopic atom in the transition state, only a small secondary isotope effect will be expected. If a transition state changes from being reactant-like (α close to zero) to being product-like (α close to unity) the isotope effect should rise and fall, being a maximum when the proton is half transferred. A correlation of α and isotope effects can be obtained by using a quadratic-fitted Bronsted plot, eq. [1.49].

$$\log k_{HA} = A + B (\log K_{HA}) + C (\log K_{HA})^2 \qquad [1.49]$$

$$d \log k_{HA}/d \log K_{HA} = B + 2C \log K_{HA} \qquad [1.58]$$

For any acid of known pK, a value of α is defined from the derivative of eq. [1.49], i.e. eq. [1.58]. When the proton is half

transferred, a maximum isotope effect should result, α should be 0.5 and from eq. [1.31], $\Delta G^{o} = 0$ (i.e. $\Delta pK = 0$).

Experimental evidence for these predictions is difficult to obtain, requiring precision of k_H/k_D values, a curved Bronsted plot and ΔpK values close to zero. Kreevoy and Oh obtained an expected correlation of k_H/k_D and pK for the hydrolysis of diazoacetate anion catalyzed by trialkylammonium ions, eq. [1.59], (KO73).

$$R_1R_2R_3\overset{+}{N}H + N_2CHCOO^- \longrightarrow R_1R_2R_3N + \overset{+}{N}_2CH_2COO^- \quad [1.59]$$

$$\downarrow$$

Products

Kemp and Casey did not find any significant trends in the isotope effects for the proton abstraction from benzoisoxazoles by tertiary amines, eq. [1.60], (KC73a). Despite a total variation in rate by a factor of 10^{11}, no significant variation in linearity of the Bronsted plot was observed.

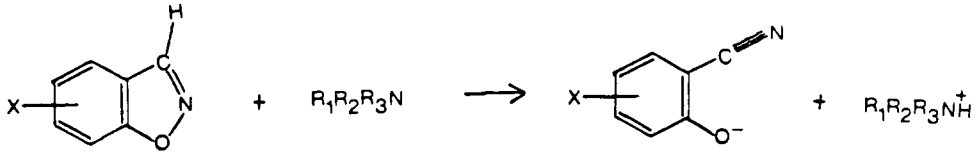

[1.60]

Dixon and Bruice in their study of the primary amine catalyzed ionization of nitroethane found linear Bronsted plots for both the ^1H and ^2H substrates with β values of 0.57 ± 0.02 (DB70). Surprisingly, their plot of k_H/k_D vs. pK showed a bell shaped curve, albeit a poor one, with a maximum close to the pK of nitroethane, 8.5. A change of

solvent from H_2O to 50% dioxane-water (v/v) changes the pK of nitroethane to 10.7. Now, the plot of k_H/k_D vs. pK rises towards a pK value of 10.7. They could not determine if the curve drops at pK values greater than 10.7, owing to experimental difficulties. Considering that linear Bronsted plots were found for this data, the authors conclude that "primary kinetic isotope effects are a more sensitive probe of transition state than are Bronsted plots."

Bordwell and Boyle in 1971 briefly reviewed the topic of kinetic isotope effects as guides to transition state structures in deprotonation reactions (BB71). The authors question the evidence of the maxima in k_H/k_D vs. ΔpK correlations that have been reported. Instead they consider the possibility that many of the reactions have an inherent experimental inaccuracy, that steric and tunnelling effects may exist and that low k_H/k_D values in cases of positive ΔpK values may be due to pre-rate-limiting equilibria. They conclude that there is no simple correlation of Bronsted coefficients and isotope effects with the extent of proton transfer in the transition state.

Bruniche-Olsen and Ulstrup have used a fundamentally different approach to isotope effects in proton transfer reactions from those discussed so far (BU79). They used the quantum theory of elementary processes in condensed media to predict the kinetic isotope effect of proton transfer reactions in homogeneous solution. Changes in $\Delta G_o^{\neq}$ and ΔpK were assumed to be insignificant when the isotope is substituted. The authors have treated several sets of experimental data with their analysis, i.e. the best theoretical fit of a parabola to the k_H/k_D vs. ΔpK plot using a set of equations derived from their approach. Their

results support the view that a maximum isotope effect will be observed at $\Delta pK \approx 0$.

Unlike the Marcus approach which requires curvature in Bronsted plots to determine values of $\Delta G_o^{\neq}$, this approach can be used with linear Bronsted plots as long as the plot of k_H/k_D vs. ΔpK is experimentally accessible. The magnitude of $\Delta G_o^{\neq}$ is directly related to the width of the parabolic plot of k_H/k_D vs. ΔpK. Large values of $\Delta G_o^{\neq}$ imply broad curves, while small values involve sharp curves. This relationship between the rate of decrease of k_H/k_D with ΔpK and $\Delta G_o^{\neq}$ is also predicted by Marcus theory (CM68, F75).

Bunriche-Olsen and Ulstrup use the parameter E_s, which is the same as the λ parameter used by Cohen and Marcus (CM68) and Kreevoy and Oh (KO73). It is equal to $4\Delta G_o^{\neq}$ and is expressed in units of eV which can be converted to kcal mol^{-1} by means of the relationship 1 eV = 23.1 kcal mol^{-1}. The authors give an equation to determine $\Delta G_o^{\neq}$ from the coefficient of the squared term from the quadratic expression of a plot of log k vs. ΔpK using their treatment, eqs. [1.61] and [1.62].

$$\log k = A + B(\Delta pK) + C(\Delta pK)^2 \qquad [1.61]$$

$$\Delta G_o^{\neq} = E_s/4 = 2.3/16RTC \qquad [1.62]$$

Curiously, eq. [1.62] and eq. [1.50], which results from simple Marcus theory, differ only in sign and in the position of RT being in the denominator in eq. [1.62] and in the numerator in eq. [1.50]. As

the units on either side of eq. [1.62] do not balance there is obviously something amiss. One wonders if the two equations are equivalent.

$$\Delta G_o^{\neq} = -2.3RT/16C \qquad [1.50]$$

The results of Bell and Grainger from the enolization of 3-nitro-(+)-camphor are analyzed by Bunriche-Olsen and Ulstrup (BG76). The result of the best theoretical fit to the k_H/k_D vs. ΔpK plot gives a $\Delta G_o^{\neq}$ value of 1.5 kcal mol^{-1}. We have treated the quadratic expression from a plot of log k vs. ΔpK by the Marcus formalism, determining a $\Delta G_o^{\neq}$ value of 3.4 kcal mol^{-1}. The data of Bordwell and Boyle for the ionization of a group of nitroalkanes give a value of $\Delta G_o^{\neq}$ = 6.7 kcal mol^{-1} (BB75, F75). Bunriche-Olsen and Ulstrup determine a value of 4 kcal mol^{-1} for the same compounds.

The agreement between the two distinctly different treatments is not always this close, however. For example in the ionization of ethylnitroacetate, Cohen and Marcus determined a $\Delta G_o^{\neq}$ value of 13 kcal mol^{-1} from the Bronsted plot of Bell and Spencer (CM68, BS59). Bunriche-Olsen and Ulstrup derive a value of either 2.7 or 3.0 kcal mol^{-1} respectively depending on whether two pyridine bases are included or not.

Isotope effect maxima have also been observed when the proton transfer occurs between a normal acid and a normal base. This process, (proton transfer between oxygen or nitrogen) is generally very fast while that involving a pseudo acid e.g. $CH_3COCH\underline{H}COCF_3$ (proton transfer

from carbon), is generally much slower (E64). For example, the rate of protonation of the anions of acetic acid and the acid just mentioned differ by a factor of 7×10^7 as shown below (C75), even though the pK_{HA} values of both acids are practically the same.

$$CH_3CO_2^- + H^+ \xrightarrow{5 \times 10^{10}\ M^{-1}sec^{-1}} CH_3CO_2H \qquad pK = 4.76 \qquad [1.63]$$

$$CH_3\overset{-}{C}HCOCF_3 + H^+ \xrightarrow{7.5 \times 10^{2}\ M^{-1}sec^{-1}} CH_3COCH_2COCF_3 \quad pK = 4.70 \qquad [1.64]$$

Kresge and co-workers have reported an isotope effect maximum for such a reaction, as shown below (BC78).

$$ArC(O^-)HN^+H_2OCH_3 + HA \xrightarrow{slow} ArC(OH)HN^+H_2OCH_3 + A^- \qquad [1.65]$$

The maximum isotope effect occurs at $\Delta pK \approx 0$ and the Bronsted plot shows a sharp change in slope from $\alpha = 0$ to $\alpha = 1$ in the same region, as expected for a normal acid/base proton transfer (E64). The small size of the k_H/k_D maximum observed (≈ 3) suggests that the proton transfer never becomes fully rate determining.

Clearly, isotope effects are important in the study of proton transfer processes. While some experimental results give support to our concepts of the process, other results illustrate possible flaws therein.

Tunnel effects which were briefly mentioned earlier play a

definite role in isotope effects, though the magnitude of their contribution is a debatable subject. The term 'tunnel effect' is used "to describe the motion of particles across energy barriers which would be impossible according to classical mechanics but which is predicted by quantum theory" (B80). The probability of such non-classical penetration of the energy barrier increases with decreasing mass of the isotope involved; thus the proton is more prone to tunnelling than the deuteron thereby resulting in anomalously large k_H/k_D values. It has been suggested that tunnel effects undermine any expected correlation of Bronsted coefficients and isotope effects (BB71, L76). However, as tunnel effects overlay the 'classical' effect of isotopic substitution, correlations between primary isotope effects with both transition state structure and Bronsted coefficients do have a role in our understanding of the process involved. Detailed analyses of the tunnel effect are documented in literature (L75, KW85, S87).

1.9 CURVATURE IN BRONSTED PLOTS II

In 1977, Hupe and Wu studied the base catalyzed enolization of a ketone with 30 oxyanions eq. [1.66], (HW77). The authors used bases

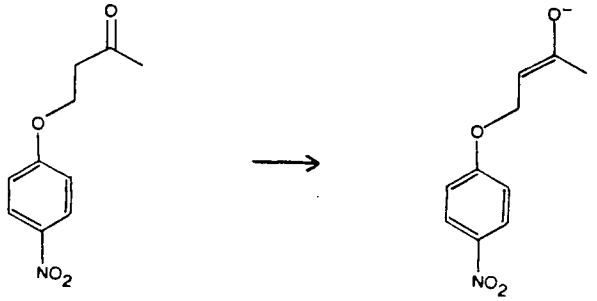

[1.66]

that vary in pK_{HA} from 4.76 (CH_3COO^-) to 16.0 ($CH_3CH_2O^-$), including hydroxide ion (pK = 15.75).

A distinctly curved Bronsted plot results. For bases of pK = 4.8 to 10.6, a β value of 0.75 is found, while above a pK of 10.6 β falls rapidly to a value of 0.3. The hydroxide ion fits onto the curve for oxygen bases of high pK. The application of Marcus theory gives a value of $\Delta G_o^{\neq}$ = 2.5 kcal mol^{-1} and W_r = 15.1 kcal mol^{-1}. The small intrinsic barrier and the large degree of curvature imply a rapidly changing transition state with changing catalyst pK, while the very large work term indicates the amount of energy needed to bring the reactants together. It may be recalled that similar results were obtained for other proton transfer reactions (Section 1.7.1).

The authors question such a small intrinsic barrier and conclude that "perturbation due to solvation of the bases" causes the Bronsted plot curvature. This effect, which is dependent only on the pK of the catalyst, causes a decrease in β for catalysts with high basicity. In 1984 Hupe and Pohl reported no significant correlation of k_H/k_D and pK in the same region where considerable curvature was present in the Bronsted plot (HP84). The authors suggest that the decreasing β value, while partly due to a large intrinsic barrier (10 kcal mol^{-1}), is mainly due to difficulty in desolvating the increasingly basic anions. The work term W_r, assumed to be a constant in Marcus theory, will increase as the solvation of the base increases.

Another example which illustrates the care needed in interpreting curved Bronsted plots comes from the work of Bernasconi and Bunnell (BB85). They studied the ionization of acetylacetone in various

DMSO-H_2O mixtures. Using just six carboxylate anions, the authors observed downward curvature in the Bronsted plot using DMSO-containing solvents. The degree of curvature increased as the content of DMSO present in the solvent mixture was increased. The curvature was attributed to the desolvation of the more basic/more solvated anions, and is therefore independent of the substrate studied. Bernasconi and Paschalis confirmed the effect by examining the ionization of another carbon acid, 1,3-indanone, and observing similar results (BP86).

Some chemists have questioned the validity of the Hammond postulate. Bordwell and Hughes drew attention to the difficulty of determining whether curvature, if present at all, is due to changes in ΔG^o or to factors such as solvation or steric and electronic effects (BH84). They conclude that "there is no compelling experimental evidence" that changing β values reflect changing ΔG^o values. Hence, they question the experimental evidence for the application of the Hammond postulate and the Leffler-Grunwald approach.

Other chemists have attempted to improve upon present concepts or to design new approaches. The use of energy surface diagrams based on two progress variables (e.g. degree of proton transfer and solvation) has been advanced by More O'Ferrall (M70, JJ77). This qualitative approach has been quantified by Grunwald (G85). Murdoch has illustrated the relationship between More O'Ferrall diagrams and Marcus rate theory (M83). Kurz has explained "anti-Hammond" behaviour, (reaction series in which the faster reactions have more product like transition states), in the context of Marcus rate theory (K83). Bernasconi has also directed his attention to this problem and developed the principle of

nonperfect synchronization (B87). Bernasconi defines an intrinsic rate constant, k_o, for the general reaction shown below so that $k_o = k_1 = k_{-1}$ when $\Delta G^o = 0$. Like the intrinsic barrier, k_o is representative of a whole reaction set and is independent of the thermodynamics of that set.

$$HA + B \underset{k_{-1}}{\overset{k_1}{\rightleftharpoons}} A^- + HB^+ \qquad [1.17]$$

Usually more than one concurrent process is involved in a reaction pathway. These processes may include bond formation/breakage, solvation/desolvation, resonance/loss of resonance, etc. and each may have made unequal progress at the transition state. In proton transfer reactions the concept of a "late" or "early" transition state is defined by the degree of bond formation or cleavage. The principle of nonperfect synchronization states that a product stabilizing factor that develops late or a reactant stabilizing factor that is lost early always lowers k_o. Conversely a product destabilizing factor that develops late or a reactant destabilizing factor that is lost early increases k_o. Thus in the two examples just discussed, solvation of the oxyanion bases, a reactant stabilizing factor, which is lost early (i.e. before proton transfer), decreases k_o causing negative deviations from the Bronsted plot, which is 'seen' as curvature. Bernasconi has developed this principle in a mathematical form (B87).

Clearly the Bronsted relation is important in helping us understand the proton transfer process. More recent developments, such as Marcus theory, are also important, although they require experimental

verification. This has been forthcoming over the past two decades, as have results that illustrate the weaknesses in our present concepts. This is progress, a little at a time. Jencks and co-workers expressed the reality of the situation in 1982; "structure-reactivity correlations provide one of the most powerful tools for probing the structure of transition states." Bronsted plot curvature "may represent a manifestation of an additional variable that affects the rate, rather than a change in transition state structure. It is important, therefore, to examine critically the reasons for nonlinear structure-reactivity correlations" (JB82).

1.10 CATALYSIS OF ENOLIZATION

Though Dawson and his co-workers and others had been studying the catalysis of acetone enolization since the early 1900's, much of the work was performed in a less than rigorous manner. One of the first definitive works on ketone enolization was published by Bell and Lidwell in 1940 (BL40). Certain aspects of this study will be discussed in detail.

The authors used a number of ketones and a number of catalysts. The enolization of the ketones was followed by measuring rates of iodination. The halogenation of the ketones in aqueous solution is first order in ketone and zero-order in halogen. The rate controlling step for the halogenation of the ketones is the conversion of the ketone to its enol form, which then reacts rapidly with halogen (LO4, ZH39).

Bell and Lidwell measured the rates of decrease of iodine concentration, equivalent to the rate of enolization, by titrating reaction samples with thiosulphate as the reaction proceeded. The rate of reaction is given by eq. [1.67], where k_{obs} is the sum of the catalytic terms, eq. [1.68].

$$\text{RATE} = -d[I_3^-]/dt = -d[\text{ketone}]/dt = k_{obs}[\text{ketone}] \qquad [1.67]$$

$$k_{obs} = k_{H_2O}[H_2O] + k_{H^+}[H_3O^+] + k_{^-OH}[^-OH] + k_{HA}[HA] + k_{A^-}[A^-] \qquad [1.68]$$

The catalytic terms include catalysis by the solvent, water, k_{H_2O} and by the carboxylic acid, HA and conjugate base, A^-. At a constant buffer ratio of the carboxylic acid and base, $n = {}^{[HA]}/_{[A^-]}$, the pH should be constant, i.e. $[H^+]$ and $[^-OH]$ are constant, for a series of varying buffer concentrations. A plot of k_{obs} vs. $[A^-]$ will be linear with slope $(k_{A^-} + nk_{HA})$ and intercept $(k_{H_2O}[H_2O] + k_{H^+}[H_3O^+] + k_{^-OH}[^-OH])$ eq. [1.69]. The combination of a number of such series at different n values leads to the determination of k_{HA} and k_{A^-}, eq. [1.70], by plotting the slope from eq. [1.69] vs. n, the buffer ratio. The slope of this line, eq. [1.70], is k_{HA} and the intercept is k_{A^-}.

$$k_{obs} = (k_{H_2O}[H_2O] + k_{H^+}[H_3O^+] + k_{^-OH}[^-OH]) + [A^-](k_{A^-} + nk_{HA}) \qquad [1.69]$$

$$\text{Slope from eq. [1.69]} = k_{A^-} + n\,k_{HA} \qquad [1.70]$$

In their study of acetone enolization, Bell and Lidwell used an acetone concentration of 0.27 M and an initial iodine concentration of between 1×10^{-3} M and 2×10^{-3} M. Under these conditions, the reaction is pseudo-zero-order in acetone. The ionic strength of each solution was adjusted to 0.11 M by the addition of sodium chloride, except in the case of monochloroacetate buffers, which will be discussed later. Ionic strength is defined by eq. [1.71], where C_i is the ion concentration and Z_i the charge of the ion (R81a). Only charged species e.g. Na^+, CH_3COO^- will contribute to the ionic strength.

$$\text{Ionic Strength } I = {}^1/_2 \sum C_i Z_i^2 \qquad [1.71]$$

The results of Bell and Lidwell for acetone enolization are given in Table 1. It can be seen that the strongest acid ($ClCH_2CO_2H$) is the best catalyst for acetone enolization, while its conjugate base ($ClCH_2COO^-$) is the worst catalyst. The statistically corrected Bronsted plots of the acid and base catalysis are shown in Fig. 8. A least-square linear correlation of the data for the acids and bases gives eq. [1.71] and [1.72] respectively, where r is the correlation coefficient, and p and q have values of 1 and 2 respectively.

Acid Catalysis $\log (k_{HA}/p) = -4.46 - 0.57 (pK + \log p/q)$ [1.71]
r = 0.9995

Base Catalysis $\log (k_{A^-}/q) = -10.9 + 0.88 (pK + \log p/q)$ [1.72]
r = 0.9997

Table 1: Data of Bell and Lidwell for acetone enolization catalyzed by acids (HA) and bases (A^-) at 25°C. Data from Ref. (BL40).

Acid	$10^7\ k_{HA}\ M^{-1}\ sec^{-1}$	Base	$10^7\ k_{A^-}\ M^{-1}\ sec^{-1}$	pK_{HA}
$ClCH_2CO_2H$	12.7	$ClCH_2CO_2^-$	0.050	2.86
$HOCH_2CO_2H$	3.25	$HOCH_2CO_2^-$	0.383	3.83
CH_3CO_2H	1.02	$CH_3CO_2^-$	2.43	4.76
$(CH_3)_3CCO_2H$	0.73	$(CH_3)_3CCO_2^-$	4.08	5.03

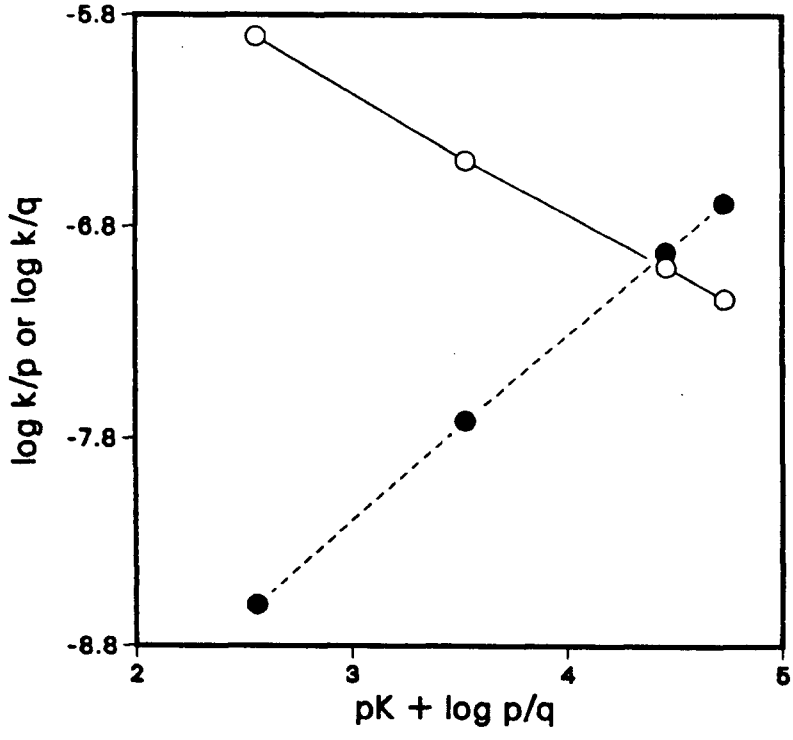

Fig. 8: Bronsted plot for acetone enolization catalyzed by acids (open circles, solid line) and bases (closed circles, dashed line). Data from Table 1, ref. (BL40).

The coefficients for the acid and base catalysis are 0.57 (α) and 0.88 (β), respectively. The authors report an α value of 0.55 using pK values of 2.86, 3.81, 4.76 and 5.04 for the four acids. The pK values used in Table 1 and Fig. 9 and indeed throughout this thesis, unless otherwise stated, are from the tabulations of Kortum and co-workers (KV61) and Serjeant and Dempsey (SD79). A least-squares linear regression using the authors' pK values gives an α value of 0.57, not 0.55 as reported.

In the case of chloroacetate buffers, Bell and Lidwell had to overcome two problems. Firstly, since k_{HA} is approximately 250 times greater than k_{A^-}, the anion will only make a meaningful contribution to the observed rate if the buffer ratios heavily favour the anion. Secondly, at the pH of such buffer solutions the contribution to the total rate from the hydronium ion was rather large and so large concentrations of buffer were needed, leading to an ionic strength of 0.2 M.

The authors also determined rate constants of hydroxide (0.25 M^{-1} sec^{-1}) and water ($8.33 \cdot 10^{-12}$ M^{-1} sec^{-1}) for acetone enolization. The rate constant of the hydronium ion ($2.73 \cdot 10^{-5}$ M^{-1} sec^{-1}) is given by the measurements of Dawson and Powis (DP13). The conventional pK values for hydroxide and hydronium ion are 15.74 and −1.74 respectively derived from a value of 55.5 M for $[H_2O]$ (B73e). Substitution of the value for pK of H_3O^+ and ^-OH into eq. [1.71] and [1.72], respectively, affords us calculated values of $k_{H_3O^+}$ and k_{-OH}. As was mentioned earlier, while p = 3 for H_3O^+ there is some disagreement about whether to use q = 2 or q = 1 for H_3O^+. For ^-OH p = 2 but q could be 1 or 3 depending on how one counts the number of basic sites in the ion. The calculated values for

H_3O^+ and ^-OH are given in Table 2 along with the ratio of calculated rate constants (k_{calc}) to observed rate constants (k_{expt}).

Table 2: Calculated rate constants for H_3O^+ and ^-OH from eqs. [1.71] and [1.72] and ratios k_{calc}/k_{expt}

Catalyst	p	q	k_{calc} M^{-1} sec^{-1}	k_{calc}/k_{expt}
^-OH	2	1	$1.80 \cdot 10^3$	7×10^3
	3	3	$2.06 \cdot 10^3$	8×10^3
H_3O^+	3	1	$5.71 \cdot 10^{-4}$	21
	3	2	$8.48 \cdot 10^{-4}$	31

The choice of p and q values does not affect the conclusion that hydroxide ion and hydronium ion are much less effective as catalysts than is expected on the basis of the Bronsted relationship for the other four catalysts.

In most cases, acid and base catalysis of ketone enolization occurs at the same time. The two types of catalyses will be discussed separately.

1.10.1. Base Catalyzed Enolization

(a) Curvature

Bell and Lidwell determined β values for carboxylate ion catalyzed enolization of a number of acetone derivatives, as well as acetone. The Bronsted correlation for each derivative was linear and the β values obtained (acetone, 0.88; chloroacetone, 0.82; dichloroacetone, 0.82) suggest that the proton is more than half transferred in the transition state. In terms of the Hammond postulate, the transition state resembles products. A trend which was obvious to Bell and Lidwell, and which further research supported, linked decreasing β values with increasing substrate reactivity (B73f). Bell compiled a mass of data for the reaction shown in eq. [1.17] where HA is a ketone, an ester or a ketoester and B is any base, including carboxylate ions, phenolate ions and pyridines (B73f).

$$HA + B \longrightarrow A^- + BH^+ \qquad [1.17]$$

A plot of log k vs. log (K_{HA}/K_{BH^+}) with appropriate statistical correlations gave a curve, representing the decrease that occurs in the β value with increasing reaction rate and increasing exothermicity. This trend is predicted by the Hammond, Leffler-Grunwald and Marcus treatments. Many authors have quoted this example in illustrating the relationship between the free energy of activation $\Delta G^{\neq}$ and the free energy of reaction ΔG^{o}. Others have suggested a different explanation

i.e. separating the data for the monocarbonyls from that of the dicarbonyls leads to two distinct linear correlations, the slope of the dicarbonyl set being less than that of the monocarbonyl set (KC73, BH85).

Hupe and Wu have fitted a line for the curved plot with $\Delta G_o^{\neq}$ = 10 kcal mol^{-1} and W_r = 4 kcal mol^{-1} by using the Marcus treatment, eq. [1.30] (HW77). This large intrinsic barrier implies a very gradually changing transition state structure. This analysis of Bell's data by using eq. [1.30] reveals a weakness; the carbon acid substrate HA has been varied, negating the assumption used in the equation's derivation that $\Delta G_o^{\neq}$ is a constant. These same authors illustrate elegantly how solvation causes downward curvature in a base catalyzed enolization, as discussed previously (Section 1.9).

The base catalyzed enolization of acetylacetone was studied by Ahrens and co-workers (AE70). The data was fitted to eq. [1.30] by Kreevoy and Oh with the inclusion of hydroxide ion and water giving a low intrinsic barrier (3.3 kcal mol^{-1}) and a large work term (10.5 kcal mol^{-1}) (KO73). The inclusion of hydroxide and water, (catalysts which deviate markedly from Bronsted plots, Section 1.10), is the cause of a sharply curving line giving rise to a small intrinsic barrier. Of course such a treatment is pointless, and without the two "curve-causing" catalytic constants and two bifunctional monoanions, a reasonably linear Bronsted plot is evident, with a β value of 0.58 (obtained by including five carboxylate bases and four phenoxide bases).

The study by Bell and Grainger of the enolization of 3-nitro-(+)-camphor catalyzed by six carboxylate bases (including one dianion) and

monohydrogen phosphate dianion is of special interest as it combines the Bronsted plot with primary isotope effects (see also Section 1.8). The isotope effect is at a maximum at $\Delta pK \approx 0$, while the Bronsted plot shows concave curvature, curvature which relies predominantly on the presence of the two dianions. As was mentioned previously, the k_H/k_D vs ΔpK plot has been used to determine an intrinsic barrier of 1.5 kcal mol^{-1} (BU79, see p. 32). The use of the Marcus equation involves fitting the log (k/q) vs. ΔpK plot to a quadratic expression in ΔpK and this gives the result shown.

$$\log (k/q) = 0.67 - 0.39\ \Delta pK - 0.025\ (\Delta pK)^2 \qquad [1.73]$$

The correlation coefficient (0.9955) is better than that obtained from a linear correlation of log (k/q) to ΔpK (0.9844). The coefficient of the squared term (0.025 ± 0.008) can be used to give an intrinsic barrier of 3.4 ± 1.1 kcal mol^{-1}. The inclusion of bases of different types is a weakness, and as the five carboxylate monoanions give a good linear Bronsted line ($\beta = 0.45$, $r = 0.9970$), we could consider the two dianions to be deviating from this line. This example illustrates the care necessary in interpreting curvature in Bronsted plots, and the caution that should be exercised in comparing different types of catalyst. Having said that, the curvature present in the Bronsted plot for 3-nitro-(+)-camphor enolization could be due in whole or in part to a change in $\Delta G^{\neq}$ with respect to ΔG^{o}. Some indication of the validity of including dianions with monoanions in Bronsted correlations is needed before a more definitive conclusion is evident.

The results of Hupe and co-workers and those of Bernasconi and co-workers (Section 1.9) show the relevance of solvation in enolization and other proton transfer reactions, another factor which must be considered in any enolization study.

(b) Isotope Effects

Primary kinetic isotope effects corresponding to k_H/k_D ratios for base-catalyzed enolization of acetone and acetone-d_6 were first reported in 1939, only seven years after the discovery of deuterium (RK39). The base studied was acetate ion and a k_H/k_D ratio of 7 resulted. The use of hydroxide ion as base provided values of 10.2 (B59), 7.5 (P59) and 9.2 (J65). These values are all close to or above the theoretically expected maximum k_H/k_D of 6.9 (which comes from considering the zero-point energies of C-H and C-D bonds) and shows that the carbon hydrogen bond is broken in the rate controlling step.

Jones obtained values of the isotope effect of hydroxide ion as the base at several temperatures; a decrease in k_H/k_D with increasing temperature was observed (J65). The decrease resulted from vibrational energy differences between C-H and C-D decreasing as the temperature rises, the k_H/k_D values being 13.5 at 1°C, 9.8 at 25°C and 7.9 at 43°C.

In 1967, Jones varied the structure of the ketone using hydroxide ion as the base and examined k_H/k_T isotope effects (JM67). The ketones studied were all substituted acetophenones and the isotope effects varied from 12.1 (4-nitroacetophenone) to 18.2 (4-methoxyacetophenone).

A study involving variation of the base with one ketone substrate was reported in 1976 (BG76). Bell and Grainger examined the bromination of 3-nitro-(+)-camphor and 3-deuterio-3-nitro-(+)-camphor as was mentioned previously (Section 1.8). A maximum isotope effect, k_H/k_D = 7.5, was observed at $\Delta pK \approx 0$.

A similar result was reported earlier in the hydroxide ion catalyzed enolization of (-)-menthone (BC70). Bell and Cox used water-dimethyl sulfoxide (DMSO) solvent mixtures and found that k_H/k_D reached a maximum value (6.5), in the solvent mixtures containing 30-40 mole % DMSO. Acidity function values for hydroxide ion in aqueous DMSO suggest that pK_{H_2O} becomes roughly equal to the pK of the substrate, (-)-menthone, in 30-40 mole % DMSO.

The results are in agreement with the concepts discussed previously (Section 1.8).

1.10.2 Acid Catalyzed Enolization

(a) Mechanism

The general acid catalyzed mechanism of ketone enolization is shown in eq. [1.10] for acetone, and is credited to Pedersen (P34).

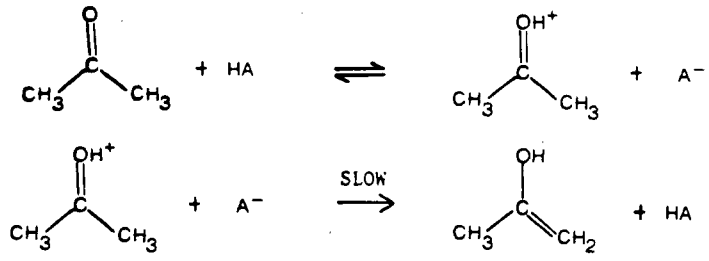

[1.10a]

[1.10b]

The observed rate for the reaction is given by eq. [1.74]. Substituting for $[ZH^+]$ with $([Z][H^+]/K_{ZH^+})$, and for $[A^-]$ with $(K_{HA}[HA]/[H^+])$ leads to eq. [1.75].

$$k_{obs} = k'_A [ZH^+][A^-] \qquad [1.74]$$

$$k_{obs} = (k'_A K_{HA}/K_{ZH^+})[Z][HA] = k_{HA}[Z][HA] \qquad [1.75]$$

Linear Bronsted relationships were found for acetone and cyclohexanone, giving α values of 0.57 and 0.74, respectively (BL40, LW69). These values are related to the β values for proton abstraction by eq. [1.10b], $\beta = 1 - \alpha$. Thus β is 0.43 for protonated acetone and 0.26 for protonated cyclohexanone), suggesting transition states in which the proton is less than half-transferred.

Evidence supporting the mechanism described was accumulated by many workers over the years. The magnitude of primary isotope effects measured for the general acid catalyzed enolization showed that the rate determining step involved breaking of the C–H bond (RK39, SS58). The absence of any solvent isotope effects (using H_2O and D_2O) for catalysis by the general acid suggests that proton abstraction by the solvent does not occur (SD58).

Lienhard and Wang compared the mechanism for the hydrolysis of enol ethers, which involves rate determining proton transfer to the β-carbon of the enol ether eq. [1.76], with the reverse of eq. [1.10b], ketonization (LW69).

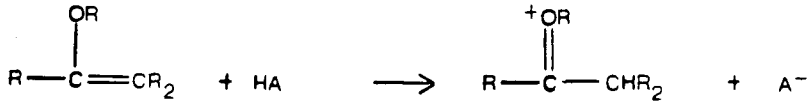

[1.76]

[1.10b]

Similar rates and α values are found for the two processes. The agreement between solvent isotope effects for enol ketonization and enol ether hydrolysis further supports the accepted mechanism (TD74).

The value of k_H/k_D for hydronium ion catalyzed enolization of acetone reported by Reitz in 1939, 5.0, was determined by using acetone-d_6 of only 92% isotopic purity (RK39). Values of 6.5 (HK72) and 6.7 (TD74) have since been reported, values that are close to the theoretical maximum value and thus correspond to half transfer of the proton.

For hydronium ion catalyzed enolization evidence has accumulated that suggests that the transition state contains molecules of water (T82). The decrease in enolization rates at very strong acid concentrations (CS79), the large negative entropy of activation (-16.5 cal mol^{-1} K^{-1} for acetone, DT73), and the large negative volume of activation (-2.1 cm^3 mol^{-1} for acetone, BW64) are all consistent with such a transition state.

(b) Proton Activating Factor

We can determine the rate constant for proton abstraction from the protonated ketone by a general base, k'_{A^-}, knowing k_{HA}, K_{ZH^+} and K_{HA}, eq. [1.77].

$$k'_{A^-} = (k_{HA}\, K_{ZH^+}/K_{HA}) \qquad [1.77]$$

This rate constant can be compared with the rate constant for proton abstraction from the unprotonated ketone by a general base, k_{A^-}, eq. [1.78].

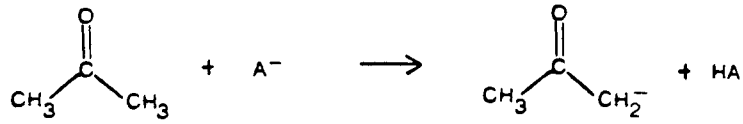

[1.78]

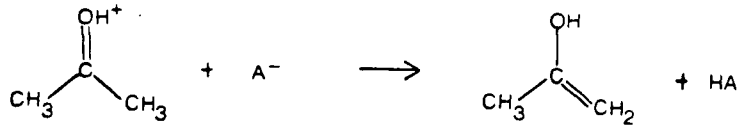

[1.10b]

The ratio of rate constants (k'_{A^-}/k_{A^-}) has been called the proton activating factor (paf) and was introduced by Stewart and Srinivasan (SS78). Using a pK_{ZH^+} of -2.9 for acetone, paf values of 3×10^7 and 2×10^7 for water and acetate bases respectively were calculated (S85d).

With carboxylates as bases, β = 0.43 (i.e. 1 - 0.57) for eq. [1.10b], and 0.88 for eq. [1.78]. The small β value in the case of eq. [1.10b] reflects the earlier transition state resulting from protonation

of the acetone. This increase in reactivity of the substrate is measured by the paf and is quite large for the deprotonation of ketones.

1.10.3 Third Order Term

The observed rate law used by Bell and Lidwell (BL40) for the general acid and base catalyzed enolization of acetone with acetate buffers, for example, is represented by eq. [1.79] where k_{sum} includes the solvent, hydronium ion and hydroxide ion contributions ($k_{H_2O}[H_2O]$ + $k_{H^+}[H_3O^+]$ + $k_{^-OH}[^-OH]$.

$$k_{obs} = k_{CH_3COOH}[CH_3COOH] + k_{CH_3COO^-}[CH_3COO^-] + k_{sum} \qquad [1.79]$$

As the reaction is subject to both acid and base catalysis, there exists the possibility for simultaneous involvement of acid and base with the substrate. The possibility of such catalysis was first sugested in 1925 (LF25) and in 1930 a third-order term involving both CH_3COOH and CH_3COO^- was detected in acetate buffers (DS30).

The presence of this term has been confirmed no fewer than three times since then (BJ53, HJ75a, AG82). The mechanism of such a process is shown below (S85e). The amount that such a concerted process contributes to the observed rate is small and indeed large concentrations of buffer are necessary (0.4 M) in order to observe the third order term in the rate expression.

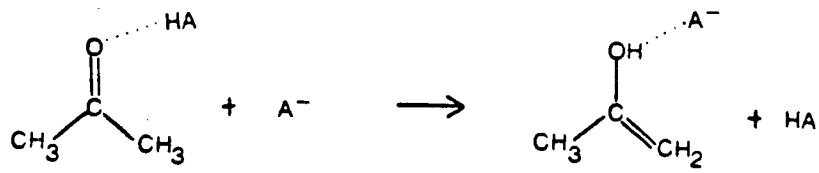

[1.80]

Hegarty and Jencks examined the third order term in acetone enolization at an ionic strength of 2 M; they used seven carboxylate buffers and determined a β value of 0.15 (HJ75a). The smallness of the slope reflects the cancelling of effects in going from strong acids/weak conjugate bases (e.g. $ClCH_2COOH$, $ClCH_2COO^-$) to weaker acids/stronger conjugate bases (e.g. CH_3COOH, CH_3COO^-). Using acetone and acetone-d_6, the authors determined a value of 5.8 for a primary isotope effect using acetate buffers. This suggests a considerable degree of C — H bond breaking in the transition state. A rather large solvent isotope effect (H_2O/D_2O) of 2.0 indicates the involvement of the carboxylic acid proton in the transition state.

The authors suggest that the two proton transfers in the reaction are simultaneous. Recent work with H_2O-D_2O mixtures supports such a push-pull mechanism (AG82).

The presence or absence of the third-order term, $k_{A^-.HA}[A^-][HA]$, will be obvious from the kinetic results at different buffer ratios. At a given buffer ratio n ($[HA]/[A^-]$) a plot of k_{obs} vs [HA] or $[A^-]$ will be linear if the third-order term is insignificant (Section 1.10). Upward curvature in such a plot, on the other hand, could be an indication of the presence of the third-order term in the rate law (HJ75b). If this is the case eq. [1.81] can be transformed to eq. [1.82].

$$k_{obs} = k_{HA}[HA] + k_{A^-}[A^-] + k_{A^-.HA}[A^-][HA] + k_{sum} \qquad [1.81]$$

$$k_{obs} - k_{sum} = k_{HA}n[A^-] + k_{A^-}[A^-] + k_{A^-.HA}n[A^-]^2 \qquad [1.82]$$

Rewriting eq. [1.82] as eq. [1.83] gives a linear relationship between the left-hand side of eq. [1.83] and $[A^-]$, with slope $k_{A^-.HA}n$ and intercept $(k_{HA}n + k_{A^-})$.

$$1/[A^-] (k_{obs} - k_{sum}) = k_{HA}n + k_{A^-} + k_{A^-.HA}n[A^-] \qquad [1.83]$$

Thus, $k_{A^-.HA}$ can be determined; when a number of such intercepts for different buffer ratios are plotted against n, k_{HA} (slope) and k_{A^-} (intercept) are obtained (BW66).

1.11 BIFUNCTIONAL CATALYSIS

The third-order term in acetone enolization involves simultaneous proton donation by one catalyst (HA) and proton acceptance by another catalyst (A^-). It has been called bifunctional catalysis (HJ75a) but it is important to distinguish it from simultaneous proton donation and proton acceptance by a bifunctional catalyst containing both acidic and basic groups. It is preferable to restrict the use of the term 'bifunctional catalysis' to the latter definition and use the more self-explanatory 'third-order term' for acetone enolization that involves acid, base and acetone reacting simultaneously.

One of the earliest reported examples of bifunctional catalysis is the epimerization of tetramethylglucose in benzene catalyzed by 2-pyridinone (SB52, EB83). The simultaneous transfer of two protons in a proton transfer reaction holds a special interest for chemists, especially as it relates to enzyme catalysis (J69).

Cox and Jencks have reported bifunctional catalysis in the general acid and general base catalyzed reaction of methoxyamine with phenylacetate (CJ81a, CJ81b).

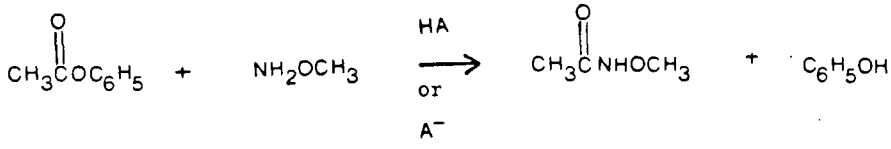

[1.84]

For the strong acids (pK $\leq$ 2) the rate limiting step involves nucleophilic attack by the amine on the carbonyl group assisted by a molecule of general acid, HA. As the acid becomes weaker, the rate limiting step becomes the protonation of the oxygen anion by the acid, eq. [1.85]. A curved Bronsted plot results from this change in rate determining step.

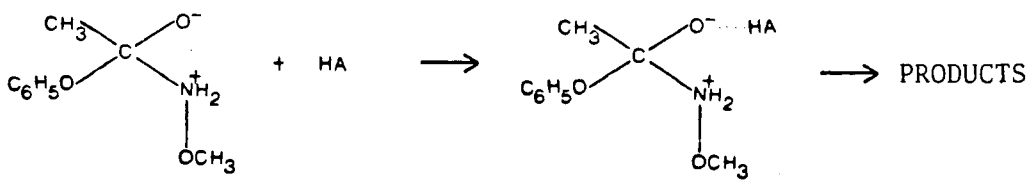

[1.85]

With the monoanions of certain diacids (e.g. $Cl_3CPO_3H^-$, $OP(OH)_2O^-$ and $O_2C(OH)O^-$), rate accelerations up to 10^3 times that expected were observed. This rate acceleration was credited to concerted protonation of the oxygen anion and deprotonation of the nitrogen cation eq. [1.86].

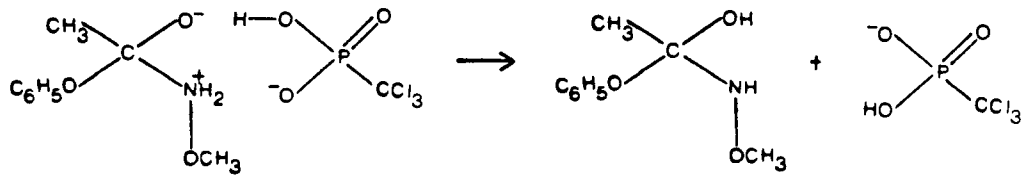

[1.86]

The ability to form eight membered rings in the transition state is a common feature of bifunctional catalysis (S85f).

Lienhard and Andersen examined three reactions, including the enolization of acetone, in searching for bifunctional catalysis by the monoanions of dicarboxylic acids (LA67). Such concerted general acid - general base catalysis would operate as shown below.

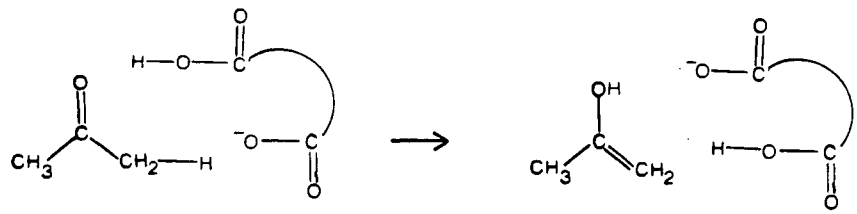

[1.87]

The authors used various buffer ratios and by an analogous treatment to that discussed previously (Section 1.10) they measured the rate constants for the monoanion k_{HA^-} and the dianion $k_{A^{2-}}$. In the absence of bifunctional catalysis the authors expected to find rate constants that were close to the sum of the rate constants for the acid and base portions of the monoanions. These two contributions were calculated on the basis of the Bronsted plots for monocarboxylic acids and bases (BL40). The contribution of the monoanion as an acid, k_{acid}, can be calculated from eq. [1.88] knowing the second equilibrium constant of the diacid, K_2. The contribution of the monoanion as a base k_{base} can

be calculated from eq. [1.89], knowing the first equilibrium constant of the diacid, K_1.

$$\log k_{acid} = 0.55 \log (2K_2) - 4.40 \qquad [1.88]$$

$$\log k_{base} = -0.88 \log (K_1/2) - 10.82 \qquad [1.89]$$

In this regard it may be noted that footnote C of table III in ref. (LA67) has an error, 'k_A =' and 'k_B =' should read 'log k_A =' and 'log k_B =' respectively. The results of their calculations are shown in Table 3.

Table 3: Data of Lienhard and Anderson for acetone enolization catalyzed by monoanions, k_{HA}-(obs) and calculated values k_{HA}-(calcd) (see text). Data from ref. (LA67).

Catalyst	10^8 k_{HA}-(obs) M^{-1} sec^{-1}	10^8 k_{HA}-(calcd) M^{-1} sec^{-1}
Oxalate monoanion	7.83	28.8
Succinate monoanion	12.5	5.83
1,1-cyclobutane-dicarboxylate monoanion	23.3	29.3

The authors concluded from these results that the monoanions studied are not "unusually effective catalysts" for the enolization of acetone. They found the same result for the mutarotation of glucose and the hydration of acetaldehyde.

A study by Spaulding and co-workers of other potential bifunctional catalysts of acetone enolization gave the same result (SS77). These authors examined the effectiveness of the phosphate dianion, $OP(OH)O_2^{2-}$ and the arsenate dianion, $OAs(OH)O_2^{2-}$, and found no noticeable rate acceleration attributable to bifunctional catalysis.

These results lead to a question left unanswered by both groups of authors. If these catalysts containing both acidic and basic functionalities are not acting as bifunctional catalysts, are they acting then as general acids or as general bases?

1.12 STERIC EFFECTS

1.12.1 General Base Catalysis

An extensive study of general base catalyzed enolization of several ketones was reported by Feather and Gold in 1965 (FG65). They studied the effectivenesss of a number of alkyl pyridines as catalysts, observing no acid catalysis by pyridinium ions. While a linear Bronsted plot was determined for acetone with 3-,4- and 5-substituted pyridines (β = 0.7), 2-substituted pyridines deviated from this line. The 2,6-substituted pyridines produced still larger deviations. This retardation of

rate constants was also evident in the enolization of other ketones. The magnitude of the deviations increased along the ketone series from acetone (CH_3R, R = $COCH_3$) to isopropylmethyl ketone ($(CH_3)_2CHR$) to pinacolone ($(CH_3)_3CR$).

The use of pyridine bases in the dedeuteration of 2-deuterio-isobutyraldehyde gave the same result (HH65). Unhindered pyridine bases produced a good Bronsted line (β = 0.5), while the 2- and 6-alkyl pyridines deviated from that line. Once again the deviation is greater for the 2,6-substituted pyridines than for the 2-substituted pyridines. The use of meta and para phenolate anions produced a Bronsted line practically coinciding with that for the pyridines and having the same slope. The two ortho-phenolates studied (chloro and methyl) fit on the line. The absence of steric effects in the phenoxides was attributed to the effect of moving the basic atom one atom away from the ring.

Other examples of such rate retardation in general base catalysis due to alkyl pyridines include the mutarotation of glucose (CW63) as well as the ionization of glyceraldehyde, dihydroxyacetone (GR67) and 2-nitropropane (BG66). Recent examples are the hydrolysis of phenylacetates (N87) and the deprotonation of 1,2,3-trimethylpyrazinium ions (NL86).

The use of 2-alkyl anilines in the latter example also leads to steric deactivating effects relative to the Bronsted line for the unhindered anilines. The degree of deviation is less than that observed for the hindered pyridines, probably reflecting the effect of moving the basic atom away from the ring.

In the base catalyzed ionization of 2-nitropropane, 2,6-dimethyl-

pyridine gave a primary kinetic isotope effect of 19 (BG66). Studies in aqueous alcohol yielded values of k_H/k_D = 10 for pyridine, while for 2,4-dimethyl, 2,6-dimethyl and 2,4,6-trimethylpyridine k_H/k_D values of 15, 24 and 24 respectively were observed (LF67). The relation between steric hindrance and increased kinetic isotope effects has been discussed by Calman and co-workers (CC69) and by Lewis (L75). The effect is attributed to tunnelling in the case of protium compounds. A recent example of steric hindrance and tunnelling involves proton transfer from a phenylnitromethane to substituted phenylguanidines (P87).

Steric effects in the opposite direction i.e. rate accelerations were reported by Bell and co-workers for base catalyzed halogenations of ketones and esters (BG49). Using a variety of carbonyl compounds (bromoacetylacetone, benzoylacetone, acetylacetone, ethyl acetoacetate, ethyl α-bromoacetoacetate and diethyl bromomalonate) and a range of base catalysts (twelve or more, ranging in pK from 2.86 to 5.03), a series of Bronsted lines were determined. Catalysts containing large groups e.g. $CH_3CH(C_6H_5)CO_2^-$ are more effective than is expected on the basis of a Bronsted line defined by $CH_3CO_2^-$, $HOCH_2CO_2^-$ and $ClCH_2CO_2^-$. This rate acceleration is more pronounced for the substrate ketones containing large groups e.g. bromoacetylacetone. The authors attribute such deviations to "the proximity of a large group in the catalyst to a similar group in the substrate, which will affect the transition state of the reaction, but not contribute anything to the dissociation constant" of the catalyst.

Another proton transfer reaction exhibiting such steric rate acceleration is the base catalyzed exchange of the methylene protons in

1,3-dimethyl-2-iminoimidazolin-4-one hydroiodide, eq. [1.90] (SS76a). A Bronsted line was determined for 47 bases which included aliphatic monocarboxylates, meta- and para-substituted benzoates and pyridines (β = 0.79). Enhanced catalytic activity was exhibited by 12 ortho-substituted benzoates, the deviation showing some correlation with substituent size.

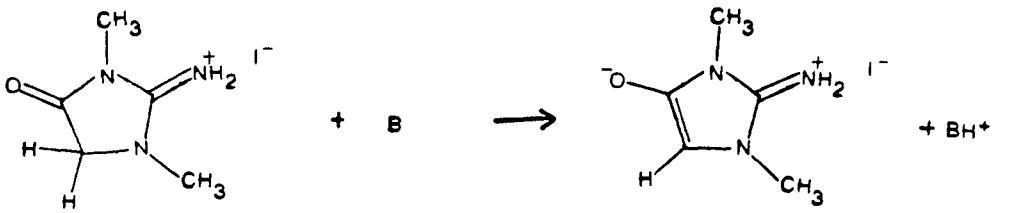

[1.90]

The authors consider first the effect on the equilibrium basicity of benzoates of ortho substituents i.e. ortho benzoates being weaker bases than their meta and para counterparts. This effect had been attributed to steric hindrance to resonance between the carbonyl group and the benzene ring in the neutral acid molecule (E69). Another explanation for the effect involves hindrance to solvation of the neutral molecule (SS67). Thus, in the proton loss from the substrate, catalyzed by ortho-benzoates, the "incipient acid molecule partly formed in the transition state must be subject to steric hindrance to resonance (or solvation) to a considerably smaller extent than the fully formed acid molecule."

Steric compression in transition states (e.g. base catalysis by 2-alkyl pyridines) has been linked to increased isotope effects caused by proton-tunelling (p. 60). The absence of steric compression in this transition state is reflected in the isotope effects for the ortho-

benzoates. These effects are lower than those observed for monocarboxylate and meta- and para-benzoates of similar basicity (SS76b).

Similar rate accelerations for ortho-benzoates were observed in the deprotonation rates of 1,2,3-trimethylpyrazinium ion, eq. [1.91] (NL85). As was discussed previously, pyridines (and to a lesser extent anilines) show conventional steric effects in this reaction i.e. rate decelerations.

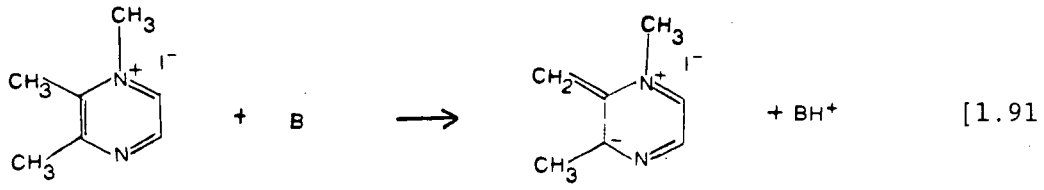

[1.91]

The effect of varying the location of the alkyl groups in the substrate in eq. [1.91] has also been studied (LS86). Using a single base ($^-$OD), the authors discover that adjacent alkyl groups activate the methyl group towards proton transfer. This example of steric rate acceleration is indeed remarkable when one considers the deactivating polar effect of the adjacent alkyl groups.

Another example of a sterically hindered substrate showing steric acceleration is that of the enolization of 2,4,6-trimethylacetophenone, which reacts faster than acetophenone under comparable conditions by a factor of 10^3 (PG84).

1.12.2 General Acid Catalysis

A report of steric hindrance in acid catalysis involves the inversion of menthone (CW63). The use of 2-methyl or 2,6-dimethylpyridinium ion leads to rate decelerations by factors of 2 and 30 respectively from the Bronsted relationship for pyridinium ion and its 3- and 4-methyl derivatives.

Pyridinium ion catalysis is often undetectable in the presence of pyridine base ($k_B >>> k_{BH^+}$) for those reactions subject to both general acid and general base catalysis.

As in general base catalysis, there are examples of steric acceleration in general acid catalysis. One of the cases discussed in base catalysis involved pyrazine derivatives and the exchange of their activated methyl protons (LS86). This exchange is also catalyzed by D_3O^+ and CF_3CO_2D and activation by adjacent methyl groups is observed here also.

The hydrolysis of cyanoketenedimethylacetal is subject to general acid catalysis, $\alpha = 0.62$, eq. [1.92] (GW68). The effectiveness of

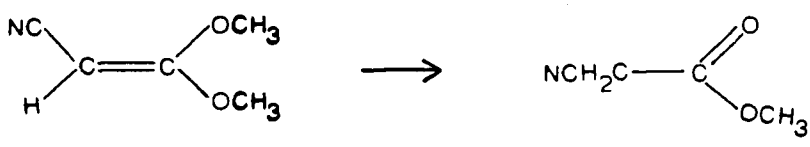

[1.92]

pivalic acid (trimethylacetic acid) is greater than expected on the basis of the Bronsted line defined by all nine carboxylic acids by a

factor of 1.2. Formic acid on the other hand, deviates negatively from the Bronsted line by a factor of 1.6.

Deviations of this type, though small, were consistently observed in a study involving five ketene acetals (KS83). While formic and cyanoacetic acid were below the Bronsted line in each case, chloroacetic and methoxyacetic acid were consistently above the lines. These authors suggest that the interaction of bulky catalysts and substrate must lower the free energy of the hydrolysis transition state.

The effect of introducing bulk into the substrate is shown by the acid catalyzed enolization of cyclohexanone as compared to acetone (LW69). In the acid catalyzed enolization of acetone, pivalic acid showed no steric effects when compared to acetic, glycolic and chloroacetic acid (BL40). With cyclohexanone as the substrate, pivalic acid is more effective as a catalyst by a factor of 3 than is predicted from the Bronsted plot for the other carboxylic acids. This effect is also present in the hydrolysis of 1-methoxycyclohexanone. The authors attribute the effect to stabilization of the transition state by hydrophobic bonding.

Obviously the role of steric effects in proton transfer reactions is not straightforward, as both rate acceleration and retardation have been observed in different situations.

2. SCOPE OF THE INVESTIGATION

The aim of this investigation is to examine a number of effects in general acid and general base catalysis. The reaction that has been chosen for study is the enolization of ketones, in particular, acetone, a substance that has come to be regarded as the prototypical carbonyl compound.

We were specifically interested in the following matters.

1. The effect of changing the acid catalyst from a monoprotic acid to a diprotic acid and conversely the effect of changing the base from a monoanion to a dianion. By using a variety of monocarboxylic acids RCOOH and dicarboxylic acids $R(COOH)_2$ as well as a group of phosphonic acids RPO_3H_2, these effects could be evaluated.
2. Whether or not monoanions of diacids act as bifunctional catalysts, and if they do not, whether they act as general acids or general bases.
3. The effect of steric bulk in the catalyst; i.e. does it cause rate acceleration, deceleration or no change from that expected on the basis of the Bronsted line for sterically unhindered catalysts. Previously quoted literature examples have shown all three effects.
4. Whether curvature in the acid and base Bronsted plots for acetone enolization can be observed over a wide span of catalyst pK values.

3. RESULTS

The results presented here cover a range of catalysts divided into two broad types; carboxylic acids and carboxylate bases, and phenylphosphonic acids and phenylphosphonate bases. These results are discussed in Chapter 4, which also includes results of further experimentation, results that were needed to help answer some of the questions arising from analysis and discussion of these data. Full experimental details of all the work included in this thesis are in Chapter 5.

The method of choice for measuring the rates of enolization of acetone is to measure the rates of iodination of the enol or enolate anion with a spectrophotometric technique, eq. [3.1].

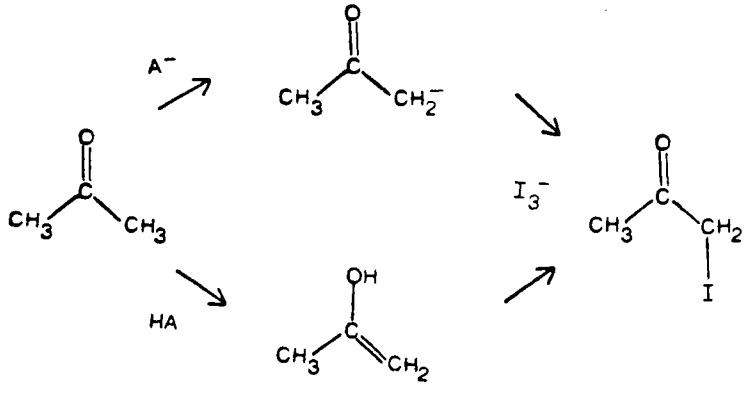

[3.1]

Using pseudo first-order kinetics (as had been done by previous workers in this area, BL40, LW69, SS77, WM78) the decrease in the absorbance of the triiodide ion (I_3^-) at a particular wavelength can be related to the rate of enolization as follows: the rate of disappearance of I_3^- can be determined from the linear plot of absorbance against time. Of course this plot is linear since the reaction is zero-order in

triiodide ion, because the concentration of acetone used (0.1 to 0.5 M) greatly exceeds that of triiodide (4×10^{-5} to 5×10^{-4} M). For example, suppose the reaction was set up so that the initial concentrations of acetone and triiodide were 0.1 M and 5×10^{-4} M respectively. Following the reaction till the concentration of triiodide has decreased to 1×10^{-4} M will decrease the acetone concentration from 0.1 M to 0.0996 M, or 0.4%. Experimentally, the reaction will show first-order kinetics (in acetone) with a rate constant k_{obs} (units of sec^{-1}). The system is said to follow pseudo first-order kinetics to call attention to the fact that the behaviour is first-order only under certain conditions. The linear plot of absorbance against time (in seconds) is related to the rate of reaction by eq. [3.2] where S is the slope of such a plot and ϵ is the extinction coefficient (molar absorptivity) of triiodide ion at the chosen wavelength (units of $M^{-1}\ cm^{-1}$).

$$\text{RATE} = -\ d[I_3^-]/dt = -\ d\,[\text{acetone}]/dt$$

$$= k_{obs}\,[\text{acetone}] = -\ S/\epsilon_{I_3^-} \qquad (\text{units of M sec}^{-1}) \qquad [3.2]$$

This relationship follows from Beer's law (the Bougeur-Lambert-Beer law, R81b), i.e. absorbance = $\epsilon_{I_3^-} \cdot [I_3^-] \cdot \ell$ where ℓ is the cell path length (1 cm). The slope of absorbance, A vs. time, t, is related to $\epsilon_{I_3^-}$ by eq. [3.3].

$$S = d[A]/dt = \epsilon_{I_3^-}\, d[I_3^-]/dt \qquad [3.3]$$

Hence k_{obs} can be determined and related to the sum of the catalytic terms present in the system under investigation eq. [3.4].

$$k_{obs} = -S/(\epsilon_{I_3^-} [\text{acetone}]) = \Sigma\, k_{cat} [\text{cat}] \qquad [3.4]$$

This work was done at low concentrations of catalyst that preclude the involvement of third-order terms in eq. [3.4]. Thus, second-order rate constants for a variety of catalyst types were measured. The results of these measurements are described in detail in the following sections.

3.1 CARBOXYLIC ACIDS AND CARBOXYLATE BASES

3.1.1 Monoprotic Acids and Monoanionic Bases

Though Bell and Lidwell had measured the rate constants for acetone enolization catalyzed by four carboxylic acids and their conjugate bases (Table 1, p. 41), we decided to extend the series to include a number of sterically crowded catalysts.

There are two ways of determining the rate constants for reactions which follow rate laws such as eq. [1.68].

$$k_{obs} = k_{H_2O}[H_2O] + k_{H^+}[H_3O^+] + k_{^-OH}[^-OH] + k_{HA}[HA] + k_{A^-}[A^-] \qquad [1.68]$$

The first method, which was discussed previously (p. 39), involves

measuring the rates of reaction at a constant buffer ratio ($n = [HA]/[A^-]$) while varying the concentration of acid and base in a number of such runs. The data obtained using different buffer ratios can be combined to give values of k_{HA} and k_{A^-} by using eq. [1.70]. This approach, which we call the buffer-ratio method, is thorough but time-consuming, requiring at least nine kinetic runs (preferably more) for each pair of acid/base catalysts.

$$\text{Slope of } k_{obs} \text{ vs. } [A^-] = k_{A^-} + nk_{HA} \qquad [1.70]$$

A second method makes use of the known values for the catalytic rate constants of hydronium ion, hydroxide ion and water. Subtracting the sum of these three contribitons, k_{sum}, from the observed rate at a particular pH leads to an equation with two unknowns, k_{HA} and k_{A^-}, eq. [3.5]. Measuring the rate at another pH will give a second equation, which can be combined with the first equation to give both k_{HA} and k_{A^-} values. The results of this method are briefly described here and it is shown that the method is the least preferred approach to the determination of the rate constants. The buffer ratio method (p. 75) is the method of choice.

$$k_{obs} - k_{sum} = k_{HA}[HA] + k_{A^-}[A^-] \qquad [3.5]$$

Cross-solving a number of simultaneous equations can lead to a number of values of the acid and base rate constants. For instance four kinetic runs produce six values each of k_{HA} and k_{A^-}.

This second approach, which we call the simultaneous equation method, gave the results shown in Table 4 for acetic acid. Values used for the catalytic constants of H_3O^+ and ^-OH were those listed by Hine and co-workers (HK72): The values of k_{H^+} and $k_{^-OH}$ being 2.84×10^{-5} M^{-1} sec^{-1} and 0.166 M^{-1} sec^{-1} respectively, values which differ from those determined by Bell and Lidwell (p. 43), these rate constants being the average of a number of results compiled from the literature. The rate constant used for water catalyzed enolization is the value of Bell and Lidwell, 8.33×10^{-12} M^{-1} sec^{-1} which when multiplied by the concentration of H_2O (i.e. 55.5 M, B73e) gives a value of 4.62×10^{-10} M^{-1} sec^{-1} for $k_{H_2O}[H_2O]$. The concentrations of acetic acid, [HA], and acetate ion, $[A^-]$, were determined from eq. [3.6] knowing the sum of [HA] and $[A^-]$.

$$\log ([HA]/[A^-]) = pK^I - pH \qquad [3.6]$$

This equation results from $pK^I = -\log ([A^-][H^+]/[HA])$ where pK^I is the pK of the acid HA at the ionic strength at which the pH was measured. This concentration dependent pK is related to the thermodynamic pK (concentration independent, value at zero ionic strength), denoted by pK^T, by eq. [3.7] where I is the ionic strength (AS84a).

$$pK^I = pK^T - (0.5115 \sqrt{I}/(1 + 1.5 \sqrt{I})) \qquad [3.7]$$

An ionic strength of 0.1 M was used in the determination of k_{obs}, resulting in pK^I being 0.11 units less than pK^T. The effect of the

Table 4: (a) Data for the cross-solving of simultaneous equations $k_{obs} - k_{sum} = k_{HA}[HA] + k_{A^-}[A^-]$ for acetic acid/acetate ion with $pK^I = 4.76 - 0.11 = 4.65$, 0.1 M ionic strength, 25°C.
(b) Results of the cross-solving of the equations I - V.

(a)

$10^8 k_{obs}$ sec^{-1}	pH	$10^8 k_{sum}$ sec^{-1}	$10^8(k_{obs}-k_{sum})$ sec^{-1}	[HA],M	$[A^-]$,M	Equation
1.431	3.83	0.467	0.964	0.08375	0.01268	I
1.364	4.11	0.267	1.10	0.07766	0.02240	II
1.486	4.42	0.159	1.33	0.06655	0.03919	III
1.744	4.925	0.094	1.65	0.03416	0.06435	IV
2.105	5.44	0.102	2.00	0.01430	0.08816	V

(b)

$10^7 k_{A^-}$ \ $10^8 k_{HA}$	I	II	III	IV	V
I	-	8.61	8.58	8.29	8.27
II	1.91	-	8.54	7.95	7.94
III	1.93	1.94	-	7.04	7.25
IV	2.12	2.14	2.19	-	7.92
V	2.14	2.14	2.15	2.14	-

$$k_{HA} = 8.04 \pm 0.54\ 10^{-8}\ M^{-1}\ sec^{-1}$$

$$k_{A^-} = 2.08 \pm 0.11\ 10^{-7}\ M^{-1}\ sec^{-1}$$

acetone on the pK was assumed to be negligible, as it comprised a maximum of only 3.7% by volume of the solvent (0.5 M). The cross-solving of the five simultaneous equations for acetic acid/acetate ion gave ten values of each rate constant; the average values and the standard deviations are shown in Table 5 along with the results for ten other acids.

The pH values were chosen so as to favour the species that had the smaller rate constant, but this had a limitation in that pH values more than 1.5 units from pK^I resulted in a disappearance of triiodide that was not zero-order. Presumably this was due to poor buffer capacity. Generally the smaller rate constant of the acid/conjugate base pair shows the larger standard deviation, chloroacetate being the worst with a deviation of ±60%. In the case of the smaller rate constants of each pair, even those with acceptable standard deviations (i.e. reasonable precision), the accuracy of the values is in doubt; these values are generally larger than that expected on the basis of Bell and Lidwell's Bronsted lines and as further investigation illustrated, the values are in fact larger than the presumably more accurate values obtained by the buffer-ratio method. The Bronsted plots using the results of the simultaneous equation method is shown in Fig. 9, with the values of Bell and Lidwell for comparison. The Bronsted equations are shown below.

Acid catalysis $\log k_{HA} = -4.63 - 0.52\ (pK + \log 1/2)$ [3.8]
r = 0.9808

Base catalysis $\log (\log k_A - /2) = -8.88 + 0.45\ (pK + \log 1/2)$ [3.9]
r = 0.9225

Table 5: k_{HA} and k_{A^-} values for acetone enolization catalyzed by carboxylic acids and carboxylate bases at 25° and 0.1 M ionic strength, determined by the simultaneous equations method, $pK^I = pK^T - 0.11$, Σ is the number of values of each rate constant determined.

Acid	$10^7 k_{HA}$ M^{-1} sec^{-1}	$10^7 k_{A^-}$ M^{-1} sec^{-1}	pK^T	Σ
$ClCH_2CO_2H$	10.4 ± 1.2[a]	0.613 ± 0.370	2.86	6
$C_6H_5CH(OH)CO_2H$	6.72 ± 0.81	0.761 ± 0.449	3.41	15
$CH_3OCH_2CO_2H$	4.97 ± 0.61	0.524 ± 0.199	3.57	10
$HOCH_2CO_2H$	3.31 ± 0.38	0.492 ± 0.215	3.83	10
$C_6H_5CH_2CO_2H$	1.78 ± 0.13	1.68 ± 0.30	4.31	8
CH_3CO_2H	0.804 ± 0.054	2.08 ± 0.11	4.76	10
$(CH_3)_2CHCO_2H$	1.16 ± 0.02	2.82 ± 0.35	4.86	10
$CH_3CH_2CO_2H$	0.849 ± 0.249	3.10 ± 0.22	4.87	15
$C_6H_{11}CO_2H$	0.898 ± 0.180	3.53 ± 0.10	4.91	10
$(CH_3)_3CCH_2CO_2H$	1.21 ± 0.08	4.26 ± 0.18	5.01[b]	6
$(CH_3)_3CCO_2H$	0.887 ± 0.037	3.94 ± 0.03	5.03	6

[a] standard deviation

[b] pK^T determined in this work, see experimental.

The poor degree of fit of the data (especially in the case of the bases) necessitated a thorough redetermination of these rate constants by the buffer-ratio method before any conclusions could be reached.

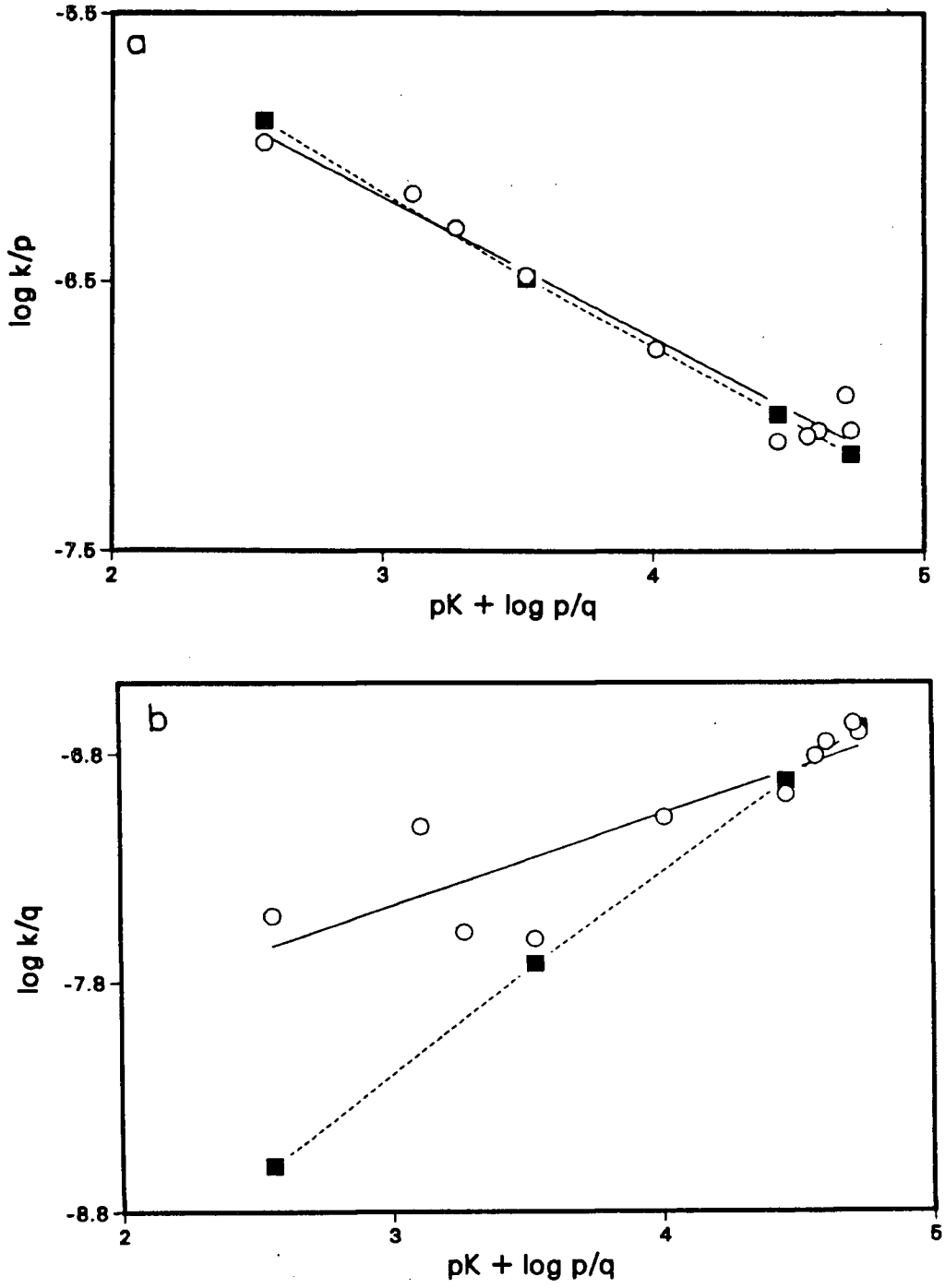

Fig. 9: Bronsted plots for acetone enolization catalyzed by (a) carboxylic acids (open circles) data from Table 5 (b) carboxylate bases (open circles) data from Table 5. Rate constants determined by simultaneous equation method. Bell and Lidwell's data (closed squares, broken lines) added for comparison in both (a) and (b) (BL40).

The following points should be noted concerning the buffer ratio method.

1. The rate constants can be determined by a plot of the slope of k_{obs} vs. $[A^-]$ against n, the buffer ratio as previously described. Such a plot gives k_{HA} as the slope and k_{A^-} as the intercept, eq. [1.70]. This was done for acid/conjugate base pairs where $k_{HA} < k_{A^-}$. The correlation coefficient gives a measure of the degree of precision of the k_{HA} measurement, precision which was generally less than that obtained for the (larger) k_{A^-} rate constants. In cases where $k_{HA} > k_{A^-}$, the slope of k_{obs} vs. [HA] was plotted against 1/n, giving k_{A^-} as the slope and k_{HA} as the intercept, eq. [3.10].

$$\text{Slope of } k_{obs} \text{ vs. } [A^-] = k_{A^-} + n\ k_{HA} \qquad [1.70]$$

$$\text{Slope of } k_{obs} \text{ vs. } [HA] = k_{HA} + (1/n)\ k_{A^-} \qquad [3.10]$$

The standard deviation of the smaller rate constant is a minimum when that rate constant is the slope, rather than the intercept, of such plots.

2. In any given set of buffer solutions at the same buffer ratio, n, the pH should be constant throughout the set. Generally the average pH of each set of carboxylate solutions had an average deviation no greater than 0.02 pH units.

3. It follows from eq. [3.6] that at a n value of 1, the pH of the solutions equals pK^I. Likewise, at n = 2, pH = pK^I − 0.3 and at n = 0.5, pH = pK^I + 0.3.

4. Experimental results showed, not surprisingly, that there is a limit to the range of buffer ratios possible. That is to say, outside the

range of $5 \geq n \geq 0.2$, the buffer capacity diminished to the point where there were significant changes in pH within the buffer set which, in turn, produced non zero-order decreases of triiodide ion absorbance (i.e. non-linear decreases were observed).

5. For certain acid/conjugate base pairs the much greater magnitude of the acid rate constant made a meaningful determination of the conjugate base rate constant impossible. This despite the fact that the choice of buffer ratios is always such that it favours the smaller contributor (within the experimental limitation of $5 \geq n \geq 0.2$). In cases where k_{A^-} is negligible, the value of k_{HA} can be determined from a plot of k_{obs} vs. [HA], as eq. [3.5] reduces to eq. [3.11].

$$k_{obs} = k_{sum} + k_{HA}\,[HA] \qquad [3.11]$$

The results for acetic acid/acetate buffers at four buffer ratios are shown in Table 6 and plotted in Fig. 10(a). Generally each buffer ratio involved four concentrations, though three concentrations were used on a few occasions. The plots of k_{obs} vs. [HA] or $[A^-]$ had r (correlation coefficient) ≥ 0.9990 in all cases.

The average pH value of each individual buffer-ratio set agrees with that expected on the basis of $pK^I = 4.65$. At $n = 1$, $pH_{calc} = 4.65$, $pH_{expt} = 4.63$ and at $n = 2.3$ and 4 the values are $pH_{calc} = 4.34$, 4.17 and 4.05, respectively, with $pH_{expt} = 4.345$, 4.16 and 4.04, respectively. The agreement was not always this good, the pH_{expt} generally having an average deviation of $\pm$ 0.03 from the pH_{calc} value.

Table 6: Results of plotting k_{obs} vs. $[A^-]$ for acetic acid/acetate ion buffers at 4 n values (n = $[HA]/[A^-]$) at 25°C and 0.1 M ionic strength.

n	pH	$[A^-]$,M	$10^8 k_{obs}$ sec^{-1}	r	10^8 Intercept sec^{-1}	10^7 Slope $M^{-1}sec^{-1}$
	4.62	0.05046	1.800			
1	4.64	0.03154	1.211	0.9996	1.72	3.240
	4.63	0.01892	0.774			
	4.345	0.03362	1.605			
2	4.35	0.02522	1.260	1.0000	2.22	4.115
	4.34	0.01681	0.916			
	4.345	0.00841	0.567			
	4.16	0.02582	1.570			
3	4.15	0.01936	1.262	0.9998	2.95	4.962
	4.16	0.01291	0.944			
	4.16	0.00645	0.608			
	4.04	0.02029	1.499			
4	4.03	0.01522	1.204	1.0000	3.39	5.704
	4.05	0.01015	0.917			
	4.04	0.00507	0.631			

The slopes of the plots of k_{obs} vs. $[A^-]$ (final column, Table 6) are plotted vs. n to provide the rate constants k_{HA} (slope) and k_{A^-} (intercept), Fig. 10(b).

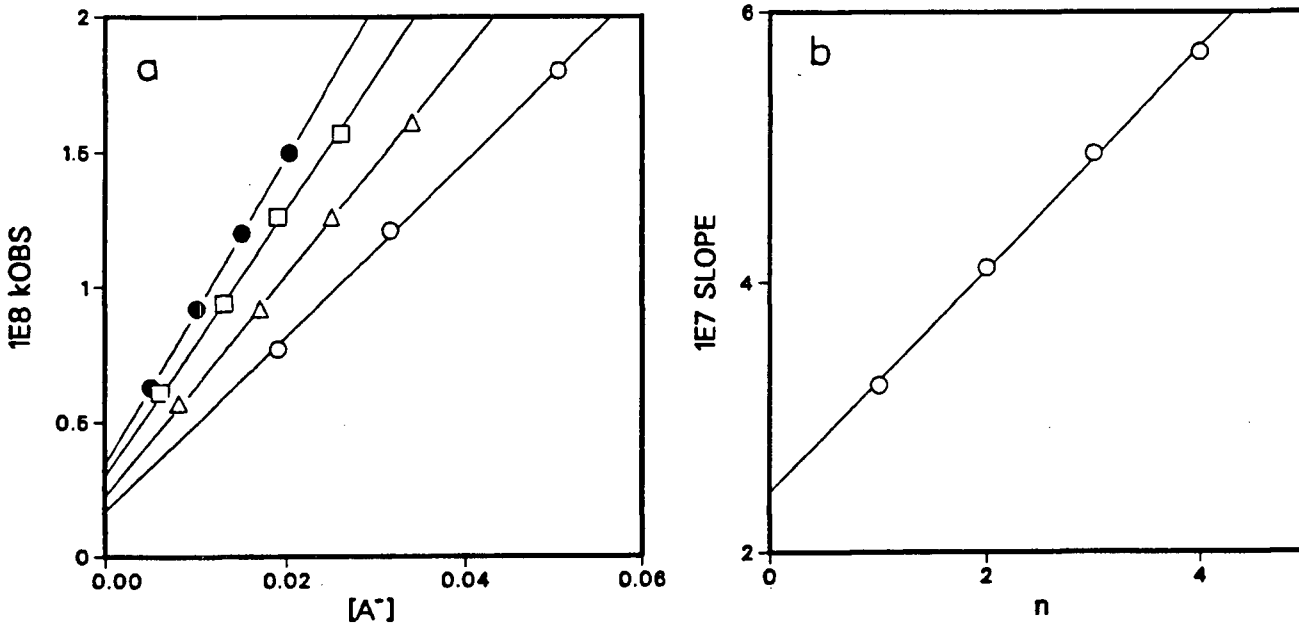

Fig. 10: (a) Plots of k_{obs} vs. $[A^-]$ for acetic acid/acetate buffers.
(b) Plot of (slope of k_{obs} vs. $[A^-]$) vs. n for acetic acid/acetate ion giving r = 0.9993,
$k_{HA} = 8.24 \pm 0.22\ 10^{-8}\ M^{-1}\ sec^{-1}$ (slope) and
$k_{A^-} = 2.45 \pm 0.06\ 10^{-7}\ M^{-1}\ sec^{-1}$ (intercept).

The results for methoxyacetic acid are shown in Fig. 11. The large standard deviation of k_{A^-} reflects the fact that the ratio of k_{HA} to k_{A^-} is large (≈20).

The results for both chloroacetic acid and iodoacetic acid buffers show negligible catalysis by the carboxylate base. This can be seen from Fig. 12(a), where for chloroacetic acid buffers, the slope of k_{obs}

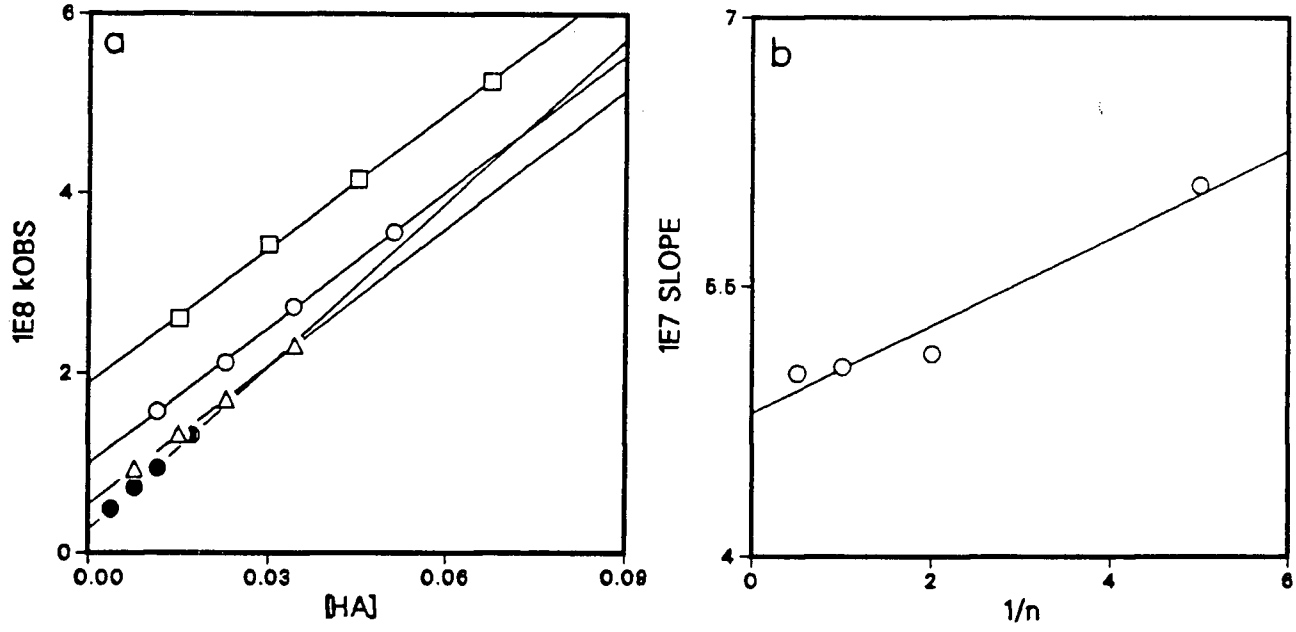

Fig. 11: (a) Plots of k_{obs} vs. [HA] for methoxyacetic acid/methoxyacetate buffers. (b) Plot of (slope of k_{obs} vs. [HA]) vs. 1/n for methoxyacetic acid/methoxyacetate ion giving r = 0.9752, k_{HA} = 4.80 ± 0.11 10^{-7} M^{-1} sec^{-1} (intercept) and k_{A^-} = 2.43 ± 0.39 10^{-8} M^{-1} sec^{-1}.

vs. [HA] is plotted against 1/n. The poor correlation coefficient and the very large standard deviation of the slope illustrate the negligible contribution of the chloroacetate ion. Plots of k_{obs} vs. [HA] are shown in Fig. 12(b); the slopes of these lines are k_{HA} values (eq. [3.11], their average value agreeing with that obtained from the intercept of Fig. 12(a).

The results of fourteen carboxylic acid/conjugate base pairs subjected to the buffer-ratio method are given in Table 7. The results generally show much lower standard deviations than the results of the simultaneous-equations method, Table 5. The results for the larger rate

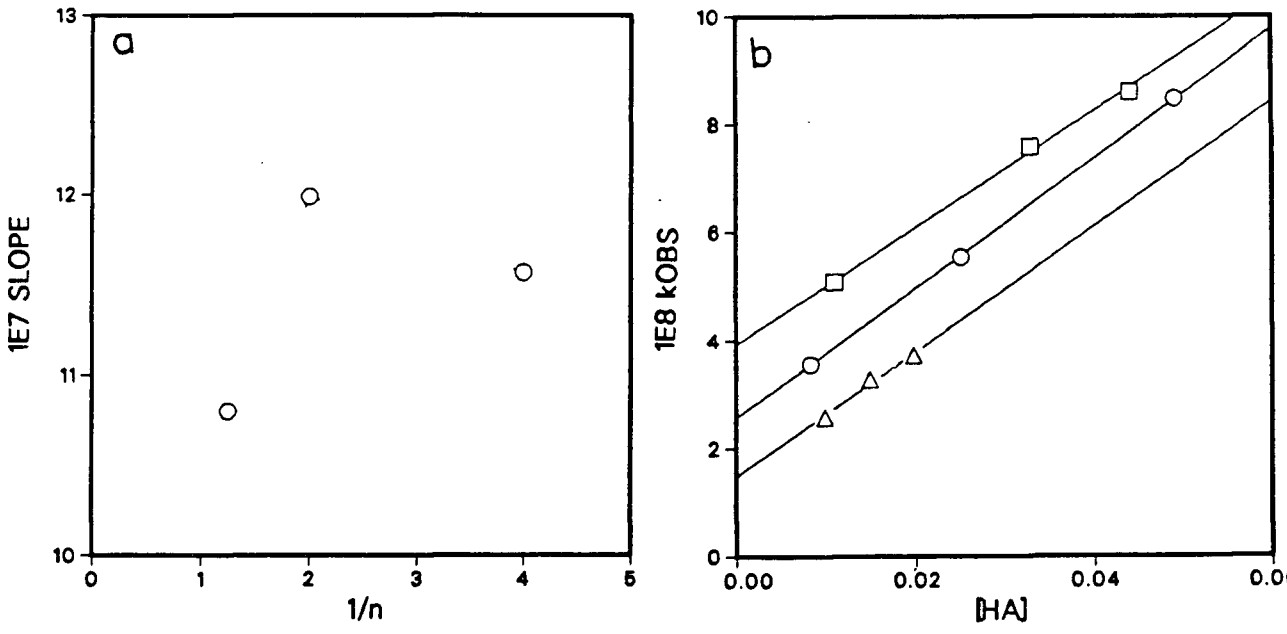

Fig. 12: (a) Plot of (slope of k_{obs} vs. [HA]) vs. 1/n for chloroacetic acid/chloroacetate ion giving r = 0.4610, k_{HA} = 11.0 ± 1.0 10^{-7} M^{-1} sec^{-1} (intercept) and k_{A^-} = 1.75 ± 3.81 10^{-9} M^{-1} sec^{-1} (slope). (b) Plots of k_{obs} vs. [HA] for chloroacetic acid/chloroacetate buffers, average of three slopes , k_{HA} = 11.5 ± 0.6 10^{-7} M^{-1} sec^{-1}.

constants of the acid/base pairs from both methods agree well, while there is a greater discrepancy between the smaller rate constants from both methods. Presumably the simultaneous-equation method leads to oversized values of the smaller rate constant of the acid/base pair. The more accurate results from the buffer-ratio method (Table 7) are discussed later.

It is not possible to determine the rate constants for carboxylic acids stronger than chloroacetic acid using the buffer-ratio method. Unlike the case of chloroacetic acid and weaker acids, we found that

Table 7: k_{HA} and k_{A^-} values for acetone enolization catalyzed by carboxylic acids and carboxylate bases at 25°C and 0.1 M ionic strength, determined by the buffer ratio method, br is the number of buffer ratios used.

Acid	$10^7 k_{HA}$ $M^{-1} sec^{-1}$	$10^7 k_{A^-}$ $M^{-1} sec^{-1}$	pK^T	br	Method[a]
$ClCH_2CO_2H$	11.0 ± 1.0	0.017 ± 0.038	2.86	3	I
	11.5 ± 0.6	-			III
ICH_2CO_2H	9.50 ± 0.16	0.098 ± 0.051	3.18	3	I
	9.77 ± 0.23	-			III
$C_6H_5CH(OH)CO_2H$	7.61 ± 0.19	0.143 ± 0.058	3.41	3	I
$CH_3OCH_2CO_2H$	4.80 ± 0.11	0.243 ± 0.039	3.57	4	I
$HOCH_2CO_2H$	3.09 ± 0.10	0.339 ± 0.031	3.83	3	I
$C_6H_5CH_2CO_2H$	1.92 ± 0.12	1.19 ± 0.09	4.31	4	I
CH_3CO_2H	0.824 ± 0.022	2.45 ± 0.06	4.76	4	II
CD_3CO_2H	0.837 ± 0.047	2.31 ± 0.13	4.77[b]	3	II
$CH_3CH_2CH_2CO_2H$	0.881 ± 0.018	2.79 ± 0.05	4.82	3	II
$(CH_3)_2CHCO_2H$	0.670 ± 0.155	3.03 ± 0.41	4.86	3	II
$CH_3CH_2CO_2H$	0.654 ± 0.083	3.22 ± 0.02	4.87	3	II
$C_6H_{11}CO_2H$	0.774 ± 0.153	3.19 ± 0.41	4.91	3	II
$(CH_3)_3CCH_2CO_2H$	0.879 ± 0.020	4.24 ± 0.05	5.01[c]	3	II
$(CH_3)_3CCO_2H$	0.717 ± 0.027	4.02 ± 0.09	5.03	3	II

[a] Methods

		Slope	Intercept
I	(Slope of k_{obs} vs. [HA]) vs. 1/n	k_{A^-}	k_{HA}
II	(Slope of k_{obs} vs. $[A^-]$) vs. n	k_{HA}	k_{A^-}
III	Plot of k_{obs} vs. [HA]	k_{HA}	k_{sum}

[b] pK values from ref. (SK63).

[c] pK determined in this work, see experimental.

with the stronger carboxylic acid buffers, the pH varied considerably with concentration. At any buffer-ratio, the lower the buffer concentration, the higher is the pH. A different kinetic treatment was therefore used for these carboxylic acids.

For each carboxylic acid solution at a particular pH, the contribution to the observed rate constant, k_{obs}, is given by eq. [3.12]. This expression results from eq. [1.68] since both the hydroxide ion and the carboxylate monoanion will have negligible contributions to k_{obs}. It may be recalled that for chloroacetic acid, the conjugate monoanion showed negligible catalysis (p. 68).

$$k_{obs} = k_{H_2O}[H_2O] + k_{H^+}[H_3O^+] + k_{^-OH}[^-OH] + k_{HA}[HA] + k_{A^-}[A^-] \qquad [1.68]$$

$$k_{obs} = k_{H_2O}[H_2O] + k_{H^+}[H_3O^+] + k_{HA}[HA] \qquad [3.12]$$

For carboxylic acid solutions below pH 2.5 or so, the involvement of the water term (4.62×10^{-10} sec^{-1}) in eq. [3.12] can be safely ignored, as it will comprise less than 0.5% of k_{obs}. For example, at a pH of 2.5, the contribution of the hydronium ion will be (3.16×10^{-3} M x 2.84×10^{-5} M^{-1} sec^{-1}), i.e. 8.97×10^{-8} sec^{-1}, or 99.5% of the total contribution of hydronium ion and water. Involvement of the carboxylic acid in the rate expression will further reduce the significance of the water term.

Hine and coworkers have reported a value for k_{H^+} (2.84×10^{-5} M^{-1} sec^{-1}) which is the average of 18 literature rate constants for the acid-catalyzed halogenation of acetone (HK72). We measured the value,

under our experimental conditions, using hydrochloric acid. The rate expression for this system is shown below.

$$k_{obs} = k_{H^+}[H_3O^+] \qquad [3.13]$$

A number of hydrochloric acid solutions varying in concentration from 1.9×10^{-3} to 1.9×10^{-1} M were used. The plot of k_{obs} against the stoichiometric concentration of hydronium ion provides the value of k_{H^+} as the slope (with negligible intercept) and is shown in Fig. 13. Eight of the thirty two kinetic runs involved addition of between 1/3 and 4/5 equivalents of sodium hydroxide, with appropriate corrections for the

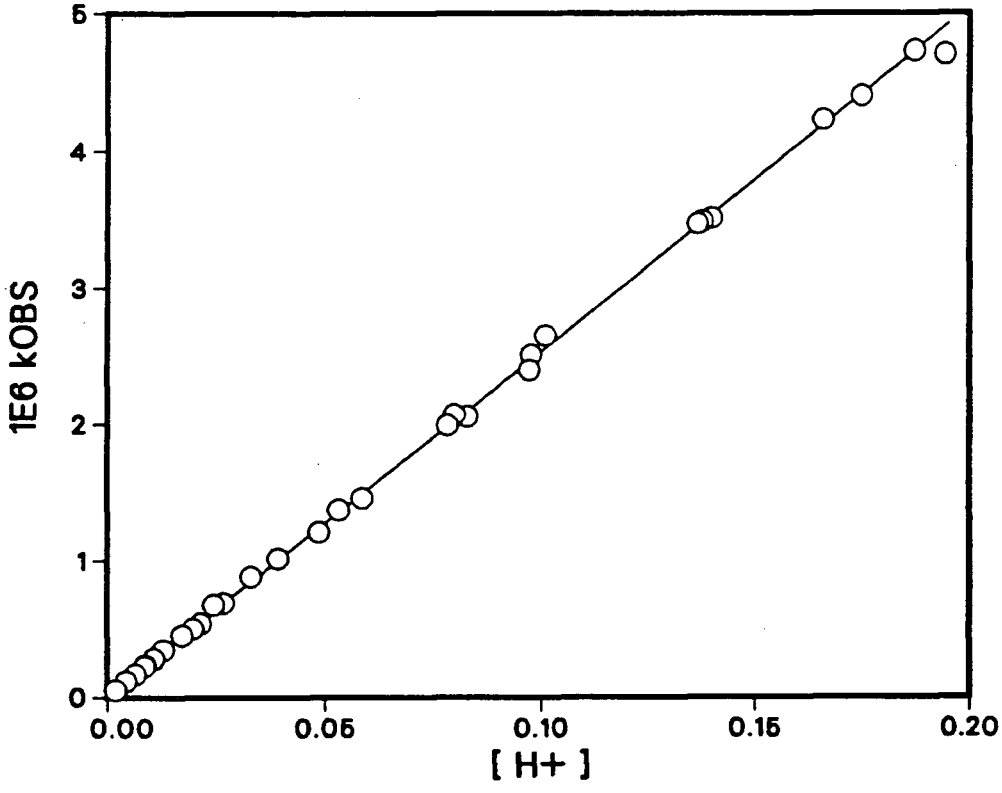

Fig. 13: Plot of k_{obs} vs. $[H_3O^+]$ (stoichiometric concentration) for hydrochloric acid giving r = 0.9995, $k_{H^+} = 2.51 \pm 0.02 \times 10^{-5}$ M^{-1} sec^{-1} (slope), and intercept $1.9 \pm 1.5 \times 10^{-8}$ sec^{-1}. Ionic strength was varied from 0.01 to 0.2 M.

concentration of hydronium ion. These results alone give a value of $2.43 \pm 0.03 \times 10^{-5}$ M^{-1} sec^{-1} for k_{H^+} compared with the value of $2.51 \pm 0.02 \times 10^{-5}$ M^{-1} sec^{-1} for all thirty two kinetic runs.

There is a small but consistent difference between the stoichiometric concentration of hydronium ion and the concentration determined from the measured pH of each solution. This latter 'pH' concentration is always found to be slightly smaller than the stoichiometric concentration, determined by titration with sodium hydroxide. Thus a k_{H^+} value determined by using the H_3O^+ 'pH' concentrations will be slightly larger than the value obtained using the stoichiometric H_3O^+ concentrations. The plot of k_{obs} vs. $[H_3O^+]$ determined from the pH for the same thirty two kinetic runs which were used to determine the stoichiometric k_{H^+} value, gives the following result; $r = 0.9960$, slope $= 2.95 \pm 0.05 \times 10^{-5}$ M^{-1} sec^{-1} (k_{H^+}) and intercept $= -2.0 \pm 3.9 \times 10^{-8}$ M^{-1} sec^{-1}. While the 'stoichiometrically' derived rate constant for hydronium ion i.e. k_{H^+}(stoich.) can be considered the correct value, it may be more appropriate to use the pH-derived value i.e. k_{H^+}(pH), in a kinetic treatment where measurements of pH are used to determine hydronium ion concentrations.

The kinetic treatment is described using difluoroacetic acid as an example; a number of carboxylic acid solutions are prepared by the addition of between 1/3 and 4/5 equivalents of sodium hydroxide to the free acid. For each particular solution at a particular pH, the concentration of the difluoroacetic acid was determined from eq. [3.14], where $[HA]_o$ is the initial concentration of difluoroacetic acid, $[B^-]$ is the concentration of base added and $[H^+]$ is calculated from the pH

measurement (AS84b). The concentration of difluoroacetic acid in each solution is related to k_{obs} by eq. [3.15].

$$[HA] = [HA]_o - [B^-] - [H^+] \qquad [3.14]$$

$$k_{obs} - k_{H^+}[H_3O^+] = k_{HA}[HA] \qquad [3.15]$$

The results for difluoroacetic acid are shown in Table 8, and Fig. 14 shows the plot of $(k_{obs} - k_{H^+}[H_3O^+])$ vs. [HA]. The slope of this line is the value of k_{HA} for difluoroacetic acid, $6.37 \pm 0.12 \times 10^{-6}$ M^{-1}

Table 8: pH, k_{obs} and [HA] measurements for difluoroacetic acid solutions

pH	10^6 k_{obs}, sec^{-1}	[HA], M	10^6 $(k_{obs} - k_{H^+}[H_3O^+])^a$ sec^{-1}
1.23	2.563	0.1321	0.826
1.255	2.400	0.1163	0.760
1.34	1.948	0.0918	0.600
1.485	1.359	0.0628	0.393
1.505	1.242	0.0499	0.320
1.745	0.711	0.0298	0.180
1.875	0.511	0.0189	0.118
2.05	0.376	0.0150	0.113

a $k_{H^+} = 2.95 \times 10^{-5}$ M^{-1} sec^{-1}, $[H_3O^+]$ determined from pH.

sec^{-1}. The negligible intercept illustrates the negligible catalysis by difluoroacetate anion. The results for dichloroacetic acid are plotted in Fig. 14 also.

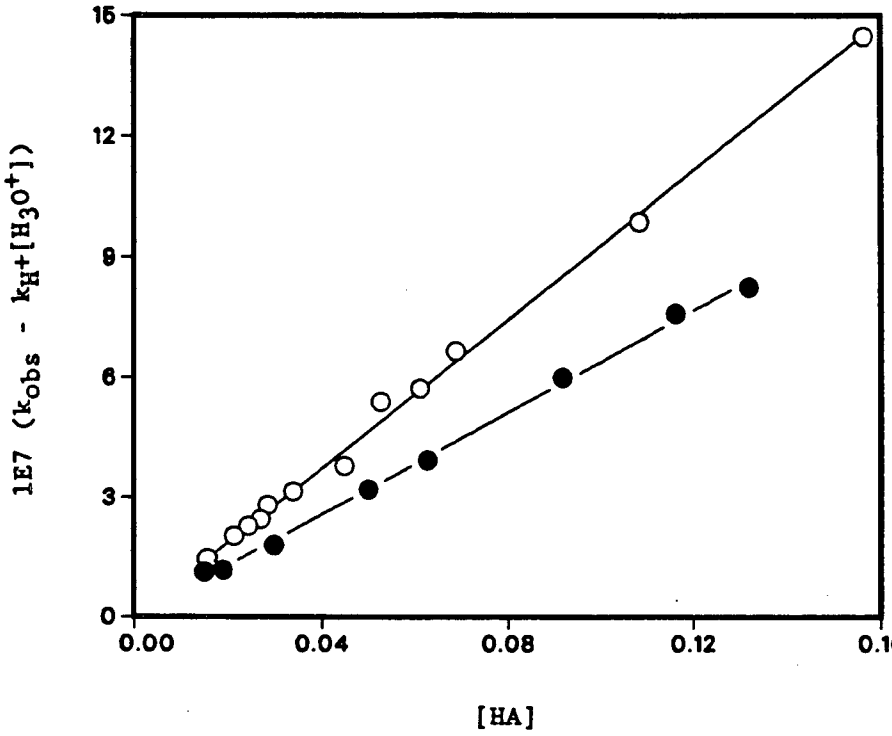

Fig. 14: Plots of (k_{obs} – k_H+[H_3O^+]) vs. [HA] for difluoroacetic acid (closed circles) giving r = 0.9990, slope, k_{HA} = 6.37 ± 0.12 x 10^{-5} M^{-1} sec^{-1} and intercept 2.1 ± 9.3 x 10^{-9} sec^{-1} and dichloroacetic acid (open circles) giving r = 0.9985, slope, k_{HA} = 9.26 ± 0.15 x 10^{-5} M^{-1} sec^{-1} and intercept 2.5 ± 9.2 x 10^{-9} sec^{-1}

The major part of k_{obs} is the contribution from hydronium ion, which in the case of difluoroacetic acid varies from 68% to 77% of k_{obs}. No attempt was made to keep the ionic strength of the difluoroacetic acid

solutions constant and from the results, with ionic strength varying from 0.1 M to 0.15 M, ionic strength effects on k_{HA} must be negligible in this range.

It may be recalled that both chloroacetic acid and iodoacetic acid showed negligible catalysis by the conjugate anion. The k_{HA} values for these two acids can be determined using this approach and compared with the results from the buffer-ratio method. As the pH of the solutions of these carboxylic acids are in the range 2.46 to 3.66, the water term should be included in the rate expression, eq. [3.12].

$$k_{obs} - k_{H^+}[H_3O^+] - k_{H_2O}[H_2O] = k_{HA}[HA] \qquad [3.12]$$

Plots of $(k_{obs} - k_{H^+}[H_3O^+] - k_{H_2O}[H_2O])$ vs. [HA] for both chloroacetic and iodoacetic acid are linear with negligible intercepts. The value of k_{HA}, i.e. the slope of the lines, is 10.9 ± 10^{-7} M^{-1} sec^{-1} for chloroacetic acid and $9.47 \pm 0.20 \times 10^{-7}$ M^{-1} sec^{-1} for iodoacetic acid. These results compare favourably with the values determined using the buffer-ratio method (Table 7); $11.0 \pm 1.0 \times 10^{-7}$ M^{-1} sec^{-1} for chloroacetic acid and $9.50 \pm 0.16 \times 10^{-7}$ M^{-1} sec^{-1} for iodoacetic acid.

A number of carboxylic acids were treated in this way and the k_{HA} values determined are listed in Table 9. No results were excluded for any acid in the plot of $(k_{obs} - k_{H^+}[H_3O^+])$ vs. [HA] in order to improve upon the degree of fit (as measured by the correlation coefficient, r). Rather, in cases where the plot was slightly scattered , a large number of kinetic runs were used to define the line. The results for protonated glycine, $H_3\overset{+}{N}CH_2CO_2H$, show the poorest correlation coefficient

Table 9: k_{HA} values for acetone enolization at 25°C, determined by plots of ($k_{obs} - k_{H^+}[H_3O^+]$)[a] vs. [HA], nk is the number of kinetic runs.

Acid	$10^7 k_{HA}$ M^{-1} sec^{-1}	pK^T	nk
ICH_2CO_2H	9.47 ± 0.20	3.18	4
$ClCH_2CO_2H$	10.9 ± 1.1	2.86	4
$Cl^-H_3N^+CH_2CO_2H$	12.8 ± 0.9	2.36[b]	16
$Cl^-(CH_3)_2\overset{+}{N}HCH_2CO_2H$	19.8 ± 0.3	1.94[b]	8
$Cl^-(CH_3)_3\overset{+}{N}CH_2CO_2H$	28.5 ± 0.8	1.83[b]	20
Cl_2CHCO_2H	92.6 ± 1.5	1.36[c], 1.36[d]	14
F_2CHCO_2H	63.7 ± 1.2	1.34[c], 1.30[d]	8
Br_3CCO_2H	280 ± 15	0.73[d]	16
Cl_3CCO_2H	273 ± 6	0.52[c], 0.69[d]	8
F_3CCO_2H	205 ± 9	0.50[c], 0.54[d]	8

a $k_{H^+} = 2.95 \times 10^{-5}$ M^{-1} sec^{-1}, water term (4.62×10^{-10} sec^{-1}) included where necessary.

b pK values from ref. (EF79).

c pK values from ref. (KF69).

d pK values determined in this laboratory (NV87).

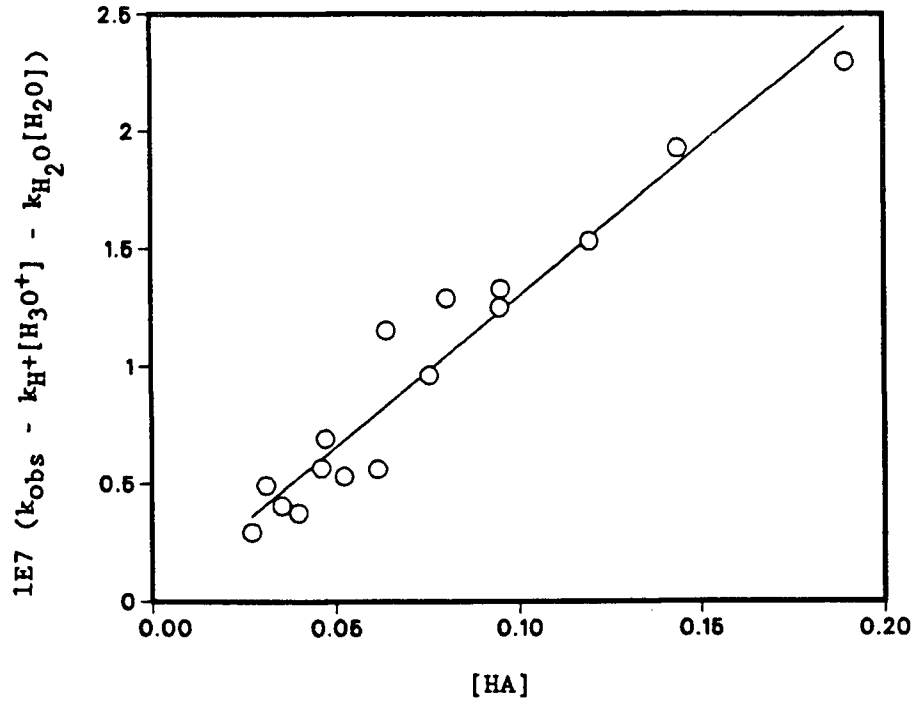

Fig. 15: Plots of ($k_{obs} - k_{H^+}[H_3O^+] - k_{H\ O}[H_2O]$) vs. [HA] for protonated glycine giving r = 0.9685, k_{HA} = 1.28 ± 0.09 x 10^{-6} M^{-1} sec^{-1} (slope) and intercept 1.4 ± 7.6 x 10^{-9}.

(0.9685) and are shown in Fig. 15. For all these acids the good degree of fit of the experimental results to eq. [3.15] is reflected by the small standard deviations of the k_{HA} values. In appropriate cases a correction for the water term is included in the rate expression (i.e. for the weaker acids and pH values greater than 2.5).

Measuring k_{HA} and k_{A^-} values for benzoic acids is extremely difficult owing to the low solubility of these acids in water. The buffer-ratio method is used, generally at buffer-ratios that favour the anion, thereby having acceptable concentrations of buffer accessible. By trial and error the maximum solubility of each acid was determined

under the experimental conditions. The acids studied are the more soluble, or rather the less insoluble, benzoic acids, which excludes 4-substituted and disubstituted benzoic acids. In any particular buffer-ratio set, comprising four solutions, only a small span of concentration is used (generally a factor of three).

The weakest benzoic acid studied, is 3-methylbenzoic acid having a pK^T of 4.27. An ionic strength of 0.1 M is used, as in the case of the aliphatic carboxylic acids. The kinetic results at three buffer ratios are shown in Table 10 and Fig. 16(a). The slope of k_{obs} vs. [HA] is plotted against 1/n in Fig. 16(b) providing k_{HA} as the intercept and k_A-as the slope. As in the aliphatic carboxylic acid buffer-ratio sets,

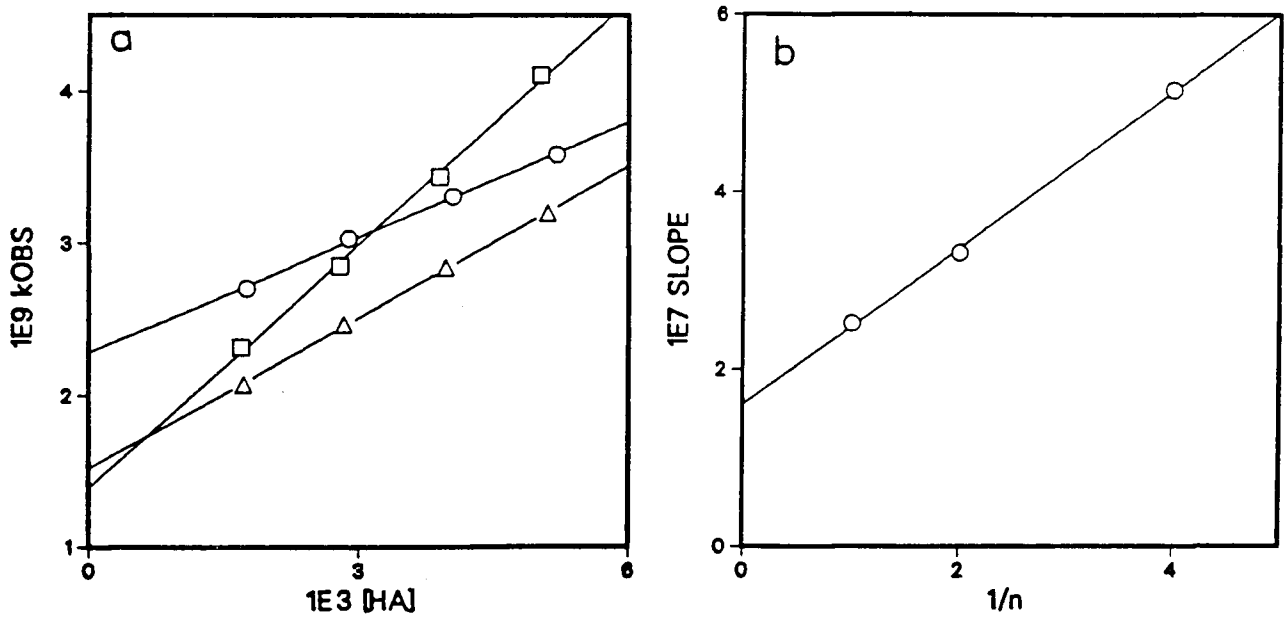

Fig. 16: (a) Plots of k_{obs} vs. [HA] for 3-methylbenzoic acid/3-methylbenzoate buffers; (b) Plot of (slope of k_{obs} vs. [HA]) vs. 1/n for 3-methylbenzoic acid/3-methylbenzoate ion giving r = 0.9995, $k_{HA} = 1.61 \pm 0.08 \times 10^{-7}$ M^{-1} sec^{-1} (intercept) and k_A- $8.81 \pm 0.31 \times 10^{-8}$ M^{-1} sec^{-1} (slope).

Table 10: Results of plotting k_{obs} vs. [HA] for 3-methylbenzoic acid/ 3-methylbenzoate ion buffers at 3 n values (n = [HA]/[A^-]) at 25°C and 0.1 M ionic strength.

n	pH	10^3 [HA], M	10^9 k_{obs} sec^{-1}	r	10^9 Intercept sec^{-1}	10^7 Slope M^{-1} sec^{-1}
	4.23	5.193	3.584			
1	4.21	4.039	3.309	0.9992	2.28	2.525
	4.205	2.885	3.030			
	4.215	1.731	2.706			
	4.54	5.093	3.200			
0.5	4.525	3.961	2.842	0.9998	1.52	3.318
	4.52	2.830	2.469			
	4.52	1.698	2.073			
	4.815	5.013	4.106			
0.25	4.845	3.899	3.437	0.9987	1.27	5.151
	4.84	2.785	2.852			
	4.81	1.671	2.319			

the average pH is close to that expected on the basis of pK^I and the value of n, the buffer ratio, eq. [3.6].

$$pH = pK^I - \log n \qquad [3.6]$$

The ratio of k_{HA} to k_{A^-} is approximately two for 3-methylbenzoic acid. As the benzoic acid chosen for study becomes stronger, this ratio will increase, making accurate determinations of k_{A^-} values more and more difficult. Until, for the stronger benzoic acids, catalysis by the conjugate benzoate anion becomes negligible. It is possible to measure k_{A^-} values for three other benzoate anions using the same method as that used for 3-methylbenzoate anion (i.e. plot of the slope of k_{obs} vs. [HA] against 1/n), albeit with standard deviations topping 20% in two of those cases. The corresponding k_{HA} values for the conjugate acids of these benzoate anions have much smaller standard deviations. The three benzoic acids which gave these results are 2-methyl, 2-ethoxy and the unsubstituted compound. The values of k_{HA} and k_{A^-} for these catalysts are given in Table 11.

Benzoic acids that are stronger than the group just mentioned give plots of the slope of k_{obs} vs. [HA] against 1/n with correlation coefficients less than 0.900 (the poor correlation coefficient reflecting the almost negligible contribution of the anion to the rate expression). For these compounds (3-fluoro, 3-nitro and 2-fluoro benzoic acids), the slopes of k_{obs} vs. $[A^-]$ are plotted against n to provide k_{HA} as the slope and k_{A^-} as the intercept. In this way, good correlation coefficients result ($\geq$0.993, reflecting the good precision

of the slope, k_{HA}) with almost negligible intercepts.

The results for 3-nitro and 2-fluorobenzoic acid are shown in Fig. 17 and are listed in Table 11, along with the results for 3-fluorobenzoic acid.

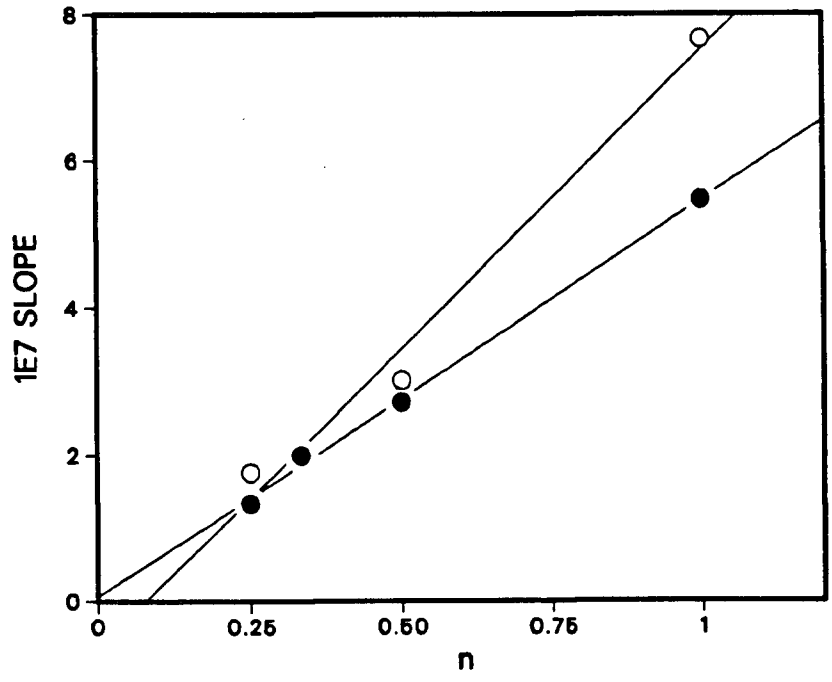

Fig. 17: Plots of (slope of k_{obs} vs. $[A^-]$) vs. n for (i) 3-nitrobenzoic acid (closed circles) giving r = 0.9990, k_{HA} = 5.40 ± 0.19 x 10^{-7} M^{-1} sec^{-1} (slope) and k_{A^-} = 6.87 ± 11.2 x 10^{-9} M^{-1} sec^{-1} (intercept) and for (ii) 2-fluorobenzoic acid (open circles) giving r = 0.9940, k_{HA} = 8.14 ± 0.69 x 10^{-7} M^{-1} sec^{-1} (slope) and k_{A^-} = -6.26 ± 4.14 x 10^{-8} M^{-1} sec^{-1} (intercept).

In addition to the seven benzoic acids discussed so far, two other benzoic acids were studied; 2-nitro and 2,6-dinitrobenzoic acid. These acids are stronger than chloroacetic acid and thus we can expect a large contribution to k_{obs} from the hydronium ion, necessitating a high concentration of HA to allow a measurement of the acid rate constants to

Table 11: k_{HA} and k_{A^-} values for acetone enolization catalyzed by benzoic acids and benzoates ions at 25°C and 0.1 M ionic strength

Substituent	10^7 k_{HA} M^{-1} sec^{-1}	10^7 k_{A^-} M^{-1} sec^{-1}	pK^T	br[a]	nk[b]	Method[c]
3-CH_3	1.61 ± 0.08	0.881 ± 0.031	4.27	3	-	I
H	2.46 ± 0.17	0.638 ± 0.069	4.20	5	-	I
2-C_2H_5O	3.05 ± 0.34	0.689 ± 0.149	4.16[d]	4	-	I
2-CH_3	4.16 ± 0.20	0.364 ± 0.071	3.91	4	-	I
3-F	3.39 ± 0.15	0.300 ± 0.087	3.86	4	-	II
3-NO_2	5.40 ± 0.19	0.069 ± 0.112	3.49	4	-	II
2-F	8.14 ± 0.69	-0.626 ± 0.414	3.27	4	-	II
2-NO_2	39.5 ± 2.4	-	2.21	-	11	IV
2,6-$(NO_2)_2$	166 ± 12	-	1.14	-	7	IV

a Number of buffer ratios used for methods I and II.

b Number of kinetic runs used for method IV.

c

Methods			Slope	Intercept
	I	(Slope of k_{obs} vs. [HA]) vs. 1/n	k_{A^-}	k_{HA}
	II	(Slope of k_{obs} vs. $[A^-]$) vs. n	k_{HA}	k_{A^-}
	IV	$(k_{obs} - k_{H^+}[H_3O^+])/[HA]$		

d pK determined in this laboratory (NV87).

be made. The relatively high solubility of these two benzoic acids makes this possible. The buffer-ratio method is of no use for these two relatively strong acids. Rather, as was the case with the di- and tri-halo aliphatic carboxylic acids (p. 83), a group of solutions at varying pH values and benzoic acid concentrations are prepared and k_{obs} measurements are made. The contribution from hydronium ion at each pH is subtracted from the corresponding k_{obs}, to provide the value of $k_{HA}[HA]$ for the appropriate benzoic acid concentration, eq. [3.15].

$$k_{obs} - k_{H^+}[H_3O^+] = k_{HA}[HA] \qquad [3.15]$$

The results for 2,6-dinitrobenoic acid are shown in Table 12. Unlike the case of the di- and tri-haloacids, which pose no solubility problems whatsoever, the range of accessible concentrations of 2,6-dinitrobenzoic acid is limited. For difluoroacetic acid (Table 8) the concentrations used spanned a factor of nine (1.3×10^{-1} M to 1.5×10^{-2} M), whereas for the benzoic acid, a concentration range of only two is possible (1.6×10^{-2} M to 7.6×10^{-3} M); the upper limit being imposed by the solubility of the acid and the lower limit being the minimum acid concentration needed for the acid to make a meaningful contribution to k_{obs}. The plot of ($k_{obs} - k_{H^+}[H_3O^+]$) against [HA] for 2,6-dinitrobenzoic acid gives a poor line ($r = 0.9716$) due to the small range of [HA] values used; Fig. 18 shows the result, with trichloroacetic acid also shown for comparison. A more appropriate means of determining k_{HA} for the pair of ortho-nitrobenzoic acids is the following; for each

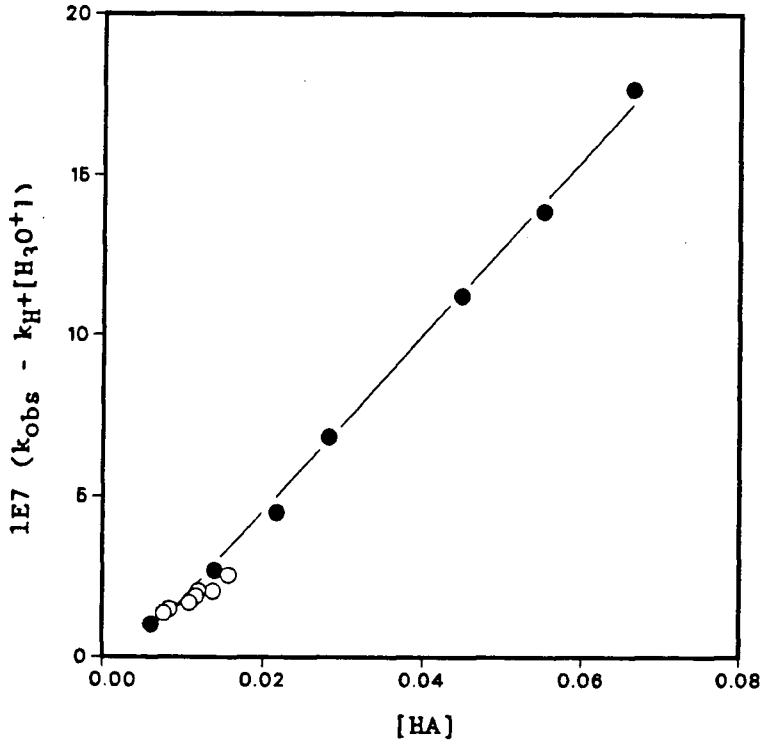

Fig. 18: Plot of ($k_{obs} - k_{H^+}[H_3O^+]$) vs. [HA] for 2,6-dinitrobenzoic acid (open circles) giving r = 0.9716, slope = 1.35 ± 0.15 x 10^{-5} M^{-1} sec^{-1} and intercept 3.31 ± 1.73 x 10^{-8} sec^{-1}. Corresponding plot for trichloroacetic acid added for comparison (closed circles).

value of ($k_{obs} - k_{H^+}[H_3O^+]$), division by [HA] provides the rate constant, k_{HA}. The resulting k_{HA} for 2,6-dinitrobenzoic acid (average value from seven kinetic runs) is 1.66 ± 0.12 x 10^{-5}, Table 12. This result and that obtained for 2-nitrobenzoic acid are at 0.1 M ionic strength and are listed in Table 11, along with the rate constants obtained for the seven other benzoic acids.

Table 12: Results of the kinetic runs for 2,6-dinitrobenzoic acid giving a value of $k_{HA} = 1.66 \pm 0.12 \times 10^{-5}$ M^{-1} sec^{-1} (obtained by dividing $(k_{obs} - k_{H^+}[H_3O^+])$ by [HA]).

pH	10^7 k_{obs} sec^{-1}	10^7 $(k_{obs} - k_{H^+}[H_3O^+])$ sec^{-1}	10^2 [HA],M	10^5 k_{HA} M^{-1} sec^{-1}
1.73	8.043	2.550	1.576	1.62
1.63	8.967	2.052	1.379	1.49
1.675	8.294	2.059	1.195	1.72
1.80	6.571	1.896	1.166	1.63
1.90	5.408	1.694	1.083	1.56
1.965	4.697	1.499	.835	1.80
1.89	5.174	1.374	.763	1.80

3.1.2 Diprotic Acids, Bifunctional Monoanions and Dianionic Bases

Carboxylic diprotic acids provide three catalytic entities for study, the neutral acid (H_2A), and monoanion (HA^-), and the dianion (A^{2-}).

In the case of dicarboxylic acids with K_1/K_2 values greater than 10^3, the two carboxylic acid ionizations are separate processes and such systems can be treated as two distinct dissociations; firstly the

diprotic acid to the conjugate monoanion; and then the monoanion to the conjugate dianion. In these situations, the appropriate kinetic treatment can be chosen from those described thus far for each acid/conjugate base pair, H_2A/HA^- and HA^-/A^{2-}. The appropriate kinetic treatment will depend on the relative magnitude of the two rate constants involved, k_{H_2A}/k_{HA^-} or $k_{HA^-}/k_{A^{2-}}$.

However, if the two pK values of the diprotic acids are separated by less than 2.7 units of pK, the two ionizations are said to overlap (AS84C). In such situations, the first dissociation (H_2A/HA^-) is not 100% complete before the next one begins (HA^-/A^{2-}) and all three species H_2A, HA^- and A^{2-} are simultaneously present to some degree. The concentrations of the three species can be determined using eqs. [3.16]-[3.19], knowing $[H^+]$, K_1^I and K_2^I (equilibrium constants at the appropriate ionic strength) and C_{TOT}, the total concentration of diacid, monoanion and dianion present (R81c).

$$D = [H^+]^2 + K_1^I[H^+] + K_1^I K_2^I \qquad [3.16]$$

$$[H_2A]/C_{TOT} = [H^+]^2/D \qquad [3.17]$$

$$[HA^-]/C_{TOT} = K_1^I[H^+]/D \qquad [3.18]$$

$$[A^{2-}]/C_{TOT} = K_1^I K_2^I/D \qquad [3.19]$$

Five aliphatic dicarboxylic acids were studied; two of these diacids have pK_1 and pK_2 values separated by more than 2.7 pK units, i.e. oxalic

acid and diethylmalonic acid; the other three diacids have 'overlapping' pK values, i.e. succinic acid, 3-methyl and 3,3-dimethylglutaric acid.

For oxalate monoanion and dianion (pK_2 = 4.29), the rate law shown in eq. [3.20] is applicable. At buffer-ratios of m = $[HA^-]/[A^{2-}]$, eq. [3.20] can be rewritten as eqs. [3.21] or [3.22].

$$k_{obs} = k_{sum} + k_{HA^-}[HA^-] + k_{A^{2-}}[A^{2-}] \qquad [3.20]$$

$$k_{obs} = k_{sum} + [HA^-]\,(k_{HA^-} + (1/m)k_{A^{2-}}) \qquad [3.21]$$

$$k_{obs} = k_{sum} + [A^{2-}]\,(k_{A^{2-}} + mk_{Ha^-}) \qquad [3.22]$$

For each buffer-ratio, m, a plot of k_{obs} vs. $[HA^-]$ will have a slope $(k_{HA^-} + (1/m)k_{A^{2-}})$. Plotting this slope against 1/m provides k_{HA^-} as the intercept and $k_{A^{2-}}$ as the slope (eq. [3.21]). Conversely the slopes of the lines resulting from plots of k_{obs} vs. $[A^{2-}]$ can be plotted against m giving $k_{A^{2-}}$ as the intercept and k_{HA^-} as the slope (eq. [3.22]).

Three buffer-ratios provided the results shown in Fig. 19 for oxalate monoanion and dianion at 0.1 M ionic strength. The larger standard deviation of the dianion rate constant compared to the monoanion rate constant reflects the fact that k_{HA^-} is approximately 13 times $k_{A^{2-}}$.

The buffer-ratios used were 0.8, 0.5 and 0.25 and the pH value of these buffer-ratio sets are close to that expected on the basis of eq.

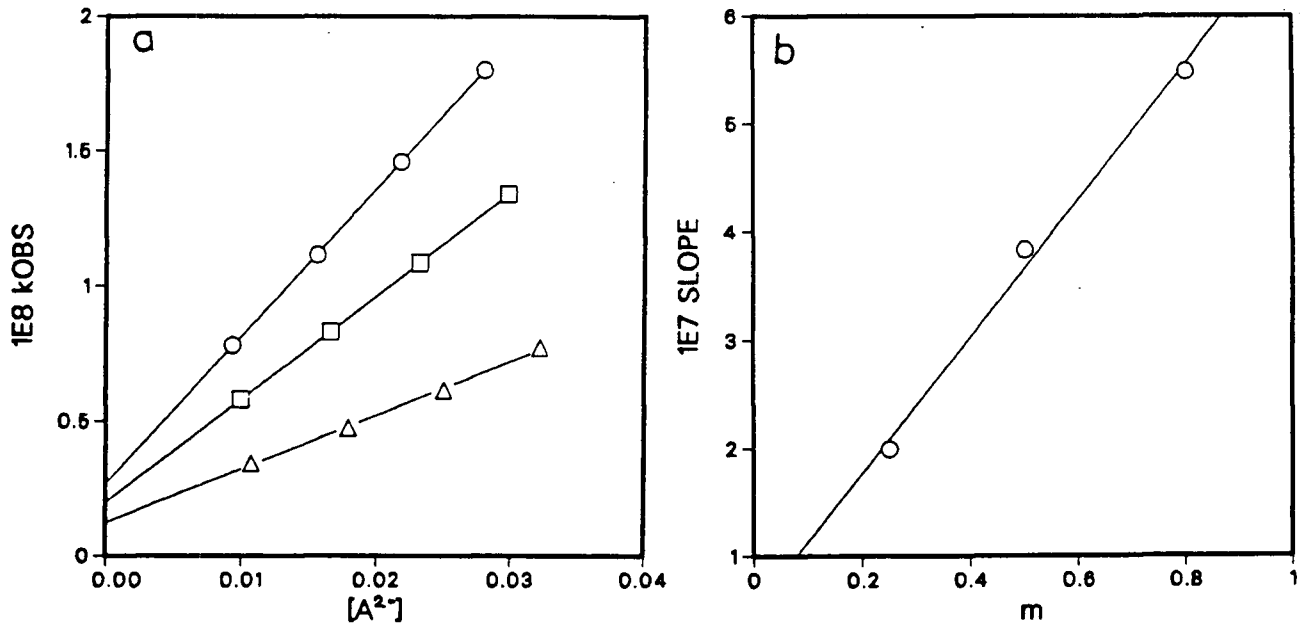

Fig. 19: (a) Plots of k_{obs} vs. $[A^{2-}]$ for oxalate monoanion/dianion buffers; (b) Plot of (slope of k_{obs} vs. $[A^{2-}]$) vs. m for oxalate monoanion/dianion giving r = 0.9965, k_{HA^-} = 6.32 ± 0.53 x 10^{-7} M^{-1} sec^{-1} (slope) and $k_{A}2^-$ = 5.05 ± 2.98 x 10^{-8} M^{-1} sec^{-1} (intercept).

[3.23], pK^I being equal to pK^T - 0.33 at 0.1 M ionic strength from eq. [3.24] (AS84d).

$$pH = pK_2{}^I - \log m \qquad [3.23]$$

$$pK_2{}^I = pK^T - (1.5345\sqrt{I})/1 + 1.5\sqrt{I}) \qquad [3.24]$$

As $pK_2{}^T$ = 4.29, $pK_2{}^I$ = 3.96 therefore the pH_{calc} values are 4.06, 4.26 and 4.56, at m values of 0.8, 0.5 and 0.25. The experimental pH values for the buffer solution are 4.08 (m = 0.8) 4.29 (m = 0.5) and

4.57 (m = 0.25), each value being the average ± 0.01, of the four members of that particular buffer-ratio set.

For oxalic acid and oxalate monoanion (pK_1 = 1.25), the rate law shown in eq. [3.25] is applicable. As in the case of the di- and tri-halo aliphatic carboxylic acids, the buffer-ratio method cannot be used for the diacid and monoanion species since the pK_1 value is so low.

$$k_{obs} = k_{H^+}[H_3O^+] + k_{H_2A}[H_2A] + k_{HA^-}[HA^-] \qquad [3.25]$$

Unlike the case of the halo aliphatic carboxylic acids, the conjugate base of the diacid, HA^-, does contribute to the observed rate. It may be recalled that the anion, A^-, does not contribute to the rate for the halo acids. The presence of the monoanion term, $k_{HA^-}[HA^-]$, is evident from the kinetic results shown in Table 13, where the results of eight individual kinetic runs are shown. Use of eq. [3.26] gives 8 values of k_{H_2A}, obtained by dividing ($k_{obs} - k_{H^+}[H_3O^+]$) by $[H_2A]$, that show a large degree of scatter.

$$k_{obs} - k_{H^+}[H_3O^+] = k_{H_2A}[H_2A] \qquad [3.26]$$

$$k_{obs} - k_{H^+}[H_3O^+] - k_{HA^-}[HA^-] = k_{H_2A}[H_2A] \qquad [3.25]$$

On the other hand use of eq. [3.25], which includes the monoanion term gives more consistent values of k_{H_2A}, Table 13.

The rate constant used for HA^- is that determined from the kinetics at various m buffer-ratios values ($[HA^-]/[A^{2-}]$), as described

Table 13: Results of the kinetic runs for oxalic acid giving a value of $k_{H_2A} = 13.6 \pm 2.5 \times 10^{-6}$ M^{-1} sec^{-1} using eq. [3.26] and $k_{H_2A} = 11.6 \pm 1.5 \times 10^{-6}$ M^{-1} sec^{-1} using eq. [3.25]

pH	10^6 k_{obs} sec^{-1}	$[H_2A]$, M	$[HA^-]$, M	10^6 k_{H_2A}[a] M^{-1} sec^{-1}	10^6 k_{H_2A}[b] M^{-1} sec^{-1}
1.21	3.367	0.1411	0.1631	11.0	10.2
1.235	3.041	0.1243	0.1495	10.7	9.89
1.31	2.503	0.0970	0.1463	10.9	9.95
1.37	2.190	0.0587	0.1440	15.9	14.3
1.51	1.554	0.0502	0.1120	12.8	11.4
1.75	0.968	0.0295	0.1124	15.0	12.6
1.93	0.636	0.0187	0.1030	15.5	12.0
2.04	0.526	0.0152	0.1065	16.8	12.4

[a] Using eq. [3.26], excluding monoanion term.

[b] Using eq. [3.25], including monoanion term.

previously, i.e. 6.32×10^{-7} M^{-1} sec^{-1}. The concentrations of H_2A and HA^- are given by eqs. [3.27] and [3.28], where $[H_2A]_o$ is the initial concentration of oxalic acid, $[B^-]$ is the concentration of base added and $[H^+]$ is calculated from the pH measurement (AS84b).

$$[H_2A] = [H_2A]_o - [B^-] - [H^+] \qquad [3.27]$$

$$[HA^-] = [B^-] + [H^+] \qquad [3.28]$$

The mean value of k_{H_2A} is $11.6 \pm 1.5 \times 10^{-6}$ M^{-1} sec^{-1}; the plot of $(k_{obs} - k_{H^+}[H_3O^+] - k_{HA^-}[HA^-])$ vs. $[H_2A]$ gives a reasonable line with $r = 0.9852$, $k_{H_2A} = 9.51 \pm 0.68 \times 10^{-6}$ M^{-1} sec^{-1} (slope) and a negligible intercept of $9.39 \pm 5.46 \times 10^{-8}$ M^{-1} sec^{-1}. The ionic strength of the solutions was not kept constant and varied from 0.2 to 0.1 M, the variation showing no dramatic effects on resulting k_{H_2A} values.

The second dicarboxylic acid studied was diethylmalonic acid. At m buffer-ratios of 2 and 1, the kinetic results showed negligible catalysis by the monoanion and so eq. [3.20] simplifies to eq. [3.29]

$$k_{obs} = k_{sum} + k_{HA^-}[HA^-] + k_{A^{2-}}[A^{2-}] \qquad [3.20]$$

$$k_{obs} = k_{sum} + k_{A^{2-}}[A^{2-}] \qquad [3.29]$$

Use of eq. [3.21] which provides k_{HA^-} as the intercept and $k_{A^{2-}}$ as the slope, showed a negligible value for the intercept. Accordingly eq. [3.29] was used for each buffer ratio (plot of k_{obs} vs. $[A^{2-}]$) giving a

value of k_A2- for the slope and k_{sum} for the intercept. The results of two buffer-ratios gave an average value of $k_A2^- = 1.59 \pm 0.15 \times 10^{-6}$ M^{-1} sec^{-1}, at 0.05 M ionic strength. At an ionic strength of 0.15 M (m = 0.5), a k_A2-value of 1.63×10^{-6} M^{-1} sec^{-1} resulted, a value very close to that at 0.05 M ionic strength, illustrating the very small effect of ionic strength on the k_A2^- value.

The value of k_{H_2A} for diethylmalonic acid is determined using eq. [3.26] in a similar treatment to that used for oxalic acid. (Note that the monoanion is not involved in the rate law.) A plot of ($k_{obs} - k_H+[H_3O^+]$) against $[H_2A]$ gives a straight line, r = 0.9988, with $k_{H_2A} = 1.32 \pm 0.04 \times 10^{-6}$ M^{-1} sec^{-1} (slope) and a negligible intercept $1.30 \pm 0.28 \times 10^{-8}$ M^{-1} sec^{-1}. Thus for diethylmalonic acid, the monoanion makes no significant contribution to k_{obs} at pH values close to either pK_1 or pK_2.

Of the three aliphatic dicarboxylic acids studied that have overlapping pK_1 and pK_2 values (i.e. $pK_2 - pK_1 < 2.7$), 3-methylglutaric acid ($pK_1 = 4.35$, $pK_2 = 5.44$) has the smallest difference between pK_1 and pK_2 i.e. the greatest degree of overlap of the two dissociations. Ignoring this overlap and treating this diacid in the same manner as oxalic acid gives the result shown in Fig. 20; the plot of the slope of (k_{obs} vs. $[HA^-]$) against 1/m giving k_A2^- as the slope and k_{HA^-} as the intercept. The buffer-ratios are chosen to minimize the extent of the overlap of both ionizations; m values favouring the dianion i.e. m = 0.8, 0.5 and 0.25 will result in small concentrations of the diacid being present.

It is possible to use this experimental data, taking account of the overlapping ionization constants, to determine the concentrations of all

three species using eqs. [3.16]-[3.19]. When this is done, we find that the concentration of the diacid, H_2A, is only between 0.3-2.2% of the total concentration and is assumed to make a negligible contribution to k_{obs}. Plots of k_{obs} vs. $[HA^-]$ thus calculated are linear. A subsequent plot of the slope of these lines against the calculated 1/m values is shown in Fig. 20 along with the result obtained by ignoring the overlapping dissociation constants. The end results of the two approaches are very similar; ignoring the overlapping K values gives $k_{HA^-} = 3.17 \times 10^{-7}$ M^{-1} sec^{-1} and $k_A2^- = 4.10 \times 10^{-7}$ M^{-1} sec^{-1}; considering the overlapping K values (and ignoring the $k_{H_2A}[H_2A]$ term) gives $k_{HA^-} = 3.33 \times 10^{-7}$ M^{-1} sec^{-1} and $k_A2^- = 4.02 \times 10^{-7}$ M^{-1} sec^{-1}.

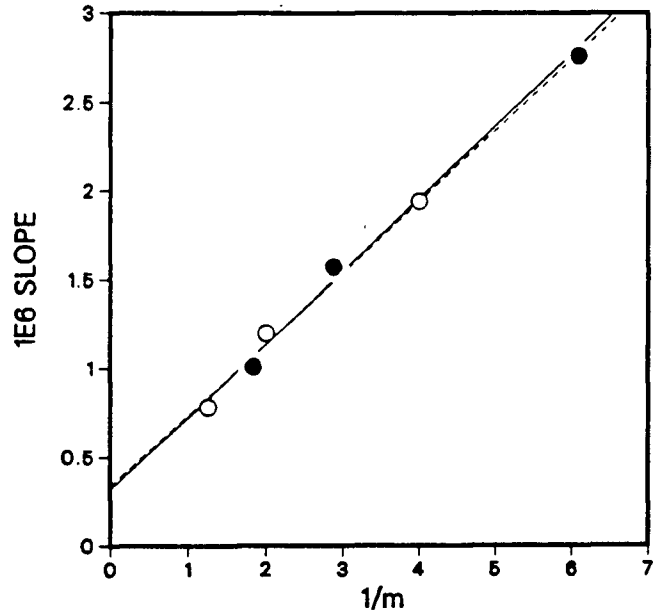

Fig. 20: Plots of (slope of k_{obs} vs. $[HA^-]$) vs. 1/m for 3-methylglutarate monoanion/dianion; (a) ignoring the overlapping K values (open circles, solid line) giving r = 0.9952, $k_{HA^-} = 3.17 \pm 1.07 \times 10^{-7}$ M^{-1} sec^{-1} (intercept) and $k_A2^- = 4.10 \pm 0.40 \times 10^{-7}$ M^{-1} sec^{-1} (slope). (b) considering the overlapping K values (closed circles, dashed line) giving r = 0.9966, $k_{HA^-} = 3.33 \pm 1.33 \times 10^{-7}$ M^{-1} sec^{-1} (intercept) and $k_A2^- = 4.02 \pm 0.33 \times 10^{-7}$ M^{-1} sec^{-1} (slope).

It is possible to include a correction for k_{H_2A} in the latter treatment. Since the pK_1 of the diacid (4.35) is close to that of phenylacetic acid (4.31), the k_{HA} value for the monoacid (Table 7, p. 80) could be used as an approximate value for k_{H_2A}. Using this value (1.92×10^{-7} M^{-1} sec^{-1}) and the concentrations determined previously, appropriate $k_{H_2A}[H_2A]$ terms are subtracted from k_{obs} prior to the plotting of k_{obs} vs. $[HA^-]$. The net result is little change in the monoanion and dianion rate constants from that obtained by ignoring any involvement of the diacid; $k_{HA^-} = 3.18 \pm 1.35 \times 10^{-7}$ M^{-1} sec^{-1} and $k_{A^{2-}} = 4.04 \pm 0.34 \times 10^{-7}$ M^{-1} sec^{-1}.

From these calculations and similar treatment of the data for 3,3-dimethylglutaric acid and succinic acid, it is obvious that ignoring the overlapping dissociations and assuming two distinct ionizations has only a little effect on the values of rate constants obtained.

For the sake of simplicity, the results quoted are those obtained by treating the two dissociations (H_2A/HA^- and HA^-/A^{2-}) as separate steps. For the second dissociation buffer-ratios ($[HA^-]/[A^{2-}]$) less than 1 are generally chosen to help negate the small errors resulting from this approach, i.e. buffer ratios with the dianion as the major of the three species and negligible diacid concentrations. For the first dissociation (k_{H_2A}/k_{HA^-} measurments), buffer ratios ($[H_2A]/[HA^-]$) greater than 1 are chosen i.e. buffer ratios with the diacid as the major of the three species and negligible dianion concentrations.

The results for succinic acid from both the $n([H_2A]/[HA^-])$ and $m([HA^-]/[A^{2-}]$ buffer-ratios are shown in Fig. 21; the two values of k_{HA^-} resulting from each treatment agree reasonably well. The result from n

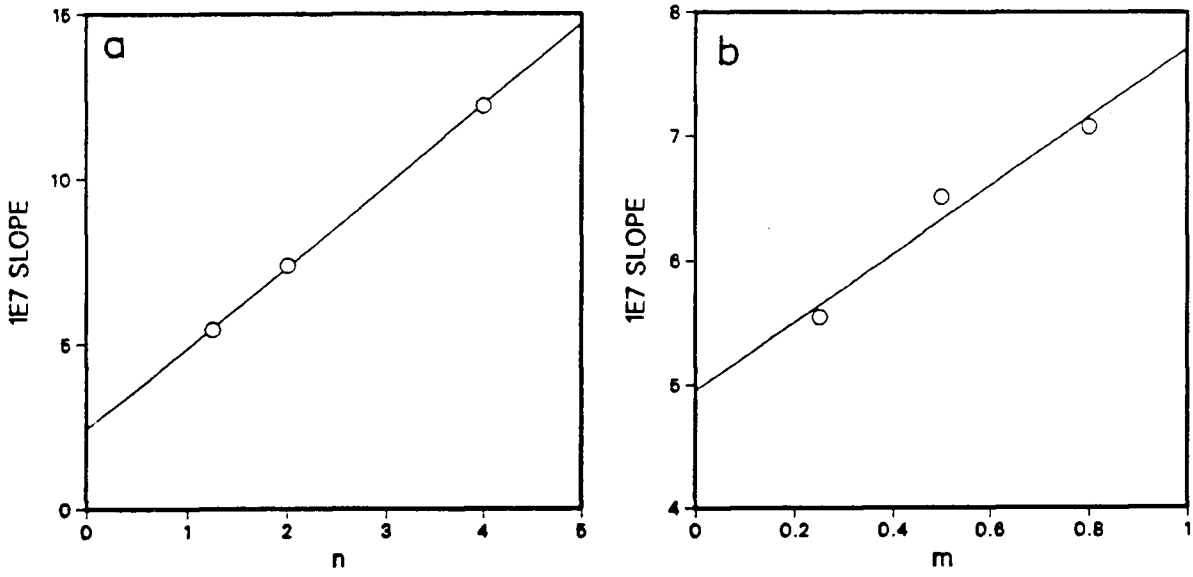

Fig. 21: (a) Plot of (slope of k_{obs} vs. $[HA^-]$) vs. n for succinic acid/monoanion buffers giving r = 0.9998, k_{H_2A} = 2.44 ± 0.04 x 10^{-7} M^{-1} sec^{-1} (slope) and k_{HA^-} = 2.45 ± 0.11 x 10^{-7} M^{-1} sec^{-1} (intercept). (b) Plot of (slope of k_{obs} vs. $[A^{2-}]$) vs. m for succinate monoanion/dianion buffers giving r = 0.9793, k_{HA^-} = 2.75 ± 0.57 x 10^{-7} M^{-1} sec^{-1} (slope) and $k_{A^{2-}}$ = 4.96 ± 0.32 x 10^{-7} M^{-1} sec^{-1} (intercept).

buffer-ratios gives a value of k_{HA^-} = 2.45 ± 0.11 x 10^{-7} M^{-1} sec^{-1}, while a value of 2.75 ± 0.57 x 10^{-7} M^{-1} sec^{-1} is obtained from the m buffer ratios.

For 3,3-dimethylglutaric acid, it was impossible to determine a value of k_{HA^-} at the second dissociation buffer values as it was swamped by the larger dianion rate constant. The plot of k_{obs} vs. $[A^{2-}]$ at M values of 0.5 and 1 gives an average value of $k_{A^{2-}}$ = 7.74 ± 0.02 x 10^{-7} M^{-1} sec^{-1} (slope). At buffer ratios close to the first dissociation, both k_{HA^-} and k_{H_2A} can be determined by plotting the slope of (k_{obs} vs. $[H_2A]$) against 1/n, giving r = 0.9976, k_{H_2A} = 2.44 ± 0.07 x 10^{-7} M^{-1} sec^{-1} (intercept) and k_{HA^-} = 7.95 ± 0.55 x 10^{-8} M^{-1} sec^{-1} (slope).

For the five diacids just discussed, solubility is no problem and the only limitations to obtaining a particular rate constant are either

(i) a reaction of the species present wth triiodide ion or (ii) the fact that the rate constant makes a negligible contribution to the rate expression In the case of aromatic dicarboxylic acids, solubility is a problem and measurements of k_{H_2A} values are impossible. However, by working at buffer ratios favouring the dianion (i.e. $m < 1$), the solubility factor can be mitigated somewhat, and measurements of k_{HA^-} and $k_{A^{2-}}$ can be made.

For phthalic acid, a plot of (slope of k_{obs} vs. $[A^{2-}]$) against m at four buffer ratios gave the following results (0.05 M ionic strength); r = 0.9876, $k_{A^{2-}} = 2.78 \pm 0.11 \times 10^{-7}$ M^{-1} sec^{-1} (intercept) $k_{HA^-} = 1.59 \pm 0.18 \times 10^{-7}$ M^{-1} sec^{-1} (slope). These results, and the results of the five aliphatic carboxylic acids are shown in Table 14.

In order to further evaluate the steric effect of ortho substituents in aromatic carboxylic acids, we decided to study a group of isophthalic acids. Measurements of the k_{H_2A} values are impossible due to the poor solubility of the diacid in water. However, values of both k_{HA^-} and $k_{A^{2-}}$ should be accessible.

We needed a set of self-consistent pK values (measured in water) for a group of both 5-substituted (meta) and 2-substituted (ortho) isophthalic acids. While data exist for an extensive set of 5-substituted derivatives in 50 wt % aqueous methanol (GS84); pK values in water have not been reported, except for the unsubstituted isophthalic acid; $pK_1 = 3.62$, $pK_2 = 4.60$ (KV61).

Accordingly, we measured the first and second dissociation constants of seven 2-substituted isophthalic acids and corrected them to the standard state. These acids are soluble enough to allow accurate

Table 14: k_{H_2A}, k_{HA^-} and $k_{A^{2-}}$ values for acetone enolization at 25°C for a group of aliphatic carboxylic acids and phthalic acid. Ionic strength 0.10 M unless otherwise stated.

Acid	10^7 k_{H_2A} M^{-1} sec^{-1}	10^7 k_{HA^-} M^{-1} sec^{-1}	10^7 $k_{A^{2-}}$ M^{-1} sec^{-1}	pK_1	pK_2
Oxalic	95.1 ± 6.8[a]	6.32 ± 0.53	0.505 ± 0.298	1.25	4.29
Diethylmalonic	13.2 ± 0.4	-	15.9 ± 1.5[b]	2.21	7.29
3-Methylglutaric	-	3.17 ± 1.07[b]	4.10 ± 0.40[b]	4.35	5.44[c]
3,3-Dimethyl-glutaric	2.44 ± 0.07	0.795 ± 0.055	7.74 ± 0.02[b]	3.85	6.45[c]
Succinic	2.44 ± 0.04	2.45 ± 0.11	4.96 ± 0.32	4.20	5.63[d]
Phthalic	-	1.59 ± 0.18[b]	2.78 ± 0.11[b]	2.91	5.41[e]

[a] Ionic strength varied from 0.1 to 0.2 M.

[b] Ionic strength 0.05 M.

[c] pK values from ref. (BB65).

[d] pK values from ref. (AS84d).

[e] pK values determined in this laboratory (NV87)

determinations of the pK_1 values. A group of seven 5-substituted isophthalic acids was also examined with the limitation of decreased solubility as compared to the 2-substituted acids. Accordingly the pK_1 values determined for these seven acids have a relatively large average deviation of ± 0.05; the results are listed in Table 15 along with those of the 2-substituted acids and the unsubstituted compound. The average deviation for all the pK values quoted, excluding the pK_1 values of the 5-substituted acids, is ± 0.02. For 5-bromoisophthalic acid, questionable results were obtained for pK_2. The value of 4.57 is too high on the basis of the values of the other 5-halo acids (5-F, 4.39; 5-I, 4.41) and so it was discarded. Instead, both pK_1 and pK_2 for this bromo acid were determined from the Hammett plot for six 5-substituted isophthalic acids. In the case of 5-methylisophthalic acid, where solubility is a major problem, pK values were also calculated from the Hammett plots.

The Hammett plots are shown in Fig. 22 using σ values recommended by Perrin, Demsey and Serjeant for meta substituents (PD81), values that are listed in Table 15.

The resulting Hammett equations for pK_1 and pK_2 are shown in eqs. [3.30] and [3.31]. The poorer correlation coefficient for the pK_1 line reflects the poorer degree of accuracy of the pK_1 measurements due to poor solubility. From these lines, pK_1 and pK_2 values for 5-bromo and 5-methylisophthalic acid are determined, and these are listed in Table 15.

Table 15: Dissociation constants of isophthalic acids in water at 25°C, corrected to zero ionic strength[a]

Substituent	pK_1	pK_2	σ_{meta}
H	3.61	4.75	0.00
5-OH	3.56	4.62	0.13
5-OCH_3	3.46	4.67	0.12
5-I	3.28	4.41	0.35
5-F	3.24	4.39	0.34
5-NO_2	2.88	4.04	0.71
5-Br	3.21[b]	4.36[b]	0.39
5-CH_3	3.68[b]	4.82[b]	-0.06
2-CH_3	2.92	4.25	-
2-OCH_3	2.91	4.32	-
2-$NHCOCH_3$	3.10	4.52	-
2-Cl	2.12	3.38	-
2-Br	1.91	3.28	-
2-I	1.94	3.32	-
2-NO_2	1.85	3.01	-

a pK values determined in this laboratory (NV87).

b pK values calculated from the Hammett plots, see text.

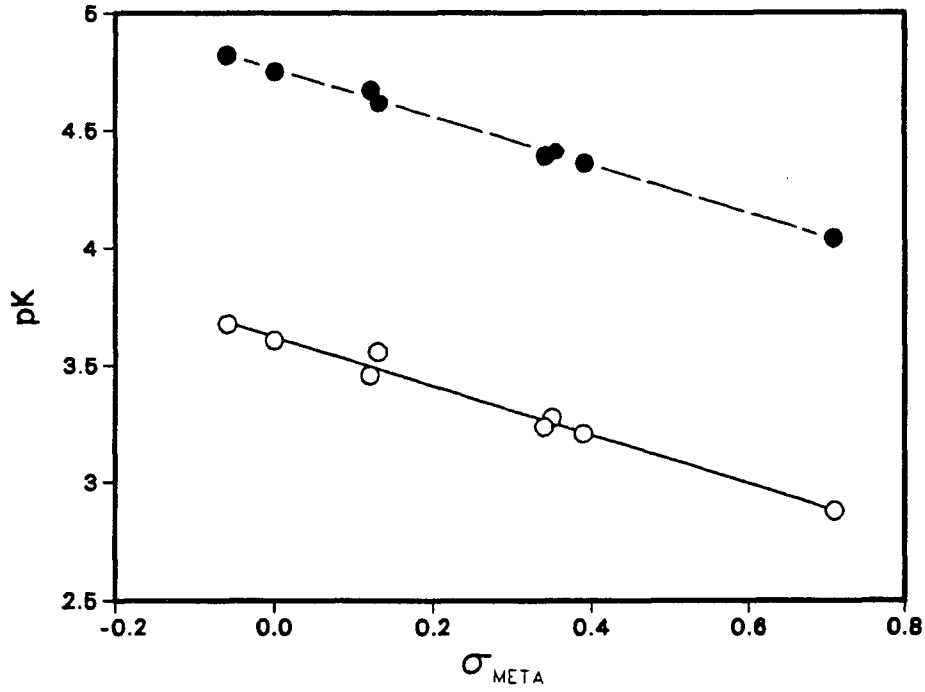

Fig. 22: Plot of pK_1 (lower line) and pK_2 (upper line) for 5-substituted isophthalic acids in water at 25°C against the Hammett meta-substituent constant; the ρ values are 1.05 (pK_1) and 1.02 (pK_2).

$$r = 0.9893 \qquad pK_1 = -1.05\,\sigma + 3.62 \qquad [3.30]$$

$$r = 0.9973 \qquad pK_2 = -1.02\,\sigma + 4.76 \qquad [3.31]$$

The kinetic treatment used to determine k_{HA^-} and $k_{A^{2-}}$ values is the same as that used for phthalic acid. Using at least three buffer ratios favouring the dianion (m = 0.8, 0.5, 0.33, and 0.25), and ignoring the overlapping dissociations, plots of the slope of (k_{obs} vs. $[A^{2-}]$) against m afford $k_{A^{2-}}$ as the intercept and k_{HA^-} as the slope. For most of the isophthalic acids studied, catalysis by the dianion was negligible. The results for isophthalic, 5-nitroisophthalic and 2-bromoisophthalic acids are shown in Fig. 23.

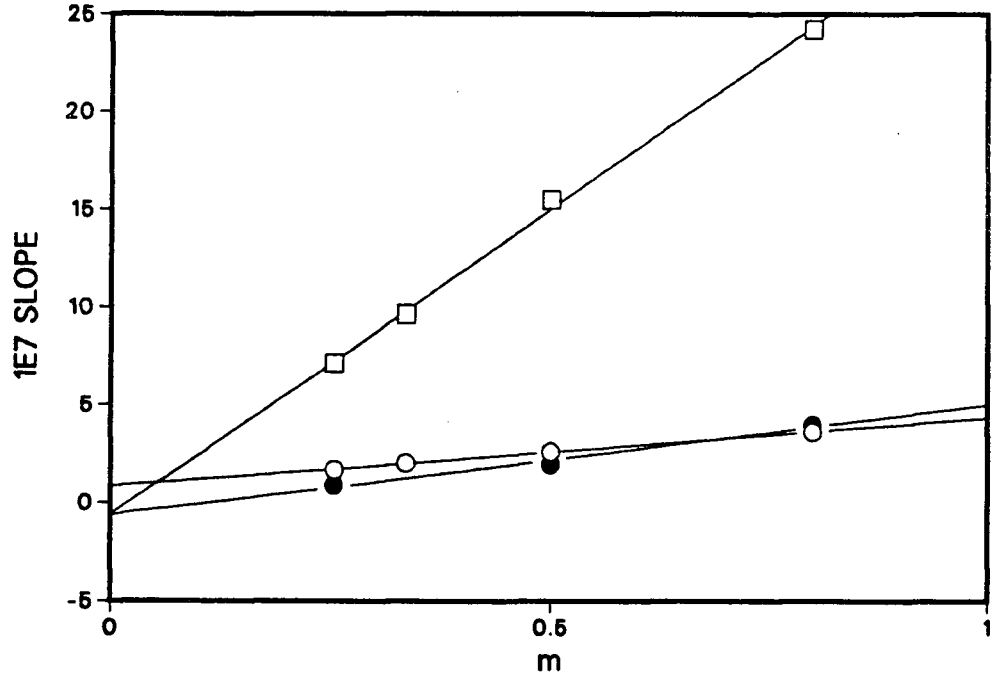

Fig. 23: Plots of (slope of k_{obs} vs. $[A^{2-}]$) vs. m for (a) isophthalic acid (open circles) giving r = 0.9996, k_{HA^-} = 3.45 ± 0.07 x 10^{-7} M^{-1} sec^{-1} (slope) and k_A2^- = 8.49 ± 0.37 x 10^{-8} M^{-1} sec^{-1} (intercept). (b) 5-Nitroisophthalic acid (closed circles) giving r = 0.9924, k_{HA^-} 5.59 ± 0.69 x 10^{-7} M^{-1} sec^{-1} and and k_A2^- = -6.23 ± 3.90 x 10^{-8} M^{-1} sec^{-1}. (c) 2-Bromoisophthalic acid (open squares) giving r = 0.9992, k_{HA^-}= 3.12 ± 0.09 x 10^{-6} M^{-1} sec^{-1} and k_A2^- = -5.86 ± 4.54 x 10^{-8} M^{-1} sec^{-1}.

The results for eleven isophthalic acids (including six 2-substituted) are listed in Table 16; only two meaningful values of k_A2^- were obtained, i.e. values for 5-methyl and the unsubstituted acid.

The experimental results can be used to determine k_{HA^-}/k_A2^- values taking account of the overlapping dissociations of the two carboxylic acid moieties, as was illustrated previously for 3-methylglutaric acid (p. 105) using eqs. [3.16]-[3.19]. The results differ slightly from those obtained by treating the two dissociations as distinct processes;

Table 16: k_{HA}- and (some) k_A2- values for acetone enolization at 25°C and 0.05 M ionic strength for a group of isophthalic acids. Rate constants are determined by ignoring the overlapping dissociations.

Substituent	10^7 k_{HA}- M^{-1} sec^{-1}	10^7 k_A2- M^{-1} sec^{-1}	br[a]
5-CH_3	2.86 ± 0.33	0.917 ± 0.123	3
H	3.45 ± 0.07	0.849 ± 0.037	4
5-Br	3.88 ± 0.23	-0.184 ± 0.085	3
5-I	3.97 ± 0.29	0.047 ± 0.110	3
5-NO_2	5.59 ± 0.69	0.623 ± 0.390	3
2-OCH_3	6.56 ± 0.26	-0.195 ± 0.098	3
2-CH_3	7.95 ± 0.61	-0.084 ± 0.230	3
2-Cl	25.2 ± 0.4	-0.521 ± 0.231	4
2-Br	31.2 ± 0.9	-0.586 ± 0.454	4
2-I	34.7 ± 1.5	1.44 ± 0.56	3
2-NO_2	34.6 ± 0.6	-0.600 ± 0.237	3

[a] Number of buffer ratios used.

the values of k_{HA^-} are all increased by a factor of approximately 1.2. The results using this method are listed in Table 17. All the results for the dicarboxylic acids will be discussed in detail later.

Table 17: k_{HA^-} and (some) k_A2^- values for acetone enolization at 25°C and 0.05 M ionic strength for a group of isophthalic acids. Rate constants are determined by considering the overlapping dissociations.

Substituent	10^7 k_{HA^-} M^{-1} sec^{-1}	10^7 k_A2^- M^{-1} sec^{-1}	br[a]
5-CH_3	3.28 ± 0.27	1.09 ± 0.05	3
H	4.09 ± 0.06	0.985 ± 0.020	4
5-Br	4.77 ± 0.03	0.383 ± 0.004	3
5-I	4.88 ± 0.16	0.512 ± 0.039	3
5-NO_2	6.88 ± 0.47	0.157 ± 0.132	3
2-OCH_3	7.23 ± 0.23	0.319 ± 0.057	3
2-CH_3	8.09 ± 0.95	0.460 ± 0.266	3
2-Cl	32.6 ± 0.9	0.289 ± 0.288	4
2-Br	43.3 ± 1.1	0.147 ± 0.331	4
2-I	47.2 ± 2.1	0.422 ± 0.586	3
2-NO_2	44.3 ± 3.9	1.08 ± 0.88	3

3.2 Arylphosphonic acids

3.2.1 pK determinations

There are a number of reports in the literature of the effect of substituents on the pK_1 and pK_2 values of arylphosphonic acids, most notably those of Jaffe and co-workers (JF53, JF54) and of Nuallain (N74). The data of Jaffe and co-workers include ortho, meta and para derivatives but the pK values are not thermodynamic values; the data of Nuallain, which are much less extensive, have been corrected for ionic strength effects but include only two ortho compounds. Since we needed a set of self-consistent pK values for our catalytic work we have measured the first and second dissociation constants of 36 arylphosphonic acids and corrected them to the standard state, and these are listed in Table 18.

As in the case of carboxylate buffers the rates of enolization of acetone were determined iodometrically by following the decrease in the absorbance of the triiodide ion. Since $K_1/K_2 \approx 10^5$, the two ionizations of the diacid are distinct processes; the catalytic activity of the diacid and dianion can therefore be treated separately, while the monoanion will be involved with both of these species.

3.2.2 Phosphonate dianions

The dependence of k_{obs} upon the composition of the buffers is given

Table 18: Dissociation constants of arylphosphonic acids in water at 25°C, corrected to zero ionic strength[a]

Substituent	pK_1	pK_2
H	1.86	7.51
3-CH_3	1.95	7.64
4-CH_3	2.00	7.68
4-C_2H_5	1.99	7.65
3-CH_3O	1.74	7.42
4-CH_3O	2.00	7.68
4-C_2H_5O	2.00	7.65
3-F	1.53	7.16
3-Cl	1.53	7.10
4-Cl	1.58	7.23
4-Br	1.54	7.18
4-CN	1.27	6.79
3-NO_2	1.20	6.69
4-NO_2	1.19	6.67
4-NH_2	-	7.84
β-naphthyl	- [b]	7.42
3-carboxy	1.55	7.78[c,d]
4-carboxy	1.51	7.64[c,e]
3,4-$(CH_3)_2$	2.04	7.76
3,5-$(CH_3)_2$	2.01	7.73
2-CH_3	2.08	7.92
2-C_2H_5	2.11	8.09
2-$(CH_3)_2CH$	2.13	8.18
2-CH_3O	2.21	8.21
2-C_2H_5O	2.32	8.42
2-F	1.49	7.19
2-Cl	1.56	7.39
2-Br	1.53	7.37
2-I	1.56	7.46
2-NO_2	1.28	7.05
α-naphthyl	- [b]	7.64
2,3-$(CH_3)_2$	2.17	8.07
2,4-$(CH_3)_2$	2.17	8.07
2,5-$(CH_3)_2$	2.10	8.00
2,6-$(CH_3)_2$	2.39	8.62
2,4,6-$(CH_3)_3$	2.53	8.82

[a] pK values determined in this laboratory (NS87).
[b] Erratic values obtained, likely because of low solubility.
[c] pK_3
[d] $pK_2 = 4.37$
[e] $pK_2 = 4.27$

by eq. [3.20] which can be rewritten as eqs. [3.21] or [3.22], where m is the buffer ratio of monoanion to dianion ($[HA^-]/[A^{2-}]$).

$$k_{obs} = k_{sum} + k_{HA^-}[HA^-] + k_{A}^{2-}[A^{2-}] \qquad [3.20]$$

$$k_{obs} = k_{sum} + [HA^-]\{k_{HA^-} + (1/m)k_{A}^{2-}\} \qquad [3.21]$$

$$k_{obs} = k_{sum} + [A^{2-}]\{k_{A}^{2-} + m \cdot k_{HA^-}\} \qquad [3.22]$$

So a plot of k_{obs} vs. $[HA^-]$ should give a line with slope $\{k_{HA^-} + (1/m)k_{A}^{2-}\}$, which can be plotted vs. 1/m to give k_{HA^-} (intercept) and k_{A}^{2-} (slope).

The results for phenylphosphonate buffers are shown in Table 19, and plotted in Fig. 24, showing negligible catalysis by the monoanion. Likewise, the results for 3,4-dimethylphenylphosphonate are listed in Table 20, and shown in Fig. 25.

Individual sets of buffer ratios showed more internal scatter in pH values (± 0.05) than was the case with monocarboxylic acids (± 0.02), the variance being more pronounced in the higher pH values. This was attributed to the low concentrations of buffer used (0.002-0.02 M) and the wide span of concentrations used at each buffer-ratio (generally a factor of 8). All the measurements for phosphonate dianions were made at 0.05 ionic strength, which resulted in a pK_2^I value = pK_2^T - 0.26, as calculated from eq. [3.24] (AS84d). Ionic strength effects are greater for monoanion/dianion equilibria (eq. [3.24]) than for acid/monoanion equilibria (eq. [3.7]); for example using this latter equation

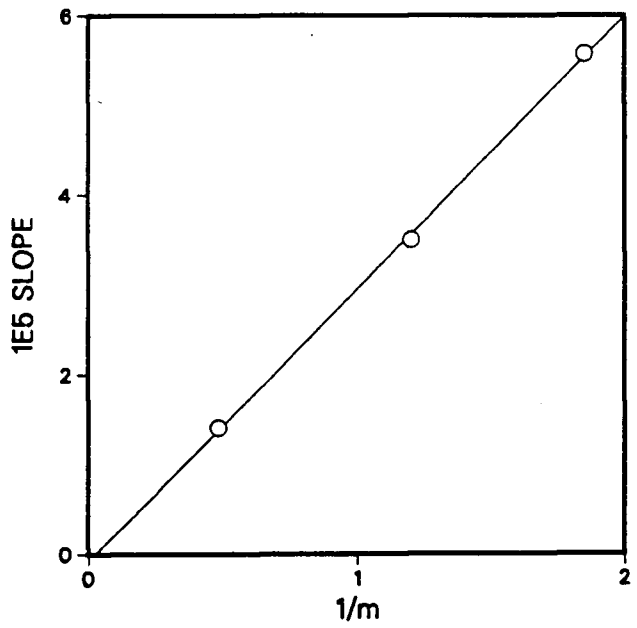

Fig. 24: Plot of (slope of k_{obs} vs. $[HA^-]$) vs. 1/m for phenylphosphonate buffer giving r = 0.9997, k_{HA^-} = -8.0 ± 10.2 x 10^{-7} (intercept) and $k_A{}^{2-}$ = 3.03 ± 0.08 x 10^{-5} (slope).

Table 19: Results of plotting k_{obs} vs. $[HA^-]$ for phenylphosphonate monoanion/dianion buffers at 3 m values ($m = [HA^-]/[A^{2-}]$) at 25°C and 0.05 M ionic strength.

1/m	pH	10^2 $[HA^-]$ M	10^7 k_{obs} sec^{-1}	r	10^8 intercept sec^{-1}	10^5 Slope M^{-1} sec^{-1}
	6.98	1.367	2.12			
0.481	6.97	0.820	1.35	1.0000	1.99	1.41
	6.93	0.273	0.58			
	7.40	0.460	2.07			
1.20	7.38	0.276	1.48	0.9987	4.74	3.50
	7.34	0.092	0.78			
	7.47	0.355	2.64			
1.85	7.45	0.213	1.82	0.9999	6.52	5.57
	7.38	0.071	1.05			

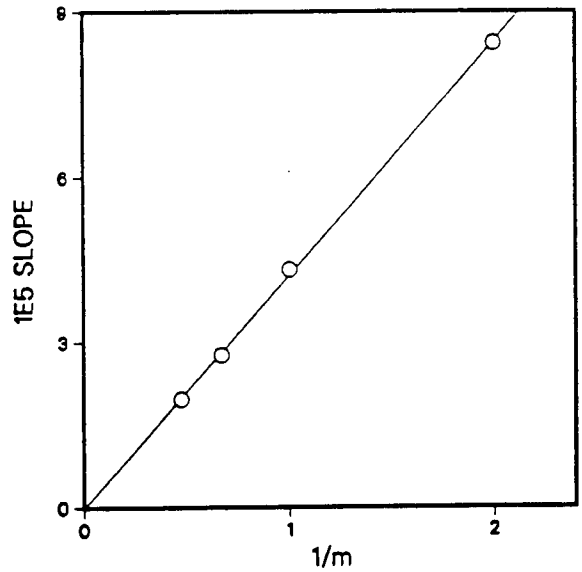

Fig. 25: Plot of (slope of k_{obs} vs. $[HA^-]$) vs. 1/m for 3,4-dimethylphenylphosphonate buffer giving r = 0.9997, k_{HA^-} = 1.3 ± 8.7 x 10^{-7} (intercept) and $k_A{}^{2-}$ = 4.24 ± 0.07 x 10^{-5}

Table 20: Results of plotting k_{obs} vs. $[HA^-]$ for 3,4-dimethylphenylphosphonate monoanion/dianion buffers at 4 m values (m = $[HA^-]/[A^{2-}]$) at 25°C and 0.05 M ionic strength

1/m	pH	10^2 $[HA^-]$ M	10^7 k_{obs} sec^{-1}	r	10^8 intercept sec^{-1}	10^5 Slope M^{-1} sec^{-1}
	7.14	0.708	1.70			
0.472	7.09	0.425	1.15	1.0000	3.13	1.96
	7.09	0.014	0.589			
	7.23	0.454	1.62			
0.667	7.24	0.182	0.889	0.9983	3.72	2.77
	7.21	0.091	0.654			
	7.18	0.045	0.461			
	7.47	0.379	2.32			
1.00	7.44	0.227	1.74	0.9977	7.01	4.33
	7.38	0.076	1.00			
	7.72	0.378	4.33			
2.00	7.67	0.270	3.45	0.9993	11.7	8.43
	7.67	0.162	2.60			
	7.64	0.054	1.58			

with an ionic strength of 0.05 gives $pK^I = pK^T - 0.09$ for a monoacid/monoanion dissociation.

HA^-/A^{2-} $$pK^I = pK^T - (1.5345\sqrt{I})/(1 + 1.5\sqrt{I}) \quad [3.24]$$

HA/A^- $$pK^I = pK^T - (0.5115\sqrt{I})/(1 + 1.5\sqrt{I}) \quad [3.7]$$

The average pH value of each buffer ratio set generally agreed with the calculated pK^I value using eq. [3.24].

As catalysis by the monoanion is negligible, eq. [3.20] reduces to eq. [3.29] and k_A2- will simply be the slope of the line obtained from a plot of k_{obs} vs. $[A^{2-}]$.

$$k_{obs} = k_{sum} + k_A2- [A^{2-}] \quad [3.29]$$

The results of phenylphosphonate and 3,4-dimethylphenylphosphonate buffers using eq. [3.29] give values for k_A2- which agree well with those obtained from Figs. 24 and 25: for phosphonate the results are $3.03 \pm 0.08 \times 10^{-5}$ (Fig. 24) and $2.95 \pm 0.05 \times 10^{-5}$ (average of 3 values, eq. [3.29], Fig. 26); for 3,4-dimethylphenylphosphonate the results are $4.24 \pm 0.07 \times 10^{-5}$ (Fig. 25) and $4.21 \pm 0.08 \times 10^{-5}$ (average of 4 values, eq. [3.29], Fig. 27).

Accordingly for the other buffer systems, k_A2- was simply determined from the slopes of the lines using eq. [3.29]. Two buffer ratios were studied (m = 2, 1 or 0.5); the values of k_A2- from these determinations generally agreed within ± 3% of the average value. Generally four

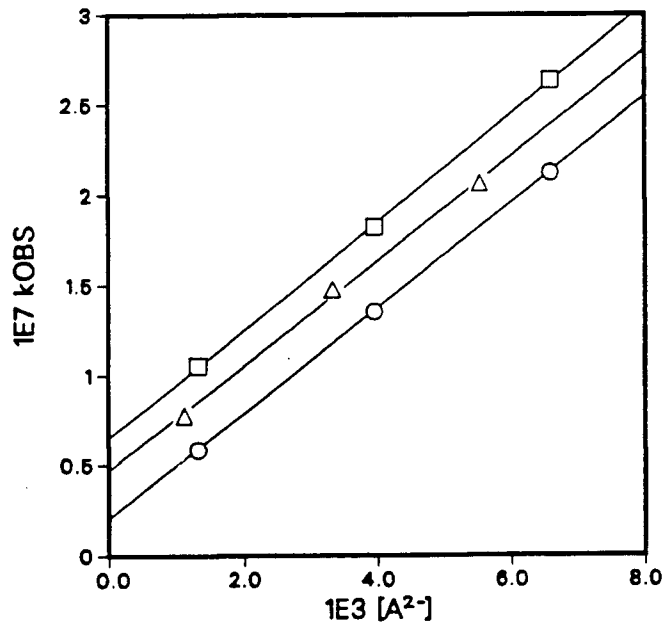

Fig. 26: Plots of k_{obs} vs. $[A^{2-}]$ for phenylphosphonate buffers, m = 2.08 (open circles), slope = 2.93 x 10^{-5}; m = 0.833 (open triangles), slope = 2.91 x 10^{-5}; m = 0.540 (open squares), slope = 3.01 x 10^{-5}; average slope = k_A2- = 2.95 ± 0.05 x 10^{-5} M^{-1} sec^{-1}

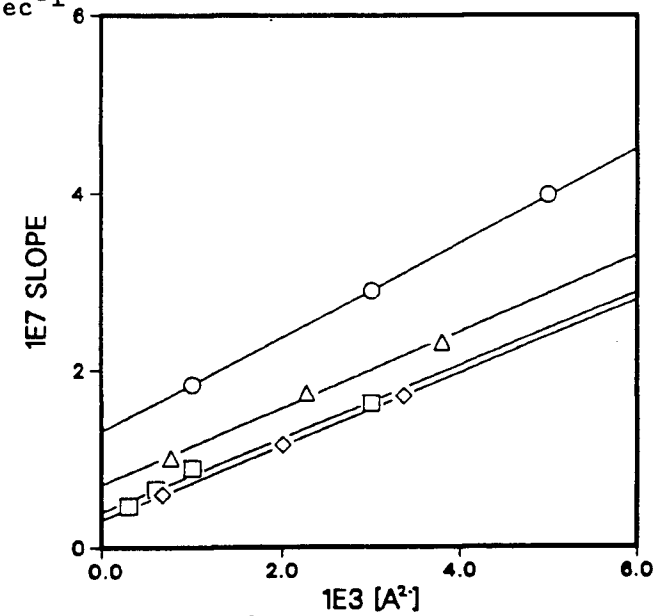

Fig. 27: Plots of k_{obs} vs. $[A^{2-}]$ for 3,4-dimethylphenylphosphonate, m = 2.00 (open circles), slope = 4.22 x 10^{-5}; m = 1.00 (open triangles), slope 4.33 x 10^{-5}; m = 0.667 (open squares), slope = 4.15 x 10^{-5}; m = 0.472 (open diamonds), slope = 4.16 x 10^{-5}; average slope = k_A2- = 4.21 ± 0.08 x 10^{-5} M^{-1} sec^{-1}.

different concentrations at each buffer ratio were examined. The results for twenty seven arylphosphonate dianions are shown in Table 21, along with the results of two phosphonate-carboxylate trianions. In the case of these latter catalysts, the dependence of k_{obs} upon the buffer composition is given by eq. [3.32] where ℓ is the buffer ratio of dianion to trianion ($[HA^{2-}]/[A^{3-}]$).

$$k_{obs} = k_{sum} + [A^{3-}] \{k_A3- + \ell\ k_{HA}2-\} \qquad [3.76]$$

In these cases, $K_2/K_3 > 10^3$ and involvement of H_2A^- in the rate expression is negligible. The trianion catalytic constants are determined from the slopes of the lines obtained from plots of k_{obs} vs. $[A^{3-}]$. The consistency of results obtained in this way at different buffer ratios, ℓ, indicates the absence of any significant catalysis by the dianion, HA^{2-}. The buffer ratios used were 0.8 and 0.5 and while the average deviation for 4-CO_2^- phosphonate trianion is a relatively large 7%, the use of eq. [3.32] leads to a similar value of k_A3- but a negative value of $k_{HA}2-$. This indicates that the 7% average deviation is a manifestation of experimental error rather than the presence of a contribution from HA^{2-} to the k_{obs} value.

3.2.3 Phosphonic diacids

Unlike the case of $[HA^-]/[A^{2-}]$ buffers, with $[H_2A]/[HA^-]$ buffers, the pH varied with concentration, as in the case of the $[HA]/[A^-]$

Table 21: k_A2^- values for acetone enolization catalyzed by arylphosphonates at 25°C and 0.05 M ionic strength, determined by plots of k_{obs} vs. $[A^{2-}]$ (eq. [3.29]), br is the number of buffer ratios used.

Substituent	10^5 k_A2^- M^{-1} sec^{-1}	br
4-NO_2	0.670 ± 0.040[a]	2
3-NO_2	0.732 ± 0.002	2
4-CN	0.788 ± 0.024	2
3-Cl	1.48 ± 0.00	2
3-F	1.42 ± 0.01	2
4-Br	1.77 ± 0.02	2
4-Cl	1.67 ± 0.02	2
2-Naph	2.24 ± 0.07	2
H	2.95 ± 0.05	3
3-CH_3	3.22 ± 0.13	2
4-CH_3	3.48 ± 0.07	2
4-C_2H_5	3.48 ± 0.03	2
3,5-$(CH_3)_2$	3.88 ± 0.23	2
3,4-$(CH_3)_2$	4.21 ± 0.08	4
3-COO^-	2.36[b] ± 0.02	2
4-COO^-	2.34[b] ± 0.16	2
2-NO_2	1.09 ± 0.01	2
2-F	1.42 ± 0.00	2
2-Cl	1.96 ± 0.02	2
2-Br	2.35 ± 0.05	2
2-I	3.12 ± 0.12	4
1-Naph	3.44 ± 0.10	2
2-CH_3	4.99 ± 0.05	2
2,5-$(CH_3)_2$	5.72 ± 0.06	2
2,3-$(CH_3)_2$	6.20 ± 0.12	2
2,4-$(CH_3)_2$	6.51 ± 0.07	2
2-C_2H_5	6.52 ± 0.20	2
2-$CH(CH_3)_2$	7.85 ± 0.16	2
2,6-$(CH_3)_2$	15.9 ± 0.3	2

[a] Deviations quoted are average deviations in the case of 2 buffer-ratios and standard deviations in the case of 3 or more buffer ratios.

[b] k_A3^-.

buffers for di- and tri-halo aliphatic carboxylic acids. A relatively concentrated solution of buffer is needed for the neutral acid to make a significant contribution to the observed rate. For several of these compounds low solubility prevents values of k_{H_2A} being obtained. The magnitude of the k_{H_2A} values determined is such that catalysis by the monoanion is negligible, a fact that is evident from the kinetic results and so eq. [3.26] is applicable.

$$k_{obs} = k_{H^+}[H_3O^+] + k_{H_2A}[H_2A] \qquad [3.26]$$

Some of the phenylphosphonic acids that were examined are soluble in water to such an extent as to allow a range of acid concentrations to be examined (0.01 – 0.1 M). For example, for 2-fluorophenylphosphonic acid, the data in Table 22 can be used to provide the k_{H_2A} value by plotting ($k_{obs} - k_{H^+}[H_3O^+]$) against [$H_2A$], as was done for the di- and tri-halo acetic acids using the previously determined k_{H^+} value (p. 83, 2.95×10^{-5} M^{-1} sec^{-1}). The resulting plot is shown in Fig. 28 with a slope, k_{H_2A}, of $2.67 \pm 0.03 \times 10^{-5}$ M^{-1} sec^{-1}. On the other hand, a value of k_{H_2A} can be calculated for each kinetic run by dividing ($k_{obs} - k_{H^+}[H_3O^+]$) by [$H_2A$], as was done for 2-nitro and 2,6-dinitrobenzoic acid, to give a value of $2.54 \pm 0.12 \times 10^{-5}$ M^{-1} sec^{-1} for k_{H_2A} (individual values for each kinetic run are given in Table 22). For most of the phosphonic acids studied only a limited range of acid concentration was accessible, undermining the applicability of determining k_{H_2A} as the slope of ($k_{obs} - k_{H^+}[H_3O^+]$) against [$H_2A$]. Rather the second method described above is used to calculate k_{H_2A} values. The

Table 22: Results of the kinetic runs for 2-fluorophenylphosphonic acid giving a value of $k_{H_2A} = 2.54 \pm 0.12 \times 10^{-5}$ M^{-1} sec^{-1}, obtained by dividing $(k_{obs} - k_{H^+}[H_3O^+])$ by $[H_2A]$, or $k_{H_2A} = 2.67 \pm 0.03 \times 10^{-5}$ M^{-1} sec^{-1}, slope of $(k_{obs} - k_{H^+}[H_3O^+])$ against $[H_2A]$.

pH	10^7 k_{obs} sec^{-1}	10^7 $(k_{obs} - k_{H^+}[H_3O^+])$ sec^{-1}	$10^2[H_2A]$, M	10^5 k_{H_2A} M^{-1} sec^{-1}
2.21	3.347	1.528	0.641	2.38
2.11	4.903	2.613	1.110	2.35
2.12	5.142	2.904	1.173	2.48
2.07	6.806	4.295	1.632	2.63
2.04	8.438	5.748	2.231	2.58
1.80	12.42	7.745	3.047	2.54
1.99	13.74	10.72	4.006	2.68
1.74	18.52	13.15	5.122	2.57
1.685	28.23	22.14	8.339	2.66

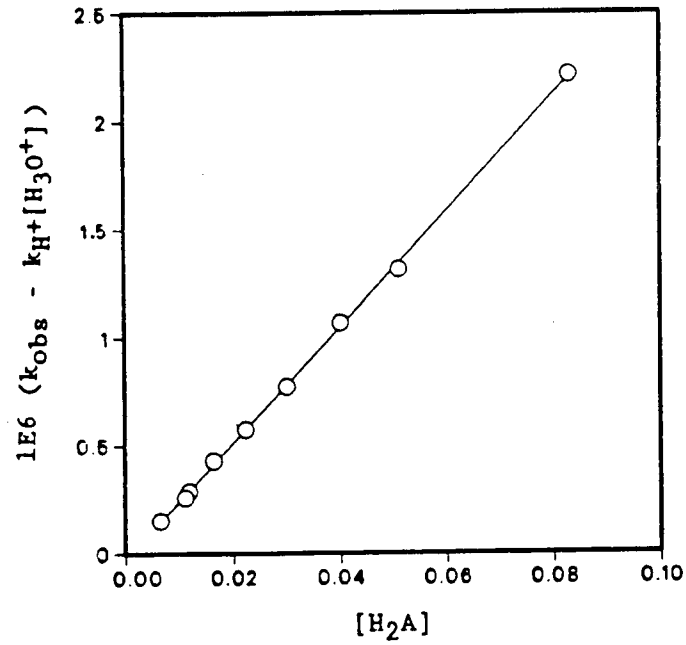

Fig. 28: Plot of ($k_{obs} - k_{H^+}[H_3O^+]$) vs. $[H_2A]$ for 2-fluorophenyl-phosphonic acid giving r = 0.9997, $k_{H_2A} = 2.67 \pm 0.03 \times 10^{-5}$ M^{-1} sec^{-1} (slope) and intercept $-2.3 \pm 1.0 \times 10^{-8}$ sec^{-1}.

The results for 20 arylphosphonic acids are given in Table 23 using this method.

The consistency of the k_{H_2A} values obtained for different kinetic runs at varying concentrations of the monoanion, HA^-, illustrates the negligible involvement of that species in the rate law. This is not surprising when one considers that the order of magnitude of the k_{H_2A} values is comparable to the k_A2^- values, which were shown previously to completely swamp the monoanion rate constant.

The k_{H_2A} values listed in Table 23 differ slightly from those reported in ref. (NS87), in which we used the figure of 2.84×10^{-5} M^{-1} sec^{-1} (HK72) for k_{H^+}, rather than our own value of 2.95×10^{-5} M^{-1} sec^{-1}.

Table 23: k_{H_2A} values for acetone enolization catalyzed by arylphosphonic acids at 25°C and 0.1 M ionic strength, determined by dividing (k_{obs} - $k_H+[H_3O^+]$) by $[H_2A]$ for a number of kinetic runs (nk).

Substituent	10^5 k_{H_2A} - M^{-1} sec^{-1}	nk
4-NO_2	3.09 ± 0.21	4
3-NO_2	3.15 ± 0.05	3
4-CN	2.89 ± 0.10	3
3-Cl	2.23 ± 0.08	4
3-F	2.46 ± 0.04	4
H	1.83 ± 0.13	14
3-CH_3	1.69 ± 0.04	4
3,4-$(CH_3)_2$	1.43 ± 0.03	4
3-COOH	2.39 ± 0.08	3
3-CH_3O	1.87 ± 0.05	4
2-NO_2	3.18 ± 0.14	4
2-F	2.54 ± 0.12	9
2-Cl	2.40 ± 0.10	4
2-Br	2.82 ± 0.15	6
2-I	2.65 ± 0.10	4
2-CH_3	1.62 ± 0.07	4
2-C_2H_5	1.43 ± 0.05	4
2-$CH(CH_3)_2$	1.29 ± 0.07	4
2,6-$(CH_3)_2$	1.03 ± 0.02	4
2-CH_3O	1.36 ± 0.03	4

3.2.4 Phosphonate Monoanions

At pH values between pK_1 and pK_2 for phenylphosphonic acids, the observed rate law is given by eq. [3.33] and the concentration ratio of monoanion to both diacid and monoanion is approximately one hundred, i.e. $[HA^-]/[H_2A] \approx [HA^-]/[A^{2-}] \approx 10^2$.

$$k_{obs} = k_{sum} + k_{H_2A}[H_2A] + k_{HA^-}[HA^-] + k_{A^{2-}}[A^{2-}] \qquad [3.33]$$

Knowing k_{sum} and the concentration of the catalytic species H_2A and A^{2-} (from the pH), as well as k_{H_2A} and $k_{A^{2-}}$ (Tables 23 and 24), it should be possible to determine the contribution from the monoanion to k_{obs}, and hence determine k_{HA^-}. Attempts were made with 3-nitrophenylphosphonic acid, phenylphosphonic acid and 3,4-dimethylphenylphosphonic acid to determine k_{HA^-}. Inconsistent results were obtained despite the fact that (a) $[HA^-]$ generally constituted between 95% and 99% of C_{TOT} and (b) $k_{HA^-}[HA^-]$ constituted between 9% and 60% of k_{obs}. The results are given in Table 24 with 3-nitrophenylphosphonate monoanion showing a relatively small 25% standard deviation, while the other two monoanions have much larger deviations.

Table 24: k_{HA^-} values for acetone enolization catalyzed by arylphosphonate monoanions at 25°C and 0.1 M ionic strength

Substituent	10^7 k_{HA^-} M^{-1} sec^{-1}	nk[a]
3-NO_2	1.09 ± 0.26	3
H	1.43 ± 1.24	4
3,4-$(CH_3)_2$	1.97 ± 1.16	4

[a] Number of kinetic runs.

4. DISCUSSION

4.1 CARBOXYLATE BASE CATALYSIS

4.1.1 Monoanions

The data in Table 7, p. 81 include rate constants for fourteen aliphatic carboxylate bases which can be used to define a Bronsted line. We feel, however, that the data for both chloroacetate and iodoacetate should be excluded from the linear regression as the standard deviations for those particular rate constants are so high, (as a result of the greater magnitude of the carboxylic acid rate constant).

Data for seven benzoate anions are given in Table 11, p. 94. Five of these k_A- values can be used in a Bronsted plot, while the negligible value for 2-fluorobenzoate anion (a negative value) and the large standard deviation for 3-nitrobenzoate anion leads us to omit those two anions from any linear regression.

The Bronsted plot for the twelve aliphatic carboxylate anions is shown in Fig. 29 and leads to eq. [4.1]. Values of p and q are 1 and 2, respectively, and the pK values at zero ionic strength have been used in the correlation. The agreement between eq. [4.1] and the correlation using the data of Bell and Lidwell eq. [1.72] is very good (BL40, p. 40).

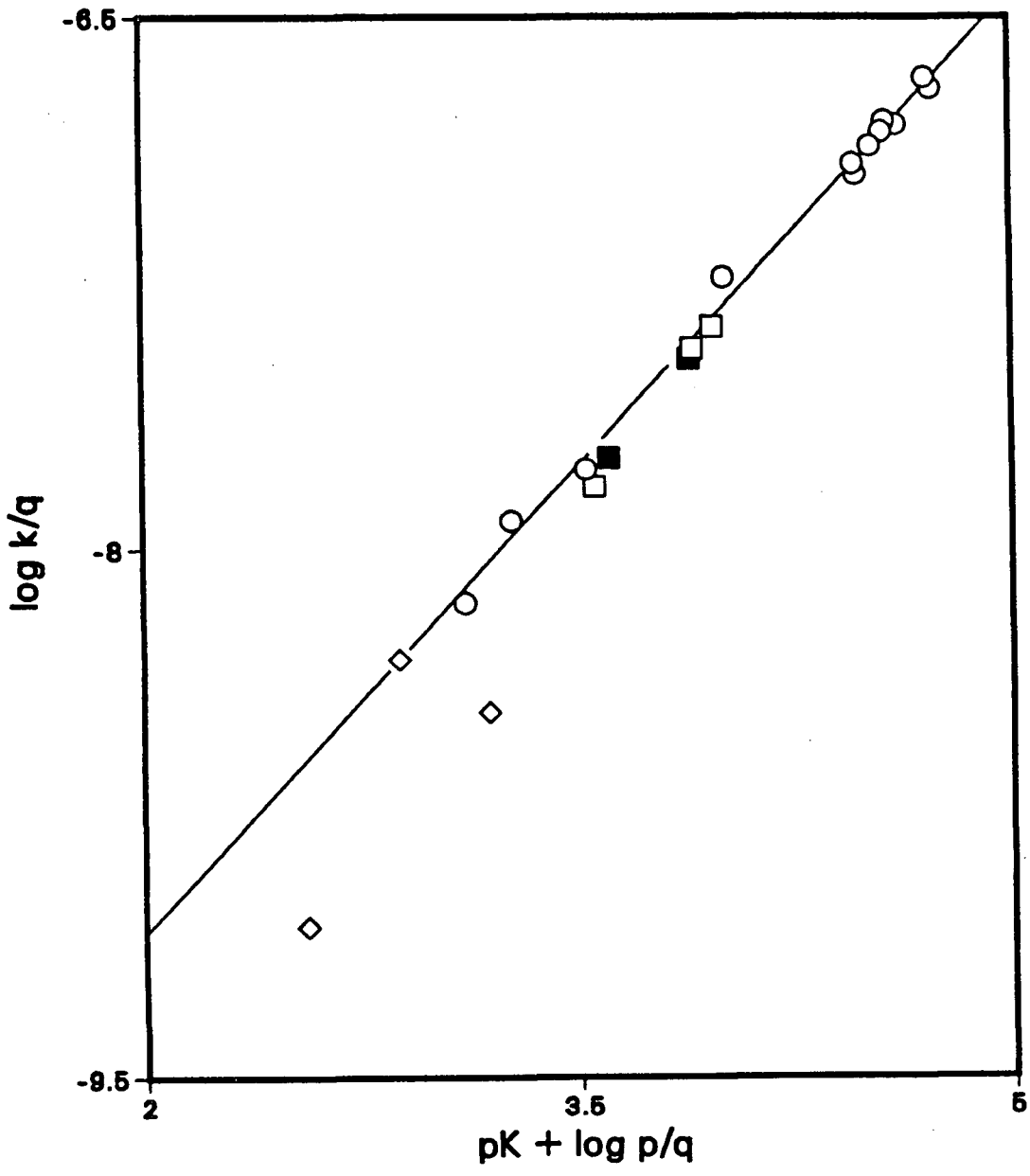

Fig. 29: Bronsted plot for catalysis of acetone enolization by carboxylate monoanions; aliphatic bases (open circles), meta benzoate bases (open squares), ortho benzoate bases (closed squares) and three bases with large standard deviations (open diamonds); line drawn with respect to the aliphatic bases.

12 bases
r = 0.9974

$$\log (k_A^-/q) = -10.9 \pm 0.1 + 0.885 \pm 0.020 \ (pK + \log p/q) \qquad [4.1]$$

4 bases
r = 0.9997

$$\log (k_A^-/q) = -10.9 + 0.879 \ (pK + \log p/q) \qquad [1.72]$$

The k_A^- values for chloroacetate, iodoacetate and 3-nitrobenzoate anion are shown in Fig. 29, but have not been included in the correlation, for the reason discussed previously. The results for five benzoates (two meta, two ortho and the unsubstituted anion) are also shown in Fig. 29 and will be discussed presently.

The following points should be noted:

1. These results confirm the work of Bell and Lidwell (BL40), using a much larger data set (twelve k_A^- values as opposed to four). The β value obtained, 0.89 ± 0.02, indicates a late (i.e. a product-like) transition state involving almost complete transfer of the proton from acetone to the carboxylate anion. This is illustrated in eq. [1.78], where A^- is a carboxylate anion.

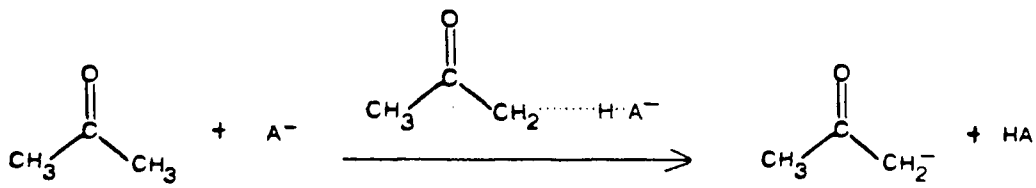

[1.78]

2. The five benzoate anion k_A^- values included in Fig. 29 fit reasonably well on the line defined by the twelve aliphatic carboxylate anions. The inclusion of the three meta benzoates in the correlation of the twelve aliphatic bases gives eq. [4.2] (β = 0.91), which differs

slightly from the original correlation, eq. [4.1]; the addition of the two ortho benzoates (eq. [4.3]) has no effect on the statistics of eq. [4.2].

15 bases $\log (k_A\text{-}/q) = -11.0 \pm 0.1 + 0.906 \pm 0.024 \ (pK + \log p/q)$ [4.2]
r = 0.9955

17 bases $\log (k_A\text{-}/q) = -11.0 \pm 0.1 + 0.911 \pm 0.022 \ (pK + \log p/q)$ [4.3]
r = 0.9955

In the case of the two ortho benzoates neither a steric accelerating effect nor a steric decelerating effect is evident.

3. It can be suggested that the small number of benzoates studied and the inherent scatter in the Bronsted plot is masking any small steric effect. However, the sterically crowded aliphatic carboxylate bases (e.g. pivalate and cyclohexane carboxylate anion) fit very well on the defined line in Fig. 29. This fact corroborates the absence of any steric effects in the carboxylate base catalyzed enolization of acetone.

4.1.2 Dianions

Combining the dianion data of Table 14, p. 109 and Table 16, p. 114 gives us eight k_A2- values for acetone enolization catalyzed by carboxylate dianions. The Bronsted plot for these eight dianions is

shown in Fig. 30(a) (involving pK_2 of course) eq. [4.4]. The aliphatic monoanion Bronsted line is included in Fig. 30(a) for a comparison with the dianions. While the value of p for both types of base is 1, the value of q (number of equivalent sites for proton attachment) is 2 for the carboxylate monoanions and 4 for the carboxylate dianions.

8 bases $\quad \log (k_A 2\text{-}/q) = -9.71 \pm 0.30 + 0.516 \pm 0.061 \ (pK_2 + \log p/q)$ [4.4]
r = 0.9610

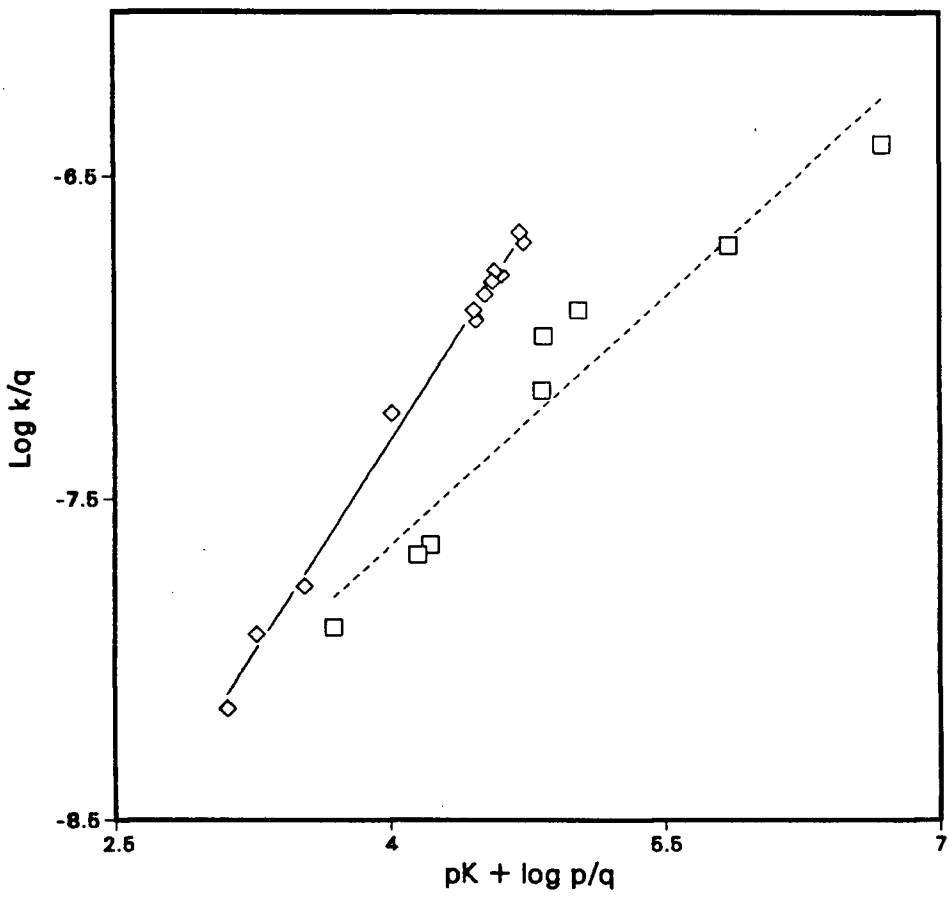

Fig. 30(a): Bronsted plot for catalysis of acetone enolization by carboxylate dianions (open squares, dashed line); Bronsted line for carboxylate monoanions added for comparison (open diamonds, solid line).

These results require detailed discussion.

1. All the dianions in Fig. 30(a) are less effective as catalysts than is expected on the basis of the Bronsted line for the carboxylate monoanions. Similar deviations have been observed previously; Spaulding and co-workers in their study of acetone enolization drew attention to the negative deviation of diethylmalonate dianion from the Bronsted line for monoanions defined by Bell and Lidwell's data (SS77); Srinivasan and Stewart discovered that the presence of an additional unit of negative charge in the catalyst reduced the effectiveness of the carboxylate base in removing a proton from the methylene carbon of a cationic creatine derivative, eq. [1.90] p. 61 (SS76a).

2. The values of k_A2- used in Fig. 30(a) are listed in Table 25, which also contains the values for three of those dianions that were previously reported by other workers, values that agree reasonably with our data. The negative deviation of the dianion rate constants from the monoanion Bronsted line cannot be attributed to an ionic strength effect. As was illustrated previously in our measurements of k_A2- for diethylmalonate (p. 104), ionic strength effects on the dianion rate constant are minimal; while the use of pK_2^I values (pK at the ionic strength at which k_A2- or k_A- is measured) may be more appropriate in Fig. 30, such an adjustment still leads to negative deviations for the dianions with respect to the monoanions' Bronsted line, albeit a slightly smaller deviation (for k_A- at 0.1 M I, $pK^I = pK^T - 0.11$; for k_A2- at 0.1 M I, $pK_2^I = pK_2^T - 0.33$ and at 0.05 M I, $pK_2^I = pK_2^T$ -

0.26). It is also worth noting that the use of the statistical factors, p and q, has no bearing on the magnitude of the deviation.

Table 25: k_A2^- values for acetone enolization catalyzed by carboxylate dianions at 25°C and 0.05 M ionic strength unless otherwise stated. Literature values are included where available

Dianion	pK_2	10^7 k_A2^- M^{-1} sec^{-1}	Literature value
Oxalate	4.29	0.505[a]	0.617[b]
Isophthalate	4.75	0.849	-
5-Methylisophthalate	4.82	0.917	-
Phthalate	5.43	2.78	-
3-Methylglutarate	5.44	4.10	-
Succinate	5.63	4.96[a]	5.17[b]
3,3-Dimethylglutarate	6.45	7.74	-
Diethylmalonate	7.29	15.9	21.0[c]

[a] Ionic strength 0.1 M

[b] Data from ref. (LA67), 0.2 M ionic strength

[c] Data from ref. (SS77), 0.1 M ionic strength

3. Another striking feature of the k_A2^- values in Fig. 30(a) (after the deviation is observed), is the relatively poor correlation of the data to a linear regression, r = 0.9610. The β value for the eight dianions, 0.52 (± 0.06), is very different from the value of 0.89 (± 0.02) obtained for the twelve aliphatic monoanions, suggesting a much earlier transition state. Perhaps the dianion data is better represented by a curve (concave to the pK axis) than a linear regression; or maybe the scatter in the plot is a manifestation of the variance in the structural type of catalyst used or a randomness attributable to experimental error.

4. Analysis of the dianions on an individual basis has led us to the following conclusion: two of the dianions are deviating negatively from a Bronsted line defined by the other six dianions, Fig. 30(b). The exclusion of diethylmalonate and 3,3-dimethylglutarate from the Bronsted correlation leads to eq. [4.5], an equation that is a statistical improvement upon eq. [4.4]. The β value of 0.78 (± 0.07) resembles the value obtained for the monoanions.

6 bases
r = 0.9831

$$\log (k_A2^-/q) = -\underset{\pm 0.3}{10.8} + \underset{\pm 0.072}{0.776} (pK_2 + \log p/q) \qquad [4.5]$$

The evidence supporting this conclusion will now be presented. For most dicarboxylic acids a statistical factor of 4 and an electrostatic effect account for the value of the K_1/K_2 ratio (S85g). The statistical factor follows from the fact that K_1 will be twice as large as it would

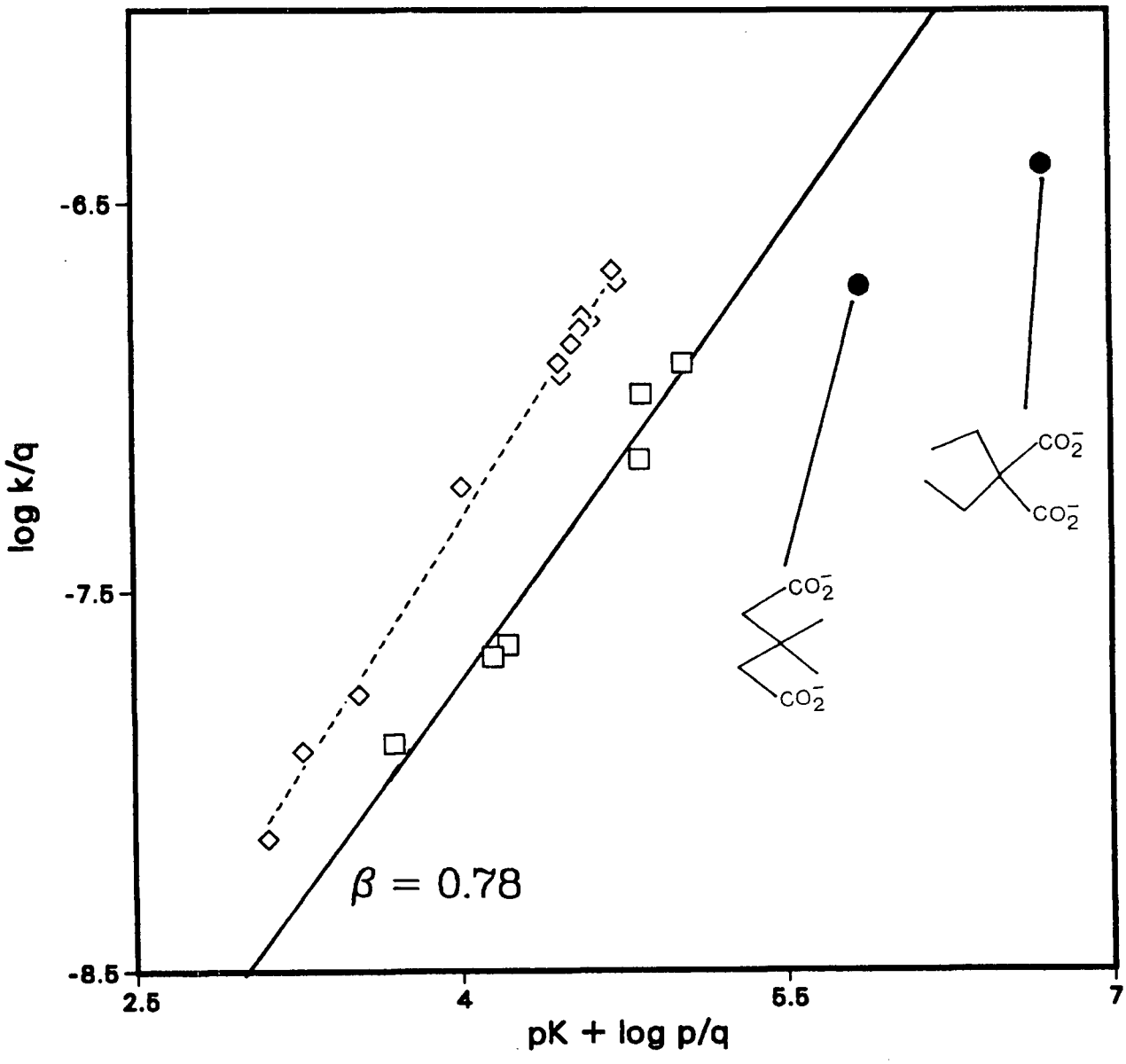

Fig. 30(b): Bronsted plot for catalysis of acetone enolization by six carboxylate dianions (open squares, solid line) with two deviating dianions (closed circles); Bronsted line for carboxylate monoanions added for comparison (open diamonds, dashed line).

otherwise be and K_2 is half as large as it would otherwise be. The electrostatic effect deals with the dissociation of the second carboxyl group in the molecule already possessing one unit of negative change; this effect depends on the distance between the two carboxyl groups (HW82).

For some dicarboxylic acids a third factor is relevant to the K_1/K_2 ratio. In the monoanion of the diacid, hydrogen-bonding may occur between the carboxyl hydrogen and the carboxylate group; this will result in a larger K_1 and a smaller K_2 than would otherwise be the case. The departure of $K_1/4K_2$ from unity is a measure of both the electrostatic effect and the hydrogen-bonding effect. In 1956, Westheimer and Benfey formulated a method for the quantitative evaluation of the hydrogen-bonding in the monoanion (WB56). They suggested a comparision of K_1, the dissociation constant of the dicarboxylic acid, with K_E the dissociation constant of the monomethyl ester of that acid. Without any hydrogen-bonding, K_1 should be twice as great as K_E, due to the statistical factor, assuming that the electronic effects of carboxyl and carbomethoxyl are equivalent. However, in the presence of hydrogen-bonding, K_1 should be more than $2K_E$; how much more reflects the degree of hydrogen-bonding in the monoanion of the diacid. Thus the departure of $K_1/2K_E$ from unity is a measure of the hydrogen-bonding effect.

The first dissociation constant of phthalic acid is 1.2×10^{-3} (K_1) while the dissociation constant of mono-methyl phthalate is 0.6×10^{-3} (K_E); thus for these compounds $K_1/2K_E \approx 1$, illustrating the absence of any hydrogen-bonding effect. On the other hand, for diethylmalonic acid $K_1/2K_E \approx 16$, illustrating the presence of a hydrogen-bonding effect

(WB56). In the case of (±)-2,3-di-tert-butylsuccinic acid, a value of 10^3 is obtained for $K_1/2K_E$ whereas the value for succinic acid is 1 (S85 g). The former is a typical case of the Thorpe-Ingold effect, where the hydrogen-bonded monoanion relieves some of the steric strain resulting from the presence of the two tert-butyl groups (JG84).

We have investigated the relationship between the degree of deviation of all the dianions from the monocarboxylate Bronsted line (Fig. 30(a)) and the degree of hydrogen-bonding in the monoanion. The latter quantity is measured by the value of $K_1/2K_E$. The former quantity is measured by the ratio of the calculated second dissociation constant of the diacid, K_2^{calc}, to the measured second dissociation constant of the diacid K_2^{obs}. The value of K_2^{calc} is available from eq. [4.1] by substituting the measured value for k_A2^- into eq. [4.1], the Bronsted line defined by the twelve aliphatic monobasic carboxylates. Thus K_2^{calc} is the dissociation constant of the monoanion, HA^-, expected on the basis of the monobasic (A^-) Bronsted line.

$$\log (k_A2^-/4) = -10.9 + 0.885 (pK_2 + \log 1/4) \qquad [4.1]$$

The results of both $K_1/2K_E$ and K_2^{calc}/K_2^{obs} for the eight dianions catalysts are given in Table 26. While the $K_1/2K_E$ values for three of the catalysts studied are available (S85g, WB56), we needed the K_E values for five mono-methyl esters. For the two mono-methyl isophthalates (meta-methyl and unsubstituted), pK_E values can be calculated on the basis of the Hammett equation for substituted benzoic acids, (eq. [4.6]), using substituent constant (σ) values of 0.32 for meta-CO_2CH_3

Table 26: $K_1/2K_E$ and K_2^{calc}/K_2^{obs} values for eight carboxylic diprotic acids

Acid	$K_1/2K_E$	K_2^{calc}/K_2^{obs}
Oxalic	1.0	2.0
Isophthalic	0.93	3.2
5-Methylisophthalic	0.91	3.5
Phthalic	1.1	4.0
3-Methylglutaric	1.0	2.6
Succinic	1.1	3.3
3,3-Dimethylglutaric	5.0	13
Diethylmalonic	16	41

and -0.06 for meta-CH_3 (PD81). Thus pK_E of 3.88 (H) and 3.94 (meta-CH_3) are obtained for the mono-methyl isophthalates

$$pK = 4.20 - \Sigma \sigma \qquad [4.6]$$

The final three mono-methyl esters (oxalate, 3-methylglutarate and 3,3-dimethylglutarate) were synthesized in our laboratory and the pK_E values determined (NV87).

The data in Table 26 show a correlation between the degree of hydrogen-bonding in the monoanion (as measured by $K_1/2K_E$) and the degree of horizontal deviation (along the pK axis) of the dianion from the monocarboxylate Bronsted line (as measured by K_2^{calc}/K_2^{obs}). For the six diacids with $K_1/2K_E$ values close to 1.0 (± 0.1), suggesting the absence of a hydrogen-bonding effect, the values of K_2^{calc}/K_2^{obs} are close to 3 (± 1), reflecting a small but consistent negative deviation from the monocarboxylate Bronsted line. Thus these six dianions should be grouped together, to give a Bronsted line, almost parallel to but displaced below the monocarboxylate Bronsted line, eq. [4.5] Fig. 30(b).

On the other hand, diethylmalonic and 3,3-dimethylglutaric acid have $K_1/2K_E$ values well above unity (16 and 5.0 respectively), illustrating the presence of a hydrogen-bonding effect in the monoanion, the effect being greater for the diethylmalonate monoanion. The values for K_2^{calc}/K_2^{obs} correlate with the $K_1/2K_E$ values for these substrates, the larger K_2^{calc}/K_2^{obs} value (i.e. greater deviation from the monocarboxylate Bronsted line) occurring for diethylmalonate dianion.

It can now be seen that a more appropriate view of the situation is to consider the two dianions whose conjugate acids HA^- possess internal hydrogen-bonding as deviating from the Bronsted line for the other six dianions, eq. [4.5]. This deviation is a horizontal displacement along the pK axis and can be explained as follows. The K_2 values of diethylmalonic acid and 3,3-dimethylglutaric acid are larger than would otherwise be expected, owing to the presence of hydrogen-bonding in the monoanion. If the proton transfer from acetone to the ion A^{2-} is normal in the sense that the effect of nearby substituents on the transition

state and on the products is similar, we would expect no deviations from the Bronsted line. The fact that deviations are observed indicates that there is a difference in the effect of hydrogen-bonding on the dianion/monoanion equilibrium and the effect in the transition state. If the hydrogen-bonding in the monoanion is neither a hindrance nor a help to the proton abstraction from acetone by the dianion, the k_A^{2-} values for the two dianions will reflect the K_2 value expected on the basis of no hydrogen-bonding.

We can calculate the K_2 values of the 'deviating' dianions expected on the basis of no hydrogen-bonding in the monoanion with eq. [4.5], the Bronsted line for six dianions. The results can be compared with the observed values of K_2, the ratio indicating the acid weakening effect of hydrogen-bonding in the monoanion, i.e. K_2^{calc}/K_2^{obs}. Of course, for the six dianions used to define the dianion Bronsted line, values of K_2^{calc}/K_2^{obs} are close to unity (± 0.4). (The ratio K_2^{calc}/K_2^{obs} used here differs from that used in Table 26, where the monocarboxylate Bronsted line (eq. [4.4]) was used as the basis for defining K_2^{calc}).

This could be the first quantitative measure of the hydrogen-bonding effect on K_2 values of diprotic carboxylic acids. It comes over thirty years since Westheimer and Benfey quantified the effect of hydrogen-bonding on K_1 values of such acids (WB56). Thus, for 3,3-dimethylglutaric acid, the acid strengthening effect on K_1 due to hydrogen-bonding in the monoanion is 5.0 ($K_1/2K_E$); the acid weakening effect on K_2 due to hydrogen-bonding in the monoanion is 3.8 (K_2^{calc}/K_2^{obs}). In the case of diethylmalonic acid, the acid strengthening effect on K_1 is 16 while the acid weakening effect on K_2 is 10. A plot of K_2^{calc}/K_2^{obs}

against $K_1/2K_E$ is shown in Fig. 31, illustrating the linear relationship between the two quantities. The slope of the line is 0.6 (obtained by either including all eight points in the correlation or just including the two 'hydrogen-bonded' points); thus the acid strengthening effect on K_2 of hydrogen-bonding in the monoanion is approximately 60% of the related acid weakening effect on K_1. It must be said, though, that more data are needed (i.e. k_A2-values and hence K_2^{calc} values) before a thorough, critical assessment of the relationship between K_2^{calc}/K_2^{obs} and $K_1/2K_E$ can be made; while more k_A2- values that coincide with eq. [4.5] would help towards a refinement of that Bronsted line (and thus a refinement of the degree of deviation of certain k_A2- values), several

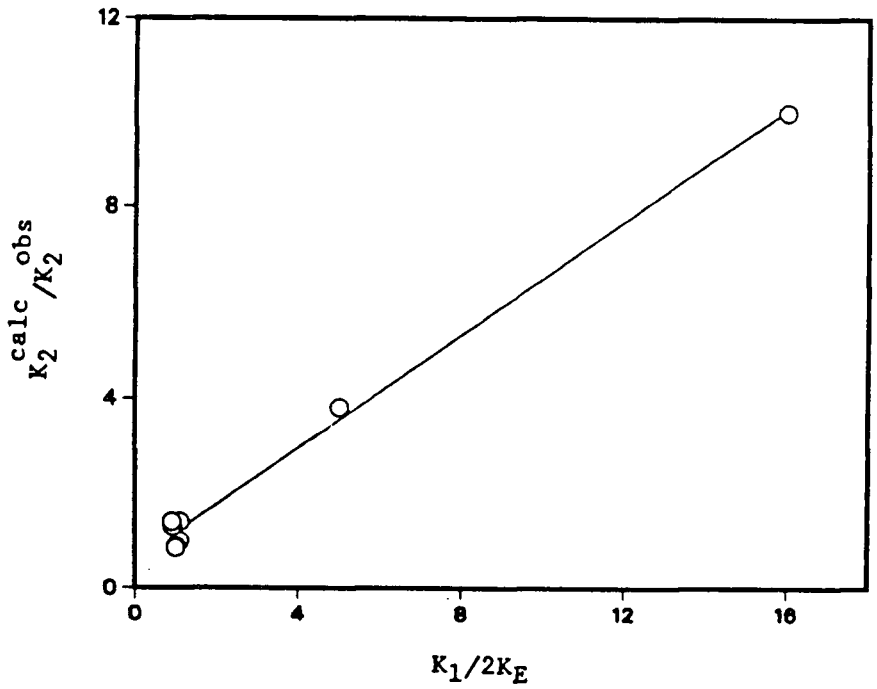

Fig. 31: Plot of K_2^{calc}/K_2^{obs} against $K_1/2K_E$ for a set of dicarboxylic acids; K_2^{calc} values calculated from eq. [4.5]; line drawn for all points giving r = 0.9968, slope = 0.59 ± 0.02, intercept = 0.57 ± 0.12.

more deviating k_A2^- values are needed to probe the aforementioned relationship. The choice of diacids to study in order to observe deviations from the dianion Bronsted line is obvious from the large compilation of $K_1/2K_E$ values available (S85g).

This discussion presupposed the absence of an effect in the transition state attributable to hydrogen-bonding in the monoanion. However, as shown below, the system could be operating such that an effect is felt by the transition state i.e. the second carboxylate could be coordinating the proton that is being abstracted by the first carboxylate unit.

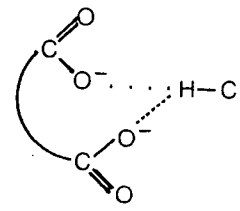

The slope of 0.6 that was derived from our correlation of K_2^{calc}/K_2^{obs} and $K_1/2K_E$, could be related to the magnitude of the hydrogen-bonding effect in the transition state, i.e. this latter factor may be only 40%, (100-60%), of the role played by hydrogen-bonding in the equilibrium acid strength of the monoanion. If this is the case, the deviation for these dianions could be dependent on the catalyst, the substrate and the reaction. On the other hand, if the first explanation is the correct one, (K_2^{calc}/K_2^{obs} measuring the hydrogen-bonding effect on K_2) changing either the substrate or the reaction will have no effect on the magnitude of the effect. A study could be undertaken to decipher the correct interpretation.

5. The large deviation of diethylmalonate dianion from that expected on the basis of the monocarboxylate Bronsted line for acetone enolization has been reported previously (SS77). The deviation (circa 1 log unit) has also been observed in the hydration of a number of aliphatic aldehydes and the mutarotation of glucose, reactions subject to both general acid and general base catalyses (PD69). Until now, no adequate explanation has been offered for the abnormally low catalytic activity of this dianion. (Unfortunately the data for all these reactions is very sparse, making an analysis, as described in p. 146, inconclusive.)

6. It may be recalled that a study of the enolization of 3-nitro-(+)-camphor catalyzed by five monocarboxylate bases, one dicarboxylate base (malonate dianion) and mono-hydrogen phosphate dianion, affords a curved Bronsted plot (BG76, p. 46). The curvature is dependent on the inclusion of the two dianions in the Bronsted plot and is therefore questionable in the light of our results for a wide structural range of dicarboxylate dianions. A better interpretation of the data is to consider a linear Bronsted line defined by the five monoanions, with the two dianions deviating negatively from this line, an interpretation supported by our results.

7. A critical question has been purposely left unanswered in our discussion thus far. Why are dicarboxylate bases less effective as catalysts than monocarboxylate bases in the enolization of acetone?

One of the prerequisites to obtaining a linear Bronsted plot is that the catalysts used in the correlation must be structurally similar; this

is partly an empirical observation suggested by consideration of the vast number of documented Bronsted correlations. Deviations from Bronsted lines, when catalysts of different structural type are included, are credited to an effect due to the difference in the types of catalyst studied. Information can also be gleaned from Bronsted plots where catalysts of different structural type collectively give a linear correlation. It has long been observed that catalysts of different charge type can often lead to deviations, both positive and negative (K73).

A study by Kresge and co-workers involving the hydrolysis of vinyl ethers illustrates such a situation (KC73b, CE77). This reaction involves rate determining proton transfer from a general acid to the substrate ($A\text{-}S_E2$, eq. [1.9], p. 6) and leads to a good Bronsted correlation for a set of neutral carboxylic acids. A group of amino acids forms a distinct line, parallel to but displaced downward from the carboxylic acid line, generally by a factor of two in k_{HA}. On the other hand, a number of alkyl monohydrogen phosphonate anions define a line of larger slope, above the carboxylic acid line. The rate acceleration factor varies, depending on the substrate studied, but is greater than the deceleration factor for the amino acids. The authors attribute such effects to a charge interaction in the transition state, where the substrate is taking on positive charge. An interaction between this charge and the positive charge in the amino acids will be repulsive, raising the energy of the transition state and leading to negative deviations from the Bronsted line for neutral carboxylic acids. In the case of phosphonate monoanions, which are acids possessing a negative

substituent, the interaction will be attractive and have the opposite effect to that for the amino acids. These interactions are affecting $\Delta G^{\neq}$, not ΔG^{o}, and thus lead to deviations from the rate-equilibrium correlation. The greater magnitude of the positive deviation as compared to the negative deviation reflects (i) the close location of the negative charge to the acidic proton in the phosphonate monoanions and (ii) the intrinsic aim of both systems to minimize the transition state energy (i.e. maximum rate acceleration and minimum rate deceleration).

Our results for base catalyzed enolization of acetone could be electrostatic in nature. The negative deviation of the dianions from the monoanion line would then be credited to an interaction that raises the transition state energy. The role of an additional unit of negative charge in the catalyst causing a repulsive, energy-raising interaction is unclear. Such an interaction should be related to the distance separating the two carboxylates; increasing this distance should decrease the effect and therefore minimize, if not obliterate, the deviation for the dianions. This is not the case; the set of dicarboxylates which form the Bronsted line in Fig. 30(b) cover a wide structural type but display no related perceivable trend in their degree of deviation from the monocarboxylate line. Thus an electrostatic interaction that is lowering the transition state energy seems implausible. We will discuss other possible explanations for this effect at a later stage.

4.2 CARBOXYLIC ACID CATALYSIS

4.2.1 Monoprotic acids

The data in Table 7, p. 81 and Table 9, p. 88 include rate constants for twenty two aliphatic carboxylic acids; Table 11, p. 94 contains k_{HA} values for nine benzoic acids. The Bronsted plot for all of this data is presented in Fig. 32. Careful analysis of the information available from Fig. 32 will now be presented.

Considering the fourteen aliphatic carboxylic acids inclusive of chloroacetic acid and weaker acids, we can compare our results with those of Bell and Lidwell covering the same pK range. The values of k_{HA} that are used for iodoacetic and chloroacetic are those from Table 7 (method I), p. 80. The Bronsted line for this group of acids is shown in Fig. 33, and is defined by eq. [4.7]. The agreement between this line and the results of Bell and Lidwell is reasonable (eq. [1.71], BL40).

14 acids
$r = 0.9900$

$$\log (k_{HA}/p) = -4.33 \pm 0.10 - 0.605 \pm 0.025 \ (pK + \log p/q) \qquad [4.7]$$

4 acids
$r = 0.9995$

$$\log (k_{HA}/p) = -4.46 - 0.569 \ (pK + \log p/q) \qquad [1.71]$$

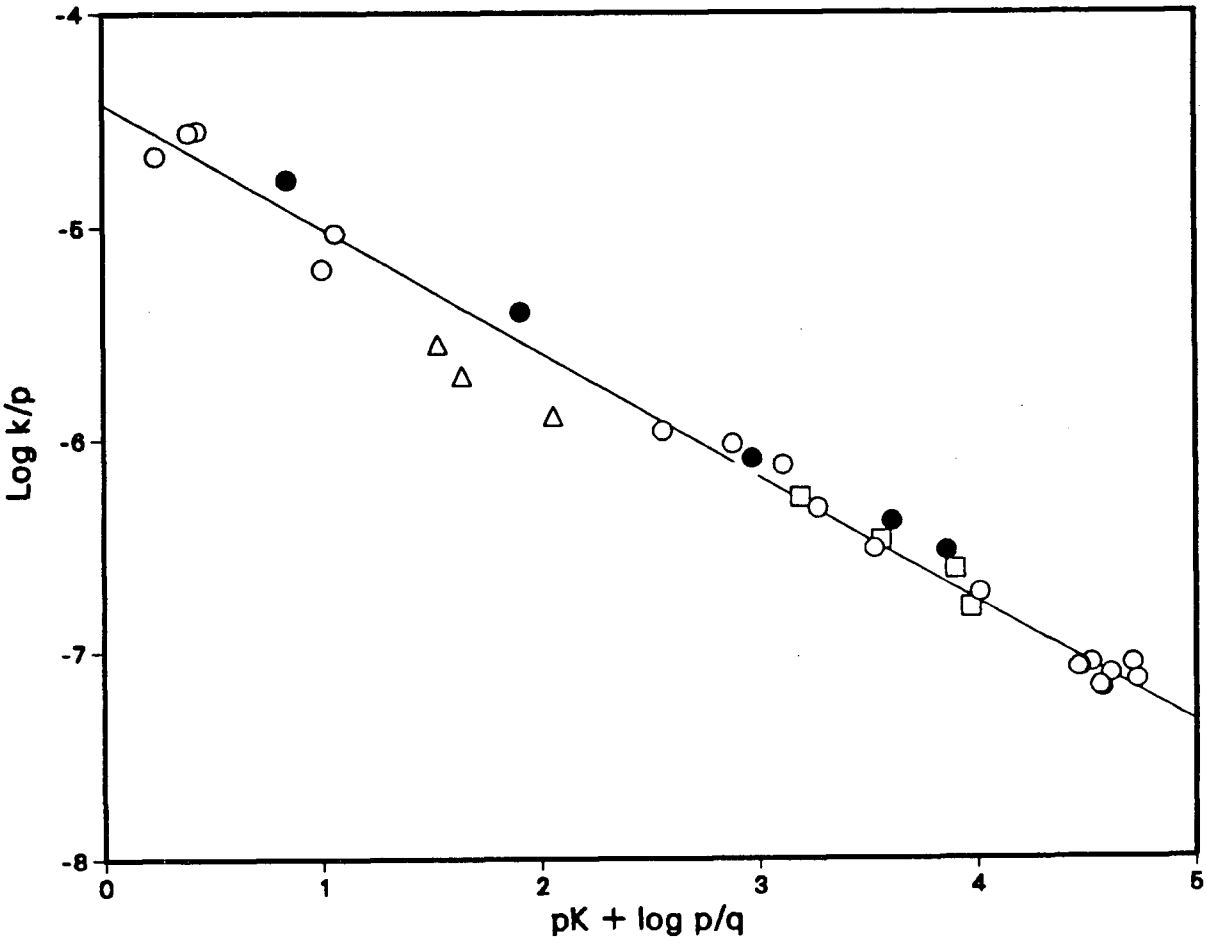

Fig. 32: Bronsted plot for catalysis of acetone enolization by carboxylic monoprotic acids; 22 aliphatic acids (open circles), 4 meta benzoic acids (open squares), 5 ortho benzoic acids (closed circles) and 3 ammonio carboxylic acids (open triangles). Line drawn for aliphatic carboxylic acids.

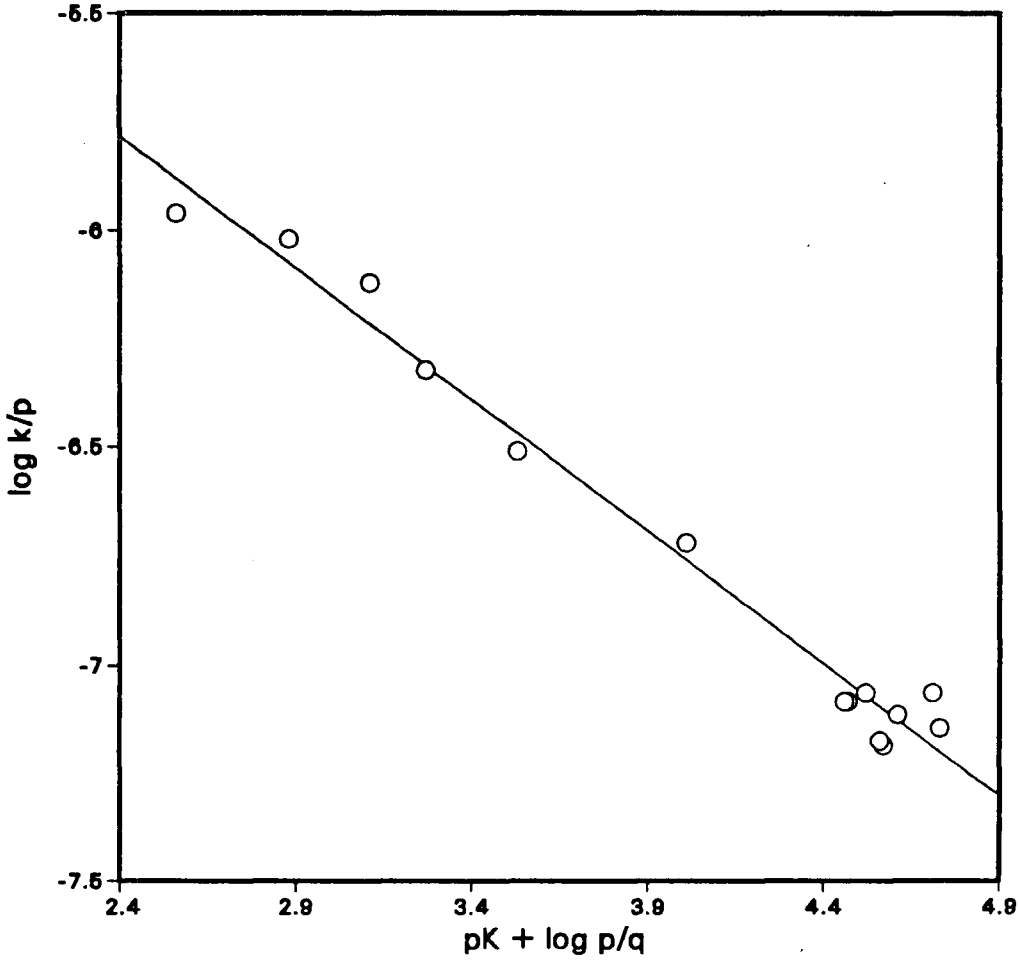

Fig. 33: Bronsted plot for catalysis of acetone enolization by carboxylic acids

The following points should be noted:

1. These aliphatic carboxylic acids give an α value of 0.605 ± 0.025, slightly larger than that obtained by Bell and Lidwell who used a much smaller data set. This α value indicates a β value of 0.395 for the base catalyzed proton abstraction from protonated acetone. It may be recalled that the general acid catalyzed enolization of acetone involves two steps; the first involves equilibrium protonation of the carbonyl

oxygen; the second involves the abstraction of a hydrogen from protonated acetone by the conjugate base of the general acid (eq. [1.10], p. 48). A β value of 0.395 for the second step indicates a transition state in which the proton is less than half-transferred, that is, a transition state that resembles reactants as shown in eq. [1.10b], HA being a carboxylic acid. The same process involving unprotonated acetone has a β value of 0.89; the much smaller β value obtained with protonated acetone reflects the degree of activation conferred on acetone on being protonated, leading to an earlier, more reactant-like transition state.

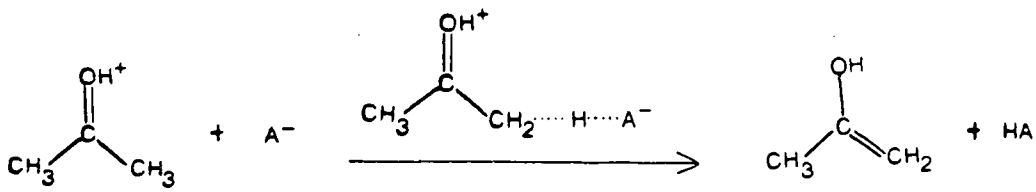

[1.10b]

One of the aims of this study is to investigate steric effects on acetone enolization. With data now available for five ortho benzoic acids and four meta benzoic acids, as well as a number of sterically crowded aliphatic acids, we can evaluate this effect. However two other effects related to the di- and tri-halo aliphatic carboxylic acids will be addressed first.

2. The Bronsted line shown in Fig. 32 is drawn for all the nineteen aliphatic acids, eq. [4.8]. The statistics of the linear regression are an improvement upon eq. [4.7], a Bronsted line obtained by excluding the five 'strong' halo-acids.

19 acids $\quad \log (k_{HA}/p) = -4.42 \pm 0.04 - 0.583 \pm 0.013 \,(pK + \log p/q)$ [4.8]
r = 0.9961

The α values of both lines are similar, eq. [4.8] having the smaller α and the smaller standard deviation, 0.583 ± 0.013. However, we believe that this group of aliphatic acids is more properly represented by a gentle curve, concave to the pK axis; a curve that includes the difluoro- and trifluoroacetic acids, but has the dichloro-, trichloro- and tribromoacetic acids as positive deviations, Fig. 34.

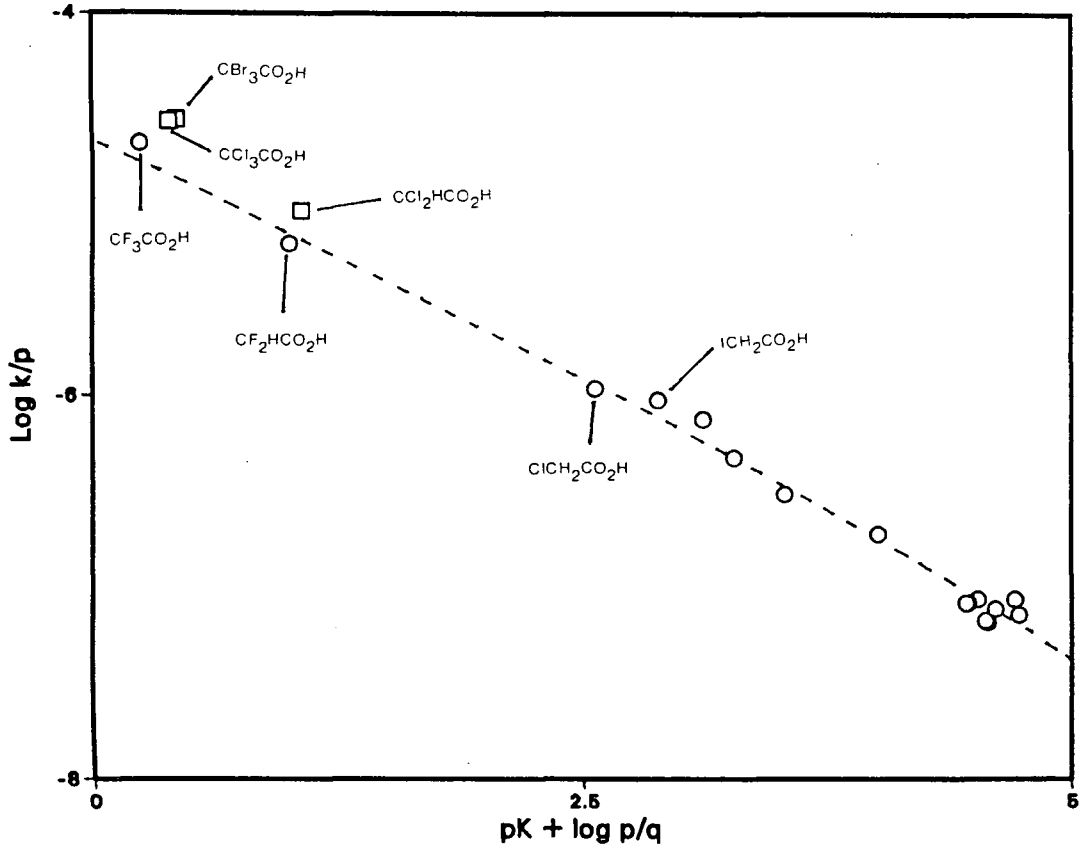

Fig. 34: Bronsted plot for catalysis of acetone enolization by nineteen carboxylic acids; curved line hand-drawn for sixteen of the acids (open circles); dichloro-, trichloro- and tribromoacetic acids also present (open squares).

The reasons for the conclusion are the following. The k_{HA} values for the 'strong' halo-acids are very precise, the standard deviations of between 2% and 5% being adequately represented by the span of the circles and squares in Fig. 34. The pK values of these acids have been measured in this laboratory. The literature results, where available, agree reasonably well with our results (Table 9, p. 88, NV87). In a comparison of the di- and tri-haloacetic acids, fluorine and chlorine being the halogens, we find that the chloro-acids are more effective as catalysts than the fluoro-acids (a factor of 1.3 for the tri-halo acids and 1.5 for the di-halo acids). This fact is clearly evident from Fig. 14, p. 86, where the plots of $(k_{obs} - k_{H^+}[H_3O^+])$ against [HA] for difluoro- and dichloroacetic acids are compared. The greater catalytic effectiveness of the chloro-acids is curious, considering that the pK measurements place the fluoro-acids as the slightly stronger acids.

The data in Fig. 34 can be interpreted in one of two ways. A linear regression including all nineteen carboxylic acids (as shown in Fig. 32) has both difluoro- and trifluoroacetic acid as negative deviations from the Bronsted line. Such a reading of the data requires an explanation for these two deviations. A second interpretation involves the gentle curve, incorporating the two 'strong' fluoro-acids while excluding the other three 'strong' halo-acids, as shown in Fig. 34. We favour the latter conclusion since the positive deviations of the dichloro-, trichloro- and tribromoacetic acids from this curve can be explained on the basis of polarizability.

A highly polarizable atom is one whose electron cloud can be easily deformed by an electric field, such as will be produced by ions in

solution (RS71). Polarization of the electron cloud would also occur in the transition state of the general acid catalyzed enolization of acetone, which involves hydrogen abstraction from protonated acetone by the conjugate base of the acid. Such a polarization will facilitate this process, and therefore lead to enhanced catalytic activity for carboxylic acids possessing polarizable substituents. This infers, of course, that polarizability exerts a larger influence on the transition state than on the equilibrium acidities. Effects of this kind have been reported previously (NL86).

Polarizability increases as one goes down a group in the Periodic Table and so a placing for the halogens in order of increasing polarizability has F < Cl < Br < I. On this basis the greater catalytic activity of tribromo- and trichloro-acetic acids over trifluoroacetic acid can be attributed to a polarizability rate-enhancement for the bromo- and chloro-acids; likewise in the case of difluoroacetic acid and dichloroacetic acid. The most polarizable halogen i.e. iodine, should show a rate constant above that expected on the basis of the Bronsted line for the other carboxylic acids. Inspection of Fig. 34 shows that iodoacetic acid is slightly on the positive side of the Bronsted line; the value for k_{HA} is almost comparable to the value for chloroacetic acid, an acid whose dissociation constant is twice that of iodoacetic acid.

We had hoped to further illustrate the role of polarizability in these systems by measuring k_{HA} value for methylthioacetic acid, the sulfur analogue of methoxyacetic acid. The polarizability of sulfur is greater than that of oxygen and so, one would expect enhanced catalytic

activity for the sulfur-containing compound. Unfortunately, the compound reacts rapidly with triiodide ion.

Further analysis of the polarizability effect, on a quantitative basis, will be presented shortly.

3. The analysis of the k_{HA} values as just described begs the question: why is the Bronsted plot curved? The curvature is in the direction predicted by the Hammond postulate and Marcus theory; the use of the twelve weaker aliphatic carboxylic acids (mandelic acid and weaker) to define one Bronsted line gives an α value of 0.621 ($\pm$ 0.035); the three stronger acids (chloroacetic and stronger) gives an α value of 0.546 $\pm$ 0.051. Having said that, the linear regression of all fifteen acids gives a much better statistical result than either of the two correlations just mentioned; a correlation coefficient of 0.9957 and an α value of 0.555 $\pm$ 0.014 result. Thus the data are quite adequately described by a linear correlation. This issue will be discussed later, after consideration of some factors that are relevant as to whether a curved or a linear correlation of this data is more appropriate.

4. We will now discuss the role of steric effects in the acid catalyzed reaction. It is evident from Fig. 32, p. 151, that while the meta benzoic acids essentially fall on the line defined by the twenty two aliphatic carboxylic acids, the five ortho benzoic acids fall slightly above such a line. The positive deviations from the defined Bronsted line are small but they are consistent. Considering that the Bronsted line (or curve) should more properly intersect the two points for the

fluoro-acetic acids in Fig. 34, the positive deviations of the two ortho-nitro benzoic acids is enhanced. The size of the deviation for the five ortho benzoic acids bears some relationship to the size of the ortho substituent; 2-fluorobenzoic acid falls just above the Bronsted line, while 2,6-dinitrobenzoic acid shows a positive deviation of greater magnitude.

The steric acceleration present in the ortho benzoic acids led us to critically examine the aliphatic acids. Using several of the aliphatic acids, acids of a structural type where little or no steric activation is expected, a Bronsted line is defined, Fig. 35. The acids used to define this line are $ClCH_2CO_2H$, $CH_3OCH_2CO_2H$, $HOCH_2CO_2H$, CH_3CO_2H, CD_3CO_2H and $CH_3CH_2CO_2H$; the result is given in eq. [4.9].

$$\begin{array}{ll} \textbf{6 acids} & \log (k_{HA}/p) = -4.37 \pm 0.06 - 0.607 \pm 0.016\ (pK + \log p/q) \\ r = 0.9985 & \end{array} \qquad [4.9]$$

The other aliphatic acids are included in Fig. 35; these acids, all possessing steric bulk, are $C_6H_5CH(OH)CO_2H$, $C_6H_5CH_2CO_2H$, $CH_3CH_2CH_2CO_2H$, $(CH_3)_2CHCO_2H$, $C_6H_{11}CO_2H$, $(CH_3)_3CCH_2CO_2H$ and $(CH_3)_3CCO_2H$. The fact that the 'sterically-crowded' catalysts appear on or above the Bronsted line in Fig. 35 leads us to conclude that a small steric accelerating effect is present in most of those catalysts. An estimation of the steric accelerating factor on k_{HA} can be made by comparing the measured k_{HA} value with the k_{HA} value calculated on the basis of the Bronsted line for those acids possessing little or no steric bulk. We can include difluoro- and trifluoro-acetic acid in this category (along with the six

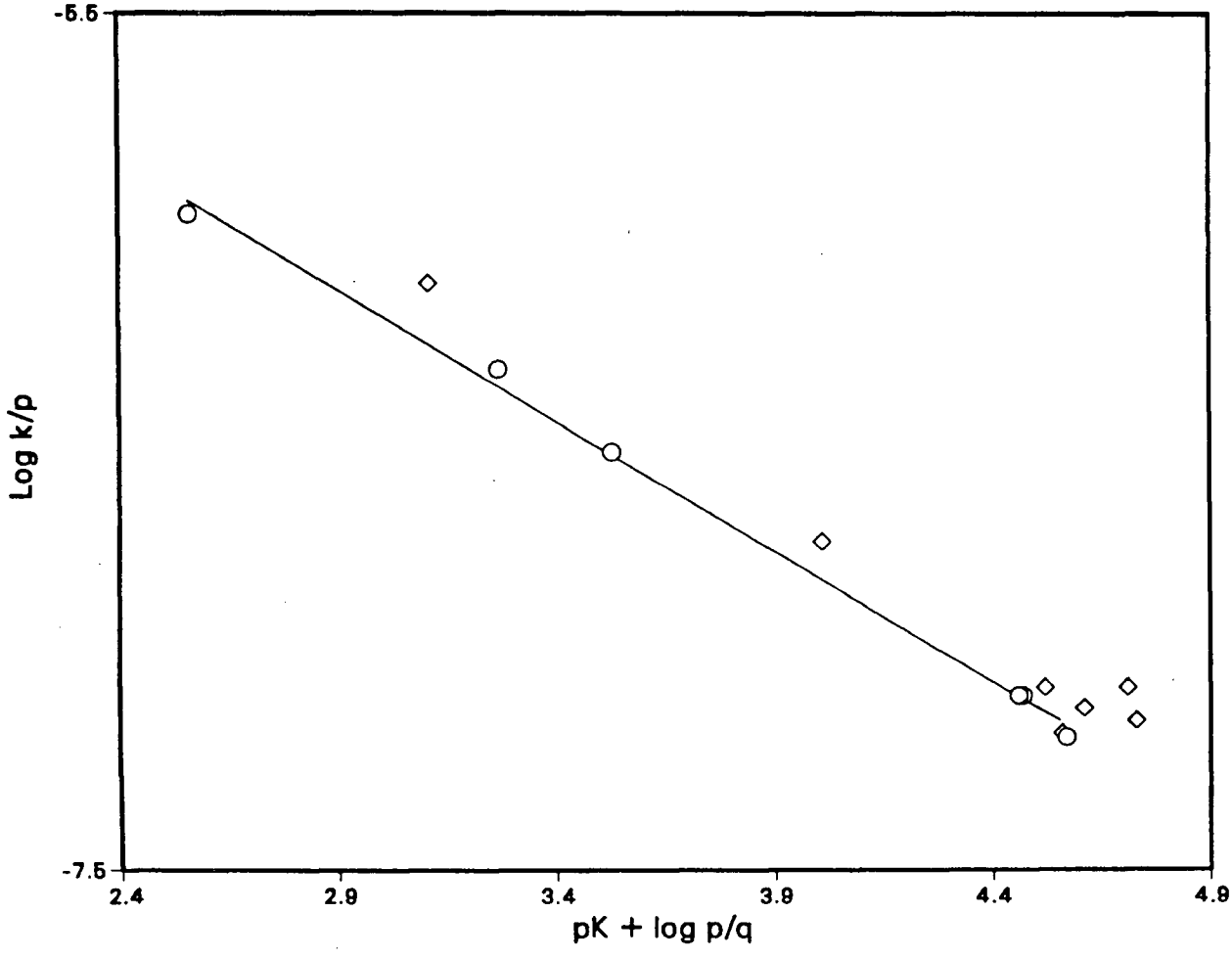

Fig. 35: Bronsted plot for catalysis of acetone enolization by thirteen aliphatic carboxylic acids; line drawn for six acids (open circles), as listed in the text; seven other acids (open diamonds), as listed in the text.

aliphatic acids listed previously). The interpretation of the Bronsted plot as a curved or a linear correlation must now be settled; the division of the aliphatic carboxylic acids into two groups, i.e. those possessing steric bulk (seven acids) and those not possessing steric bulk (eight acids), makes the decision as to the choice of correlation for the Bronsted line simpler.

The choice of a linear or a curved correlation can be made based upon an evaluation of the results of both correlations for the group of acids possessing little or no steric bulk; the results (using a quadratic expression to define the curve) are presented in eqs. [4.10] and [4.11], and shown in Fig. 36. The degree of fit is slightly better for

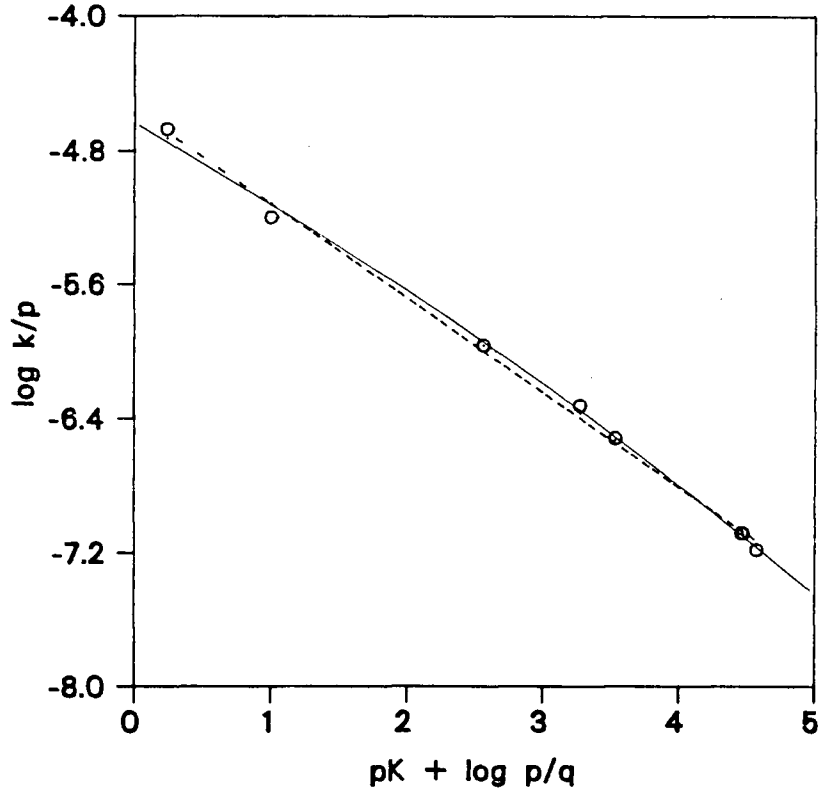

Fig. 36: Bronsted plot for catalysis of acetone enolization by aliphatic carboxylic acids possessing no steric bulk; dotted straight line, linear correlation, eq. [4.10]; solid curve line, quadratic correlation, eq. [4.11].

the quadratic expression, and an inspection of Fig. 36 suggests that the second degree curve is a more appropriate correlation of the data.

8 acids; r = 0.9985

$$\log (k_{HA}/p) = \underset{\pm 0.04}{-4.56} - \underset{\pm 0.013}{0.562}\ (pK + \log p/q) \qquad [4.10]$$

8 acids; r = 0.9990

$$\log (k_{HA}/p) = \underset{\pm 0.06}{-4.60} - \underset{\pm 0.054}{0.497}\ (pK + \log p/q) - \underset{\pm 0.01}{0.013}\ (pK + \log p/q)^2 \qquad [4.11]$$

A consideration of the ratio of the observed k_{HA} values to the k_{HA} values calculated using either eq. [4.10] or [4.11], illustrates that the quadratic expression is more appropriate. The results are given in Table 27; in the case of eq. [4.10], the linear correlation, the ratio $k_{HA}^{obs}/k_{HA}^{calc}$ shows a pattern with the values at the extremities of the line equalling one or less, while the values in the centre of the line are greater than one; on the other hand, the values of $k_{HA}^{obs}/k_{HA}^{calc}$ for eq. [4.11], the quadratic correlation, show a random scatter above and below unity. This fact favours eq. [4.11] as the correlation of choice; a choice that is also supported by the generally smaller deviations from unity for the $k_{HA}^{obs}/k_{HA}^{calc}$ values found with eq. [4.11] than with eq. [4.10].

We can now use eq. [4.11] to evaluate the magnitude of the steric acceleration effect on k_{HA} for the other seven aliphatic acids, as well as for the meta and ortho benzoic acids. The results of these calculations are given in Table 28; Fig. 37 illustrates the magnitude of the

Table 27: $k_{HA}^{obs}/k_{HA}^{calc}$ values for the group of aliphatic carboxylic acids possessing little or no steric bulk. Values of k_{HA}^{calc} calculated from a substitution of the appropriate pK value into eq. [4.10] (linear correlation) or eq. [4.11] (quadratic correlation).

Acid	$k_{HA}^{obs}/k_{HA}^{calc}$ (eq. [4.10])	$k_{HA}^{obs}/k_{HA}^{calc}$ (eq. [4.11])
F_3CCO_2H	1.00	1.07
F_2CHCO_2H	0.837	0.821
$ClCH_2CO_2H$	1.09	1.00
$CH_3OCH_2CO_2H$	1.19	1.11
$HOCH_2CO_2H$	1.07	1.01
CH_3CO_2H	0.955	0.980
CD_3CO_2H	0.982	1.01
$CH_3CH_2CO_2H$	0.873	0.908

Table 28: $k_{HA}^{obs}/k_{HA}^{calc}$ values for aliphatic carboxylic acids, meta and ortho benzoic acids. Values of k_{HA}^{calc} calculated from a substitution of the appropriate pK value into eq. [4.11].

Acid	$k_{HA}^{obs}/k_{HA}^{calc}$
Aliphatic carboxylic acids:	
$C_6H_5CH(OH)CO_2H$	1.42
$C_6H_5CH_2CO_2H$	1.22
$CH_3CH_2CH_2CO_2H$	1.14
$(CH_3)_2CHCO_2H$	0.918
$C_6H_{11}CO_2H$	1.14
$(CH_3)_3CCH_2CO_2H$	1.49
$(CH_3)_3CCO_2H$	1.25
Benzoic acids:	
H	1.34
3-CH_3	0.964
3-F	1.16
3-NO_2	1.12
2-C_2H_5O	1.57
2-CH_3	1.52
2-F	1.26
2-NO_2	1.56
2,6-$(NO_2)_2$	1.77

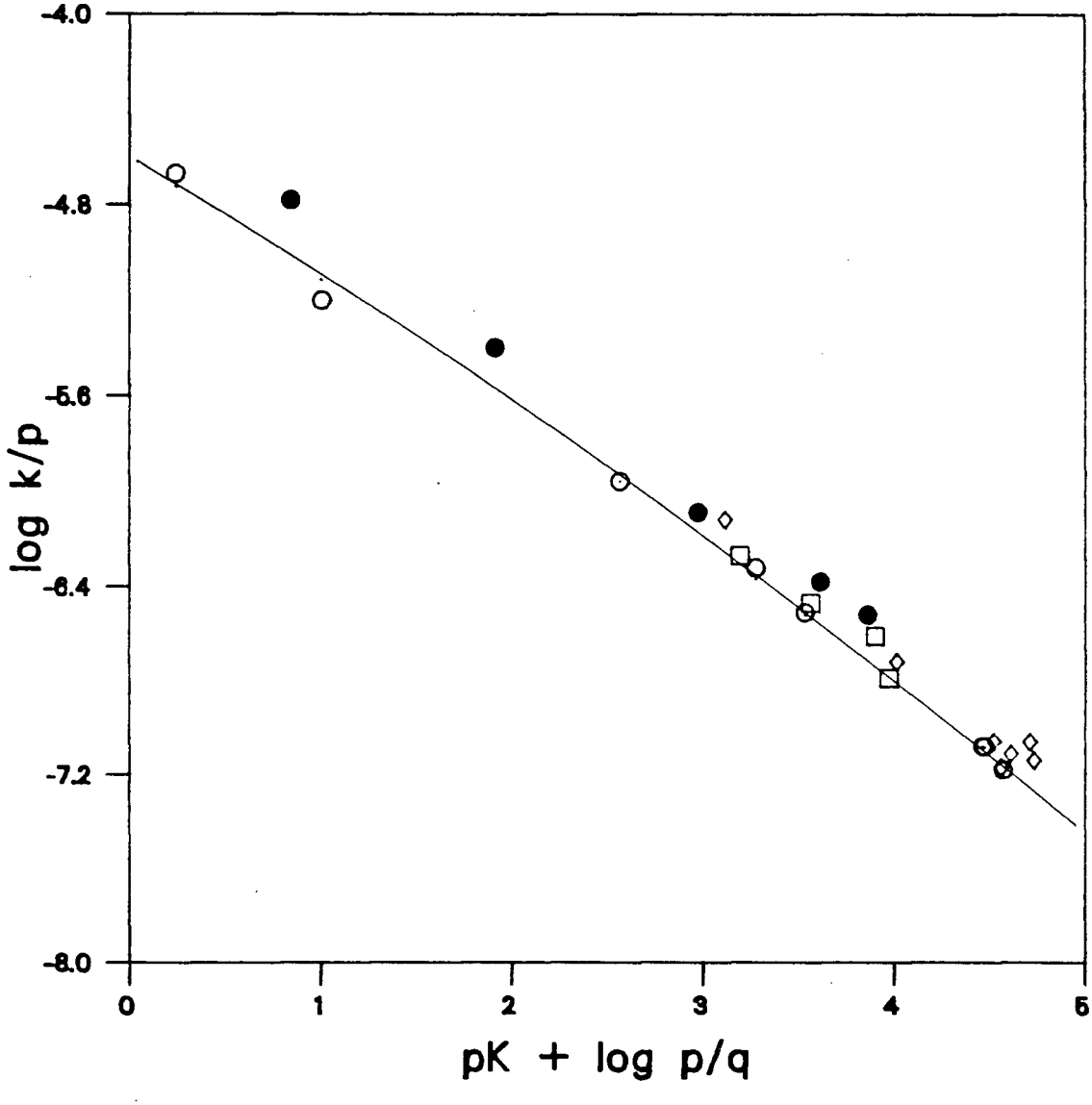

Fig. 37: Bronsted plot for catalysis of acetone enolization by carboxylic acids; second degree curve drawn for eight aliphatic acids (open circles); also shown are seven aliphatic acids possessing steric bulk (open diamonds); four meta benzoic acids (open squares) and five ortho benzoic acids (closed circles).

deviations for these acids. The largest deviations (as measured by $k_{HA}^{obs}/k_{HA}^{calc}$) are for the ortho benzoic acids, with the larger substituent generally having the greater deviation. Thus 2,6-dinitrobenzoic acid is a factor of 1.8 times more effective as a catalyst than is expected on the basis of the equilibrium acid strength. Benzoic acid and its meta derivatives have values of $k_{HA}^{obs}/k_{HA}^{calc}$ that are generally lower than those found for the ortho-substituted acids. The aliphatic carboxylic acids show varying effects; the bulky mandelic and t-butylacetic acids showing the larger deviations ($k_{HA}^{obs}/k_{HA}^{calc} \approx 1.4$), while dimethylacetic and butanoic acid have values of $k_{HA}^{obs}/k_{HA}^{calc}$ close to unity.

Incidentally the use of the linear correlation eq. [4.10] gives values of $k_{HA}^{obs}/k_{HA}^{calc}$ comparable to, and showing the same trend, as the data in Table 28. Possible explanations for such steric acceleration will be discussed after analysis of the results for all the catalytic species under investigation.

We can also use eq. [4.11] to quantify the polarizability accelerating effect discussed previously. The results are given in Table 29 and show the expected trend. The largest acceleration is for tribromoacetic acid, with trichloroacetic acid showing a comparable deviation. It is interesting that the accelerating effect of dichloroacetic and iodoacetic acid are also comparable; this indicates that the polarizability effect of two chlorine atoms is roughly the same as the polarizability of one iodine atom.

A consideration of Fig. 36 from the viewpoint of a linear correlation relies heavily on the point for trifluoroacetic acid; on the other

Table 29: $k_{HA}^{obs}/k_{HA}^{calc}$ values for aliphatic carboxylic acids possessing polarizable substituents. Values of k_{HA}^{calc} obtained using eq. [4.11]

Acid	$k_{HA}^{obs}/k_{HA}^{calc}$
Cl_3CCO_2H	1.71
Br_3CCO_2H	1.83
Cl_2CHCO_2H	1.28
ICH_2CO_2H	1.31

hand the exclusion of this acid lends further support to a curved correlation of the carboxylic acid set. It is possible that the polarizability effect is yielding a slightly oversized value of k_{HA} for trifluoroacetic acid; a quadratic correlation of the other seven acids gives a much better result (r = 1.00) than a linear correlation of the same data (eqs. [4.12] and [4.13] respectively).

7 acids, r = 0.9975

$$\log (k_{HA}/p) = -\underset{\pm 0.07}{4.58} - \underset{\pm 0.018}{0.556}(pK + \log p/q) \qquad [4.12]$$

7 acids, r = 1.0000

$$\log (k_{HA}/p) = -\underset{\pm 0.04}{4.82} - \underset{\pm 0.032}{0.351}(pK + \log p/q) - \underset{\pm 0.0054}{0.0355}(pK + \log p/q)^2 \qquad [4.13]$$

The deviation of the trifluoroacetic acid from the curve defined by eq. [4.13] as measured by $k_{HA}^{obs}/k_{HA}^{calc}$ is a factor of 1.65; the values for the four acids listed in Table 27 (trichloroacetic acid etc.) increases with the use of eq. [4.13]. The acids now have $k_{HA}^{obs}/k_{HA}^{calc}$ values of 2.50, Cl_3CCO_2H; 2.67, Br_3CCO_2H; 1.58, Cl_2CHCO_2H; 1.47, ICH_2CO_2H. (The relative magnitude of these values is unchanged from those listed previously.) It is interesting that the polarizability effect of three fluorine atoms is only slightly higher than either two chlorine atoms or one iodine atom. This treatment presumes that the effect of polarizability on difluoroacetic and chloroacetic acid is negligible.

As sterically bulky catalysts have been shown to deviate positively from the Bronsted line, the polarizability effect could well be superimposed on the steric effect, especially in the case of the tri-halo acids and, in particular the acids possessing the larger halo atoms.

An attempt to include more carboxylic acids (with pK values less than chloroacetic acid) in the Bronsted plot in order to further evaluate the curved correlation proved futile. Unfortunately, cyanoacetic acid (pK value of 2.47) reacts rapidly with triiodide ion. While we did measure the k_{HA} values for protonated glycine and two of its derivatives (pK values between 1.83 and 2.36), these acids illustrated an effect of their own.

5. It is evident from Fig. 32 that the ammonio carboxylic acids are less effective catalysts than is expected on the basis of the Bronsted line for the uncharged carboxylic acids; thus protonated glycine and its

dimethyl and trimethyl derivatives show negative deviations from that line. The magnitude of the deviation can be estimated from the value of $k_{HA}^{obs}/k_{HA}^{calc}$, k_{HA}^{calc} values available from eq. [4.11]; the average result for the three acids is 0.62 ± 0.08 illustrating catalytic retardation by a factor of 1.6.

This effect could be related to the effect discussed previously in the case of carboxylate monoanions and dianions. It may be recalled that the dianions formed a distinct Bronsted line displaced downward from the monocarboxylate line by about a factor of three in the rate constants. In this case the deviation is also in the negative direction, but involves carboxylic acids bearing positively charged substituents. The three acids examined are all structurally similar and prompted us to question the effect of increasing the distance between the positive charge and the carboxylic acid portion of the catalyst. We chose to evaluate this effect by obtaining the trimethyl ammonio derivatives of butanoic and hexanoic acid and measuring the k_{HA} values. The reported pK values for these two acids (3.98, 4.26) led us to expect a measureable k_{A^-} value for the conjugate monoanion of the carboxylic acid.

Measurements for both of these acids were made at four buffer-ratios at 0.1 M ionic strength (I) and gave excellent kinetic results. The results for 4-trimethylammoniobutanoic acid ($(CH_3)_3N^+(CH_2)_3CO_2H$) are k_{HA} = 1.59 ± 0.06 x 10^{-7} M^{-1} sec^{-1} and k_{A^-} = 8.05 ± 0.28 x 10^{-8} M^{-1} sec^{-1} (n values of 0.25, 0.5, 1 and 4). The results for 6-trimethylammoniohexanoic acid ($(CH_3)_3N^+(CH_2)_5CO_2H$) k_{HA} = 1.18 ± 0.04 x 10^{-7} M^{-1} sec^{-1} and k_{A^-}= 1.77 ± 0.09 x 10^{-7} M^{-1} sec^{-1} (n values of 0.5, 1, 2 and 4). There

is a large discrepancy, for both of these acids, between the pK^T values reported in the literature (EF79) and the pK^I values (I = 0.1 M) available from the average pH values at each n value (pK^I = pH + log n). The pK^I values are 4.13 ± 0.04 for the butyric acid derivative and 4.51 ± 0.02 for the hexanoic acid derivative (at 0.1 M ionic strength). These values have been confirmed in this laboratory by potentiometric titration of the acids (NV87). To avoid any question of ionic strength effects on pK^T causing apparent deviations for the positively charged acids, we will use pK^I values in the Bronsted plot.

In the case of the two acids just mentioned and the neutral carboxylic acids, rate constants have been measured at an ionic strength of 0.1 M. The pK^I values for the uncharged acids agree with that expected on the basis of eq. [3.7] (p. 71), i.e. pK^T - 0.11 at 0.1 M ionic strength. However measurements of k_{HA} for protonated glycine and its N-methyl derivatives have been obtained over a span of ionic strength (0.1 to 0.4 M), a variance that seemingly has no effect on k_{HA}. Values of pK^I are available from experimental data and these also show no variation with ionic strength. The results are listed in Table 30.

The Bronsted curve defined by eight uncharged acids (using pK^I) is given by eq. [4.14] (same acids as in Fig. 36). The corresponding Bronsted plot contains the results for the charged acids, Fig. 38. A measure of the degree of deviation for these acids is given by $k_{HA}^{obs}/k_{HA}^{calc}$, where k_{HA}^{calc} is the value expected on the basis of eq. [4.14]. Some deviations are obvious in Fig. 38 and the values of $k_{HA}^{calc}/k_{HA}^{obs}$ in Table 30 quantify these results. While acids possessing positive charges near the carboxylic acid centre generally deviate from the

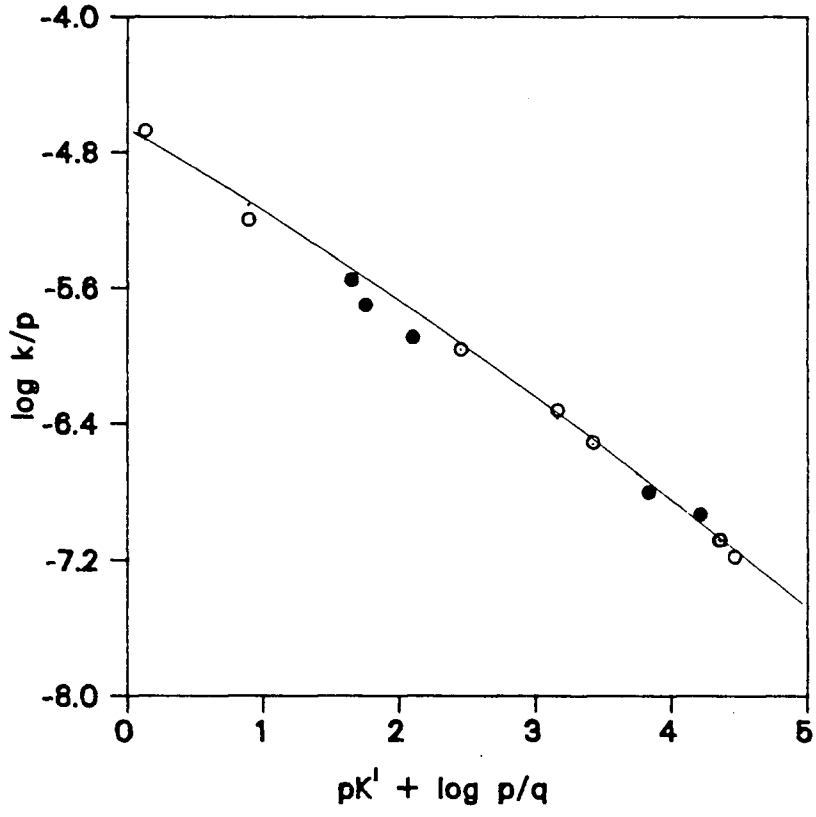

Fig. 38: Bronsted plot for catalysis of acetone enolization by aliphatic carboxylic acid; 8 uncharged acids (open circles), 5 positively charged acids (closed circles). Curve is for uncharged acids (eq. [4.14])

Bronsted line, the effect is removed by increasing the distance between the two moieties.

$$(\log k_{HA}/p) = -\underset{\pm 0.05}{4.66} - \underset{\pm 0.051}{0.500}\,(pK^I + \log p/q) - \underset{\pm 0.010}{0.131}\,(pK^I + \log p/q)^2 \qquad [4.14]$$

Table 30: pK^I and $k_{HA}^{obs}/k_{HA}^{calc}$ values for aliphatic carboxylic acids possessing positively charged substituents. Values of k_{HA}^{calc} obtained using eq. [4.14]

Acid	pK^I	$k_{HA}^{obs}/k_{HA}^{calc}$
$(CH_3)_3N^+CH_2CO_2H$	1.95 ± 0.02	0.944
$(CH_3)_2N^+HCH_2CO_2H$	2.05 ± 0.05	0.749
$H_3N^+CH_2CO_2H$	2.40 ± 0.03	0.744
$(CH_3)_3N^+(CH_2)_3CO_2H$	4.13 ± 0.04	0.930
$(CH_3)_3N^+(CH_2)_5CO_2H$	4.51 ± 0.02	1.17

In the case of trimethylglycine, it seems that a positive charge close to the carboxylic acid has no effect on k_{HA}. However, we can attribute a rate accelerating steric effect to k_{HA} for this acid, on the basis of our earlier discussion. The two factors work in opposition to one another giving the result shown. It may be recalled that t-butylacetic acid, the carbon analogue of this acid, shows a relatively large positive deviation from the Bronsted line.

The transition state for the process involves hydrogen abstraction from protonated acetone by the carboxylate base. It seems that when the base possesses a unit of positive charge close to the carboxylate, a repulsive interaction occurs which raises the energy of the transition

state. This effect is small (a rate retardation by a factor of 1.3 for protonated glycine) and may reflect an electrostatic repulsive interaction between the substrate and the catalyst. The system will try to minimize this effect and this may, in part, explain the relatively small size of the effect. If the catalyst has a structure which can minimize the interaction, it will do so and thus the degree of deviation is almost negligible for the four-carbon ammonion compound. The six-carbon ammonio compound is actually above the line to a very small extent. The role of a steric accelerating factor for these two acids should be minimal, considering the earlier result for butanoic acid.

The values of k_A- determined for the conjugate anions of the two acids just mentioned can be compared with the values expected on the basis of the Bronsted line for monobasic carboxylates (using pK^I values in the correlation). For 4-trimethylammoniobutanoate anion, the $k_A\text{-}^{obs}/k_A\text{-}^{calc}$ value is 0.946 and for 6-trimethylammoniohexanoate anion the $k_A\text{-}^{obs}/k_A\text{-}^{calc}$ value is 0.957. These results illustrate a negligible effect for base abstraction of a proton from acetone when the base possesses a unit of positive charge that is some distance from the carboxylate portion of the base. We are unable to measure k_A- values for bases possessing a positive charge closer to the carboxylate group, e.g. glycine.

A study by Cox and co-workers involved the base catalyzed enolization of two ketones that possess positively charged ammonio groups in the substrate itself (CM81). They found rates 10^3 times larger than those of the corresponding base catalyzed reactions for either the neutral aminoketone or acetophenone. The effect diminished with an

increase in the length of the alkyl chain separating the carbonyl and the ammonio moiety. The authors suggest that intramolecular electrostatic stabilization of the negative charge developing on the carbonyl oxygen in the transition state causes the rate acceleration. In our case, which is an intermolecular situation, no effect is observed, perhaps reflecting the difficulty in having the ammonio substituent in the correct position in space to stabilize the developing negative charge on the carbonyl oxygen. Another interesting study involving electrostatic effects has been reported by Dahlberg and co-workers (DK83).

4.2.2 Diprotic Acids

Table 14, p. 109 contains four k_{H_2A} values. This small group of dicarboxylic acid rate constants should provide some insight into the effect of changing the catalyst from a monoprotic acid to a diprotic acid. These k_{H_2A} values are shown in Fig. 39, which also include the Bronsted line for monoprotic carboxylic acids.

It seems, from Fig. 39, that two of the four diacids are essentially on the line for the monoacids, i.e. oxalic and succinic acid. On the other hand diethylmalonic and 3,3-dimethylglutaric acid fall below the monoacid line. It may be recalled that the dianions of these two acids deviated negatively from the Bronsted line for the other dianions, an effect which is related to the degree of hydrogen bonding in the monoanion. The same effect would qualitatively explain the results in this case.

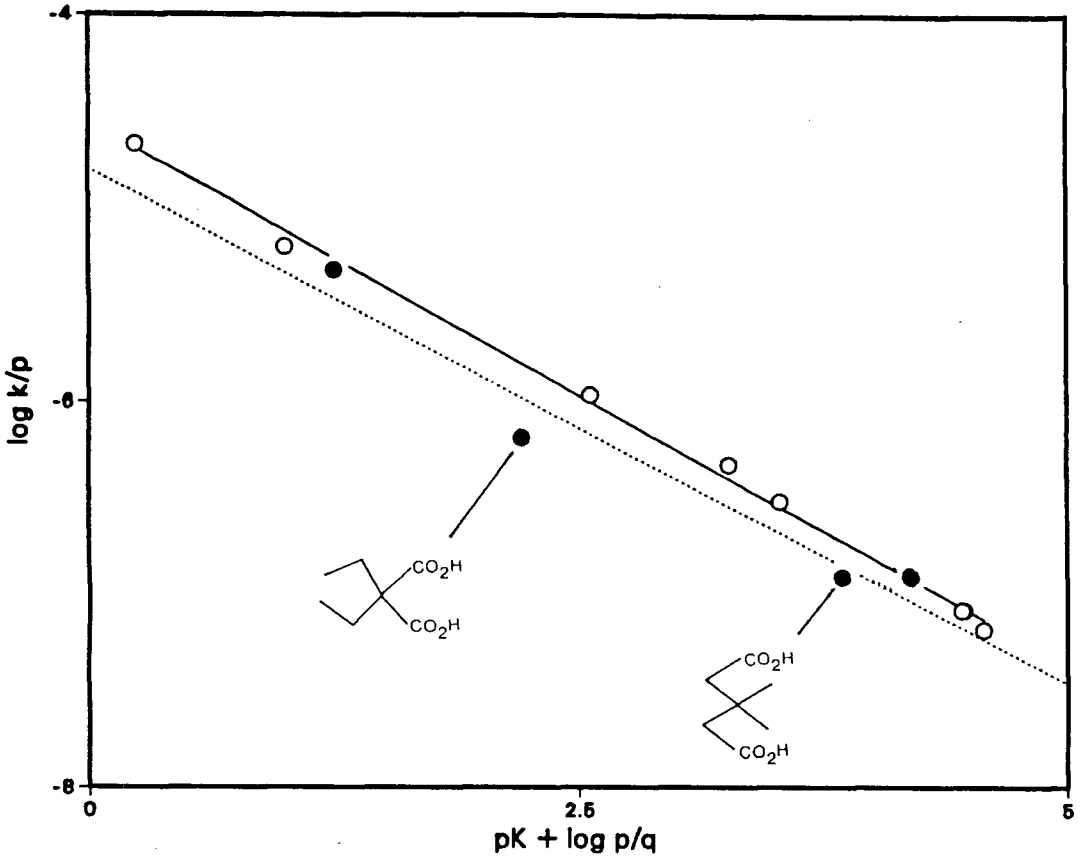

Fig. 39: Bronsted plot for catalysis of acetone enolization by aliphatic carboxylic acids; monoprotic acids (open circles, solid line) and diprotic acids (closed circles, dotted line).

While the deviation for diethylmalonic acid ($K_1^{obs}/K_1^{calc} = 4.7$) is greater than that of 3,3-dimethylglutaric acid ($K_1^{obs}/K_1^{calc} = 2.1$), the magnitude of the effect is much smaller than the effect on K_1 as measured by $K_1/2K_E$ (16 and 5.0 respectively). These results suggest that the effect of hydrogen-bonding in the transition state is only slightly less than the effect on the equilibrium acid strength of the diacid. The process is represented by eq. [1.10b] below, where A^- is the monoanion of the diacid.

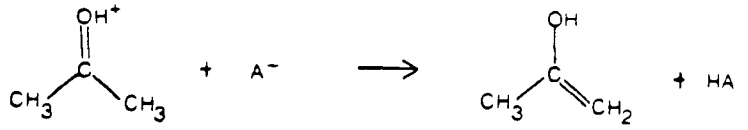

[1.10b]

4.3 BIFUNCTIONAL CATALYSTS (DICARBOXYLIC ACID MONOANIONS)

A collection of data from Table 14, p. 109, and Table 16, p. 114, provides sixteen rate constants for the monoanions of dicarboxylic acids. One of the aims of this work is to evaluate the role played by such monoanions in the enolization of acetone. Are these bifunctional monoanions (i.e. those containing both $-CO_2H$ and $-CO_2^-$ groups) acting as bifunctional catalysts (eq. [1.87] p. 56)? A study by other workers involving three monoanions suggests the absence of bifunctional catalysis (p. 54, LA67). If this is the situation, another question has to be answered; are these catalysts containing both acidic and basic functionalities acting as general acids or general bases?

1. Our approach to answering these questions involved dual analysis of the sixteen k_{HA^-} values; (i) if the monoanions are acting as general acids (i.e. protonation of acetone, followed by hydrogen abstraction from acetone by the conjugate dianion), the Bronsted plot involves a correlation of k_{HA^-} with pK_2, and should have a negative slope (since the weaker acid will be the poorer catalyst). (ii) If the monoanions are acting as general bases (i.e. hydrogen abstraction from acetone by the carboxylate functionality of the monoanion), the Bronsted plot

involves a correlation of k_{HA^-} with pK_1, and should have a positive slope (since the stronger base will be the better catalyst).

The results of both Bronsted plots could very well indicate whether general acid or general base catalysis is operative. The inclusion of the Bronsted lines for carboxylic monoprotic acids (Fig. 34, p. 154) and for their conjugate bases (Fig. 29, p. 132) in the appropriate Bronsted plot for the monoanions could answer the question of whether bifunctional catalysis is operative; if the monoanions are acting as bifunctional catalysts, we should expect considerable exaltation of the catalytic constants over values expected on the basis of the Bronsted lines for the monoprotic acids and their conjugate bases.

The two resulting Bronsted plots are shown in Figs. 40 and 41. Two features are evident from these plots: (i) Bifunctional catalysis is obviously not important since the measured k_{HA^-} values are generally of the same order of magnitude as the monoprotic acids and conjugate bases in the same pK region. (ii) The plot of the monoanions acting as bases, Fig. 41, has some scatter and produces a negative slope, which makes no sense at all. On the other hand the plot of the monoanions acting as acids, Fig. 40, shows a much better correlation, with again a negative slope, which in this case is the appropriate one. Therefore we conclude that general acid catalysis is the observed route for the monoanions of dicarboxylic acids.

2. It is interesting that these monoanions, acting as general acids, are more effective as catalysts than the neutral monoprotic acids. The transition state for the latter process involves hydrogen abstraction

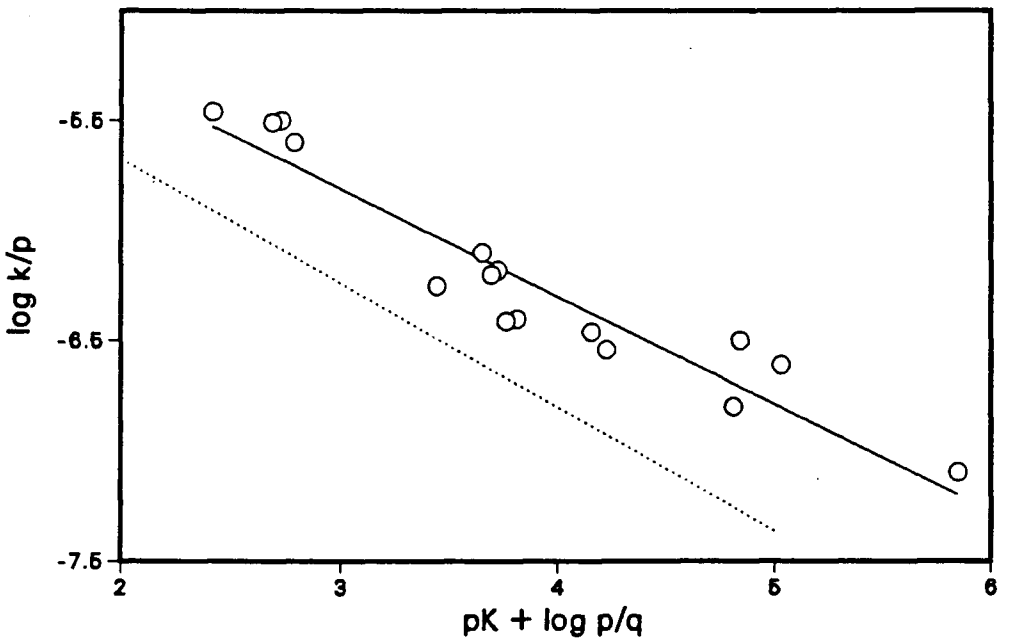

Fig. 40: Bronsted plot for catalysis of acetone enolization by the monoanions of dicarboxylic acids (solid line); monoanions acting as acids, involving pK_2, p = 1, q = 4; Bronsted line for carboxylic monoprotic acids added for comparison (dotted line).

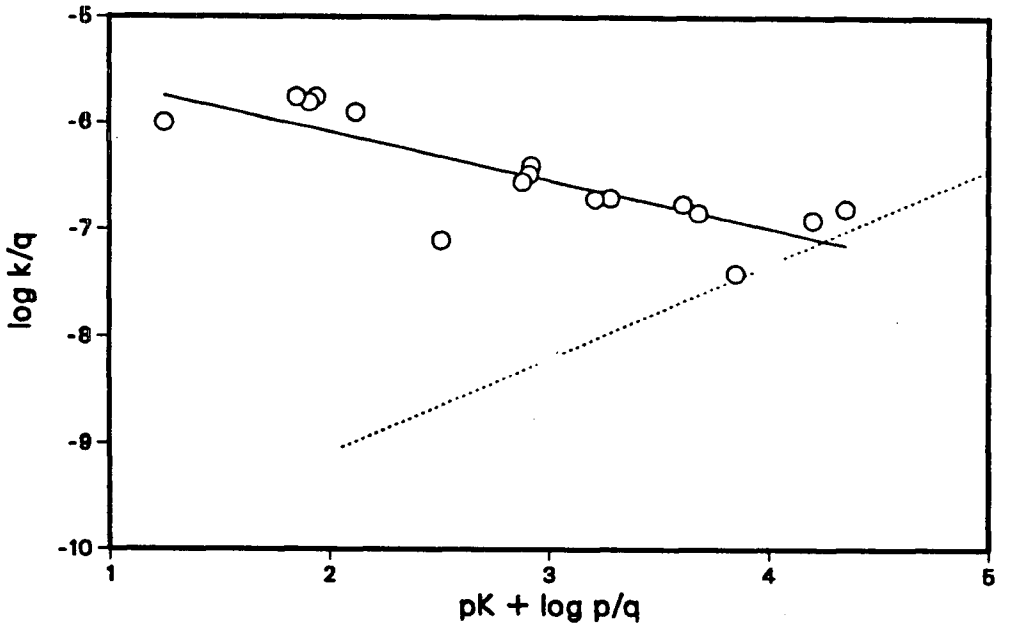

Fig. 41: Bronsted plot for catalysis of acetone enolization by the monoanions of dicarboxylic acids (solid line); monoanions acting as bases, involving pK_1, p = 2, q = 2; Bronsted line for carboxylate bases added for comparison (dotted line).

from protonated acetone by the conjugate base, A^-, while in the former process, the base is the conjugate dianion, A^{2-}. When the substrate is acetone base catalysis by dianions is less effective than monoanion catalysis (Section 4.1.2).

These two effects seem independent of the distance separating the two carboxylate moieties in the catalyst, but rather, just dependent on the presence of the additional carboxylate unit, and whether the substrate is acetone or protonated acetone.

3. The data in Fig. 40 are shown in Fig. 42 with a classification of the types of monoanion present. One of our aims in examining the isophthalic acids is to probe further the effect of ortho substituents on the rate constants of benzoic acid and benzoate anion derivatives. Unfortunately, due to relatively poor catalysis by the dianions of these acids, we are unable to study the ortho effect in benzoate anion derivatives. However, the values of k_{HA^-} for the isophthalate monoanions can provide some insight into the ortho effect in benzoic acid derivatives. (These catalysts can be considered as benzoic acid derivatives which possess a 3-CO_2^- substituent and either a 5- or a 2-substituent also).

A first step in evaluating any effects in the isophthalate monoanions is to define the general acid-catalyzed Bronsted line for the 5-substituted monoanions. (We have included the unsubstituted species in this category.) The result of a linear correlation is given in eq. [4.15], providing an α value of 0.321 ($\pm$ 0.056, Fig. 43). This slope is significantly lower than that observed for the aliphatic carboxylic

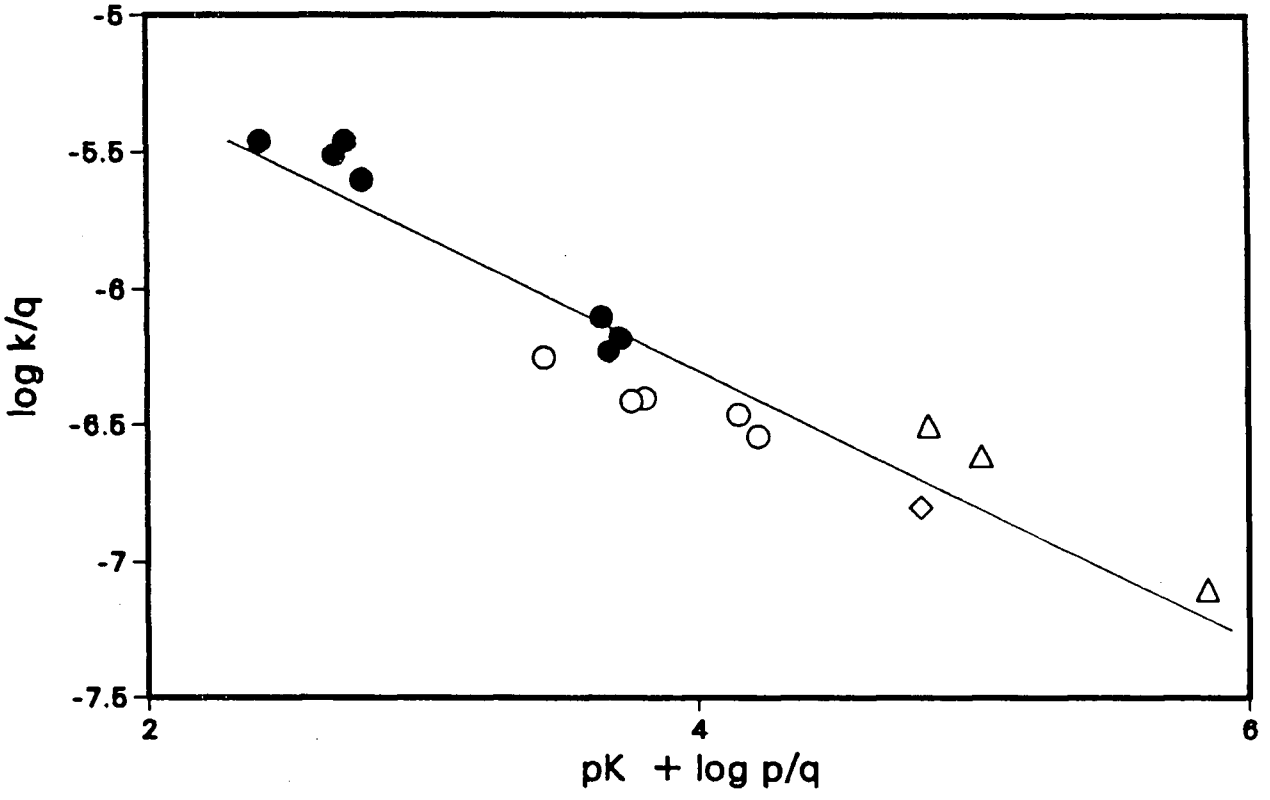

Fig. 42: Bronsted plot for catalysis of acetone enolization by the monoanions of dicarboxylic acids; aliphatic monoanions (open triangles), phthalate monoanion (open diamond), 5-substituted isophthalate monoanions (open circles) and 2-substituted isophthalate monoanions (closed circles).

acids and benzoic acid and its meta derivatives, i.e. 0.598 (± 0.024). The range of (pK + log p/q) for the isophthalate monoanion is 3.4 - 4.2, while for the neutral carboxylic acids, the range is 2.6 - 4.7.

5 monoanions $\quad \log (k_{HA}\text{-}/p) = -5.17 - 0.321(pK + \log p/q)$ [4.15]
r = 0.9581 $\qquad\qquad\qquad\qquad\qquad\qquad \pm \qquad \pm$
$\qquad\qquad\qquad\qquad\qquad\qquad\quad 0.22 \qquad 0.056$

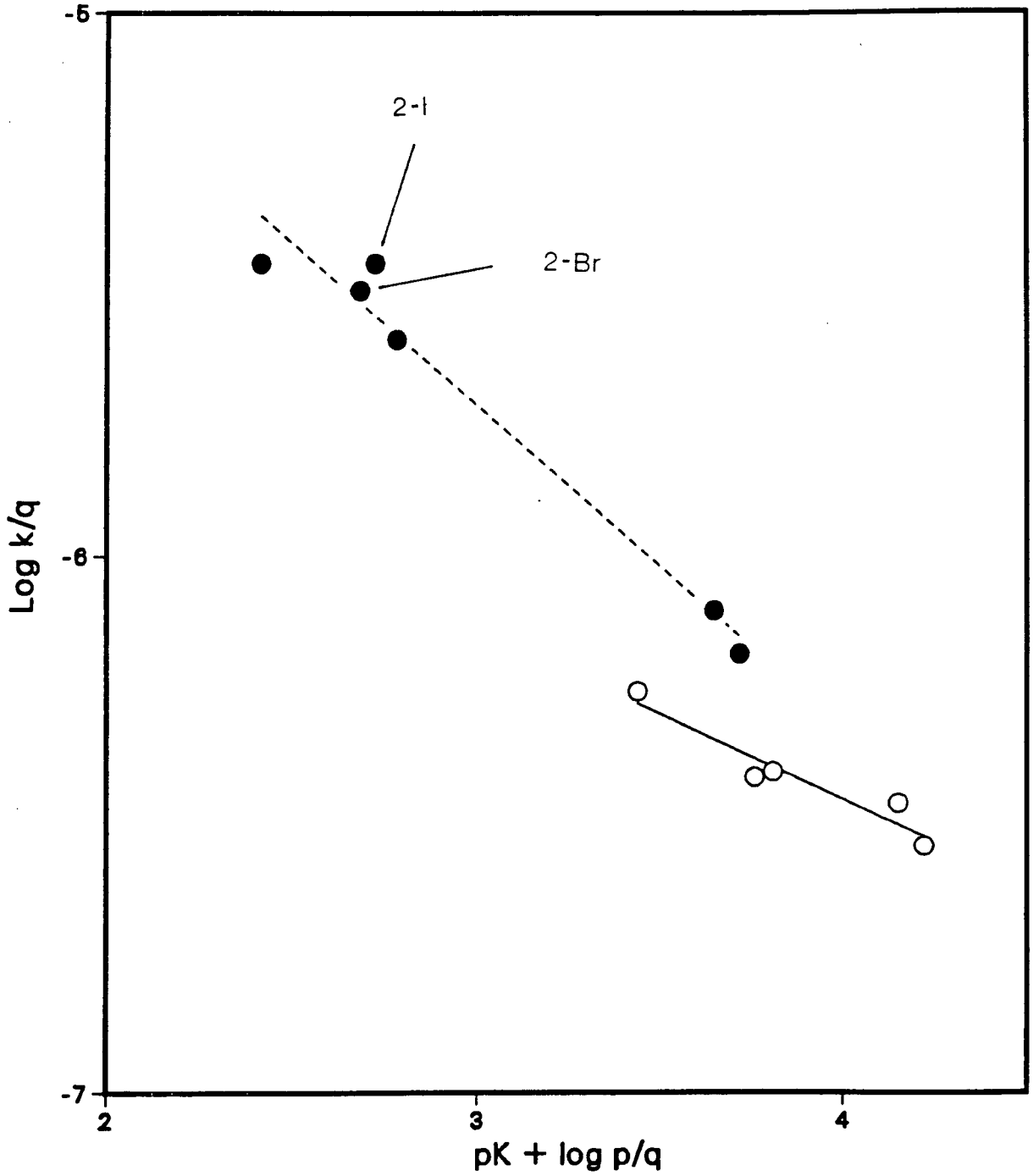

Fig. 43: Bronsted plot for catalysis of acetone enolization by isophthalate monoanion; data from Table 16, p. 114; 5-substituted isophthalate monoanions (open circles, solid line) and 2-substituted isophthalate monoanions (closed circles, dashed line).

The low correlation coefficient of eq. [4.15] reflects the random scatter of the points in a relatively small pK range. A poor correlation is also evident for benzoic acid and its meta derivatives, acids which also cover a narrow span of pK values, eq. [4.16]. Thus the significant drop in the α value in the case of eq. [4.15] from that observed for uncharged carboxylic acids (whether aliphatic and/or benzoic acids) cannot be written off as a meaningless slope of a poorly correlated linear regression.

4 benzoic acids $\log (k_{HA}/p) = -4.37 \pm 0.41 - 0.593 \pm 0.113 \, (pK + \log p/q)$ [4.16]
r = 0.9655

An interpretation of the α value (0.32) for 5-isophthalate monoanions in terms of the Hammond postulate and Marcus theory reads as follows. The β value for abstraction of the hydrogen from protonated acetone by the isophthalate dianion is 0.68 (1-α). This suggests a late transition state with the proton transfer over half complete. It may be recalled that when the base involved is a monobasic carboxylate, an earlier transition state is implied by the smaller β value (0.38 $\pm$ 0.02). The apparent high β value for the isophthalate dianions is in direct conflict with the value expected on the basis of the Hammond postulate. The more reactive isophthalate dianions should lead to an earlier transition state as compared to the monobasic carboxylates. An earlier transition state is linked to a smaller β value. However the less reactive monobasic anions have the smaller β value.

A similar contradictory effect is evident in the system involving

neutral acetone and carboxylate bases. The more reactive monobasic catalysts have the larger β value, 0.89, whereas the less reactive dibasic catalysts have the slightly smaller β value, 0.78.

The 2-substituted isophthalate monoanions show an acceleration relative to the 5-substituted monoanions. While the two groups of catalysts only share a limited range of pK values, the 2-substituted monoanions in this range (2-CH_3O and 2-CH_3) deviate positively relative to the line defined by 5-substituted isophthalate monoanions in the same range. This effect can be attributed to the presence of the ortho substituent in the catalyst. This is consistent with the effects observed with ortho-substituted benzoic acids. It is difficult to estimate the rate accelerating factor for all the 2-substituted monoanions as this would involve a tenuous extension of the 5-substituted monoanion line. However the values of $k_{HA}\text{-}^{obs}/k_{HA}\text{-}^{calc}$ for 2-methyl and 2-methoxyisophthalate monoanion can be estimated on the basis of e.q. [4.15], the 5-substituted Bronsted line. The results are 1.52 for 2-CH_3O and 1.75 for 2-CH_3; these values roughly agree with the results for 2-ethoxybenzoic acid, 1.57, and 2-methylbenzoic acid, 1.52, which are based on the monocarboxylic acid Bronsted line.

The set of 2-substituted isophthalate monoanions in Fig. 43 forms a reasonably linear Bronsted correlation, defined by eq. [4.17]. It can be seen that two of the halo-substituted monoanions (bromo and iodo) are on the positive side of this line, and considering the role of polarizability effects in the general acid catalyzed mechanism (p. 155), these monoanions could very well be deviating from the Bronsted line due to a polarizability effect. The Bronsted line for the four other monoanions

(excluding 2-I and 2-Br) is given by eq. [4.18] and is a statistical improvement upon eq. [4.17].

6 monoanions $\log (k_{HA}^-/p) = -3.95 \pm 0.17 - 0.592 \pm 0.055 \ (pK + \log p/q)$ [4.17]
r = 0.9829

4 monoanions $\log (k_{HA}^-/p) = -4.11 \pm 0.11 - 0.551 \pm 0.034 \ (pK + \log p/q)$ [4.18]
r = 0.9960

A measure of the degree of deviation from eq. [4.18] for 2-I and 2-Br will be given by $k_{HA}^{-obs}/k_{HA}^{-calc}$. The results are 1.41 for 2-I and 1.20 for 2-Br, a trend that is expected since iodine has the larger polarizability effect. The absence of an effect for the 5-I and 5-Br monoanions must be due to the large distance separating the catalytic centre and the halo atom.

The 2-substituted isophthalate monoanions seem to form a good linear Bronsted correlation displaced above, and having a larger α value than, the 5-substituted monoanion Bronsted line. A larger α value implies a smaller β value for the rate-determining proton abstraction. Thus for the 5-substituted monoanions, $\beta = 0.68$, whereas the 2-substituted monoanions have a smaller value, $\beta = 0.45$. This smaller β value may reflect the more reactive system for the 2-substituted catalysts, a greater reactivity which seems to arise as a result of the ortho-substitution. The earlier transition state in this system would then be credited to a steric rate accelerating effect.

Having said that, evidence for such a situation in the ortho-benzoic

acids when compared to other monocarboxylic acids (whether aliphatic or meta-benzoic) has not been found. The five ortho-benzoic acids studied do give a good linear Bronsted correlation, eq. [4.19], but the α value is comparable to that obtained for the other monocarboxylic acids.

$$\begin{array}{ll} \textbf{5 acids} & (\log k_{HA}/p) = -\underset{0.05}{4.30} - \underset{0.016}{0.581}\,(pK + \log p/q) \\ \textbf{r = 0.9990} & \end{array} \qquad [4.19]$$

All the effects discussed for the 2- and 5-substituted isophthalate monoanions have involved the data in Table 16, k_{HA^-} values determined by ignoring the overlapping dissociations of the diacids. If the values of k_{HA^-} are used from Table 17, values determined by considering the overlapping dissociations, these monoanions deviate to a slightly higher degree from the neutral carboxylic line (factor of 1.2). However the relative position of the isophthalate monoanions with respect to each other does not change as shown by Fig. 44.

4.4 ARYLPHOSPHONIC ACIDS. SUBSTITUENT EFFECTS ON THEIR FIRST AND SECOND DISSOCIATIONS

Before discussing the catalytic rate constants for the arylphosphonic acids and related species, an analysis of their first and second dissociations will be presented (Table 18, p. 117).

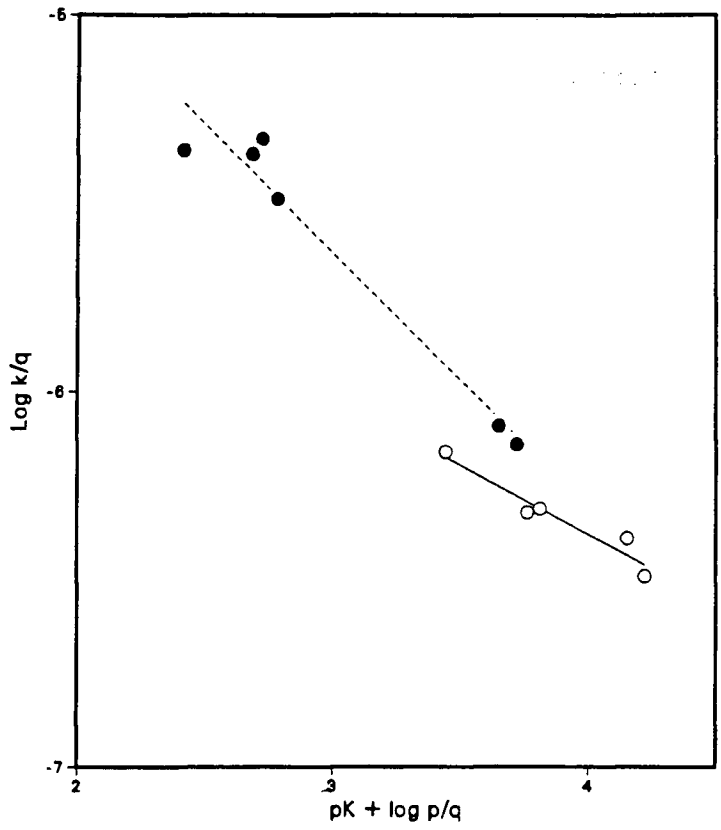

Fig. 44: Bronsted plot for catalysis of acetone enolization by isophthalate monoanions; data from Table 17, p. 115, determined by considering the overlapping dissociations of the diacid; 5-substituted isophthalate monoanions (open circles, solid line) and 2-substituted isophthalate monoanions (closed circles, dashed line).

4.4.1 Meta and Para Substituents

The π-bonding abilities of phosphorus and carbon are known to be quite different (M79). With regard to arylphosphonic acids, the degree of conjugation between aryl ring and the acidic functional group appears

to be considerably less than is the case with arylcarboxylic acids, judging from the ortho effects to be discussed later. Accordingly, one might expect that ordinary Hammett σ values would overestimate the electron releasing capacity of groups such as alkoxy in the para position of arylphosphonic acids. Thus the modified substituent constant σ^n, which is intended for use with systems that have no through conjugation, might be better for correlating the pK values of these acids (T60, HW73).

We find that our data for pK_2 are correlated very well by σ^n (Fig. 45 and eq. [4.19]) and rather poorly by σ (Fig. 46 and eq. [4.20]), indicating the degree of π bonding between the aryl ring and phosphorus to be small. The values of σ and σ^n are listed in Table 31.

17 acids
r = 0.9970

$$pK_2 = 7.55 \pm 0.01 - 1.140\sigma^n \pm 0.023 \qquad [4.19]$$

17 acids
r = 0.9778

$$pK_2 = 7.48 \pm 0.02 - 0.980\sigma \pm 0.054 \qquad [4.20]$$

It is clearly evident from Figs. 45 and 46 and the related equations that σ^n is the substituent constant of choice for the Hammett correlation of the substituents and the equilibrium constants.

The situation with respect to pK_1 is less clear, partly because the bellwether amino substituent is absent and partly because the precision of the K_1 values is less. In contrast to the results with pK_2, the

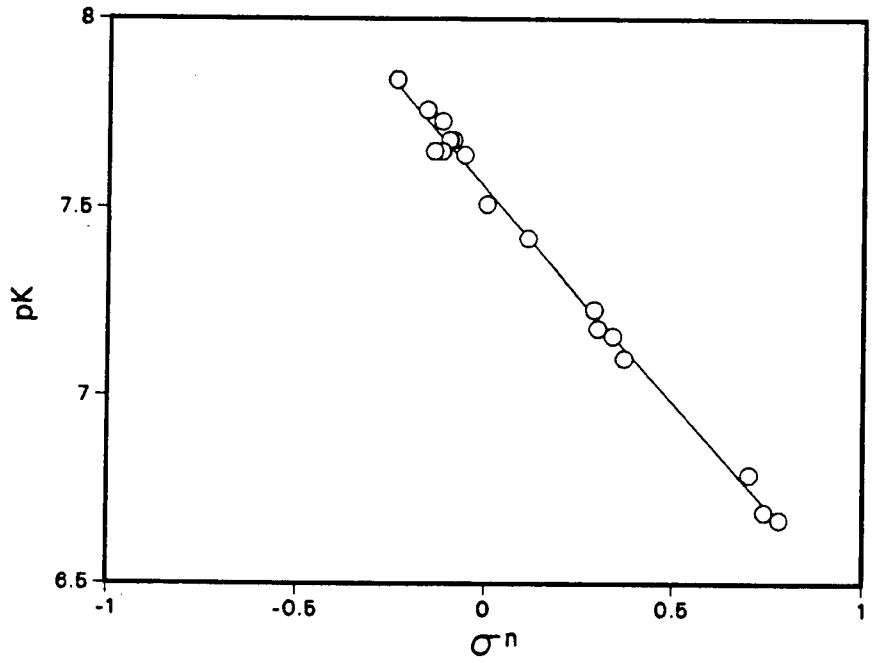

Fig. 45: Plot of pK_2 for arylphosphonic acids against the substituent constant σ^n

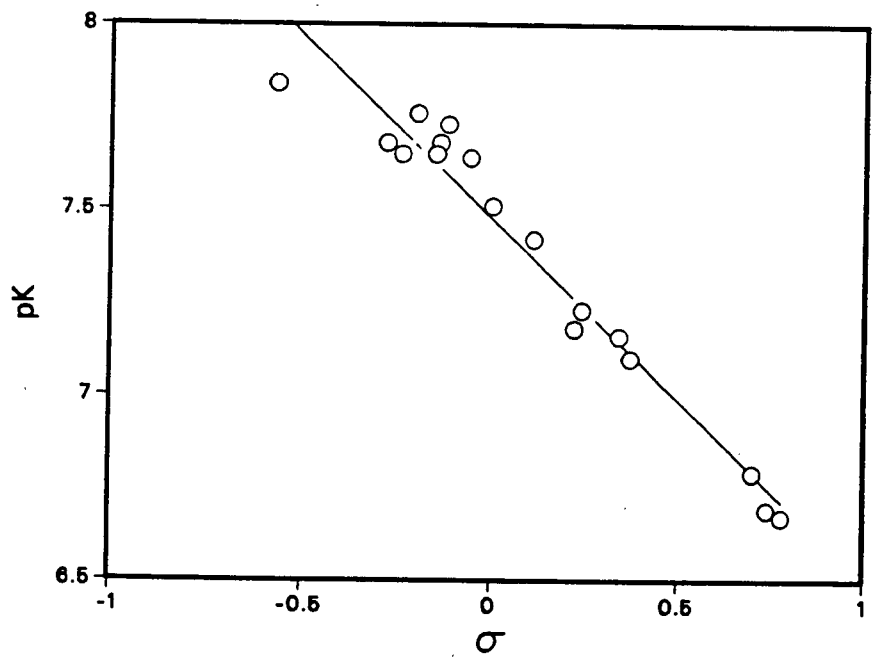

Fig. 46: Plot of pK_2 for arylphosphonic acids against the substituent constant σ

Table 31: Substituent constant values (σ and σ^n) for meta and para substituents. Data from refs. (PD81, HW73)

Substituent	σ	σ^n
H	0.00	0.00
3-CH_3	-0.06	-0.06
4-CH_3	-0.14	-0.10
4-C_2H_5	-0.15	-0.12
3-CH_3O	0.11	0.11
4-CH_3O	-0.28	-0.09
4-C_2H_5O	-0.24	-0.14
3-F	0.34	0.34
3-Cl	0.37	0.37
4-Cl	0.24	0.29
4-Br	0.22	0.30
4-CN	0.70	0.70
3-NO_2	0.74	0.74
4-NO_2	0.78	0.78
4-NH_2	-0.57	-0.24
3,4-$(CH_3)_2$	-0.20	-0.16
3,5-$(CH_3)_2$	-0.12	-0.12

correlation between pK_1 and σ^n (Fig. 47 and eq. [4.21]) is not dramatically better than for σ (Fig. 48 and eq. [4.22]) when all points are included.

16 acids
r = 0.9954

$$pK_1 = 1.88 \pm 0.01 - 0.924 \pm 0.024\ \sigma^n \qquad [4.21]$$

16 acids
r = 0.9872

$$pK_1 = 1.84 \pm 0.01 - 0.857 \pm 0.037\ \sigma \qquad [4.22]$$

When a line is drawn with respect to the compounds for which $\sigma = \sigma^n$ (i.e. meta compounds and the para nitro and cyano compounds), the values of the slope and intercept are − 0.926 and 1.89, respectively, for pK_1. These values are almost identical to those given in eq. [4.21] but are considerably different from those given in eq. [4.22]. This is conclusive evidence that σ^n, and not σ, is the parameter of choice for pK_1. The correlation involving pK_2 for the compounds having equivalent σ and σ^n values gives further support to the choice of the latter substituent constant for pK_2; the values of the slope and intercept are 1.143 and 7.55, respectively, and are almost identical to those in eq. [4.19], but significantly different from those in eq. [4.20].

The reaction constant for the first dissociation is smaller than for the second, $\rho_1^n = 0.924$ $\rho_2^n = 1.140$ (Figs. 45 and 47 respectively). We find it difficult to rationalize the somewhat greater effect of substituents on pK_2 than on pK_1. Because of our concern that the pK_1 values for the most acidic phosphonic acids might be lower than the measured

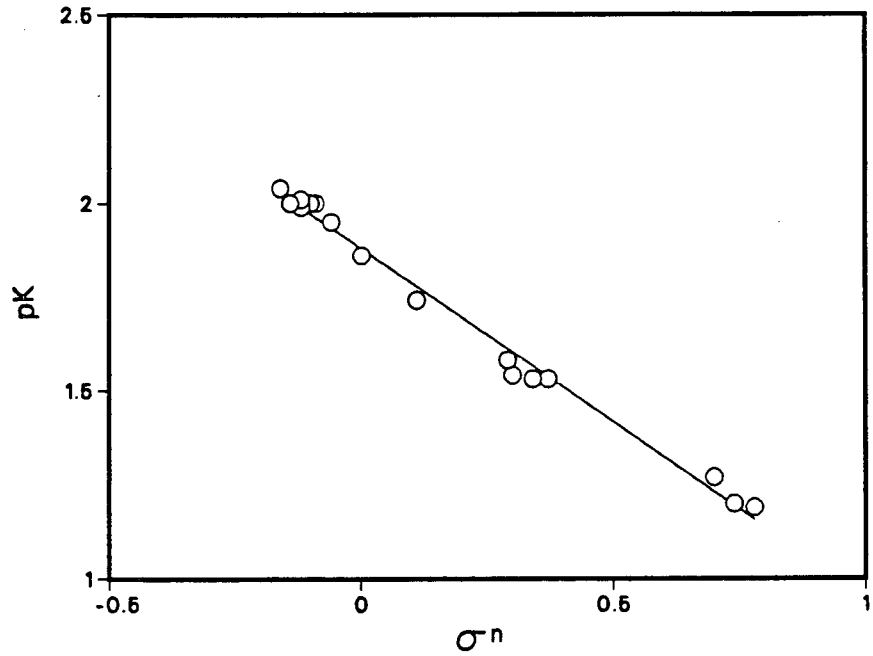

Fig. 47: Plot of pK_1 for arylphosphonic acids against the substituent constant σ^n

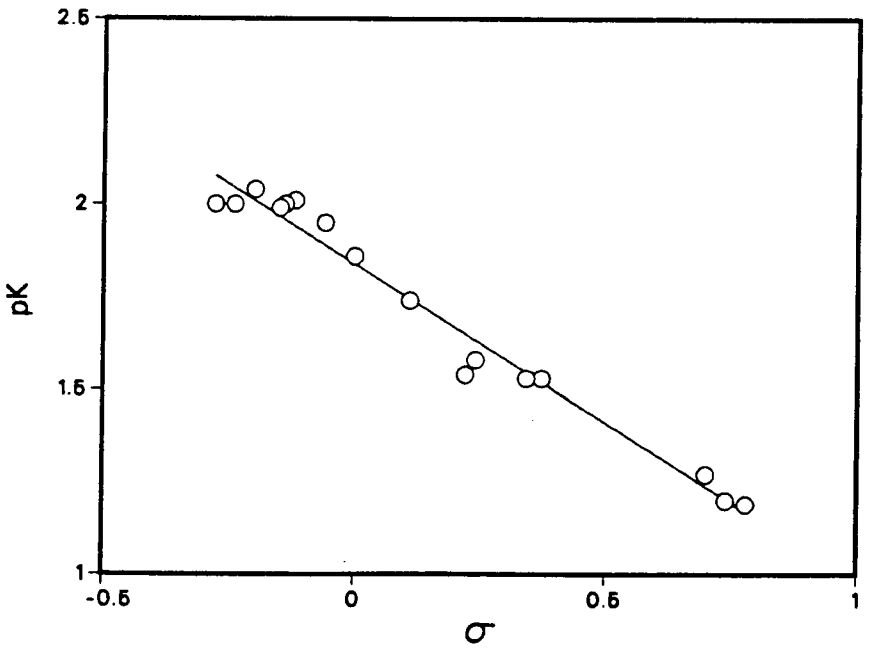

Fig. 48: Plot of pK_1 for arylphosphonic acids against the substituent constant σ

values (i.e. larger K_1 values than are measured), thus lowering the actual value of ρ_1, we considered analogous systems to which the present system could be compared. However, there is little known about the electronic effect of aryl substituents on successive dissociations of oxygen acids. It may be recalled that our result for the ρ_1 and ρ_2 values for 5-substituted isophthalic acids are very similar (p. 112, ρ_1 = 1.05, ρ_2 = 1.02). While only six acids have been used in these correlations and the degree of accuracy for pK_1 is poorer than for pK_2 due to low solubility of the diacid, a study in 50 wt % aqueous methanol involving eleven isophthalic acids also gives similar ρ_1 and ρ_2 values, 1.21 and 1.20 respectively (GS84). The limited precise data available for meta and para arylarsonic acids indicate that ρ_1 is larger than ρ_2 (NC73 and references therein). The successive dissociation constants of $C_6H_5CO_2H_2^{\cdot}$ have been determined but, unfortunately, their meta and para derivatives do not appear to have been studied (HS74).

Our concern regarding the pK_1 values of the most acidic compounds, in particular the nitro substituted phenylphosphonic acids, stems from observation of differences in the degrees of ionization and dissociation of strong and moderately strong acids (S85h and references therein). The pertinent equilibria are shown in eq. [4.23]

$$ArPO_3H_2 + H_2O \rightleftharpoons ArPO_3H^- \cdot H_3O^+ \rightleftharpoons ArPO_3H^- + H_3O^+ \qquad [4.23]$$

For weaker acids ionization and dissociation are synonymous and so pK values measured potentiometrically will correspond to the ionization process; for stronger acids this may not be so. It would be expected

that the reaction constant of a Hammett type correlation would correspond to the ionization process, which would mean that the ρ_1 we have measured might be slightly low. Since our main concern is the determination of catalytic effects in the enolization of acetone, which will depend on dissociative phenomena, the potentiometrically determined pK_1 values are all we require. (In the case of the strong halo-acetic acids ionization and dissociation are also distinct processes.) It should be noted, however, that in acid catalyzed A-S_E-2 reactions (which involves proton transfer from the acid to the substrate in the rate-controlling step), the pertinent catalytic species for strong and moderately strong acids may be the ion pair or the non-ionized acid and it is not known if the use of potentiometric pK values is appropriate. It may be recalled that the rate determining step in the acid catalyzed enolization of acetone involves proton transfer from the protonated substrate to the conjugate base of the acid.

The pK_2 values of the 3- and 4-carboxyphenylphosphonic acids refer to the dissociation of the carboxyl group and this allows a check to be made of the previously reported substituent effect of the $-PO_3H^-$ group (JF53). After being corrected to zero ionic strength our results suggest that the $-PO_3H^-$ group is electron donating relative to hydrogen ($\sigma_m = -0.17$ and $\sigma_p = -0.07$). The values reported previously indicated that the anionic moiety is electron withdrawing; however, the pK values were not corrected for ionic strength, which can be quite large for the second and higher dissociations of polyprotic acids. The relative ordering of the meta- and para-PO_3H^- acids is the same in our results as the earlier study. Since charged groups are notorious for the inconsis-

tency of their Hammett substituent constant values (HH78), the significance of the σ values we have derived is uncertain.

4.4.2 Ortho Substituents

Unlike benzoic acids, where virtually any ortho group has a marked acid-strengthening effect, most arylphosphonic acids with ortho substituents have acidities that are roughly comparable to those of their para analogues, at least when direct interactions such as hydrogen bonding are absent, and this has been remarked upon previously (JF54). The generally accepted explanation for the acid-strengthening effect of ortho groups in benzoic acids involves steric hindrance to conjugation in the neutral molecule (E69). In the case of arylphosphonic acids, in which conjugation between the acid unit and the ring is slight, we would not expect the marked acid-strengthening effect of ortho groups that is characteristic of benzoic acids.

One of the obvious limitations to Hammett plots is that they hold for meta and para substituted derivatives only. Since ortho substituents in aromatic systems involve a number of effects (steric and electronic), the quantification (parametrization) of these effects with a Hammett-type equation is difficult. Bijloo and Rekker have used a multivariate analysis method to evaluate the ortho effect based on the work of Fujita and Niskioka (BR84, FN76). In 1976 these latter workers proposed that the ortho effect is composed of a polar effect and proximity effects which can be expressed as a linear combination of

effects (as had been postulated by Charton in 1971, C71). Bijloo and Rekker have modified this approach slightly and their analysis for benzoic acids is presented after a brief explanation of the method.

The electronic effect of an ortho group is the sum of the para-substituent effect (σ_p) and an additional inductive effect only valid for ortho substituents (σ_I^o). The steric effect of an ortho group is quantified by the steric parameter E_S^o. The correlation for ortho, meta, and para benzoic acids is then defined by eq. [4.24] with σ_I^o and E_S^o being zero for the meta- and para-substituted acids and σ values for the ortho-substituents being equivalent to the values for the para-substituents.

$$pK = pK_o + \rho\sigma + \rho_I\sigma_I^o + \delta E_S^o \qquad [4.24]$$

With the omission of the two ortho parameters, eq. [4.24] reduces to the readily recognizable Hammett equation. Bijloo and Rekker correlate 46 meta and para benzoic acids and 18 ortho benzoic acids with eq. [4.24], and obtain eq. [4.25] (r = 0.9982)

$$pK = 4.21 - 0.96\sigma - 1.32\sigma_I^o + 0.40E_S^o \qquad [4.25]$$

The values of ρ (0.96) and pK_o (4.21) agree reasonably well with the values for the meta and para benzoic acids only (1.00 and 4.20 respectively). The separation of ordinary polar effects (σ), proximity polar effects (σ_I^o) and steric effects (E_S^o) is deemed a success. The sign of the coefficient for the steric parameter, δ, is positive indicating that

the steric effect is acid strengthening (E_S^o values are negative).

When all the pK data for our set of phenylphosphonic acids (Table 18, p. 117) are subjected to multivariate analysis using eq. [4.25] (using σ^n, not σ), satisfactory correlations could be obtained provided the ortho alkoxy groups were omitted; these compounds show anomalously high pK_1 and pK_2 values, presumably because of hydrogen bonding between the oxygen of the alkoxy unit and the proton(s) of the phosphonic acid (N74). The results are shown in eqs. [4.26] and [4.27].

$$\begin{array}{lll} \text{29 acids} & pK_1 = & 1.86 - 0.87\sigma^n - 0.32\sigma_I^o - 0.13E_S^o \\ r = 0.9864 & & \pm \quad\quad \pm \quad\quad \pm \quad\quad \pm \\ & & 0.02 \quad 0.04 \quad 0.07 \quad 0.02 \end{array} \qquad [4.26]$$

$$\begin{array}{lll} \text{30 acids} & pK_2 = & 7.52 - 1.07\sigma^n - 0.29\sigma_I^o - 0.33E_S^o \\ r = 0.9884 & & \pm \quad\quad \pm \quad\quad \pm \quad\quad \pm \\ & & 0.02 \quad 0.06 \quad 0.09 \quad 0.02 \end{array} \qquad [4.27]$$

The values of σ^n for the meta and para substituents are available in Table 31, while the three parameters for the ortho substituents are listed in Table 32. The high correlation coefficients, the closeness of the ρ values to those found when meta and para compounds only are used (eqs. [4.19] and [4.21]) and the close agreement between the experimental and calculated pK values of the unsubstituted compound suggest that the ortho effects have been successfully treated using eq. [4.24]. The agreement is not nearly as good when a comparison is made between the meta and para series alone (eqs. [4.19] and [4.21]) and the ortho series alone (eqs. [4.28] and [4.29]) although satisfactory correlation coefficients are obtained in all cases.

Table 32: σ^n (= σ^n para), σ_I^o and E_S^o values for ortho substituents. Data from refs (HW73, BR84).

Substituent	σ^n	σ_I^o	E_S^o
2-CH_3	-0.10	0.00	-1.24
2-C_2H_5	-0.12	0.00	-1.31
2-$(CH_3)_2CH$	-0.14	0.00	-1.71
2-F	0.18	0.54	-0.46
2-Cl	0.29	0.47	-0.97
2-Br	0.30	0.47	-1.16
2-I	0.31	0.40	-1.40
2-NO_2	0.78	0.67	-1.01
2,3-$(CH_3)_2$	-0.18	0.00	-1.24
2,4-$(CH_3)_2$	-0.20	0.00	-1.24
2,5-$(CH_3)_2$	-0.18	0.00	-1.24
2,6-$(CH_3)_2$	-0.20	0.00	-2.48
2,4,6-$(CH_3)_3$	-0.30	0.00	-2.48

17 acids
r = 0.9970
meta, para

$$pK_2 = 7.55 \pm 0.01 - 1.14\sigma^n \pm 0.02 \quad [4.19]$$

14 acids
r = 0.9889
ortho

$$pK_2 = 7.42 \pm 0.03 - 0.60\sigma^n \pm 0.22 - 0.63\sigma_I^o \pm 0.25 - 0.43E_S^o \pm 0.04 \quad [4.28]$$

16 acids
r = 0.9884
meta, para

$$pK_1 = 1.88 \pm 0.01 - 0.92\sigma^n \pm 0.02 \quad [4.21]$$

14 acids
r = 0.9879
ortho

$$pK_1 = 1.82 \pm 0.05 - 0.49\sigma^n \pm 0.17 - 0.64\sigma_I^o \pm 0.19 - 0.19E_S^o \pm 0.03 \quad [4.29]$$

The poor agreement between the individual sets of meta/para compounds and ortho compounds is a weakness in this analysis (BR84). Perhaps the poor agreement reflects the fact that for the ortho compounds, eqs. [4.28], we are correlating four variables for only fourteen compounds; this also results in the relatively large standard deviation of the constants and, particularly, the coefficients in both of these equations. The standard deviations are greatly reduced in eqs. [4.26] and [4.27], in which the meta/para series is added giving multivariate equations that involve over twice the number of compounds as previously correlated. Thus a fairer comparison may involve the meta/para series and the meta/para/ortho series, where the agreement has been shown to be very good.

What is the significance of the coefficients related to the ortho substituents? The values of ρ_I, the ortho-inductive reaction constant,

are fairly modest, (0.32 for pK_1, 0.29 for pK_2), and are much smaller than the value for benzoic acids, (1.32, eq. [4.25]). This is not surprising since there is less conjugation in this system compared to the benzoic acids. The coefficients of the steric parameters, δ, are negative, meaning that steric effects are acid weakening, the reverse of the situation with benzoic acids. The values of −0.13 and −0.33 for pK_1 and pK_2 can be compared with the value of +0.40 for benzoic acids (eq. [4.25]). The steric effect of ortho groups in this case is probably associated principally with hindrance to solvation and, if this is so, the larger δ for pK_2 than for pK_1 is reasonable, indicating a greater change in solvation going from monoanion to dianion than from netural acid to monoanion (MG64). Indeed, the neutral molecule, being highly acidic, may be quite highly solvated, particularly if the ion-pair form is present in significant amounts (eq. [4.23]). The differential steric effect of ortho groups can be seen in Fig. 49 where pK_1 is plotted against pK_2. The horizontal displacement of the ortho compounds from the line for the meta and para compounds can be considered to be a measure of the enhanced steric effect on the second dissociation.

4.5 ARYLPHOSPHONATE DIANION CATALYSIS

The data in Table 21, p. 124, contains 16 meta- and para- and 13 ortho-substituted phosphonate dianion rate constants. For these catalysts p and q have values of 1 and 3, respectively.

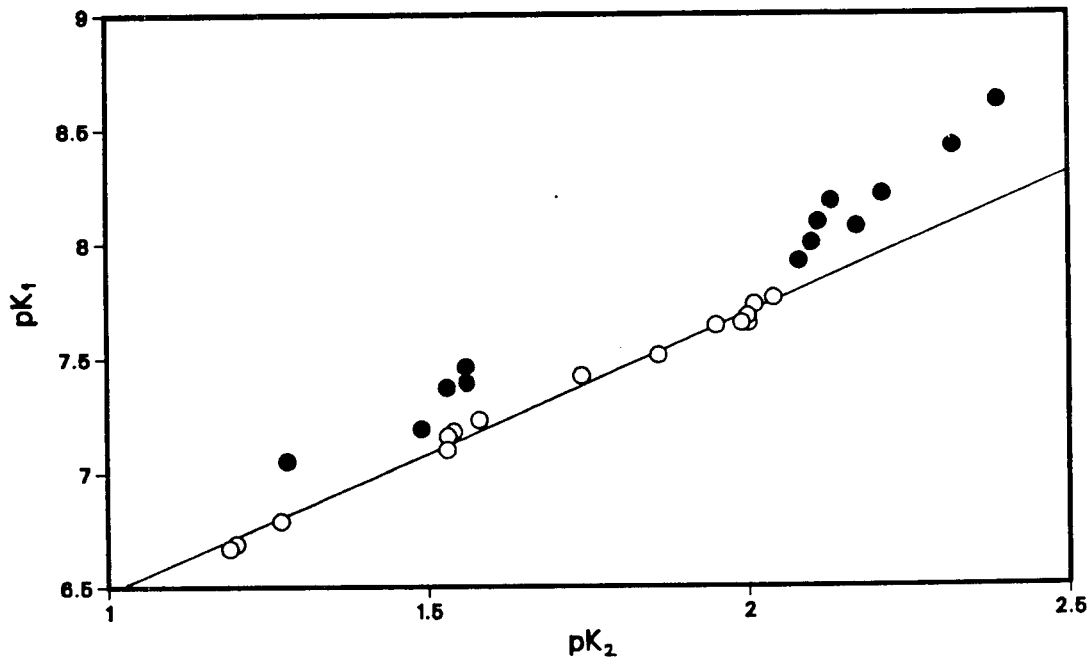

Fig. 49: Plot of pK_1 against pK_2 for arylphosphonic acids; meta and para compounds (open circles) and ortho compounds (closed circles). Line drawn from meta and para compounds.

1. For all these phosphonate dianions a very good Bronsted relationship is obtained when the points for the charged substituent $-CO_2^-$ are omitted. The effect of this substituent will be discussed later. The Bronsted plot is shown in Fig. 50 and the line defined by the fourteen meta and para phosphonate dianions is given by eq. [4.30]. The value of β, 0.71 ($\pm$ 0.02), suggests a transition state in which the proton is just under three quarters transferred. It is interesting that this more reactive series of dianions has a smaller β value than either the carboxylate monoanion (0.89) or dianion (0.78) bases. This trend is in agreement with the Hammond postulate where the more reactive system has an earlier transition state.

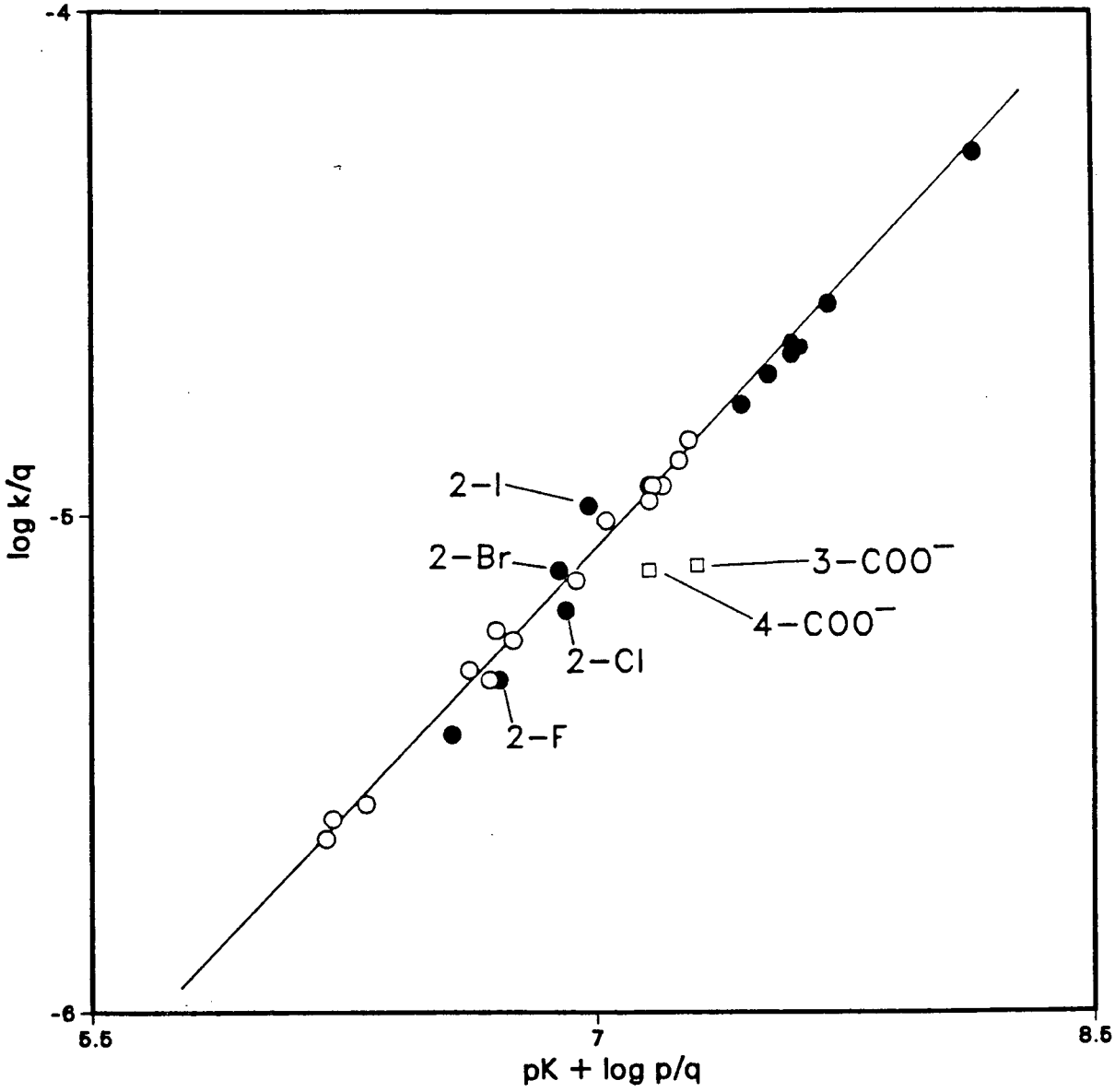

Fig. 50: Bronsted plot for catalysis of acetone enolization by arylphosphonate dianions; meta and para compounds (open circles), ortho compounds (closed circles) and 3- and 4-CO_2^- compounds (open squares); line drawn with respect to the meta and para compounds

14 dianions $\log (k_A2\text{-}/q) = -10.0 \pm 0.1 + 0.712 \pm 0.018 \ (pK_2 + \log p/q)$ [4.30]
r = 0.9960

2. Ortho substituents in the dianion conform well to the Bronsted line drawn with respect to the meta and para compounds. Defining a line for the ortho substituted dianions leads to eq. [4.31] which is very similar to eq. [4.30].

13 dianions $\log (k_A2\text{-}/q) = -10.1 \pm 0.2 + 0.712 \pm 0.029 \ (pK_2 + \log p/q)$ [4.31]
r = 0.9907

However, it can be seen that while eleven of these dianions fall either on or just below the meta and para line, the 2-iodo and 2-bromo-substituted compounds deviate just above such a line. The standard deviations of the points in Fig. 50 is adequately represented by the span of the circles and squares shown, and the deviation cannot be blamed on experimental error. The fact that it is the bromo and iodo compounds which deviate, and considering our experience with these substituents in both isophthalate monoanions and aliphatic carboxylic acids, we credit their enhanced catalytic activity to polarizability.

We can estimate the degree of activation involved by calculating the $k_A2\text{-}^{obs}/k_A2\text{-}^{calc}$ value. The calculated dianion rate constant is that expected on the basis of the other eleven ortho dianions. The Bronsted line for this set of catalysts is given by eq. [4.32] and is a statistical improvement upon eq. [4.31]; a fact which further favours the

exclusion of the iodo and bromo compounds from the ortho dianion Bronsted line.

11 dianions $\log (k_A2\text{-}/q) = -\underset{0.1}{10.3} + \underset{0.013}{0.742}\ (pK_2 + \log p/q)$ [4.32]
r = 0.9986

The resulting $k_A2\text{-}^{obs}/k_A2\text{-}^{calc}$ values are 1.37 for 2-I and 1.21 for 2-Br. These values are almost identical to the results involving 2-I and 2-Br substituted isophthalate monoanions; values of $k_{HA}^{obs}/k_{HA}^{calc}$ in that system are 1.41 for 2-I and 1.20 for 2-Br, p. 183. Since there is less conjugation between the ring and the acid moiety in this system, we might have expected a lessening of the ortho polarizability effect but this appears not to be the case.

3. With the exception of iodo and bromo, there appears to be no special proximity effect on the rate of reaction. That is, ortho groups exert essentially the same effect on the dissociation equilibrium of the monoanions as on the rate of proton abstraction by the arylphosphonate dianions; this is in agreement with the result observed for carboxylate monoanion bases, both aliphatic and aromatic. While this latter series includes a number of sterically bulky aliphatic bases, it does not provide the scope of ortho benzoate anion catalysts one would wish for in such a study. However, the phosphonate dianion series is more extensive in this regard and clearly no significant rate accelerating or decelerating effects are present. It should be noted that the ortho compounds include both the 2-$CH(CH_3)_2$ and the 2,6-$(CH_3)_2$ compounds. It

is also interesting to consider the carboxylate dianion set discussed previously from this perspective; while the size of the series is very limited and a number of hidden effects could be operating due to the range of structural-types of catalyst involved, phthalate dianion (in effect an ortho benzoate base) does not show an enhanced activation (Fig. 30(b), p. 139).

4. When the arylphosphonate dianion includes a negatively charged substituent, a small negative deviation is observed. Similar deviations for dicarboxylate ions compared to monocarboxylate ions have been observed previously in this work (p. 147) and by others (SS76a). The degree of deviation in the rate constant k_A3^- from the Bronsted line defined by the meta and para dianions, (eq. [4.30]), is a factor of 1.8 ± 0.2 (average of the deviations for the $3\text{-}CO_2^-$ and $4\text{-}CO_2^-$ phosphonates). These factors are less than we observed in the case of carboxylate dianions in comparison to carboxylate monoanions, where deviations by factors of between 2 and 3 were observed. Considering the larger ionic strength effect on pK values in the case of dianion/trianion dissociations than for monoanion/dianion dissociations, the degree of deviation for the phosphonate trianions is probably less than is suggested by Fig. 50. At an ionic strength of 0.05 (as is used for the phosphonates), $pK_2^I = pK_2^T - 0.26$ whereas $pK_3^I = pK_3^T - 0.43$. Taking account of the difference in pK^I due to the ionic strength effect (0.17 pK units), the deviation factor is only between 1.35 ± 0.15. Clearly, while the phosphonate trianions deviate slightly from the dianion line, the deviation is small, especially in comparison to the

carboxylate situation. A similarity between the two situations is that the distance separating the negatively charged units does not seem significant. Perhaps the rate retardation effect in going from A^- to A^{2-} to A^{3-} is a progressively weakening one; a comparison of a carboxylate trianion with the set of dianions would be interesting in this regard.

4.6 ARYLPHOSPHONIC ACID CATALYSIS

The data in Table 23, p. 128, contains 10 meta- and para- and 10 ortho-substituted phosphonic acid rate constant. For these diacids, p and q are both equal to 2.

1. For catalysis by the neutral phosphonic acids the Bronsted plot shows some divergence between the meta and para compounds on the one hand and the ortho compounds on the other, Fig. 51. The line defined by the ten meta and para acids is given by eq. [4.33]. The value of α, 0.38 ($\pm$ 0.02), implies a β value of 0.62 for the proton abstraction from the conjugate acid of acetone by the phosphonate monoanions.

10 acids
r = 0.9890

$$\log (k_{H_2A}/p) = \underset{\pm 0.03}{-4.35} - \underset{\pm 0.020}{0.383} (pK + \log p/q) \qquad [4.33]$$

The value of β suggests a transition state in which the proton is more than half transferred. This is an earlier transition state than we

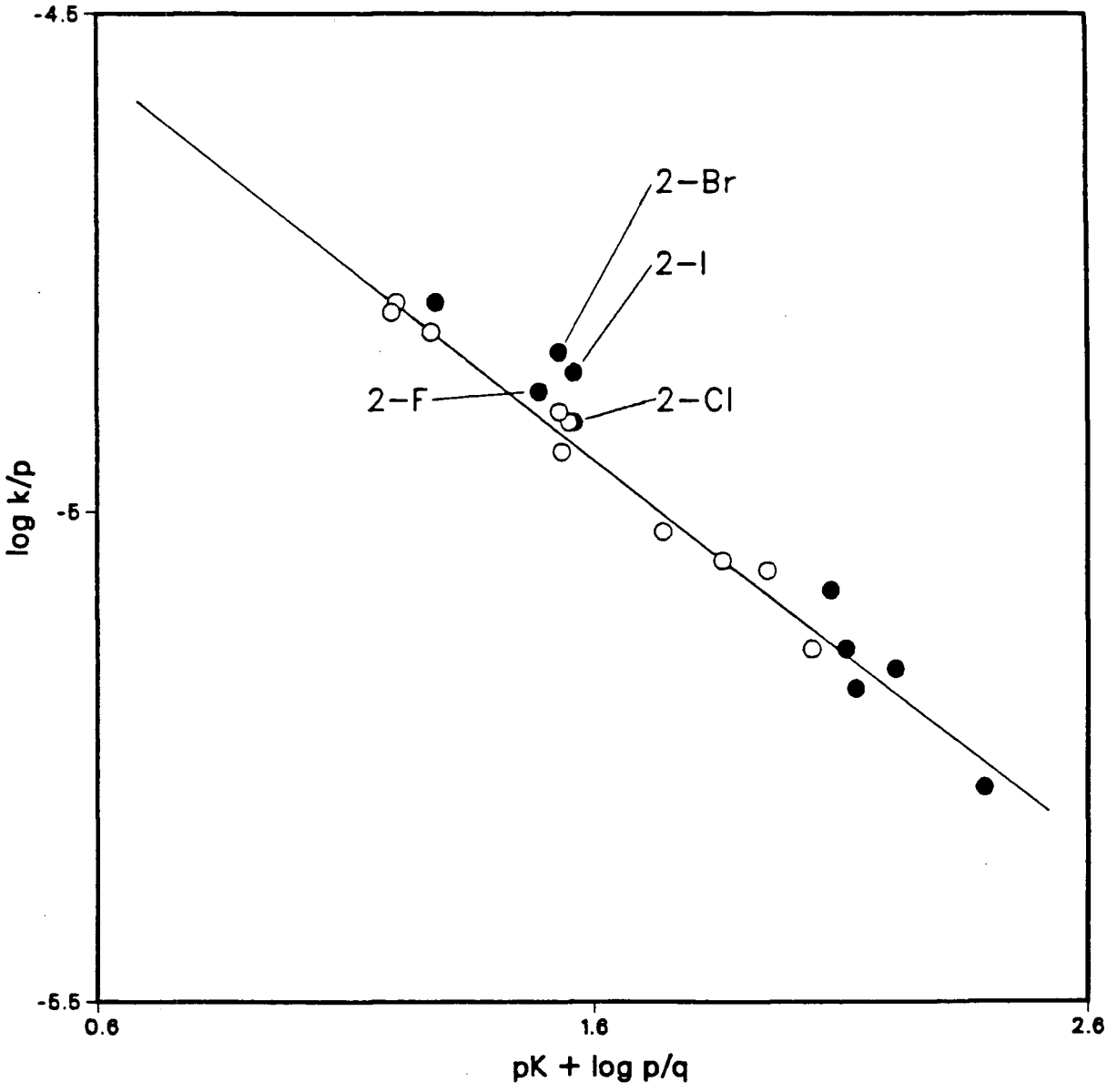

Fig. 51: Bronsted plot for catalysis of acetone enolization by arylphosphonic acid; meta and para compounds (open circles) and ortho compounds (closed circles); line drawn with respect to the meta and para compounds

observed with phosphonate dianions when neutral acetone is the substrate. This may reflect the degree of activation conferred on the system by protonating the substrate, leading to an earlier transition state. This is dramatically illustrated in the comparison of carboxylate anions when acetone is the substrate (β = 0.89) and when protonated acetone is the substrate (β = 0.38). However, in this case the catalysts are different (phosphonate monoanions with protonated acetone and phosphonate dianions with neutral acetone), and a comparison of the β values may be unfair.

2. The ortho compounds deviate to a small extent in the positive direction in comparison to the meta and para compounds. The deviations, which are not large, are more pronounced for the more acidic compounds, suggesting a slightly larger Bronsted coefficient may govern the reactivity of the ortho rather than that of the meta and para compounds. Even when the ortho compounds are omitted, there is more scatter in the Bronsted plot for catalysis by $ArPO_3H_2$ (Fig. 51) than in that for catalysis by $ArPO_3^{2-}$ (Fig. 50), an effect that is probably due to the precision of the measurements of both pK_1 and k_{H_2A} being somewhat lower than the measurements of pK_2 and k_A2-.

A similar effect for the 2-I and 2-Br catalysts is observed in this case, as is evident in phosphonate dianion catalysis; the catalysts possessing these ortho-polarizable substituents show enhanced reactivity. The other two ortho-halo catalysts, which possess less polarizable halogens, show no such effect, as in the case of the dianions (i.e. 2-Cl and 2-F). This example of a rate accelerating effect has now been

observed in four different series of catalysts and shows two expected trends; the degree of positive deviation is directly related to the polarizability of the substituent, and is also related to the proximity of the substituent to the catalytic centre. The Bronsted line defined by the ortho substituents, excluding the iodo and bromo compounds, is given by eq. [4.34]. The values of $k_{H_2A}{}^{obs}/k_{H_2A}{}^{calc}$ for 2-Br and 2-I are 1.12 and 1.09, respectively; these values are smaller than is observed for the dianions, and are also more prone to error due to the inherent scatter in the Bronsted plot. However, it may have some significance in that the reaction constant for pK_1 is lower than for pK_2 and accordingly a proximity polarizability effect may well be expected to be less for k_{H_2A} than the k_A2-.

8 acids
r = 0.9893

$$\log (k_{H_2A}/p) = -4.26 \underset{0.05}{\pm} - 0.419 \underset{0.025}{\pm} (pK + \log p/q) \qquad [4.34]$$

3. While the scatter in Fig. 51 is a hindrance to analysis of the results, the ortho compounds do appear to form a line with a slightly higher slope than that for the meta and para compounds. This implies a smaller β value for the rate determining second step of the general acid catalyzed enolization. It may be recalled that the 2-isophthalate dianions with protonated acetone as the substrate had a smaller β value than the 5-isophthalate dianions, a fact, we suggested, that can be linked to a steric activation effect leading to an earlier transition state (smaller β value). A similar situation might be operative here,

with the effect being apparently smaller than for the isophthalate system.

4.7 ARYLPHOSPHONATE MONOANION CATALYSIS

We had hoped to determine a number of arylphosphonate monoanion rate constants, but unfortunately, as was mentioned in Section 3.2.4, accurate k_{HA^-} values were inaccessible due to the much larger k_{H_2A} and $k_{A^{2-}}$ values. Table 24, p. 130, does contain three k_{HA^-} values but the very large standard deviations for two of these values makes an analysis of the rate constants difficult.

1. If the arylphosphonate monoanions are acting as acids the second dissociation constant is involved and we can predict an estimate of the k_{HA^-} values by extending the H_2A Bronsted line into the pK_2 range (eq. [4.33], $ArPO_3H_2$ catalysis). For example, the 3-nitrophenylphosphonate monoanion (pK_2 = 6.69) should have a k_{HA^-} value of 1.9×10^{-7} M^{-1} sec^{-1} on this basis (p = 1, q = 3 for HA^- as an acid). On the other hand, if the monoanions are acting as bases, the first dissociation constant is involved. An extension of the A^{2-} Bronsted line into the pK_1 range (eq. [4.30], $ArPO_3^{2-}$ catalysis) provides a rough value for k_{HA^-} acting as a base. The result for the 3-nitro monoanion (pK_1 = 1.20, p = 2, q = 2) suggests a k_{HA^-} value of 1.4×10^{-9} M^{-1} sec^{-1}. Furthermore, if bifunctional catalysis were important, the catalytic constants would be expected to be considerably increased over the values calculated on the

basis of the Bronsted plots for both $ArPO_3H_2$ and $ArPO_3^{2-}$.

The value of k_{HA^-} determined for the 3-nitro monoanion (1.1×10^{-7} M^{-1} sec^{-1}) is of the same order of magnitude as that predicted on the basis of this species acting as an acid. The value expected, if the monoanion acts as a base, is two orders of magnitude smaller than the experimentally determined rate constant. We conclude that the phosphonate monoanions are acting as general acids, not general bases, and bifunctional catalysis appears to be absent. The monoanions of the dicarboxylic acids that were studied also act as general acids.

2. Since the $-PO_3H^-$ group behaves as an acid in the enolization of acetone, the phosphonic acid with the lower pK_2 value has the more effective monoanion catalyst, while simultaneously having the less effective dianion catalyst. Thus phosphonic acids with lower pK_2 values than those in the extensive set already examined might allow an accurate determination of some k_{HA^-} values. On this basis we decided to study a few alkylphosphonic acids, whose pK_2 range spans from 4.93 ($Cl_3CPO_3H_2$) to 8.71 ($(CH_3)_3CPO_3H_2$) (KT77).

In a similar manner to that employed for the arylphosphonates, using buffers of HA^- and A^{2-}, we attempted to measure k_A2^- and k_{HA^-}. For the two weaker acids, HA^-, (i.e. the phosphonate monoanions, high pK_2 values) catalysis by the monoanion was not detectable while values of k_A2^- could be obtained (methyl phosphonate and t-butylphosphonate dianions). In the case of chloromethylphosphonate buffers, we were able to detect a small catalytic effect attributable to the monoanion, though the dianion is more effective as a catalyst by a factor of at least 15 ;

a plot of the (slope of k_{obs} vs. $[AH^-]$) against 1/m had a noticeable, but small, intercept i.e. k_{HA^-}, eq. [3.21] (see p. 118).

$$k_{obs} = k_{sum} + [HA^-]\ (k_{HA^-} + (1/m)k_A2^-) \qquad [3.21]$$

When we examined buffers of trichloromethylphosphonate, we found an interesting result; the monoanion is more effective as a catalyst than the dianion (factor of 5, approximately). The results for the alkyl phosphonates are given in Table 33.

Table 33: k_A2^- values and k_{HA^-} values (where measurable) for acetone enolization catalyzed by alkylphosphonates at 25°C and 0.05 M ionic strength

Acid	pK_2[a]	$10^7\ k_{HA^-}$ $M^{-1}\ sec^{-1}$	$10^6\ k_A2^-$ $M^{-1}\ sec^{-1}$	br[b]	Method[c]
$(CH_3)_3CPO_3H_2$	8.71	-	206 ± 3	2	I
$CH_3PO_3H_2$	8.00	-	60.8 ± 3	2	I
$ClCH_2PO_3H_2$	6.59	3.05 ± 2.74	4.42 ± 0.27	3	II
$Cl_3CPO_3H_2$	4.93	7.62 ± 0.09	0.157 ± 0.004	3	II

a Thermodynamic pK_2 values from ref. (KT77).

b Number of buffer ratios

c Method I plots of k_{obs} vs. $[A^{2-}]$
Method II (slope of k_{obs} vs. $[HA^-]$) vs. 1/m giving k_A2^-, slope and k_{HA^-}, intercept.

While the k_{HA}- value for $ClCH_2PO_3H^-$ (pK, 6.59) has a large standard deviation it is slightly larger than the value for 3-nitrophenylphosphonate monoanion (pK, 6.69) and smaller than the value for $Cl_3CPO_3H^-$ (pK, 4.93); a general acid catalysis Bronsted line based on these monoanions will only give an approximate value of α as the deviations of the two smaller k_{HA}- values is rather large. The resulting α value is 0.24 with the combination of $Cl_3CPO_3H^-$ and $ClCH_2PO_3H^-$, or, on the other hand, 0.48 with the combination of $Cl_3CPO_3H^-$ and $3\text{-}NO_2\text{-}ArPO_3H^-$. Obviously an interpretation of these Bronsted coefficients is very difficult as the β value for $-PO_3^{2-}$ $(1-\alpha)$ has a large average deviation, being roughly equal to 0.64 ± 0.12. Further work in this area with a set of alkylphosphonates in a pK range of 4 to 6 would provide a more rigorous β value.

3. The k_A2- values determined for the alkylphosphonates can be compared with the set of aryl dianions discussed previously. The Bronsted plot for all these phosphonate dianions is shown in Fig. 52 and shows an interesting trend. The values for chloro- and especially trichloromethyl phosphonate fall slightly below the extension of the Bronsted line for the meta and para arylphosphonates. The fact that the methyl- and t-butyl-phosphonates fall on or close to that line illustrates the validity of considering the alkyl and aryl dianions as a homogeneous group. The trend, obvious from Fig. 52, is that a slightly curved line may be a better representation of the Bronsted line than a linear correlation. The curvature is in the direction predicted by the Hammond postulate and Marcus theory; the less reactive catalysts possessing the

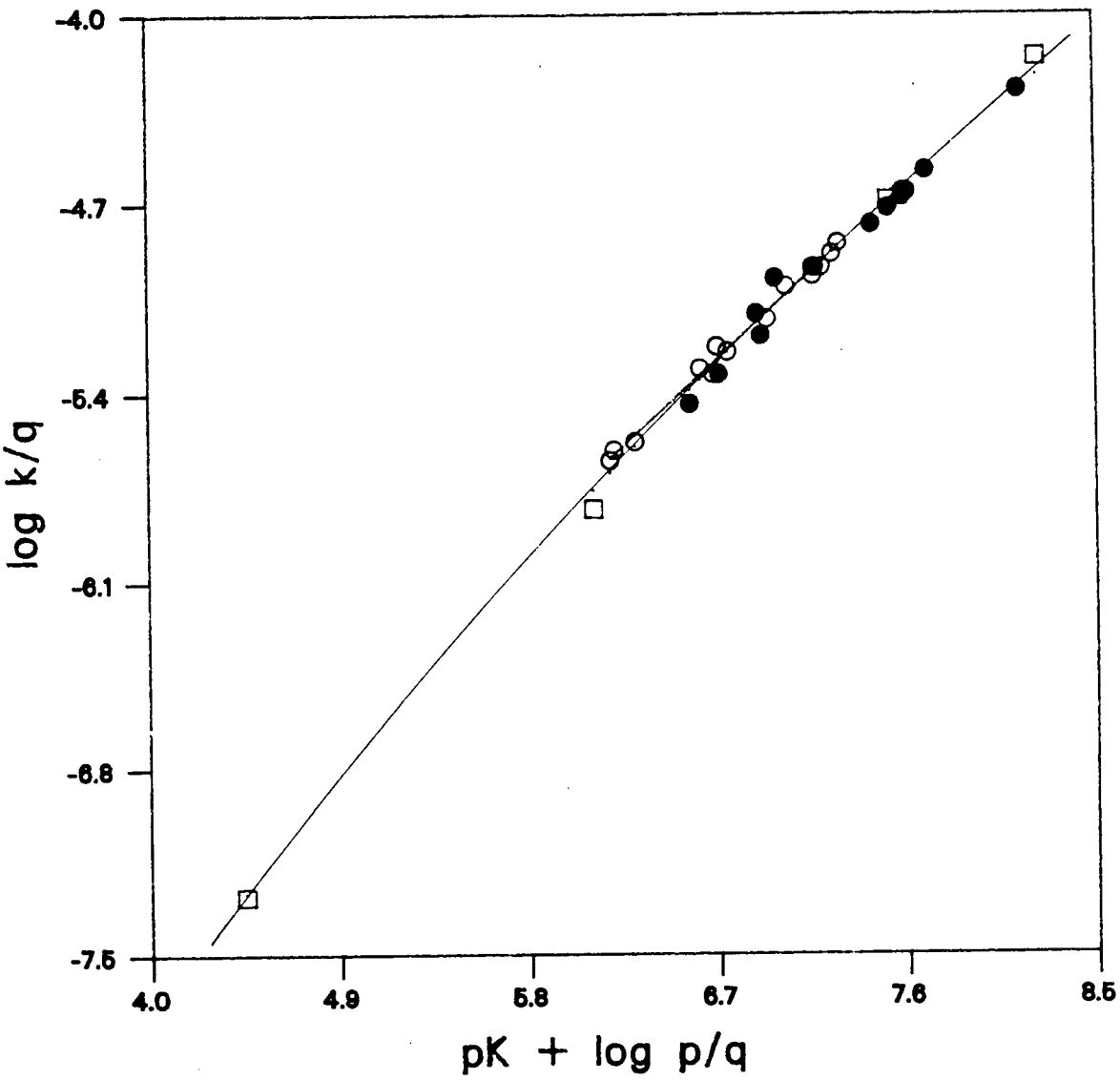

Fig. 52: Bronsted plot for catalysis of acetone enolization by phosphonate dianions; meta and para aryl compounds (open circles), ortho aryl compounds (closed circles) and alkyl compounds (open squares), solid line drawn with respect to the meta and para arylphosphonates, dotted line (quadratic, eq. [4.45]) drawn with respect to all the phosphonates

larger β values, implying a later transition state. For example, the Bronsted line defined by the meta and para aryl dianions and the alkyl dianions, inclusive of phenylphosphonate dianion and weaker bases ($pK_2 \leq 7.51$), is given by eq. [4.35]; the linear correlation is quite good for this set of catalysts and a β value of 0.875 ($\pm$ 0.025) results. A Bronsted line for the same type of catalysts inclusive of phenylphosphonate dianion and stronger bases ($pK_2 \geq 7.51$) is defined by eq. [4.36]; once again, the linear correlation is quite good but a smaller β value is evident, 0.732 ($\pm$ 0.019).

11 dianions $\log (k_A 2\text{-}/q) = -\underset{\pm 0.2}{11.1} + \underset{\pm 0.025}{0.875} (pK_2 + \log p/q)$ [4.35]
$r = 0.9964$

8 dianions $\log (k_A 2\text{-}/q) = -\underset{\pm 0.1}{10.2} + \underset{\pm 0.019}{0.732} (pK_2 + \log p/q)$ [4.36]
$r = 0.9979$

The curvature present in Fig. 52 would be undetectable, if only the alkylphosphonates had been studied; this set of four dianions gives a very acceptable linear correlation, $r = 0.9996$ and $\beta = 0.83$. A further point is that the trichloromethylphosphonate dianion may be enhanced due to a polarizability effect (which is evident in the 2-iodo and 2-bromophenylphosphonate dianions), and the 'true' curve may possess a greater degree of curvature than is evident from Fig. 52. A study involving a set of phosphonates in the lower regions of the curve is needed (as suggested earlier in order to obtain monoanion rate constants).

We will return to an analysis of these results when we discuss

general aspects of all this work, before finally summarizing the conclusion derived from our analysis of these results.

4.8 GENERAL DISCUSSION

4.8.1 Curvature in General Acid Catalyzed Bronsted Plots

It may be recalled that the carboxylic acid data, after removing those acids that are prone to either a steric effect or a polarizability effect, was interpreted as a curved Bronsted plot, (Fig. 36, p. 160, eq. [4.11], p. 161 or eq. [4.13], p. 166). Obviously this interpretation is open to criticism and it may well be easier and simpler to define a linear correlation and leave it at that. However our approach is to question the likelihood of such curvature, rather than ignore it. So we set about further research in this area.

1. One of the explanations advanced for curvature in rate-equilibria relationships has been desolvation of increasingly basic anions (see p. 35). While this particular consideration is not applicable to the general acid catalyzed mechanism, it does raise the matter of a solvent effect on the rate constants causing non-linear correlations of rate and equilibrium constants. We fail to see how the solvent could have such an effect in our system. However, reported values of k_{HA} in D_2O when compared to the values in H_2O for acid catalyzed bromination of acetone show a trend; the ratio of k_{HA} values (H_2O/D_2O) increases along the

series $ClCH_2CO_2H$ (1.22), $HOCH_2CO_2H$ (1.37), CH_3CO_2H (1.54) (RK39). Perhaps the trend continues for the stronger carboxylic acids and is somehow causing curvature in the Bronsted plot; thus we decided to measure k_{HA} values in D_2O (k_{DA}).

For three acids with both measurable k_{HA} and k_{A^-} values, we simply repeated the procedure followed for measurements in H_2O, replacing H_2O with D_2O at all stages. The results are given in Table 34, along with the results for four other acids with negligible k_{A^-} values. These acids, chloroacetic and stronger, were studied in the same manner as before. This necessitated a measurement of k_{D^+} in order to evaluate $(k_{obs} - k_{D^+}[D_3O^+])$, and hence k_{DA}. This was done in a similar fashion to that for k_{H^+}; as in that case, both a stoichiometric and a pH(pD)-derived rate constant were obtained, the pD-derived value ($6.54 \pm 0.08 \times 10^{-5}$ M^{-1} sec^{-1}) being used in subsequent determinations of k_{DA} for the halo-acids. The pD values are obtained from the relationship, pD = 'pH reading' + 0.40 (SS76a and references therein). The stoichiometric result for k_{D^+} is $4.62 \pm 0.10 \times 10^{-5}$ M^{-1} sec^{-1} (slope of k_{obs} against $[D_3O^+]$ for 11 kinetic runs), giving a $k_{H^+}(H_2O)/k_{D^+}(D_2O)$ value of 0.543 ± 0.013. This ratio agrees with that of Toullec and Dubois and implies that D_3O^+ is a better catalyst than H_3O^+. This enhanced catalytic activity is due to the greater protonating power of D_3O^+, despite the poorer base capacity of D_2O relative to H_2O.

The general acids that were examined show a negligible solvent isotope effect except for the weaker acids which exhibit a very slight effect; $k_{HA}(H_2O)$ seems to be greater than $k_{DA}(D_2O)$ for these acids. The effect on K_{HA} of changing the solvent to D_2O is an acid

weakening one, and is generally given by eq. [4.37] at 25°C (ML62). This pK correction-factor varies little and is unlikely to be a cause of the small effects evident in Table 34.

Table 34: k_{DA} values for acetone enolization at 25°C, measured in D_2O and resulting $k_{HA}(H_2O)/k_{HA}(D_2O)$

Acid	$10^7 k_{DA}$ (D_2O) M^{-1} sec^{-1}	$k_{HA}(H_2O)/k_{DA}$ (D_2O)[a]	nk[b]	br[c]
F_3CCO_2D	218 ± 13	0.94 ± 0.07	3	-
F_2CHCO_2D	62.7 ± 1.4	1.02 ± 0.03	5	-
Cl_2CHCO_2D	101 ± 3	0.92 ± 0.03	6	-
$ClCH_2CO_2D$	11.4 ± 0.2	0.96 ± 0.10	4	-
$HOCH_2CO_2D$	2.47 ± 0.04	1.25 ± 0.05	-	3
CH_3CO_2D	0.541 ± 0.037	1.52 ± 0.11	-	3
$(CH_3)_3CCO_2D$	0.513 ± 0.044	1.40 ± 0.13	-	3

a $k_{HA}(H_2O)$ values from Tables 7 and 9, pp. 81 and 88.

b Number of kinetic runs

c Number of buffer ratios

$$pK_{DA} = 0.41 + 1.02\ pK_{HA} \qquad [4.37]$$

As mentioned earlier, the results of Reitz and Kopp show a solvent effect; the effect is similar to the one that we observe and has not been adequately explained (LR69).

The fact that the weaker acids exhibit a decreased catalytic activity while the stronger acids remain unchanged, gives rise to a greater degree of curvature for the Bronsted plot in D_2O. The significance of these results is not evident to us. The absence and presence of solvent effects in the k_{HA} values does not provide any insight into the nature of the Bronsted correlation in H_2O; in fact, it raises new questions that merit a more thorough analysis than is presented here.

2. If the carboxylic acid curvature is due to a changing transition state, i.e. different degrees of proton transfer, an analysis of the results using Marcus theory may be informative. Following on our discussion in Chapter 1, such an analysis makes use of a quadratic expression for the Bronsted curved line. For a complete treatment, it is more appropriate to calculate rate constants for proton abstraction from protonated acetone by the conjugate base of the acid, k'_{A^-}, eq. [1.77] (p. 51). This requires that three parameters be known , k_{HA}, K_{HA} and K_{ZH^+}; the latter is the dissociation constant of protonated acetone, eq. [4.38]

$$k'_{A^-} = \delta k_{HA} k_{ZH^+} / K_{HA} \qquad [1.77]$$

$$K_{ZH^+} = [Z][H^+]/[ZH^+] \qquad [4.38]$$

There is disagreement about the acid strength of protonated acetone; estimates of pK_{ZH^+} range from -2.2 to -7.2 (A82 and references therein). Values of -2.9 and -6 have both been used in previous studies (S85d, A82); in order to see how critical the magnitude of the values are to our analysis, we chose to use both pK_{ZH^+} values (leading to k'_{A^-} values which differ by 10^3). The data in Table 35 contains the k'_{A^-} results for the set of carboxylate bases which we wish to examine, i.e. the eight carboxylates free of both polarizability and steric effects.

The quadratic expression for this data in terms of eq. [1.53], p. 25 is given by eq. [4.39] (p and q have values of 1 and 2, respectively). The use of pK_{HA} instead of log K_{HA} results in a change of sign in the coefficient of the linear term, E, eq. [4.40]. We will use the form of eq. [4.39], as it clearly illustrates the log k – log K relationship as well as being a tidier expression than eq. [4.40].

$$\log k_B = D + E\ (\log K_{BH^+}) + F\ (\log K_{BH^+})^2 \qquad [1.53]$$

$$\log (k'_{A^-}/q) = D + E\ (\log K_{HA}q/p) + F\ (\log K_{HA}q/p)^2 \qquad [4.39]$$

$$\log (k'_{A^-}/q) = D - E\ (pK + \log p/q) + F\ (pK + \log p/q)^2 \qquad [4.40]$$

Table 35: Calculated k'_A- values for acetone enolization catalyzed by carboxylate bases using eq. [1.77] with k_{ZH^+} = 800 M (k'_A-[1]) or 10^6 M (k'_A-[2])

Base	k'_A-[1] M^{-1} sec^{-1}	10^3 k'_A-[2] M^{-1} sec^{-1}	pK_{HA}[a]
$F_3CCO_2^-$	0.0564	.0711	0.54
$F_2CHCO_2^-$	0.101	.127	1.30
$ClCH_2CO_2^-$	0.633	.797	2.86
$CH_3OCH_2CO_2^-$	1.42	1.78	3.57
$HOCH_2CO_2^-$	1.66	2.09	3.83
$CH_3CO_2^-$	3.76	4.74	4.76
$CD_3CO_2^-$	3.91	4.93	4.77
$CH_3CH_2CO_2^-$	3.85	4.85	4.87

[a] pK_{HA} values at zero ionic strength

Using a value of -2.9 for pK_{ZH^+} the resulting quadratic is given by eq. [4.41]. The size of the coefficient, as well as the deviation for the squared term, (-0.016 ± 0.010), illustrates the debatable nature of the choice of a quadratic vs. linear correlation, eq. [4.42]. The correlation coefficient is slightly better for the quadratic expression, while the large standard deviation of the squared term will lead to a comparable large deviation in the intrinsic barrier.

8 bases; r = 0.9985

$$\log (k'_A\text{-}/2) = -\underset{\pm 0.05}{1.72} - \underset{\pm 0.050}{0.518}\ (\log 2K_{HA}) - \underset{\pm 0.0098}{0.0156}\ (\log 2K_{HA})^2 \qquad [4.41]$$

8 bases; r = 0.9975

$$\log (k'_A\text{-}/2) = -\underset{\pm 0.04}{1.67} - \underset{\pm 0.013}{0.440}\ (\log 2K_{HA}) \qquad [4.42]$$

Use of eqs. [1.54]-[1.56], p. 25, provides values of $\Delta G_o^{\neq}$, W_r and W_p. The results are given in Table 35 and apart, from the W_r term, the large standard deviations of the $\Delta G_o^{\neq}$ and W_p term reflect the poor statistics of the coefficient preceding $(\log 2K_{HA})^2$. This situation illustrates the difficulty in analyzing Bronsted plots using the Marcus equation; unless the degree of curvature is well defined, the resulting intrinsic barrier and work terms can only be very rough estimates.

If the data in Table 35 is analyzed after deleting the trifluoroacetate anion (which may show enhanced catalytic activity due to polarizability), a much improved quadratic equation is obtained from a statistical point of view, eq. [4.43]. The resulting parameters have now acceptable degrees of deviation, and these are also listed in Table 36.

Table 36: Results of Marcus Theory Analysis of Carboxylate Anion Data (Table 35) for Protonated Acetone Enolization; Units of kcal mol^{-1}, $pK_{ZH^+} = -2.9$

Equation	np[a]	$\Delta G_o^{\neq}$	W_r	W_p
[4.41]	8	5.5 ± 3.4	14 ± 4	19 ± 20
[4.43]	7	2.4 ± 0.4	16 ± 1	23 ± 3

[a] Number of data points

7 bases, excluding $F_3CCO_2^-$, **r = 0.9995**

$$\log (k'_{A^-}/2) = -\underset{\pm 0.05}{1.92} - \underset{\pm 0.035}{0.652} (\log 2K_{HA}) - \underset{\pm 0.0060}{0.0363} (\log 2K_{HA})^2 \qquad [4.43]$$

The results of the analysis using a pK_{ZH^+} value of -6 are quite similar to the values in Table 36, i.e. within the deviations quoted.

Clearly, while the Marcus parameters from eq. [4.41] are questionable, as is the use of a quadratic correlation, the results of eq. [4.43] seem to be quite rigorous; a quadratic correlation (Fig. 53) is a good improvement upon a linear one (r = 0.9995 and 0.9955, respectively). However, an analysis based on eq. [4.43] is both greatly dependent on excluding trifluoroacetate ion and including difluoroacetate ion. Bearing this in mind, does the Marcus treatment give results which support, or question, the assumed curvature in the Bronsted plot?

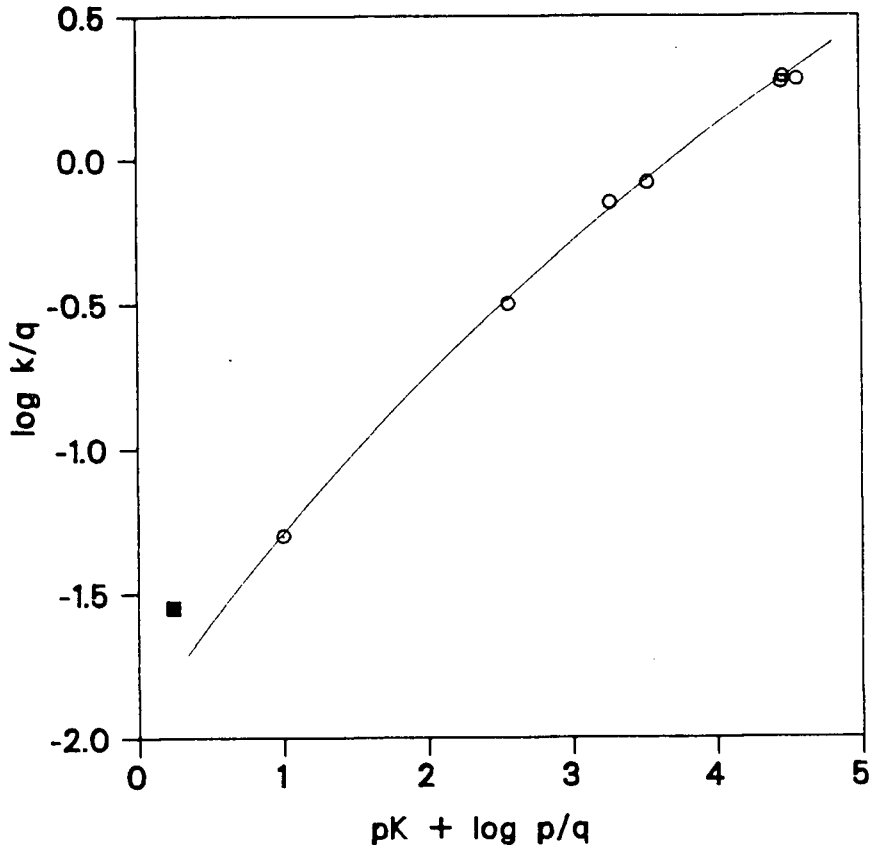

Fig. 53: Curved Bronsted plot for catalysis of 'protonated acetone' enolization by carboxylate bases, open circles, eq. [4.43]; trifluoroacetate ion, closed square.

The consequence of $\Delta G_o^{\neq}$ being small as compared to W_r (the work term needed to 'set-up' the reactants for proton transfer) has been observed before in a number of proton transfer reactions (K73). It is worth recalling the meaning of $\Delta G_o^{\neq}$, the intrinsic barrier; it is the kinetic factor of the reaction barrier for a hypothetical system where $\Delta G^o = 0$. A small value of $\Delta G_o^{\neq}$ implies a rapid proton transfer, which when linked to a large W_r term, indicates a system where organizing the reactants for the actual proton transfer is the major energy cost involved in the

reaction. If we could compare our results with some closely related system for which the Marcus parameters have been determined, an evaluation of the validity of our analysis can be made. Unfortunately, no such data exists that allows an evaluation of these parameters for a set of general bases and a protonated ketone. The reason for this is simple; curvature in the Bronsted plot has not been observed for a set of structurally similar general acid catalysts. (Actually, there is one report of such curvature in an acid catalyzed enolization, but it is due to a solvation effect in DMSO, see p. 36). On the other hand, a number of studies involving neutral ketones and curved Bronsted plots have been reported and this subject has been discussed in some detail previously (Section 1.10.1, p. 44). There are at least two interpretations of the available data; one credits rapidly changing Bronsted slopes (usually with a range of structurally dissimilar catalysts, see p. 45, KO73) with small $\Delta\overset{\neq}{G}_o$ values ($\approx$ 3 kcal mol^{-1}) and large W_r terms ($\approx$ 12 kcal mol^{-1}); another favours a gradually changing transition state with large $\Delta\overset{\neq}{G}_o$ values ($\approx$ 10 kcal mol^{-1}) and small W_r terms (see p. 45, HW77).

3. Primary isotope effects would be informative as to the degree of proton transfer in the transition state and hence to the degree of change of proton transfer along the catalyst series (See Section 1.8, p. 28).

As explained previously, similar procedures were used to determine a number of k_{HA} values with acetone-d_6 as the substrate. Using the buffer-ratio method values of k_{HA} were determined for a couple of acids, (acetic acid k_D measurement could not be measured, as the acetate anion

swamped the acid contribution to k_{obs}). In the case of the stronger carboxylic acids, this required a determination of k_{H^+} for the deuterated substrate. As in the case of acetone in H_2O and D_2O, both a stoichiometric and a pH-derived value of k_{H^+} are determined. The value of the stoichiometric k_{H^+} is $4.23 \pm 0.03 \times 10^{-6}$ M^{-1} sec^{-1} (12 kinetic runs, slope of plot of k_{obs} against $[H_3O^+]$). The value of k_H/k_D for hydronium ion is therefore 5.9 ± 0.1. This value compares with earlier values of 6.5 (HK72) and 6.7 (TD74), (see p. 50). The pH-derived value is $4.96 \pm 0.04 \times 10^{-6}$ M^{-1} sec^{-1} and it is this value that is used to subtract the $k_{H^+}[H_3O^+]$ term from k_{obs} in determining k_{HA} values. All the k_{HA} values measured using acetone-d_6 are listed in Table 37.

An examination of the k_H/k_D values illustrates two important points: (i) the values are generally close to the theoretical expected maximum of 6.9 (p. 47), indicating half transfer of the proton in the transition state; (ii) there is no apparent trend in the values that could be related to changing pK of the acid catalysts.

Consider F_3CCO_2H, $ClCH_2CO_2H$ and $HOCH_2CO_2H$; values of k_H/k_D rise and fall along the set, 7.9, 7.3 and 7.9. There may well be a trend in the isotope effects, but, if so, it is a small effect and is masked by the large standard deviations of the rate constant ratios. The absence of a noticeable change in the primary isotope effect argues against a changing transition state; such a transition state would involve changes in the degree of proton transfer and accordingly changes in k_H/k_D values. Thus, these results undermine the validity of applying Marcus theory to the rate-equilibria correlation. In other words, while curvature may or may not be present, the isotope effects indicate that a

Table 37: k_{HA} values for acetone-d_6 enolization at 25°C, measured in H_2O and the resulting k_H/k_D values

Acid	10^8 k_{HA} M^{-1} sec^{-1}	k_H/k_D[a]	nk[b]	br[c]
F_3CCO_2H	258 ± 22	7.9 ± 0.8	5	-
Cl_2CHCO_2H	132 ± 7	7.0 ± 0.4	8	-
2-$NO_2C_6H_4CO_2H$	44.7 ± 3.3	8.8 ± 0.8	3	-
$ClCH_2CO_2H$	15.1 ± 1.9	7.3 ± 1.1	4	-
$HOCH_2CO_2H$	3.92 ± 0.38	7.9 ± 0.8	-	3
$C_6H_5CH_2CO_2H$	2.54 ± 0.06	7.6 ± 0.5	-	3

[a] k_H values from Tables 7, 9, and 11, pp. 81, 88 and 94.

[b] Number of kinetic runs

[c] Number of buffer ratios

changing transition state is not occurring in the range of acids studied. The fact that β is close to 0.5 should lead us to expect isotope effects near the maximum and indeed this is so.

At this point we will leave the issue of general acid catalysis. We feel the discussion of this subject has illustrated the experimental and the interpretative difficulties in deciding whether curvature is present in Bronsted plots or not.

One last point that the reader may have noticed in Table 37. The isotope effect for 2-nitrobenzoic acid is 8.8 ± 0.8; this is the largest one measured and it may be significant. It may be recalled that large isotope effects have been associated with sterically crowded catalysts, an effect that has been linked to tunnelling (see p. 60). Obviously a study of ortho-benzoic acids would be informative. However, if k_H/k_D is high for these acids, this will make accurate determinations of k_D values difficult.

4.8.2 Curvature in General Base Catalyzed Bronsted Plots

A set of alkyl and arylphosphonates gives a non-linear Bronsted correlation, Fig. 52, p. 212. This is a more evident case of curvature than we observed with the carboxylic acids, and it merits further analysis.

1. Combining 27 $ArPO_3^{2-}$ and 4 RPO_3^{2-} species into one set provides us with a very wide range of catalyst equilibrium acid strengths and a very large number of catalysts. As was mentioned previously, a linear correlation of all the data is not the best representation of the relationship between log k and log K. In fact, as shown in Fig. 52 and by the equations below, a second degree curve is a better correlation of the data; a third degree curve provides no improvement whatsoever in the relationship.

31 dianions $\log (k_A 2\text{-}/3) = -10.6 \pm 0.1 - 0.785 (\log 3K_2)$ [4.44]
r = 0.9940

r = 0.9995 $\log (k_A 2\text{-}/3) = -12.6 \pm 0.3 - 1.42 \pm 0.10 (\log 3K_2) - 0.0489 \pm 0.0078 (\log 3K_2)^2$ [4.45]

We can use eqs. [1.54]-[1.56], p. 25, to determine the Marcus parameters. The resulting intrinsic barrier is 1.7 ± 0.3 kcal mol^{-1}; the work term, W_r, is determined to be 21 ± 3 kcal mol^{-1}. In order to determine the work term, Wp, which accounts for the separation of products, a value of K_Z is needed, i.e. the equilibrium constant for the dissociation of acetone as an acid. A highly accurate value of pK_Z has been available since 1984, based on measurements of enol-keto conversion rates in aqueous solution at 25°C: K_Z = 19.16 ± 0.04 (CK84). The value of K_Z used in eq. [1.56] is the statistically corrected one, i.e. Kq/p where p = 6 and q = 1 (thus log (K_Zq/p) = − 19.94). Hence, Wp is 21 ± 5 kcal mol^{-1}. The results of the Marcus analysis are statistically quite good; this is a measure of the excellent fit of the log k - log K correlation to a quadratic expression in log K.

The very low intrinsic barrier (2 kcal mol^{-1}) and the large work term necessary to bring the reactants together (21 kcal mol^{-1}) are of interest; analysis of other ketones with carboxylate bases gives similar results, though values of W_r are half as large as the value we have determined (KO73, AC72). One of these studies, which involves acetylacetone as the substrate, included catalysts of different structural types, a device that was required to 'observe' curvature (see p. 45).

Clearly our study is a more rigorous one, though it still has room for improvement; specifically, other catalysts in the lower pK range could be studied, and primary isotope effects could be evaluated.

The study by Hupe and Wu involving the base catalyzed enolization of a ketone with 30 oxyanions has been discussed in some detail (HW77, see p. 34). This study is relevant to our results, especially as the authors' values of $\Delta G_o^{\neq}$ (2.5 kcal mol^{-1}) and W_r (15.1 kcal mol^{-1}) are very close to ours. However, the curvature in their Bronsted plot is credited to a solvation effect and the authors suggest a $\Delta G_o^{\neq}$ value of 10 kcal mol^{-1} for such systems (see p. 45). Primary isotope effects in their system showed no significant correlation with pK, a fact that favours their argument (HP84, see p. 35).

We decided to examine the primary isotope effect in our system. A number of dianions were studied with acetone-d_6 at a single buffer ratio, the slope of k_{obs} against $[A^{2-}]$ being k_A2-. A correlation of β values and k_H/k_D values is predicted by Marcus theory, and in particular eq. [4.46], which expresses the rate of change of log k_A- as a function of changing HA, i.e. β (Section 1.8, p. 28).

$$-\beta = \text{d log k/d log K} = -1.42 - 0.0978\ (\log 3K_2) \qquad [4.46]$$

Thus, for a particular base, β can be calculated and, if a changing transition state is causing the curvature, the β values should correlate with the k_H/k_D values. (Statistical factors have been omitted from the left hand side of eq. [4.46] for clarity, however k should be read as $k_A-/3$ and K as $3K_2$). The results for seven phosphonates are given in

Table 38. The deviation of the k_A2^- values with acetone-d_6 is assumed to be ± 3%, (average deviation of all k_A2^- values with acetone), in order to calculate the deviation of k_H/k_D. The dianions which were examined were partly chosen on the basis of a smaller than average standard deviation in k_A2^-.

Table 38: k_A2^- values for acetone-d_6 enolization at 25°C, in water, and the resulting k_H/k_D values; β values calculated from eq. [4.46] on the basis of log $K_{2q/p}$, q = 3, p = 1.

Base	log $K_{2q/p}$	10^7 k_A^{2-} M^{-1} sec^{-1}	k_H/k_D	β
$ClCH_2PO_3^{2-}$	-6.11	15.0	2.9 ± 0.2	0.82
$4\text{-}CNC_6H_4PO_3^{2-}$	-6.31	24.9	3.2 ± 0.1	0.80
$3\text{-}ClC_6H_4PO_3^{2-}$	-6.62	42.7	3.5 ± 0.1	0.77
$3,4\text{-}(CH_3)_2C_6H_3PO_3^{2-}$	-7.28	92.8	4.5 ± 0.2	0.71
$2,4\text{-}(CH_3)_2C_6H_3PO_3^{2-}$	-7.59	141	4.6 ± 0.1	0.68
$2,6\text{-}(CH_3)_2C_6H_3PO_3^{2-}$	-8.14	303	5.2 ± 0.2	0.62
$(CH_3)_3CPO_3^{2-}$	-8.23	298	6.9 ± 0.2	0.62

[a] k_H values from Tables 21 and 32 (pp. 124 and 210)

Since the k_A2-values for both acetone and acetone-d_6 are precise, the values of k_H/k_D show a low standard deviation. There is a trend in the primary isotope effect, the value is a maximum when ΔpK is a minimum, Δ pK being the difference in pK between the monoanion, HA^- and acetone. There is also a clear link between the calculated β values and the measured k_H/k_D values; the largest isotope effect is associated with the β value nearest to 0.5 whereas when β is 0.82 the isotope effect is small (2.9). We believe that these results illustrate, rather elegantly, the changing position of the proton in the transition state. The Hammond postulate and its mathematically derived form, the Marcus equation, is followed almost perfectly by our substrate and set of catalysts. In fact, the results for base catalysis can be considered as evidence of the applicability of these concepts.

It is unclear why the study by Hupe and Wu gives fundamentally different results. While both systems involve base-catalyzed enolization, the catalysts used in each study are quite different; it would be interesting to combine their substrate and our extensive set of phosphonate dianions. Their work aside, the values of $\Delta G_o^{\neq}$, W_r and W_p determined for our system are given credence by the isotope effects study, which illustrates a changing transition state. While Marcus theory may underestimate $\Delta G_o^{\neq}$ by a factor of roughly two (p. 26), the end result of our analysis is that the bulk of the energy required for the reaction comes from W_r, the work needed to 'organize' or 'set-up' the two reagents in a position to allow relatively facile transfer of the proton.

The two analyses of curved Bronsted plots (Section 4.8.1 and 4.8.2)

stand in stark contrast to one another. One is an interpretative maze while the other is a classic example of a blending of theoretical concepts and experimental results.

Some final points concerning base catalysis and curvature can be made. It can be seen from Fig. 54 that the points for the carboxylate monoanions and dianons fall on or near extensions of the phosphonate curve. From our measurements of k_{HA} for a few carboxylic acids we have three values of k_{A^-} for acetone-d_6. The resulting k_H/k_D values are given in Table 38 and are quite compatible with the results obtained with the phosphonates, i.e. the same trend is present and the ten combined values make a reasonable set with a minimum isotope effect of 2.2 and a maximum of 6.9.

The fact that $\beta = 0.89$ for the monocarboxylates is in keeping with the β values increasing as we move from the phosphonates to the carboxylates.

Our last comment concerns k_{-OH}. From measurements of the phosphonate dianion rate constants we have determined a value of k_{-OH} (for acetone) from the intercepts of k_{obs} vs. $[A^{2-}]$ plots and pH. The result is $0.251 \pm 0.034\ M^{-1}\ sec^{-1}$ (43 values), a value close to that of Bell and Lidwell but higher than that of Hine (BL40, HK72). The same analysis for acetone-d_6 gives a value of $2.56 \pm 0.37 \times 10^{-2}\ M^{-1}\ sec^{-1}$ for k_{-OH} (5 values), a k_H/k_D value for hydroxide is therefore 9.8 ± 1.9. This compares favourably with literature values (see p. 47). The ΔpK for hydroxide and acetone is only about 3 pK units, and thus we have reached, or are close to, the maximum isotope effect.

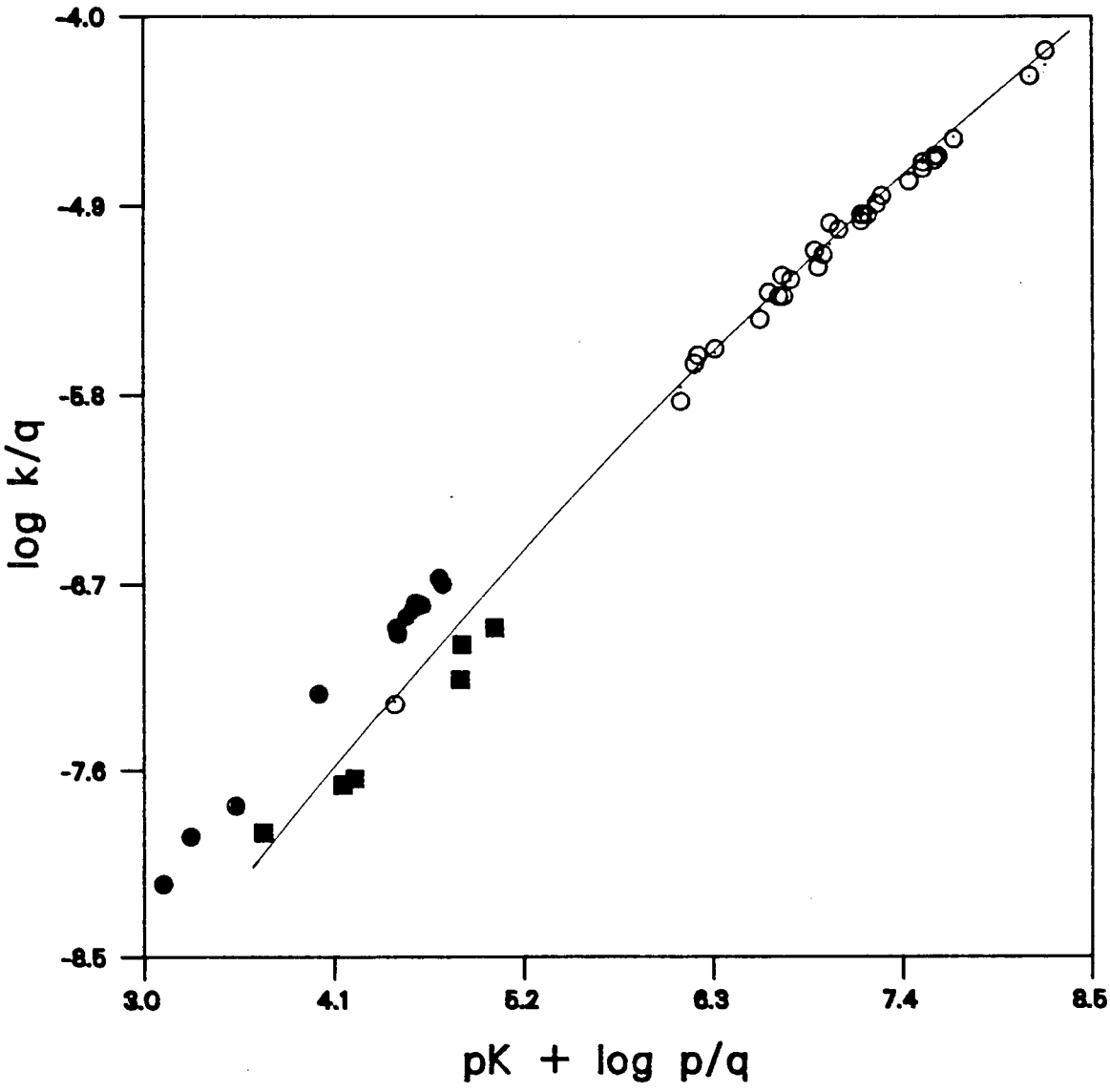

Fig. 54: Bronsted plot for acetone enolization catalyzed by phosphonate dianions (curve, open circles), monocarboxylate anions (closed circles) and dianions (closed squares).

Table 39: k_A- values for acetone-d_6 enolization at 25°C in water, and the resulting k_H/k_D values

Base	-log K q/p	10^7 k_A- M^{-1} sec^{-1}	k_H/k_D[a]
$HOCH_2CO_2^-$	3.53	0.156 ± 0.014	2.2 ± 0.3
$C_6H_5CH_2CO_2^-$	4.01	0.441 ± 0.005	2.7 ± 0.2
$CH_3CO_2^-$	4.46	0.781 ± 0.041	3.1 ± 0.2

[a] k_H values from Table 7, p. 81.

It may be recalled that the curved Bronsted line of Hupe and Wu incorporated hydroxide ion (HW77). The curved line for the phosphonates is such that k_{-OH} deviates negatively, i.e. it falls below the line, by a factor of 13 or 43 depending on the choice of p and q.

4.9. CONCLUSIONS

A number of β values have been determined in this work, for both acetone, Z, and protonated acetone, ZH^+, using a variety of catalysts. The results are listed in Table 40, and a number of conclusions can be

Table 40: Bronsted coefficients for proton abstraction from acetone (Z) and from protonated acetone (ZH^+)

Row No.	Substrate	Catalysts[a]		β
1	Z	RCO_2^-		0.89
2	ZH^+	RCO_2^-		0.40
3	Z	$R(CO_2^-)_2$,	$Ar(CO^-)_2$	0.77
4	ZH^+	$Ar(CO_2^-)_2$	5-subst	0.68
5	ZH^+	$Ar(CO_2^-)_2$	2-subst	0.45
6	Z	$ArPO_3^{2-}$	meta, para	0.71
7	Z	$ArPO_3^{2-}$	ortho	0.74
8	ZH^+	$ArPO_3H^-$	meta, para	0.62
9	ZH^+	$ArPO_3H^-$	ortho	0.58

[a] R = alkyl; Ar = aryl

summarized on the basis of the size of the Bronsted coefficients.

1. In a comparison between the same type of catalyst reacting with protonated or neutral acetone, the smaller β value is always observed with protonated acetone. This is interpreted as the more reactive system having an earlier transition state i.e. proton transfer occurs sooner along the reaction coordinate. This is predicted by the Hammond postulate. (Compare rows 1 and 2; 3 and 4; and 6 and 8, although the

latter involve slightly different catalysts.

2. In the case of 2-substituted isophthalate monoanions, steric acceleration is observed (when compared to 5-substituted isophthalates). This is reflected in the relative β values of reactions involving ZH^+ and the conjugate dianions; the more reactive 2-substituted catalysts lead to an earlier transition state (rows 4 and 5). A similar but smaller effect is observed with arylphosphonate monoanions, rows 8 and 9, the ortho-catalysts possess the smaller β value and show a steric accelerating effect.

3. In the case of arylphosphonate dianions the ortho-compounds fall on or just below the Bronsted line for the meta- and para-compounds; the larger β for the ortho series (row 7) may reflect a slight steric retardation effect.

4. As was discussed previously, (p. xxx), a comparison of the effects for monocarboxylate bases and dicarboxylate bases does not make sense in terms of the Hammond postulate (compare rows 1 and 3, and 2 and 4). Perhaps this is an example of a breakdown in the concept of a more reactive system having an earlier transition state. It is also possible that the additional unit of negative charge (in the dianion) is having a large unexplained effect. In fact a comparison of the two types of catalyst, $-CO_2^-$ and $(-CO_2^-)_2$, may be inappropriate; it seems that a combination of $-PO_3^{2-}$ and $-CO_2^-$ results (rows 1 and 6) may be a more valid comparison, considering our recent discussion (p. 232). Despite

the difference in the catalytic moiety, the $-PO_3^{2-}$ charge is more localized than in the carboxylate dianions, and therefore may resemble the $-CO_2^-$ to a greater degree. As well as the deductions concerning the magnitude of β values just discussed, a number of other conclusions have been made on the basis of our results.

5. A relationship exists between the degree of hydrogen-bonding in the monoanions of dicarboxylic acids and the degree of deviation of the dianion from the Bronsted line for dianions whose conjugate monoanions have no hydrogen bonding.

6. In both acid and base catalyzed enolization, polarizable substituents cause the catalyst to display an enhanced catalytic activity.

7. Ortho benzoic acids, 2-substituted isophthalate monoanions and sterically crowded aliphatic carboxylic acids all show varying degrees of enhanced reactivity in the acid catalyzed enolization of acetone. The effect seems absent in the general base catalyzed process and therefore might be linked to the use of protonated acetone as opposed to neutral acetone as the substrate. However, why the protonated substrate should cause an effect while the neutral substrate does not, is not obvious. The fact that Bell and coworkers have observed steric acceleration in base catalyzed enolization with very bulky catalysts and substrates (see p. 60, BG49) may mean that we will not observe any effect until a bulky substrate is used. In this regard, the reported rate enhancement by a factor of three for pivalate anion in cyclohexa-

none enolization seems relevant (LW69). The role of steric factors in these processes is unclear. It has been suggested that hydrophobic bonding causes rate accelerations in some of these cases (BG49).

8. There appears to be curvature in the Bronsted plot for carboxylic acid catalysts. Primary isotope effects suggest that the curvature is not due to changes in transition state structure.

9. On the other hand, curvature in a set of phosphonates has been related to isotope effect variations, all of which suggests that there is a change in the degree of proton transfer (at the transition state) as the equilibrium base strength of the catalyst is changed. Marcus theory analysis implies that the proton transfer itself is facile while setting-up the reagents for such a transfer is energetically expensive.

10. A group of monoanions that were studied act as general acids, not general bases, in the enolization of acetone.

11. The inclusion of catalysts of different structure and/or charge in one Bronsted correlation must be done with caution.

A glance at the scope of this investigation as outlined in p. 65 is recommended. We have answered many of our original questions and some more besides. However, as always happens in research, new questions arise out of an analysis of our results. These questions have assumed a higher level of complexity than before and the answers to them must be

the next step in our progress.

4.10 SUGGESTIONS FOR FURTHER WORK

1. A study involving a sterically bulky substrate (e.g. 2,4-dimethylpentanone) would be informative. Would there be an increase in the steric acceleration factors over that observed for general acid catalyzed enolization of acetone? Would steric acceleration be evident in the general base catalyzed process?

2. A number of halo-substituted alkylphosphonic acids would be very helpful in further evaluating the curved Bronsted plot for all the phosphonates. This would also allow the construction of a Bronsted plot for phosphonate monoanions.

3. As recommended previously, more work is needed in the correlation of deviating dianions and the degree of hydrogen-bonding in their conjugate monoanions.

In closing this discussion, a retrospective view of the main thrust of this thesis may be worthwhile. Throughout this work, we have critically examined the reasons for deviations from Bronsted lines as well as the causes for non-linear Bronsted correlations.

The non-linearity observed in the case of phosphonate dianions has been credited to a changing transition state and this result gives support to the Hammond postulate and to Marcus theory. It should be

remembered, however, that our present concepts and theories of transition state energetics are models and should be considered as such. These models require both experimental support and constructive criticism. Results which agree with our present concepts suggest that we are on the right track. Results which appear to undermine our present concepts should not solicit blanket criticism of the model. On the contrary, they illustrate the limitations of our approach.

There is a paucity of experimental evidence, devoid of debatable facets, for the Hammond postulate. We believe that the curved phosphonate Bronsted plot and related primary isotope effects is a worthwhile contribution in this regard.

EXPERIMENTAL

5.1 General Kinetic Measurements

Unless otherwise stated, the following are implied. Distilled water was used throughout this work. Acetone was of spectrophotometry grade (BDH Chemicals); it was refluxed with potassium permanganate (0.1 g/400 mL) for 2 hours, fractionally distilled, and stored overnight over calcium carbonate. The liquid was filtered and fractionally distilled a second time, and was stored in a dark bottle fitted with a septum cap, for up to twelve weeks. Buffer solutions of the acids and their conjugate bases were prepared by the addition of either hydrochloric acid to the sodium salt of the acid, or sodium hydroxide to the free acid. Solutions of both sodium hydroxide and hydrochloric acid were prepared by dilution of concentrated volumetric solutions available from BDH chemicals. The sodium hydroxide was standardized by titration with potassium hydrogen phthalate (gold label, Aldrich Chemical Co.) using phenolphthalein as indicator; this was done on a daily basis. The hydrochloric acid was standardized by titration with the standardized sodium hydroxide, using the same indicator; this was done on a weekly basis.

The general method of preparing buffer solutions was as follows. The free acid was placed in a 10 mL or 25 mL volumetric flask. A volume of sodium hydroxide was added in order to obtain a chosen buffer-ratio, n, ($[HA]/[A^-]$). The number of equivalents of hydroxide necessary for a

particular n value is given by $1/(n + 1)$. In cases where the acid was used as its sodium salt, hydrochloric acid was added. The number of equivalents of hydrochloric acid necessary for a particular n value is given by $n/(1 + n)$. Aliquots from these stock solutions of buffer were placed in 5 mL or 10 mL volumetric flasks. The ionic strength of these solutions was made up to a constant value by the addition of sodium chloride. Acetone was added via a 250 μL syringe to each preweighed volumetric flask; the concentrations of acetone that were used varied from 0.1 to 0.5 M. Each solution was made up to the appropriate volume with water. Generally four solutions were prepared from each stock solution at a particular n value.

The rates of enolization of acetone were determined iodometrically by following the decrease in the absorbance of the triiodide ion at 353, 400 or 440 nm (pp. 66-68). A 3 mL sample of a particular solution was temperature equilibrated at 25°C for 15 min in a closed cuvette. The iodination was initiated by the addition of 50 μL of triiodide ion solution. The decrease in absorbance was followed with a Cary 16 spectrophotometer equipped with a cell holder thermostatted at 25 ± 0.1°C. The rate of reaction is given by eq. [3.2], p. 67; each observed first-order rate constant (k_{obs}) was calculated from the linear slope of the plot of absorbance against time by use of the relationship k_{obs} = -slope/($\epsilon_{I_3^-}$ [acetone]), where $\epsilon_{I_3^-}$ is the extinction coefficient of triiodide ion at the chosen wavelength. The concentration of acetone was corrected for the dilution factor, caused by the addition of 50 μL I_3^- solution, as were the concentrations of acid and base buffers.

The values of $\epsilon_{I_3^-}$ used were 2.45×10^4 M^{-1} cm^{-1} at 353 nm (AB65), 5.9×10^3 M^{-1} cm^{-1} at 400 nm (value determined in this work) and 1818 M^{-1} cm^{-1} at 440 nm (SS76b). A wavelength of 353 nm was used unless (a) the buffer species absorb at that wavelength (e.g. nitro-substituted catalysts) (b) the disappearance of tri-iodide ion was too fast to follow at that wavelength (e.g. highly acidic buffer solutions). The concentrations of triiodide ion varied from 4×10^{-5} to 5×10^{-4} M, and were chosen to give an initial absorbance reading of approximately 0.9. The fact that all plots of absorbance against time were linear from the time of the first reading (about 30 sec after the addition of the triiodide aliquot) until at least 70% of the iodine had reacted show that the kinetics of iodine consumption are zero order. Stock solutions of triiodide ion were prepared with 0.5 M KI and concentrations of I_2 that depended on the wavelength chosen; 2.2×10^{-3} M at 353 nm, 6.9×10^{-3} M at 400 nm and 2.1×10^{-2} M at 440 nm. The equilibrium between KI, I_2 and $K^+I_3^-$ favours $K^+I_3^-$ (K = 714, AB65) and all the solutions of triiodide ion will contain negligible amounts of I_2.

The pH values of buffer solutions before and after rate measurements showed little change, ± 0.02 pH units at the worst, generally less. A Radiometer Model 26 pH meter and a Radiometer GK2421C combined glass electrode were used for pH measurements. The pH meter was standardized with aqueous buffer solutions at pH 2.00 ± 0.02, 4.00 ± 0.01 and 7.00 ± 0.01 (BDH Chemicals and Fischer Scientific).

For all the acid/base pairs which were examined, a 'blank' reaction (i.e. no acetone) with triiodide ion was carried out. In most cases, there was no reaction between the buffers and I_3^-. In some cases, a

rapid non-linear decrease of I_3^- was observed, precluding the measurements of rate constants associated with that particular buffer pair. In a few cases, the disappearance of triiodide in the absence of acetone was a slow first-order reaction that could be satisfactorily corrected for. The enolization process is zero order in iodine and it could be shown that the reaction of iodine with the buffer anion has a negligible effect on the measured rate of enolization.

In the case of buffer ratios involving diprotic acids and the conjugate monoanions, the treatment described for monoprotic acids is applicable. However, for any particular buffer ratio of the monoanion and its conjugate base (the dianion), i.e. m, the number of equivalents of hydroxide needed for a particular m value is $(m + 2)/(m + 1)$. Thus the proportion of dianion is taken to be the fraction in excess of one equivalent, that of the monoanion to be unity minus this fraction, and that of the diacid to be zero. This treatment presupposes two distinct acid dissociations. A method has been described previously which considers overlapping dissociations, and allows a calculation of $[H_2A]$, $[HA^-]$ and $[A^{2-}]$ (pp. 97-98).

The extinction coefficient for triiodide ion at 400 nm was determined as follows. A plot of $[I_3^-]$ against absorbance gives $\epsilon_{I_3^-}$ as the slope, with the intercept being negligible. The concentration of I_3^- was determined by titration with a standard sodium thiosulfate solution that had just been titrated with potassium dichromate (V51). The result of two determinations of $\epsilon_{I_3^-}$ at 400 nm gave a value of $5.9 \pm 0.2 \times 10^3$ M^{-1} cm^{-1}. Values of the extinction coefficient at 353 nm and 400 nm, which were also determined, are close to the reported values (2.52 ±

0.11×10^4 M^{-1} cm^{-1} at 353 nm and 1824 ± 55 M^{-1} cm^{-1} at 440 nm).

5.2 CARBOXYLIC ACIDS

Most of the monoprotic aliphatic acids were purified as their sodium salts. Commercially available acids were mixed with diethyl ether and washed with 0.95 equivalents of sodium hydroxide. The aqueous layer was separated, washed twice with diethyl ether, and the water was removed under reduced pressure to give the sodium salt of the acid. The salts were recrystallized from ethanol/ethyl acetate mixtures, dried in vacuo. Acids purified in this manner are listed in Table 7, p. 80. In the case of iodoacetic acid, the sodium salt was obtained from a commercial source (Aldrich Chemical Co.), and washed with acetone to remove the yellow colour, dried at 80°C for two hours and used directly for the kinetic measurements. Sodium acetate-d_3 was obtained from MSD Isotopes. Buffer solutions of these acids were prepared by the addition of hydrochloric acid.

For the stronger aliphatic acids inclusive of dichloroacetic acid and stronger halo-acids, the acid was purified by distillation at reduced pressure, except in the case of tribromoacetic acid, which was sublimed at 80°C/2 mm Hg. As was described previously, buffer-ratio control proved difficult for these acids. Consequently, a different kinetic treatment was used, and this has been discussed already, p. 82. Stock solutions of these acids were prepared and titrated, and a subsequent dilution was used to provide solutions of various concentra-

tions. Hydroxide was then added in varying amounts (between 1/3 and 4/5 equivalents) and the k_{obs} values for each solution were measured.

Three of the ammonio carboxylic acids are commercially available. Glycine, N,N-dimethylglycine hydrochloride and N,N,N-trimethylglycine hydrochloride were all recrystallized from alcohol. Stock solutions of the latter two compounds were titrated and kinetic results obtained in the same manner as that used for the strong halo-acids. Glycine hydrochloride buffers were prepared by the addition of hydrochloric acid to various amounts of glycine. The concentration of acid HA present in any particular solution is $[A^-] + [HCl] - [H^+]$, where A^- is glycine itself, and $[H^+]$ is available from the pH measurements.

4-Trimethylammoniobutanoic acid chloride was prepared from 4-dimethylaminobutanoic acid hydrochloride following a reported method (AK81). In the same way 6-trimethylammoniohexanoic acid chloride was synthesized from 6-aminohexanoic acid. Both of these compounds were recrystallized from DMF, and gave satisfactory end points upon titration with standardized hydroxide solution (±3% of the calculated result). The melting point of the butanoic acid derivative (213 – 216 °C) compares favourably with the reported value (214 – 219°C). The hexanoic acid derivative (mp 200-202°C) gave the following elemental analysis; found; C: 51.6; H: 9.57; N: 6.64; expected: C: 51.5; H: 9.61; N: 6.68. The kinetic treatment for these two acids was quite straightforward and has been described already.

The benzoic acids that were studied were all recrystallized from water.

A number of acid buffers reacted with triiodide ion and thus we

could not measure any rate constants for these monoprotic acids or their conjugate bases. Included in this group are cyanoacetic, 3,4-dinitrobenzoic, bromoacetic, dibromoacetic and 4-aminobutanoic acid. We synthesized methylthioacetic acid, following a literature method (CS70), but it also reacted with I_3^-. An acid, which was to extend the upper pK range of the monoprotic acids in our Bronsted plot, is trimethylsilylacetic acid (pK = 5.22); it was prepared from the corresponding Grignard reagent but was found to react with I_3^- (SG49).

The pK of t-butylacetic acid was determined in water at 25°C and corrected for ionic strength (AS84). This thermodynamic pK is 5.01 ± 0.02. Values for propanoic acid and benzoic acid were also determined as a check on the experimental accuracy of the pK measurement. These results are close to the literature values (4.86 ± 0.03, and 4.20 ± 0.03).

The diprotic carboxylic acids were all purified by recrystallization, from water in the case of aromatic acids, and from hexane/ethylacetate/ethanol mixtures in the case of aliphatic acids. Reactions between the buffer and triiodide ion occurred with 1,2-cis-dicarboxylic acid and methylmalonic acid. A slow reaction occurred in the case of 3-methylglutaric acid, which prevented measurements being made of k_{H_2A} but allowed us to determine k_{HA^-} and $k_{A^{2-}}$.

The 2- and 5-substituted isophthalic acids were synthesized, and their pK_1 and pK_2 values measured, by other members of our research group (GS84, NL87).

5.3 PHOSPHONIC ACIDS

Whereas, for acid catalysis poor solubility limits the range of acids for which we can measure k_{H_2A}, for phosphonate dianion catalysis, a number of buffers reacted with triiodide. These included all the buffers containing appreciable concentrations of arylalkoxy-dianions. The synthesis and pK determinations of the arylphosphonic acids have been reported (NS87). The alkylphosphonic acids were synthesized by other members of our group (NV87).

5.4 ISOTOPE MEASUREMENTS

Deuterium oxide (99.8 atom % D) and acetone-d_6 (99.9 atom % D) were obtained from MSD isotopes. D_2O was used directly in the preparation of buffer solution, and in the dilution of concentrated NaOD and DCl solutions (laboratory stock). The rate measurements in D_2O were obtained in an identical manner as that for H_2O. Solutions of I_3^- were prepared in D_2O. While most of the acids were used in the form of their sodium salts difluoroacetic and trifluoroacetic acid-d were used directly. Acetone-d_6 was distilled and dried in an identical manner to that of acetone.

5.5 STATISTICS

All linear correlations are the result of a least-squares regression analysis using the minitab program available on the UBC MTSG system. The same program was used for the quadratic correlations. Uncertainties (i.e. ± deviations) in the case of addition, subtraction, multiplication and division are calculated by the standard equations (R81d).

6. APPENDIX

I. RATE-ACIDITY PROFILE

For each buffer-ratio a value of k_{sum} (contribution to k_{obs} from hydronium ion, hydroxide ion and water) is available and thus a plot of log k_{sum} against the pH gives the rate-acidity profile for acetone enolization, Fig. 55. This allows a check on the reported value of k_{H_2O}

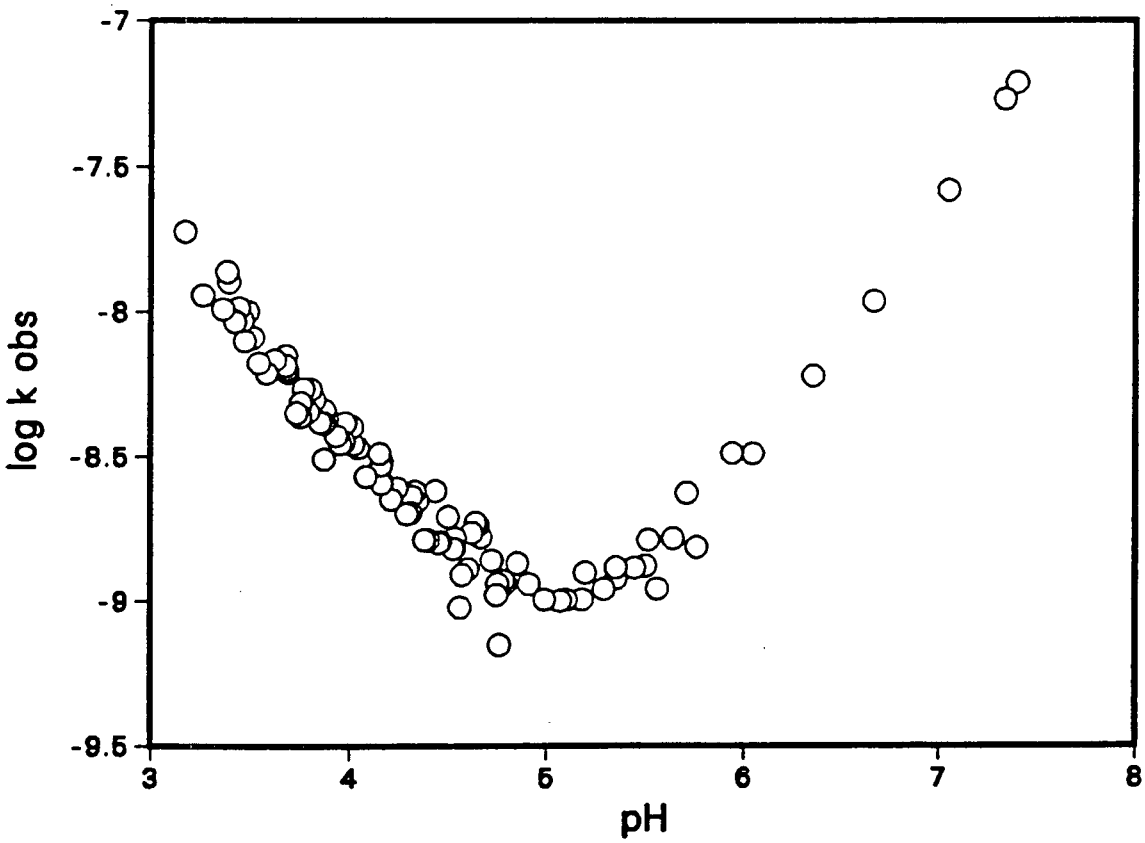

Fig. 55: Rate-acidity profile for the enolization of acetone.

(BL40). Knowing k_{H^+} (2.51×10^{-5} M^{-1} sec^{-1}) and k_{-OH} (0.251 M^{-1} sec^{-1}), we can determine the pH value at which the contribution to k_{obs} from these species is a minimum (S85i). The result is 5.0, a value which is also suggested by Fig. 55 where a plateau is evident at that pH. The contribution from H_3O^+ and ^-OH is 5.0×10^{-10} M^{-1} sec^{-1} while the k_{obs} from Fig. 55 is 1.0×10^{-9} M^{-1} sec^{-1}. Thus, the difference (5×10^{-10} M^{-1} sec^{-1}) can be credited to $k_{H_2O}[H_2O]$, and since $[H_2O]$ is 55.5 M, the catalytic constant for water is 9.0×10^{-12} M^{-1} sec^{-1} which is in good agreement with the value of Bell and Lidwell, 8.3×10^{-12} M^{-1} sec^{-1}.

II. SOLVENT ISOTOPE EFFECTS IN BASE CATALYSIS

The solvent isotope effect (H_2O/D_2O) was measured for a number of bases and the results are given in Table 41. The combination of the results for the three carboxylate bases with those of their conjugate acids (Table 34, p. 219) allows an estimation of k_{ZH^+}/K_{ZD^+}, the ratio of equilibrium constants for protonated acetone in H_2O and D_2O, given by the equation below (from eq. [1.77], p. 51).

$$K_{ZH^+}/K_{ZD^+} = k'_{A^-}(H_2O)/k'_{A^-}(D_2O) \times K_{HA}/K_{DA} \times k_{HA}(D_2O)/k_{HA}(H_2O)$$

The values of K_{HA}/K_{DA} (LR69, SS76a) and $k_{HA}(D_2O)/k_{HA}(H_2O)$ are available and we can make the following assumption; the solvent isotope effect for base catalysis involving acetone is equal to that for base catalysis involving protonated acetone. The resulting k_{ZH^+}/K_{ZD^+} value

Table 41: k_A-[a] values for acetone enolization at 25°C, measured in D_2O and resulting k_A-$(H_2O)/k_A$-(D_2O) values

Base	10^6 k_A- (D_2O) M^{-1} sec^{-1}	k_A-$(H_2O)/k_A$-(D_2O)[b]
$HOCH_2CO_2^-$	.0350 ± 0.0014	0.97 ± 0.10
$CH_3CO_2^-$	.181 ± 0.008	1.35 ± 0.07
$(CH_3)_3CCO_2^-$	.316 ± 0.012	1.27 ± 0.06
4-CN-$C_6H_4PO_3^{2-}$	7.89[c]	0.98 ± 0.03
4-CH_3-$C_6H_4PO_3^{2-}$	39.1	0.89 ± 0.03
2,6-$(CH_3)_2$-$C_6H_3PO_3^{2-}$	162	0.98 ± 0.04

a k_A2- values for phosphonate bases

b k_A-(H_2O) values from Table 7 and 21, pp. 81 and 124.

c Deviation of k_A2- values in D_2O assumed to be ± 3% (p. 229).

is 2.81 ± 0.13, slightly smaller than the effects for carboxylic acids (3.09, 3.31 and 3.16 for trimethylacetic acetate and glycolic acid respectively).

BIBLIOGRAPHY

A 82 W.J. Albery, J. Chem. Soc., Faraday Trans. 1, **78**, 1579 (1982).

AB65 W.J. Albery, R.P. Bell, and A.L. Powell, Trans Faraday. Soc. **61**, 1194 (1965).

AC72 W.J. Albery, A.N. Campbell-Crawford and J.S. Curran, J. Chem. Soc. Perkin II, 2206 (1972).

AE70 M.-L. Ahrens, M. Eigen, W. Kruse, and G. Maass, Ber. Bunsenges. Phys. Chem., **74**, 280 (1970).

AG82 W.J. Albery and J.S. Gelles, J. Chem. Soc., Faraday Trans. I, **78**, 1569 (1982).

AK81 L. Andersson, T. Kuhler, and M. Nilsson, Synthesis, 468 (1981).

AS84 A. Albert and E.P. Serjeant, The Determination of Ionization Constants, 3rd edn., Chapman and Hall, New York, (1984).

a) pp. 47-49.
b) p. 51.
c) p. 56.
d) p. 60.
e) p. 55.

B 23 J.N. Bronsted, Rec. Trav. Chim., 42, 718 (1923).

B 59 R.P. Bell, The Proton in Chemistry, 1st ed., p. 201, Cornell University, Press, Ithaca, N.Y., 1959.

B 73 R.P. Bell, The Proton in Chemistry, 2nd ed., Cornell University Press, Ithaca, N.Y., 1973.

a) Chapter 2.
b) p. 172.
c) pp. 160-164.
d) pp. 197-200
e) Chapter 10.
f) pp. 202-203
g) p. 270

B 78 R.P. Bell, Correlation Analysis in Chemistry, Recent Advances, Chapter 2, Chapman and Shorter, Plenum Press, 1978.

B 80 R.P. Bell, The Tunnel Effect in Chemistry, Chapman and Hall, London, (1980).

B 87 C.F. Bernasconi, Acc. Chem. Res., **20**, 301 (1987).

BB65 T.C. Bruice and W.C. Bradbury, J. Am. Chem. Soc., **87**, 4851 (1965).

BB71 F.G. Bordwell and W.J. Boyle Jr., J. Am. Chem. Soc., **93**, 512 (1971).

BB75 F.G. Bordwell and W.J. Boyle Jr., J. Am. Chem. Soc., **97**, 3447 (1975).

BB85 C.F. Bernasconi and R.D. Bunnell, Isr. J. Chem., **26**, 420 (1985).

BC70 R.P. Bell and B.G. Cox, J. Chem. Soc. (B), 194 (1970).

BC78 N.A. Bergman, Y. Chiang, and A.J. Kresge, J. Am. Chem. Soc., **100**, 3928 (1978).

BG49 R.P. Bell, E. Gelles, and E. Moller, Proc. R. Soc. A, **198**, 308 (1949).

BG66 R.P. Bell and D.M. Goodall, Proc. Roy. Soc. A, **294**, 273 (1966).

BG76 R.P. Bell and S. Grainger, J.C.S. Perkin II, 1606 (1976).

BH85 F.G. Bordwell and D.L. Hughes, J. Am. Chem. Soc., **107**, 4737 (1985).

BJ53 R.P. Bell and P. Jones, J. Chem. Soc., **88**, (1953).

BL40 R.P. Bell and O.M. Lidwell, Proc. Roy. Soc. (London), **A176**, 88 (1940).

BL65 D.M. Bishop and K.J. Laidler, J. Chem. Phys., **42**, 1688 (1965).

BP24 J.N. Bronsted and K.J. Pedersen, Z. Phys. Chem., **108**, 185 (1924).

BP86 C.F. Bernasconi and P. Paschalis, J. Am. Chem. Soc., **108**, 2969 (1986).

BR84 G.J. Bijloo and R.G. Rekker, Quant. Struct. Uct.-Act. Relat. Pharmacol. Chem. Biol., **3**, 91 (1984).

BS59 R.P. Bell and T.S. Spencer, Proc. Roy. Soc. A, **251**, 41 (1959).

BU79 N. Bruniche-Olsen and J. Ulstrup, J. Chem. Soc. Faraday Trans. I, **75**, 205 (1979).

BW64 B.T. Baliga and E. Whalley, Can. J. Chem., **42**, 1835 (1964).

BW66 M.L. Bender and A. Williams, J. Am. Chem. Soc., **88**, 2502 (1966).

C 71 M. Charton, Prog. Phys. Org. Chem., **8**, 235 (1971).

C 75 J.E. Crooks, in "Proton Transfer Reactions" (E.F. Caldin and V. Gold, eds.), Chapter 6, Chapman and Hall, London, 1975.

CC69 J.P. Calmon, M. Calmon and V. Gold, J. Chem. Soc. (B), 660 (1969).

CD81 B.G. Cox, P. De Maria, A. Fini, and A.F. Hassan, J. Chem. Soc., Perkin Trans. 2, 1351 (1981).

CE77 W.K. Chwang, R. Eliason, and A.J. Kresge, J. Am. Chem. Soc., **99**, 805 (1977).

CH87 Y. Chiang, M. Hojjatti, J.R. Keefe, A.J. Kresge, N.P. Schepp, and J. Wirz, J. Am. Chem. Soc., **109**, 4000 (1987) and references therein.

CJ81a M.M. Cox and W.P. Jencks, J. Am. Chem. Soc., **103**, 572 (1981).

CJ81b M.M. Cox and W.P. Jencks, J. Am. Chem. Soc., **103**, 580 (1981).

CK84 Y. Chiang, A.J. Kresge, Y.S. Tang and J. Wirz, J. Am. Chem. Soc., **106**, 460 (1984).

CM68 A.O. Cohen and R.A. Marcus, J. Phys. Chem., **72**, 4249 (1968).

CS70 J.M. Carpenter and G. Shaw, J. Chem. Soc. (C), 2016 (1970).

CS79 R.A. Cox, C.R. Smith, and K. Yates, Can. J. Chem., **50**, 3239 (1979).

CW63 F. Covitz and F.H. Westheimer, J. Am. Chem. Soc., **85**, 1773 (1963).

DB70 J.E. Dixon and T.C. Bruice, J. Am. Chem. Soc., **92**, 905 (1970).

DK83 D.B. Dahlberg, M.A. Kuzemko, Y. Chiang, A.J. Kresge, and M.F. Powell, J. Am. Chem. Soc., **105**, 5387 (1983).

DP13 H.M. Dawson and F. Powis, J. Chem. Soc., 2135 (1913).

DS30 H.M. Dawson and E. Spivey, J. Chem. Soc., 2180 (1930).

DT73 J.E. Dubois and J. Toullec, Tetrahedron, **29**, 2859 (1973).

E 64 M. Eigen, Angew. Chemie, Internat. Ed., **3**, 1 (1964).

E 69 L. Eberson in "The Chemistry of Carboxylic Acids and Esters", ed. S. Patai, Interscience, New York, 1969, Chapter 6.

EB83 K. Engdahl, H. Bivehed, P. Ahlberg, and W.H. Saunders, Jr., J. am. Chem. Soc., **105**, 4767 (1983).

EF79 J.T. Edward, P.G. Farrell, J. Halle, J. Kirchnerova, R. Schaal, and F. Terrier, J. Org. Chem., **44**, 615 (1979).

ES87 R.T. Eddin, J. M. Sullivan and J.R. Norton, J. Am. Chem. Soc., **109**, 3945 (1987).

F 75 Faraday Symposia, **10**, 89-99 (1975).

FG65 J.A. Feather and V. Gold, J. Chem. Soc., 1752 (1965).

FN76 T. Fujita and T. Nishioka, Prog. Phys. Org. Chem., **12**, 49 (1976).

G 85 E. Grunwald, J. Am. Chem. Soc., **107**, 4710 (1985).

GR67 C.D. Gutsche, D. Redmore, R.S. Buriks, K. Nowotny, H. Grassner, and C.W. Armbruster, J. Am. Chem. Soc., **89**, 1235 (1967).

GS84 S.J. Gumbley and R. Stewart, J. Chem. Soc. Perkin Trans. II, 529 (1984).

GW68 V. Gold and D.C.A. Waterman, J. Chem. Soc. B, 839 (1968).

H 40 L.P. Hammett, Physical Organic Chemistry, McGraw-Hill, New York, 1940.

HH65 J. Hine, J.G. Houston, J.H. Jensen, and J. Mulders, J. Am. Chem. Soc., **87**, 5050 (1965).

HH78 A.J. Hoefnagel, M.A. Hoefnagel, and B.M. Wepster. J. Org. Chem., **43**, 4720 (1978).

HJ75a A.F. Hegarty and W.P. Jencks, J. Am. Chem. Soc., **97**, 7188 (1975).

HJ75b E.S. Hand and W.P. Jencks, J. Am. Chem. Soc., **97**, 6221 (1975) .

HK72 J. Hine, J.C. Kaufmann, and M.S. Cholod, J. Am. Chem. Soc., **94**, 4590 (1972).

HK75 A.I. Hassid, M.M. Kreevoy, and T. Liang, Faraday Symposia, **10**, 69 (1975).

HP78 D.J. Hupe and E.R. Pohl, J. Am. Chem. Soc., **100**, 8130 (1978).

HP84 D.J. Hupe and E.R. Pohl, J. Am. Chem. Soc., **106**, 5634 (1984).

HS74 E. Hayon and M. Simic. Acc. Chem. Res., **7**, 114 (1974).

HW73 A.J. Hoefnagel and B.M. Wepster. J. Am. Chem. Soc., **95**, 5357 (1973).

HW77 D.J. Hupe and D. Wu, J. Am. Chem. Soc., **99**, 7653 (1977).

HW82 A.J. Hoefnagel and M.B. Wepster, J. Org. Chem., **47**, 2318 (1982) and references therein.

J 65 J.R. Jones, J. Chem. Soc. Faraday Trans., **61**, 95 (1965).

J 69 W.P. Jencks, Catalysis in Chemistry and Enzymology, Chap. 3, McGraw-Hill, New York, 1969.

JB82 W.P. Jencks, S.R. Bryant, J.R. Gandler, G. Fendrich and C. Nakamura, J. Am. Chem. Soc., **104**, 7045 (1982).

JF53 H.H. Jaffe, L.D. Freedman, and G.O. Doak. J. Am. Chem. Soc., **75**, 2209 (1953).

JG84 J. Jager, T. Graafland, H. Schenk, A.J. Kirby, and J.B.F.N. Engberts, J. Am. Chem. Soc., **106**, 139 (1984).

JF54 H.H. Jaffe, L.D. Freedman, and G.O. Doak. J. Am. Chem. Soc., **76**, 1548 (1954).

JJ77 D.A. Jencks and W.P. Jencks, J. Am. Chem. Soc., **99**, 7948 (1977).

JM67 J.R. Jones, R.E. Marks, and S.C. Subba Rao, J. Chem. Soc. Faraday Trans., **63**, 111 (1967).

K 73 A.J. Kresge. Chem. Soc. Rev., **2**, 475 (1973).

K 75 A.J. Kresge, in "Proton Transfer Reactions", (E.F. Caldin and V. Gold, eds.), Chapter 7, Chapman and Hall, London, 1975.

K 76 M.M. Kreevoy in "Isotopes in Organic Chemistry", (E. Buncel and C. Lee, eds.), Chapter 1. Elsevier, Amsterdam, 1976.

K 83 J.L. Kurz, J. Org. Chem., **48**, 5117 (1983).

K 84 H.F. Koch, Acc. Chem. Res., **17**, 137 (1984).

KC73a D.S. Kemp and M.L. Casey, J. Am. Chem. Soc., **95**, 6670 (1973).

KC73b A.J. Kresge and Y. Chiang, J. Am. Chem. Soc., **95**, 803 (1973).

KF69 J.L. Kurz and J.M. Farrar, J. Am. Chem. Soc., **91**, 6057 (1969).

KK73 G.W. Koeppl and A.J. Kresge, J.C.S. Chem. Commun., 371 (1973).

KL84 M.M. Kreevoy and I.H. Lee, J. Am. Chem. Soc., **106**, 2550 (1984).

KO73 M.M. Kreevoy and S. Oh, J. Am. Chem. Soc., **95**, 4805 (1973).

KS83 A.J. Kresge and T.S Straub, J. Am. Chem. Soc., **105**, 3961 (1983).

KT77 A.J. Kresge and Y.C. Tang, J. Org. Chem., **42**, 757 (1977).

KV61 G. Kortum, W. Vogel, and K. Andrusson, "Dissociation Constants of Organic Acids in Aqueous Solution", Butterworths, London, 1961.

KW85 H. Kwart and K.A. Wilk, J. Org. Chem., **50**, 817 (1985).

L 04 A. Lapworth. J. Chem. Soc., 30 (1904).

L 75 E.S. Lewis, in "Proton Transfer Reactions", (E.F. Caldin and V. Gold, eds.), Chapter 10, Chapman and Hall, London, 1975.

L 76 K.T. Leffek in "Isotopes in Organic Chemistry", (E. Buncel and C. Lee, eds.), Chapter 3. Elsevier, Amsterdam, 1976.

LA67 G.E. Lienhard and F.H. Anderson, J. Org. Chem., **89**, 2229 (1967).

LF25 T.M. Lowry and I.J. Faulkner, J. Chem. Soc., 2883 (1925).

LF67 E.S. Lewis and L.H. Funderburk, J. Am. Chem. Soc., **89**, 2322 (1967).

LG63 J.E. Leffler and E. Grunwald, "Rates and Equilibria of Organic Reactions", John Wiley, New York, 1963, p. 156.

LR69 P.M. Laughton and R.E. Robertson, in "Solute-Solvent Interactions", ed. J.F. Coetzee and C.D. Ritchie, Marcel Dekker, New York, 1969, Chapter 7.

LR87 T.H. Lowry and K.S. Richardson, Mechanism and Theory in Organic Chemistry, 3rd edn., Harper and Row, New York, 1987.

a) p. 662.
b) pp. 212-214.
c) pp. 222-229.

LS81 E.S. Lewis, C.C. Shen and R.A. More O'Ferrall, J. Chem. Soc. Perkin II, 1084 (1981).

LS86 T.W.S. Lee and R. Stewart, Can. J. Chem., **64**, 1085 (1986).

LW69 G.E. Lienhard and T. Wang, J. Am. Chem. Soc., **91**, 1146 (1969).

M 70 R.A. More O'Ferrall, J. Chem. Soc. (B), 274 (1970).

M 75 R.A. More O'Ferrall, in "Proton Transfer Reactions", (E.F. Caldin and V. Gold, eds.), Chapter 7, Chapman and Hall, London, 1975.

M 79 T.A. Modro. Phosphorus Sulfur, **5**, 331 (1979).

M 83 J.R. Murdoch, J. Am. Chem. Soc., **105**, 2660 (1983).

MG64 D.J. Martin and C.E. Griffin, J. Organomet. Chem. **1**, 292 (1964).

ML62 A.O. McDougall and F.A. Long, J. Phys. Chem., **66**, 429 (1962).

N 74 C.O. Nuallain, J. Inorg. Nucl. Chem., **36**, 339 (1974).

N 87 H. Neuvonen, J. Chem. Soc. Perkin Trans II, 159 (1987).

NC73 C.O. Nuallain and S.O. Cinneide. J. Inorg. Nucl. Chem., **35**, 2871 (1973).

NH87 P.O. Neill and A.F. Hegarty, J. Chem. Soc. Chem. Comm., 744 (1987).

NL86 K. Nagarajan, T.W.S. Lee, R.R. Perkins and R. Stewart, Can. J. Chem., **64**, 1090 (1986).

NS87 K. Nagarajan, K.P. Shelly, R.R. Perkins, and R. Stewart, Can. J. Chem., **65**, 1729 (1987).

NV87 K. Nagarajan, S. Venimadhavan, O. Lee, and R. Stewart, unpublished results.

P 34 K.J. Pedersen, J. Phys. Chem., **38**, 590 (1934).

P 59 Y. Pocker, Chem. and Ind., 1383 (1959).

P 87 P. Pruszynski, Can. J. Chem., **65**, 2160 (1987).

PD69 Y. Pocker and D.G. Dickerson, J. Phys. Chem., **73**, 4005 (1969).

PD81 D.D. Perrin, B. Dempsey, and E.P. Serjeant, "pK_a Prediction for Organic Acids and Bases", Chapman and Hall, London, 1981.

PG84 A.G. Pinkus and R. Gopalan, J. Am. Chem. Soc., **106**, 2360 (1984).

PM67 Y. Pocker and J.E. Meany, J. Phys. Chem., **71**, 3113 (1967).

R 81 R.W. Ramette, "Chemical Equilibrium and Analysis", Addison-Wesley, Reading, MA, 1981.

a) p. 91.

b) p. 137.
c) pp. 294-296.
d) pp. 63-64.

RK39 O. Reitz and J. Kopp, Z. Physik Chem., A184, 429 (1939).

RS71 J.D. Roberts, R. Stewart, and M.C. Caserid, Organic Chemistry: Methane to Macromolecules, P. 203, W.A. Benjamin, New York, 1971.

S 85 R. Stewart, The Proton: Applications to Organic Chemistry. Academic Press, Orlando, 1985.

a) p. 254.
b) pp. 259-260.
c) pp. 269-281.
d) p. 292.
e) p. 282.
f) p. 154.
g) pp. 34-36.
h) pp. 11-14.
i) p. 290.

S 87 W.H. Saunders, Jr., J. Am. Chem. Soc., 107, 164 (1987).

SA84 C.J. Schlesener, C. Amatore and J.K. Kochi, J. Am. Chem. Soc., 106, 3567 (1984).

SB52 C.G. Swain and J.F. Brown, J. Am. Chem. Soc., 74, 2538 (1952) .

SD58 C.G. Swain, A.J. DiMilo, and J.P. Cordner, J. Am. Chem. Soc., 80, 5983 (1958).

SD79 E.P. Serjeant and B. Dempsey, "Ionization constants of organic acids in aqueous solution", Pergamon, Oxford, 1979.

SG49 L.H. Sommer, J.R. Gold, G.M. Goldberg and N.S. Marans, J. Am. Chem. Soc., 71, 1509 (1949).

SK63 A. Streitwieser Jr. and H.S. Klein, J. Am. Chem. Soc., 85, 2759 (1963).

SK85 A. Streitwieser Jr., M.J. Kaufman, D.A. Bors, J.R. Murdoch, C.A. MacArthur, J.T. Murphy, and C.C. Shen. J. Am. Chem. Soc., 107, 6983 (1985).

SN87 K.P. Shelly, K. Nagarajan, and R. Stewart, Can. J. Chem., 65, 1734 (1987).

SS58 C.G. Swain, E.C. Stivers, J.F. Reuwer, Jr., and L.S. Schaad, J. Am. Chem. Soc., 80, 5885 (1958).

SS67 J. Steigman and D. Sussman, J. Am. Chem. Soc., **89**, 6406 (1967).

SS76a R. Srinivasan and R. Stewart, J. Chem. Soc. Perkin Trans. 2, 674 (1976).

SS76b R. Srinivasan and R. Stewart, J. Am. Chem. Soc., **98**, 7648 (1976).

SS77 J. Spaulding, J.E. Stein, and J.E. Meany, J. Phys. Chem., **81**, 1359 (1977).

SS78 R. Stewart and R. Srinivasan, Acc. Chem. Res., **11**, 271 (1978).

SS81 R. Stewart, R. Srinivasan and S.J. Gumbley, Can. J. Chem., **59**, 2755 (1981).

T 60 R.W. Taft. J. Phys. Chem., **64**, 1805 (1960).

T 82 J. Toullec, in "Advances in Physical Organic Chemistry" (V. Gold, and D. Bethell, eds.), Volume 18, Academic Press, London, 1982, p. 1.

TD74 J. Toullec and J.E. Dubois, J. Am. Chem. Soc., **96**, 3524 (1974).

V 51 A.I. Vogel. Quantitative Inorganic Analysis. 2nd edn., Longmans, Green and Co., London, 1951, pp. 342, 336.

W 61 F.H. Westheimer, Chem. Revs., **61**, 265 (1961).

WB56 F.H. Westheimer and O.T. Benfey, J. Am. Chem. Soc., **78**, 5309 (1956).

WM78 M.D. Waddington and J.E. Meany, J. Chem. Ed., **55**, 60 (1978).

ZH39 L. Zucker and L.P. Hammett, J. Am. Chem. Soc., **61**, 2791 (1939).